



Contracts for field projects
and supporting research on . . .

77

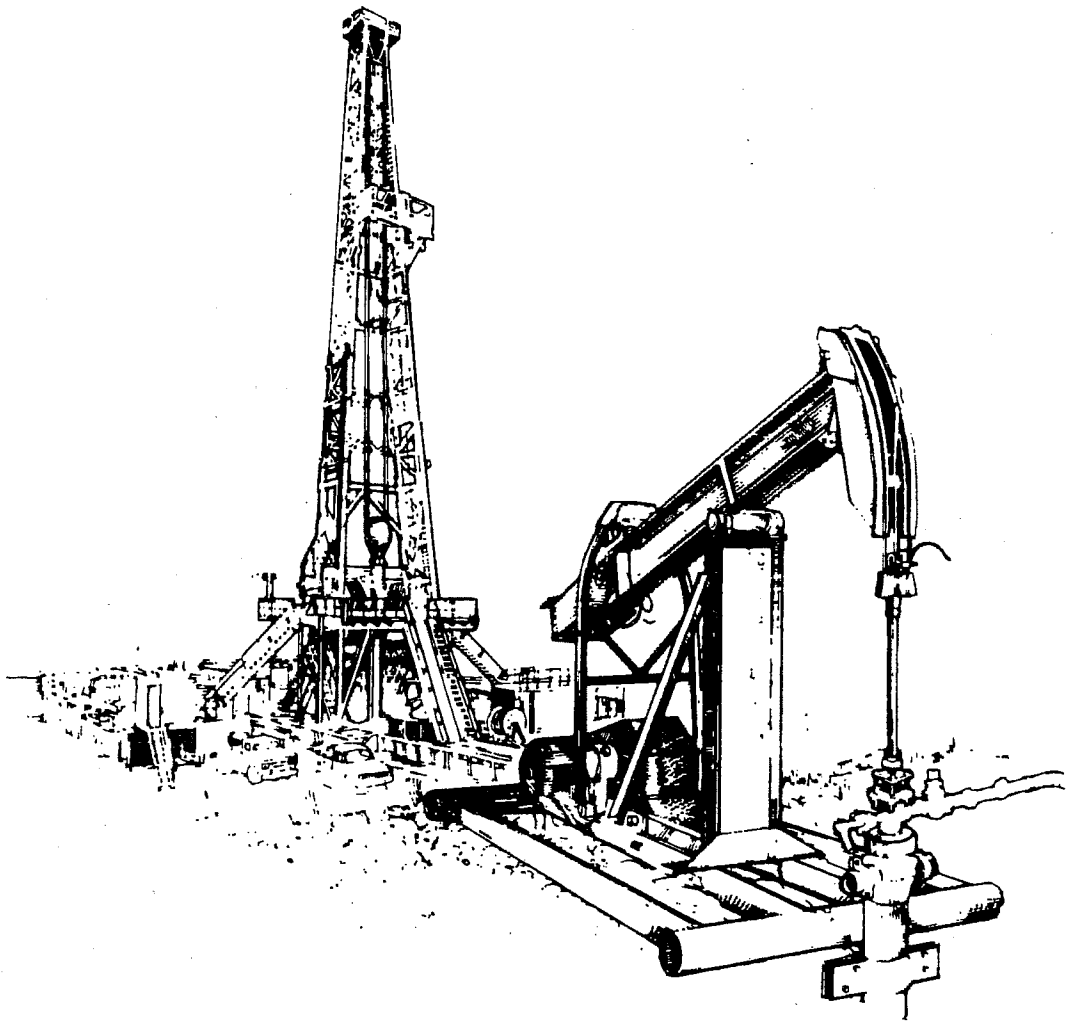
Enhanced Oil Recovery

Reporting Period October–December 1993

DOE/BC--94/1
(DE94000200)

PROGRESS REVIEW

Quarter Ending December 31, 1993



United States Department of Energy

Office of Gas and Petroleum Technology
and Bartlesville Project Office

DISCLAIMER

This report was prepared as an account of work sponsored by an agency of the United States Government. Neither the United States Government nor any agency thereof, nor any of their employees, makes any warranty, express or implied, or assumes any legal liability or responsibility for the accuracy, completeness, or usefulness of any information, apparatus, product, or process disclosed, or represents that its use would not infringe privately owned rights. Reference herein to any specific commercial product, process, or service by trade name, trademark, manufacturer, or otherwise does not necessarily constitute or imply its endorsement, recommendation, or favoring by the United States Government or any agency thereof. The views and opinions of authors expressed herein do not necessarily state or reflect those of the United States Government or any agency thereof.

Available to DOE and DOE contractors from the Office of Scientific and Technical Information, P.O. Box 62, Oak Ridge, Tennessee 37831; prices available from (615) 576-8401.

Available to the public from the U.S. Department of Commerce, Technology Administration, National Technical Information Service, Springfield, Virginia 22161; prices available from (703) 487-4650.

U.S. Department of Energy
Washington, D.C. 20545

PATRICIA GODLEY
Assistant Secretary for Fossil Energy
Room 4G-084 Forrestal Building
Telephone Number 202-586-4695

REGINAL SPILLER
*Deputy Assistant Secretary for Gas
and Petroleum Technologies*

SANDRA WAISLEY
*Director for Oil and Gas Exploration
and Production*

Bartlesville Project Office
P.O. Box 1398
Bartlesville, Oklahoma 74005
Telephone No. 918-337-4401

THOMAS C. WESSON
Director

R. M. RAY
Deputy Director

BETTY J. FELBER
*Program Coordinator,
Enhanced Oil Recovery*

HERBERT A. TIEDEMANN
*Project Manager for
Technology Transfer*

DOE/BC--94/1
(DE94000200)

Distribution Category UC-122

PROGRESS REVIEW NO. 77

CONTRACTS FOR FIELD PROJECTS AND SUPPORTING RESEARCH ON ENHANCED OIL RECOVERY

Date Published - December 1994

UNITED STATES DEPARTMENT OF ENERGY



PUBLICATIONS LIST

Bartlesville Project Office

Thomas C. Wesson, Director

AVAILABILITY OF PUBLICATIONS

The Department of Energy makes the results of all DOE-funded research and development efforts available to DOE and DOE contractors from the Office of Scientific and Technical Information, P.O. Box 62, Oak Ridge, TN 37831; prices available from (615) 576-8501, FTS 626-8401.

Available to the public from the National Technical Information Service, U.S. Department of Commerce, 5285 Port Royal Road, Springfield, VA 22161; prices available from (703) 487-4650.

Give the full title of the report and the report number.

Sometimes there are slight delays between the time reports are shipped to NTIS and the time it takes for NTIS to process the reports and make them available. Accordingly, we will provide one copy of any individual report as long as our limited supply lasts. Please help us in our effort to eliminate wasteful spending on government publications by requesting only those publications needed. Order by the report number listed at the beginning of each citation and enclose a self-addressed mailing label. Available from DOE Bartlesville Project Office, ATTN: Herbert A. Tiedemann, P.O. Box 1398, Bartlesville, OK 74005; (918) 337-4293.

Quarterly Reports

DOE/BC-93/2 Contracts for Field Projects and Supporting Research on Enhanced Oil Recovery. Progress Review No. 74. Quarter ending March 1993. March 1994. 165 pp. Order No. DE93000147. Status reports are given for various enhanced oil recovery and gas recovery projects sponsored by the Department of Energy. The field tests and supporting research on enhanced oil recovery include chemical flooding, gas displacement, thermal/heavy oil, resource assessment, geoscience technology, microbial technology, field demonstrations in high-priority reservoir classes, novel technology, and environmental technology.

DOE/BC-93/3 Contracts for Field Projects and Supporting Research on Enhanced Oil Recovery. Progress Review No. 75. Quarter ending June 1993. June 1994. 173 pp. Order No. DE94000115. Status reports are given for various enhanced oil recovery and gas recovery projects sponsored by the Department of Energy. The field tests and supporting research on enhanced oil recovery include chemical flooding, gas displacement, thermal/heavy oil, resource assessment, geoscience technology, field demonstrations in high-priority reservoir classes, novel technology, and environmental technology.

Chemical Flooding

DOE/BC/14886-6 Investigation of Oil Recovery Improvement by Coupling an Interfacial Tension Agent and a Mobility Control Agent in Light Oil Reservoirs. Surtex, Inc. Annual Report. June 1994. 88 pp. Order No. DE94000139. A study is underway of two major areas concerning co-injecting an interfacial tension reduction agent(s) and a mobility control agent. The first area defines the interactions of alkaline agent, surfactants, and polymers on a fluid-fluid and a fluid-rock basis. The second

area concerns the economic improvement of the combined technology. This report examines the interactions of different alkaline agents, surfactants, and polymer combinations on a fluid-fluid basis. Alkali and surfactant combine to reduce the interfacial tension between a low acid number, 42 API gravity crude oil and the aqueous solution to values lower than either agent alone. Surfactant structure can vary from linear chain sulfonates to alkyl aryl sulfonates to produce low interfacial tension values when combined with alkali. However as a class, the alkyl aryl sulfonates were the most effective surfactants. Surfactant olefinic character appears to be critical in developing low interfacial tensions. For the 42 API gravity crude oil, surfactants with molecular weights ranging from 370 to 450 amu are more effective in lowering interfacial tension. Ultralow interfacial tensions were achieved with all of the alkaline agents evaluated when combined with appropriate surfactants. Different interfacial tension reduction characteristics with the various alkali types indicates alkali interacts synergistically with the surfactants to develop interfacial tension reduction. The solution pH is not a determining factor in lowering interfacial tension. Surfactant is the dominate agent for interfacial tension reduction.

Thermal Recovery

DOE/BC/14899-9 Visualization and Simulation of Bubble Growth in Pore Networks - Topical Report. University of Southern California. March 1994. 36 pp. Order No. DE94000116. Bubble nucleation and bubble growth in porous media is an important problem encountered in processes, such as pressure depletion and boiling. To understand its basic aspects, experiments and numerical simulations in micromodel geometries were undertaken. Experiments of bubble growth by pressure depletion were carried out in 2-D etched-glass micromodels and in Hele-Shaw cells. Nucleation of bubbles and the subsequent growth of gas clusters were visualized. Contrary to the bulk or to Hele-Shaw cells, gas clusters in the micromodel have irregular and ramified shapes and share many of the features of an external invasion process (e.g. of percolation during drainage). A pore network numerical model was developed to simulate the growth of multiple gas clusters under various conditions. The model is based on the solution of the convection-diffusion equation and also accounts for capillary and viscous forces, which play an important role in determining the growth patterns. Numerical simulation results in good agreement with the experimental results.

NIPER-689 (Vol. 1)

The Description and LabVIEW® Executable Code of a General-Purpose Laboratory-Automation Program, Volume I. National Institute for Petroleum and Energy Research. April 1994. 132 pp. Order No. DE94000125. This report is Volume I (the description) of a two-volume series that describes a general purpose, automation computer program developed by NIPER for data acquisition/control/analysis/presentation. This software was developed to provide interactive computer control of a variety of instruments typically found in laboratories and pilot plants in order to improve efficiency in operation and safe handling of potentially

hazardous operations. For example, it is easily adaptable for operating a laboratory that conducts experiments at extreme conditions of pressure and temperature, such as those found in a steamflooding laboratory. The software was developed in an object-oriented graphical language around National Instruments' LabVIEW® which is the future trend in automation programming.

NIPER-689 (Vol. 2)

The Descriptive Panels and Diagrams for NIPER Lab WARDEN

Software, Volume 2. National Institute for Petroleum and Energy Research. April 1994. 240 pp. Order No. DE94000126. This report is the second volume of a two-volume series on the NIPER Lab WARDEN computer program, a modular laboratory or pilot plant automation software designed for data acquisition/control/analysis/presentation. Volume I of the series is the User Manual that serves all users, whereas this volume is the Reference Manual intended for advanced users examining the structure or modifying the program. Volume I contains a brief introduction of LabVIEW® and object-oriented programming, various features of the NIPER Lab WARDEN program, instruction on how to use these features, and several example problems and their step-by-step solutions. This volume (Volume 2) contains the complete program code needed to reproduce or modify the program. It includes the position in hierarchy, the connector pane, the front panel, and the block diagram for each of the virtual instruments (VI) in NIPER Lab WARDEN. The panels and block diagrams contained herein are generated from the computer program described in Volume I but are arranged to show and explain the structure and interrelationship between various elements in the program.

Geoscience

DOE/BC/14448-11

Reservoir Heterogeneity in Carboniferous Sandstone of the Black Warrior Basin. Final Report. Geological Survey of Alabama. June 1994.

196 pp. Order No. DE94000134. Although oil production in the Black Warrior basin of Alabama is declining, additional oil may be produced through improved recovery strategies, such as waterflooding, chemical injection, strategies, such as waterflooding, chemical injection, strategic well placement, and infill drilling. High-quality characterization of reservoirs in the Black Warrior basin is necessary to utilize advanced technology to recover additional oil and to avoid premature abandonment of fields. This report documents controls on the distribution and producibility of oil from heterogeneous Carboniferous reservoirs in the Black Warrior basin of Alabama. The first part of the report summarized the structural and depositional evolution of the Black Warrior basin and establishes the geochemical characteristics of hydrocarbon source rocks and oil in the basin. This second part characterized facies heterogeneity and petrologic and petrophysical properties of Carter and *Millerella* sandstone reservoirs. This is followed by a summary of oil production in the Black Warrior basin and an evaluation of seven improved-recovery projects in Alabama. In the final part, controls on the producibility of oil from sandstone reservoirs are discussed in terms of a scale-dependent heterogeneity classification.

DOE/BC/14660-11

Oil Recovery Improvement Through Profile Modification by

Thermal Precipitation. Final Report. University of Texas. April 1994. 60 pp. Order No. DE94000122. The objective of this research project has been to investigate the potential for using temperature-dependent (thermal) precipitation of chemicals to reduce the porosity and permeability of porous rocks. The method consists of injecting hot water that is saturated in a chemical that will precipitate upon cooling. Through this process, the permeability of thief zones in oil reservoirs could be reduced, allowing improved recovery by secondary and tertiary recovery processes. The chemical literature was reviewed for environmentally safe chemicals that have a suitable temperature-dependent solubility for the thermal precipitation process. Four suitable chemicals were identified: boron oxide, potassium carbonate, sodium borate, and potassium chloride. An

experimental apparatus was constructed to test the thermal precipitation process at high temperatures and pressures. Data was collected with clastic Berea sandstone cores using two chemicals: potassium carbonate and sodium borate. Data was also collected with limestone cores using potassium carbonate. The porosities and permeabilities were measured before and after being treated by the thermal precipitation process. A theoretical study of the process was also conducted. A model for predicting the fractional reduction in porosity was developed that is based on the temperature-dependent solubility of the chemical used. An empirical model that predicts the fractional reduction in permeability in terms of the fractional reduction in porosity was then developed for Berea sandstone. Existing theoretical models for estimating the permeability of porous media were tested against the measured data. The existing models, including the widely-used Carman-Kozeny equation, underpredicted the reduction in permeability for the thermal precipitation process. This study has shown that the thermal precipitation process has considerable potential for the controlled reduction in porosity and permeability in geologic formations. A design study to determine how the process would work in the field is recommended.

DOE/BC/14446-10

Development of Nuclear Magnetic Resonance Imaging/Spectroscopy

for Improved Petroleum Recovery. Final Report. Texas A&M University. April 1994. 160 pp. Order No. DE94000121. The overall objectives of this program are to develop and apply Nuclear Magnetic Resonance Imaging (NMRI) and CT X-Ray Scanning methods for determining rock, fluid, and petrophysical properties and for fundamental studies of multiphase flow behavior in porous media. Specific objectives are divided into four subtasks: (1) The development of NMRI and CT scanning for the determination of rock-fluid and petrophysical properties; (2) Development of NMRI and CT scanning for characterizing conventional multiphase displacement processes; (3) Development of NMR and CT scanning for characterizing dispersed phase processes; and (4) Miscible displacement studies. The final reports for each of the subtasks are provided in this document.

DOE/BC/14655-8

Use of "Rock Typing" to Characterize Carbonate Reservoir Heterogeneity. Final Report. Ikwaukolam Energy Company, Inc. March 1994.

396 pp. Order No. DE94000118. The objective of the project was to apply techniques of "rock typing" and quantitative formation evaluation to borehole measurements in order to identify reservoir and non-reservoir rock-types and their properties within the "C" zone of the Ordovician Red River carbonates in the northeast Montana and northwest North Dakota areas of the Williston Basin. Rock-typing discriminates rock units according to their pore-size distribution. Formation evaluation estimates porosities and pore fluid saturation. Rock-types were discriminated using crossplots involving three rock-typing criteria: (1) linear relationship between bulk density and porosity, (2) linear relationship between acoustic interval transit-time and porosity, and (3) linear relationship between acoustic interval transit-time and bulk density. Each rock-type was quantitatively characterized by the slopes and intercepts established for different crossplots involving the above variables, as well as porosities and fluid saturations associated with the rock-types. Another family of linear relationships involving shear wave velocity, compressional wave velocity, and porosity were used to characterize the entire "C" zone carbonate section. Slopes and intercepts derived in the combined use of shear and compressional wave velocities are characteristic of carbonates, and corroborate results predicted from other studies. The "C" zone of the Red River carbonates is extremely heterogeneous. The heterogeneities were observed in hand specimen, and corroborated by wide variabilities in porosity, permeability, grain density, the porosity-permeability crossplot, and the results from rock-typing and quantitative formation evaluation. Sixty-four different rock-types were identified in the fifty-two wells studied. Vertical distribution of rock-types shows a non-porous anhydrite rock-type, underlain, in most wells, by combinations of anhydritic dolomite and dolomite rock-types. These in turn are underlain by dolomitic limestone and limestone rock-types. Dolomitic lime-

stone and limestone rock-types are generally non-porous or have low porosities. The thickness of the non-porous dolomite rock-types varies from a few feet in some wells to over hundred feet in others.

DOE/BC/14649-15 **Analysis and Evaluation of Interwell Seismic Logging Techniques for Hydrocarbon Reservoir Characterization. Final Report. Southwest Research Institute. June 1994. 200 pp. Order No. DE94000133.** The oil and gas industry is presently emphasizing the production and recovery of established reserves rather than exploration of new fields. This has brought into focus the need for a better understanding of reservoir rock properties and geologic structures. Of particular interest are factors that directly affect the distribution of the reservoir fluids, namely the permeability of the rock and the presence and locations of fractures and impermeable boundaries that channel or constrain the movement of fluids. A new conceptual extension of sonic logging is offered in this project for specific application in heterogeneous reservoirs. This concept is one of interwell seismic logging which is made possible by the prevalence of the relatively large number of wells located in the reservoir. In this application, high resolution seismic transmission measurements between a pair of boreholes can provide information equivalent to a seismic section which uniquely is oriented in the plane of the boreholes. These interwell seismic data is analyzed to determine various petrophysical properties of the reservoir under investigation.

DOE/BC/14654-15 **Simulation Studies to Evaluate the Effect of Fracture Closure on the Performance of Fractured Reservoirs. Final Report. K & A Energy. March 1994. 176 pp. Order No. DE94000119.** A three-year research program to evaluate the effect of fracture closure on the recovery of oil and gas from naturally fractured reservoirs has been completed. The overall objectives of the study were to: (1) evaluate the reservoir conditions for which fracture closure is significant, and (2) evaluate innovative fluid injection techniques capable of maintaining pressure within the reservoir. The evaluations of reservoir performance were made by a modern dual porosity simulator, TETRAD. This simulator treats both porosity and permeability as functions of pore pressure. Simulated wellbores can assume any orientation from vertical to horizontal. The Austin Chalk in the Pearsall Field of South Texas was selected as the prototype fractured reservoir for this work. Availability of published data was the principal basis for this selection. Consequently, the simulation models were initialized with properties typical of the Pearsall Field, Austin Chalk reservoir. During the first year, simulations of vertical and horizontal well performance were made assuming that fracture permeability was insensitive to pressure change. Sensitivity runs indicated that the simulator was predicting the effects of critical reservoir parameters in a logical and consistent manner. The results confirmed that horizontal wells could increase both rate of oil recovery and total oil recovery from naturally fractured reservoirs. In the second year, the performance of the same vertical and horizontal wells was reevaluated with fracture permeability treated as a function of reservoir pressure. To investigate sensitivity to in situ stress, differing loading conditions were assumed. The highest condition assumed all principal stress components equaled the overburden stress. The lower stress cases assumed the horizontal stress components were unequal and less than the overburden stress. Simulated natural depletions confirm that pressure sensitive fractures degrade well performance. The severity of degradation worsens when the initial reservoir pressure approaches the average stress condition of the reservoir, such as occurs in over pressured reservoirs. Simulations with water injection indicate that degradation of permeability can be counteracted when reservoir pressure is maintained and oil recovery can be increased when reservoir properties are favorable.

DOE/BC/14444-16 **Oil Recovery Enhancement from Fractured, Low Permeability Reservoirs. 1991-1992 Annual Report. Texas A&M University. June 1994. 68 pp. Order No. DE94000138.** The results of the investigative efforts for this jointly funded DOE-State of Texas research project achieved during the 1991-1992 year may be summarized as follows. *Geological Character-*

ization - Detailed fracture system maps measured at outcrops along the Austin Chalk trend have been related to the subsurface. Statistical data obtained from the outcrop studies has been correlated with FMS dipmeter information obtained from Austin Chalk operators. These studies have shown the hierarchical nature and the bed contained fracture development observed in the outcrop may be extrapolated to the subsurface. Well log response in Austin Chalk wells has been shown to be a reliable indicator of both organic maturity and fracturability. Multi-component, vertical-seismic-profile, VSP shear-wave data were reduced to their true orthogonal components by balancing or rotating the source magnitudes and geophone couplings. The resultant method appears to be useful to detect the negligible displacement fractures in the Austin Chalk. Production decline curves have been related to well test or transient pressured analysis methods. Studies on daily production records of Austin Chalk horizontal wells have shown that analysis of production records may be substituted for the more expensive and difficult to obtain transient pressure data. *Development of the EOR Imbibition Process* - Magnetic Resonance Imaging, MRI studies have shown the carbonated water-imbibition displacement process significantly accelerates and increases recovery from oil saturated, low permeability rocks. These studies applied to flow in open and dead-end micro-fractures have shown significant volumes of oil remain undisturbed in the dead-end micro-fractures even when carbonated water is used as the imbibing fluid. *Transfer of Technology* - A number of presentations and publications were made at technical meetings and symposia. Two conferences concerning the results of our investigative efforts on the Austin Chalk were held at Texas A&M.

DOE/BC/14968-1 **National Data Repository System. American Geological Institute. March 1994. 72 pp. 500 copies. Order No. DE94000120.** The American Geological Institute (AGI) has completed the first phase of a study to assess the feasibility of establishing a National Geoscience Data Repository System to capture and preserve valuable geoscientific data. The study was initiated in response to the fact that billions of dollars worth of domestic geological and geophysical data are in jeopardy of being irrevocably lost or destroyed as a consequence of the ongoing downsizing of the U. S. energy and minerals industry. This report focuses on two major issues. First, it documents the types and quantity of data available for contribution to a National Geoscience Data Repository System. Second, it documents the data needs and priorities of potential users of the system. A National Geoscience Data Repository System would serve as an important and valuable source of information for the entire geoscience community for a variety of applications, including environmental protection, water resource management, global change studies, and basic and applied research. The repository system would also contain critical data that would enable domestic energy and minerals companies to expand their exploration and production programs in the United States for improved recovery of domestic oil, gas, and mineral resources. The results of the initial phase of the feasibility study are extremely positive. Major oil companies, large independent petroleum producers, and minerals companies have indicated they would consider contributing vast amounts of data to a National Geoscience Data Repository System.

DOE/BC/14951-5 **Integrated Approach Towards the Application of Horizontal Wells to Improve Waterflooding Performance. Annual Report. University of Tulsa. June 1994. 54 pp. Order DE94000137.** This annual report describes the progress during the first year of the project on Integrated Approach Towards the Application of Horizontal Wells to the Department of Energy's Class I program which is targeted towards improving the reservoir performance of mature oil fields located in fluvial-dominated deltaic deposits. The project involves an integrated approach to characterize the reservoir followed by drilling of horizontal injection wells to improve production performance. The type of data we intend to integrate includes cross borehole seismic surveys, geological interpretation based on logs and cores, and engineering information. This report covers the first phase of the project which includes a detailed reservoir description of the field based on the available information, followed by flow simulation

of the Self Unit to compare the simulated result with the historical performance. Based on the simulated results, a vertical test well was drilled to validate our reservoir description. The well will also be used as a source well for a cross borehole seismic survey. This report discusses the related geophysical, geological, and engineering activities leading to the drilling of the vertical test well. The validation phase and the collection of the cross borehole survey has just begun, and the results will be presented in the next annual report.

DOE/BC/14959-5

Revitalizing a Mature Oil Play: Strategies for Finding and Producing Unrecovered Oil in Frio Fluvial-Deltaic Reservoirs of South Texas. Annual Report for October 1992-December 1993. The University of Texas. May 1994. 100 pp. Order No. DE94000131. Progress achieved during the first year of the project consisted of screening production and geologic databases of fields within the Frio Fluvial-Deltaic sandstone play to determine fields suitable for detailed characterization studies, selecting two South Texas fields for detailed studies, and performing initial reservoir studies of each field. Tabulation and statistical analysis of production and engineering data from 346 reservoirs throughout the Frio Fluvial-Deltaic oil play were performed in order to characterize average reservoir parameters, generate frequency distributions for values of individual reservoir attributes, and calculate playwide resource estimates. Two fields were selected for study: Rincon field, near the Mexico border in Starr County, and T-C-B field, in the northern part of the play trend in Jim Wells County. Project personnel conducted reviews with operators of both fields. Data on drilling history, perforation intervals, formation and reservoir tops, well logs, core descriptions and analyses, limited conventional core, sidewall core samples, and fluid and pressure tests were acquired from 220 wells in Rincon field and from more than 80 wells in T-C-B field.

DOE/BC/14959-8

Identification of Remaining Oil Resource Potential in the Frio Fluvial/Deltaic Sandstone Play, South Texas. Topical Report. The University of Texas. May 1994. 73 pp. Order No. DE94000132. Reservoir attribute data were statistically analyzed from oil and gas fields throughout the geographic area covered by the Frio Fluvial/Deltaic Sandstone oil play. General reservoir attributes analyzed in detail included porosity, initial water saturation, residual oil saturation, net pay, reservoir area, and fluid characteristics. Statistical analysis of variance demonstrated no difference between oil reservoir attributes and gas reservoir attributes, indicating that oil and gas reservoirs are subsets of a larger genetically similar population. Probability functions that describe attribute frequency distributions were determined for use in risk adjusting resource calculations. Different functions were found to be most applicable for the various petrophysical reservoir attributes.

DOE/BC/14657-15

Measuring and Predicting Reservoir Heterogeneity in Complex Deposystems. The Fluvial-Deltaic Big Injun Sandstone in West Virginia. Final Report for September 20, 1991-October 31, 1993. Evidence for heterogeneity in the Big Injun reservoir-forming sandstones on a regional scale is found in the distribution of hydrocarbons into distinct fields across the basin. The easternmost fields traditionally are considered to be updip unconformity traps; those to the west appear to be regionally downdip from the truncated margin of the reservoir. Drilling history for Granny Creek suggests reservoir heterogeneity as drillers first developed the northern and central part of the field in the 1920's and 30's, then the southernmost part. There was sporadic infill drilling throughout the field since initial development. In contrast, Rock Creek field was developed in two stages, first within the shallower part of this synclinal field, then deeper when drillers accepted higher water saturations. Evaluation of waterflood performance revealed the non-uniform pressure and production behavior in several patterns in Granny Creek field. A novel approach was employed to model a fracture between a well that exhibited low injection pressures and a production well that experienced early water breakthrough. This led to successful simulation of waterflood production performance for two adjacent patterns

with substantially different behaviors. The results of simulation studies revealed that the communication path must be through a separate zone, most probably the overlying Greenbrier Limestone.

Microbial Technology

DOE/BC/14659-7

Characterization of Non-Darcy Multiphase Flow in Petroleum Bearing Formation. Final Report. University of Oklahoma. April 1994. 196 pp. Order No. DE94000123. Slow flow is most common in oil and gas reservoirs and can be adequately described by Darcy's law. Although rapid fluid flow may occur only in certain limited locations, it can affect the productive capacity of in-situ reservoirs significantly. Therefore, for accurate predictability of reservoir productivity, accurate description of deviations from Darcy's law during rapid flow is important. Although rapid flow in porous media, frequently referred to as non-Darcy flow, has been subject to numerous studies, there is still no consensus amongst the researchers as to the accurate way of describing the relevant processes. Therefore, this study has reviewed the previous studies and developed improved formulations and methodologies. In the present study non-Darcy multiphase flow in porous materials is theoretically and experimentally investigated. Background material is presented which demonstrates a need for obtaining new theoretical and experimental results in order to better characterize this important porous media flow regime. Improved models, experimental data, and mathematical correlations are necessary for scientists and engineers to develop the technology that can be used to significantly reduce the cost of finding and producing natural gas and its associated liquids. Non-Darcy multiphase flow in various consolidated porous media and unconsolidated porous media characteristic of hydraulically created propped fractures and gravel pack systems is also investigated. The experimental research is carried out in the new non-Darcy Flow Research Laboratory recently constructed at the University of Oklahoma.

DOE/ID/01570-T171

Laboratory Methods for Enhanced Oil Recovery Core Floods. Topical Report. Idaho National Energy Laboratory, EG&G Idaho. March 1994. 28 pp. Order No. DE94000117. Current research at the Idaho National Engineering Laboratory (INEL) is investigating microbially enhanced oil recovery (MEOR) systems for application to oil reservoirs. Laboratory corefloods are invaluable in developing technology necessary for a field application of MEOR. Methods used to prepare sandstone cores for experimentation, coreflooding techniques, and quantification of coreflood effluent are discussed in detail. A technique to quantify the small volumes of oil associated with laboratory core floods is described.

Novel Technology

DOE/BC/14650-15

A Novel Approach to Modeling Unstable EOR Displacements. Final Report. University of Texas at Austin. April 1994. 216 pp. Order No. DE94000128. This is the final report of a three-year research project that was aimed at developing a methodology for predicting the performance of unstable displacements in heterogeneous reservoirs. A performance prediction approach that combines numerical modeling with laboratory imaging experiments has been developed. Most enhanced oil recovery (EOR) schemes involve the displacement of a more dense and more viscous oil by a less dense and less viscous fluid in a heterogeneous porous medium. The interaction of heterogeneity with the several competing forces, namely, viscous, capillary, gravitational, and dispersive forces, can conspire to make the displacements unstable and difficult to model and to predict. The objective of this research was to develop a systematic methodology for modeling unstable fluid displacements in heterogeneous media. Flow visualization experiments were conducted using X-ray computed tomography (CT) imaging and a video imaging workstation to (a) gain new insights into the dynamics of unstable displacements, (b) acquire detailed quantitative experimental image data for calibrating numerical models of unstable displacements and (c) image and characterize heterogeneities in laboratory cores geostatistically. High-resolution

numerical models modified for use on vector-architecture supercomputers were used to replicate the image data. Geostatistical models of reservoir heterogeneity were incorporated in the numerical models in order to study the interaction of hydrodynamic instability and heterogeneity in reservoir displacements. Finally, a systematic methodology for matching the experimental data with the numerical models and scaling the laboratory results to other systems were developed. The outcome of the research is a new method for predicting the performance of unstable EOR displacements in the field based on small-scale displacements in the laboratory.

Resource Assessment Technology

DOE/BC/14658-9 **Predictability of Formation Damage: An Assessment Study and Generalized Models. Final Report. University of Oklahoma. April 1994. 300 pp. Order No. DE94000125.** The project objective is to develop improved generalized predictive models to be used for investigation of reservoir formation damage and control for various fluid and rock conditions and to account for these effects in reservoir simulation. To accomplish its objective the proposed study first critically studies and evaluates the previous modeling efforts reported in the literature. Then, generalized predictive models are formulated by combining the previous attempts and by improving and generalizing the modeling approaches to accommodate for a wide variety of conditions encountered in actual field applications. A critical review of the previous work addressing their theoretical basis, assumptions and limitations, and the generalized and improved models developed in this study are presented in a systematic manner in terms of a standardized definition and nomenclature for direct comparison.

Case studies with the improved models are presented to demonstrate their capacity and validity. Computer programs implementing the improved modeling approaches are also supplied.

Gas Displacement

DOE/BC/14852-5 **Scale-up of Miscible Flood Processes for Heterogeneous Reservoirs. 1993 Annual Report. Stanford University. May 1994. 130 pp. DE94000130.** Progress is reported for a comprehensive investigation of the scaling behavior of gas injection processes in heterogeneous reservoirs. The interplay of phase behavior, viscous fingering, gravity segregation, capillary imbibition and drainage, and reservoir heterogeneity is examined in a series of simulations and experiments. Compositional and first-contact miscible simulations of viscous fingering and gravity segregation are compared to show that the two techniques can give very different results. Also, analyzed are two-dimensional and three-dimensional flows in which gravity segregation and viscous fingering interact. The simulations show that 2D and 3D flows can differ significantly. A comparison of analytical solutions for three-component two-phase flow with experimental results for oil/water/alcohol systems is reported. While the experiments and theory show reasonable agreement, some differences remain to be explained. The scaling behavior of the interaction of gravity segregation and capillary forces is investigated through simulations and through scaling arguments based on analysis of the differential equations. The simulations show that standard approaches do not agree well with results of low IFT displacements. The scaling analyses, however, reveal flow regimes where capillary, gravity, or viscous forces dominate the flow.

INDEX

COMPANIES AND INSTITUTIONS

	Page		Page
Amoco Production Company		Sierra Energy Company	
West Hackberry Tertiary Project	76	Enhanced Oil Recovery Utilizing High-Angle Wells in the Frontier Formation, Badger Basin Field, Park County, Wyoming	115
Anderman/Smith Operating Company		Stanford University	
Secondary Oil Recovery from Selected Carter Sandstone Oil Fields—Black Warrior Basin, Alabama	110	Productivity and Injectivity of Horizontal Wells	47
Colorado School of Mines		Scaleup of Miscible Flood Processes	27
Interdisciplinary Study of Reservoir Compartments	61	Stanford University Petroleum Research Institute	
Columbia University		Research on Oil Recovery Mechanisms in Heavy Oil Reservoirs	55
Dynamic Enhanced Recovery Technologies	71	Surtek, Inc.	
Surfactant Loss Control in Chemical Flooding: Spectroscopic and Calorimetric Study of Adsorption and Precipitation on Reservoir Minerals	1	Detailed Evaluation of the West Kiehl Alkaline-Surfactant-Polymer Field Project and Its Application to Mature Minnelusa Waterfloods	44
Illinois Institute of Technology		Investigation of Oil Recovery Improvement by Coupling an Interfacial Tension Agent and a Mobility Control Agent in Light Oil Reservoirs	21
Surfactant-Enhanced Alkaline Flooding for Light Oil Recovery	6	Texaco Exploration and Production, Inc.	
Lawrence Livermore National Laboratory		Postwaterflood CO ₂ Miscible Flood in Light Oil, Fluvial-Dominated Deltaic Reservoir	95
Oil Field Characterization and Process Monitoring Using Electromagnetic Methods	52	University of Alaska	
Lomax Exploration Company		Study of Hydrocarbon Miscible Solvent Slug Injection Process for Improved Recovery of Heavy Oil from Schrader Bluff Pool, Milne Point Unit, Alaska	41
Green River Formation Waterflood Demonstration Project, Uinta Basin, Utah	107	University of Kansas	
Louisiana State University		Improved Oil Recovery in Fluvial Dominated Deltaic Reservoirs of Kansas—Near-Term	102
Assist in the Recovery of Bypassed Oil from Reservoirs in the Gulf of Mexico	68	Improving Reservoir Conformance Using Gelled Polymer Systems	16
Maurer Engineering Inc.		University of Southern California	
Horizontal Oil Well Applications and Oil Recovery Assessments	39	Modification of Reservoir Chemical and Physical Factors in Steamfloods To Increase Heavy Oil Recovery	43
Michigan Technological University		University of Southern Mississippi	
Visual Display of Reservoir Parameters Affecting Enhanced Oil Reservoirs	81	Responsive Copolymers for Enhanced Petroleum Recovery	9
New Mexico Institute of Mining and Technology		University of Texas	
Field Verification of CO ₂ -Foam	25	Geoscience/Engineering Characterization of the Interwell Environment in Carbonate Reservoirs Based on Outcrop Analogs, Permian Basin, West Texas and New Mexico	60
Improved Techniques for Fluid Diversion in Oil Recovery	18		
Integration of Advanced Geoscience and Engineering Techniques To Quantify Interwell Heterogeneity	57		
Oklahoma Geological Survey			
Continued Support of the Natural Resources Information System for the State of Oklahoma	65		

Revitalizing a Mature Oil Play: Strategies for Finding and Producing Unrecovered Oil in Frio Fluvial-Deltaic Reservoirs of South Texas	86
University of Tulsa	
Application of Artificial Intelligence to Reservoir Characterization: An Interdisciplinary Approach	58
Integrated Approach Toward the Application of Horizontal Wells To Improve Waterflooding Performance	104
University of Wyoming	
Anisotropy and Spatial Variation of Relative Permeability and Lithologic Characterization of Tensleep Sandstone Reservoirs in the Bighorn and Wind River Basins, Wyoming	62

Utah Geological Survey	
Geological and Petrophysical Characterization of the Ferron Sandstone for Three-Dimensional Simulation of a Fluvial-Deltaic Reservoir	84
Increased Oil Production and Reserves from Improved Completion Techniques in the Bluebell Field, Uinta Basin, Utah	79

CONTENTS BY EOR PROCESS

Chemical Flooding—Supporting Research	1
Gas Displacement—Supporting Research	25
Thermal Recovery—Supporting Research	39
Geoscience Technology	57
Resource Assessment Technology	65
Field Demonstrations	71

**DOE Technical Project Officers for
Enhanced Oil Recovery**

DIRECTORY

Name	Phone number	Name of contractor
U. S. Department of Energy Gas and Petroleum Technology Oil and Gas Exploration and Production 3E-028/FORS Washington, D.C. 20585		
Bartlesville Project Office P. O. Box 1398 Bartlesville, Oklahoma 74005		
Edith Allison	918-337-4390	Columbia University Lomax Exploration Company Sierra Energy Company University of Texas Utah Geological Survey
Jerry Casteel	918-337-4412	Columbia University Illinois Institute of Technology New Mexico Institute of Mining and Technology Stanford University Surtek, Inc. University of Kansas University of Southern Mississippi
Robert Lemmon	918-337-4405	Colorado School of Mines Michigan Technological University New Mexico Institute of Mining and Technology University of Texas University of Tulsa University of Wyoming Utah Geological Survey
Rhonda Lindsey	918-337-4455	University of Kansas University of Tulsa
Chandra Nautiyal		Texaco Exploration and Production, Inc.
R. Michael Ray	918-337-4403	Oklahoma Geological Survey
Thomas Reid	918-337-4233	Lawrence Livermore National Laboratory Maurer Engineering Inc. Stanford University Stanford University Petroleum Research Institute Surtek, Inc. University of Alaska University of Southern California
Metairie Site Office 900 Commerce Road, East New Orleans, Louisiana 70123		
Gene Pauling	504-734-4131	Amoco Production Company Anderman/Smith Operating Company Louisiana State University
Morgantown Energy Technology Center P. O. Box 880 Morgantown, West Virginia 26505		
Royal Watts	304-285-4218	New Mexico Institute of Mining and Technology

CHEMICAL FLOODING— SUPPORTING RESEARCH

***SURFACTANT LOSS CONTROL
IN CHEMICAL FLOODING:
SPECTROSCOPIC AND CALORIMETRIC
STUDY OF ADSORPTION AND
PRECIPITATION ON RESERVOIR
MINERALS***

Contract No. DE-AC22-92BC14884

**Columbia University
New York, N.Y.**

**Contract Date: Sept. 30, 1992
Anticipated Completion: Sept. 29, 1995
Government Award: \$602,232**

**Principal Investigator:
P. Somasundaran**

**Project Manager:
Jerry Casteel
Bartlesville Project Office**

Reporting Period: Oct. 1–Dec. 31, 1993

Objectives

The objective of this research is to elucidate the mechanisms of adsorption and surface precipitation of flooding

surfactants on reservoir minerals. The effect of surfactant structure, surfactant combinations, and other inorganic and polymeric species and solids of relevant mineralogy will also be determined. A multipronged approach consisting of microspectroscopy and nanospectroscopy, microcalorimetry, electrokinetics, surface tension, and wettability will be used to achieve the objectives. The results of this study should help in controlling surfactant loss in chemical flooding and also in developing optimum structures and conditions for efficient chemical flooding processes.

Summary of Technical Progress

The adsorption–desorption of tetradecyl trimethyl ammonium chloride (TTAC) and sodium dodecyl sulfate (SDS)–octaethylene glycol mono *n*-decyl ether ($C_{12}EO_8$) surfactant mixtures at the kaolinite–water and alumina–water interfaces were studied during this quarter. Spectroscopic techniques were used to investigate the microstructure of the adsorbed layer.

The effect of the hydrocarbon chain length of octaethylene glycol mono *n*-alkyl ether (C_nEO_8)-type nonionic surfactants on the adsorption of 1:1 mixtures of SDS– C_nEO_8 at the kaolinite–water interface was studied. The adsorption of SDS was enhanced by the presence of $C_{10}EO_8$, but this effect was not as significant as those by $C_{12-16}EO_8$. Interestingly, once the hydrocarbon chain length of the nonionic surfactant exceeded that of the SDS (12), there was no further enhancement of SDS adsorption. The results are explained in terms of

hydrocarbon chain-chain interaction and shielding of the chains from a hydrophilic environment.

Dynamic pyrene fluorescence spectroscopy was used to measure the aggregate size of 1:1 mixtures of SDS- $C_{12}EO_8$ adsorbed at the alumina-water interface. The nonionic surfactant in the mixed aggregate with the anionic SDS reduced the electrostatic repulsion and increased the total aggregate size. At the interface, the SDS aggregate was smaller than the $C_{12}EO_8$ aggregate for similar adsorption densities.

Changes in the microstructure of a TTAC adsorbed layer during adsorption and desorption were probed with the use of fluorescence spectroscopy. The TTAC aggregates at the alumina-water interface are not as tightly packed as TTAC micelles in bulk solution. The TTAC adsorption on alumina was found to be not completely reversible, and the nature of the adsorbed layer was observed to be altered upon dilution.

Adsorption of Surfactant Mixtures at Solid-Liquid Interfaces

Results reported during the previous quarter indicated that, with increasing hydrocarbon chain length of the nonionic surfactant C_nEO_8 ($n=10, 12, 14, 16$), the adsorption on kaolinite increased, but there was only partial coverage of the kaolinite surface (θ varied from 0.11 to 0.19). During this reporting period, the adsorption of 1:1 mixtures of SDS and C_nEO_8 mixtures at the kaolinite-water interface was studied. As shown in Fig. 1, the isotherms for the adsorption of SDS are

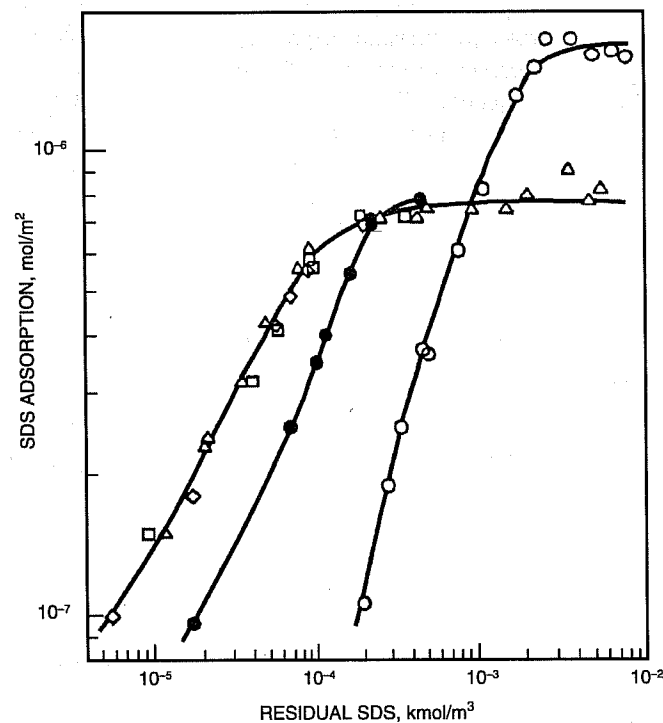


Fig. 1 Effect of nonionic surfactant hydrocarbon chain length on the adsorption of sodium dodecyl sulfate (SDS) from 1:1 SDS/ C_nEO_8 mixtures, 0.03M NaCl, pH 5.

identical when the hydrocarbon chain length of the nonionic surfactants ($C_{12}EO_8$, $C_{14}EO_8$, $C_{16}EO_8$) is equal to or longer than that of the anionic SDS (C_{12}).

When the hydrocarbon chain length of the nonionic surfactant is shorter ($C_{10}EO_8$) than that of the anionic SDS, however, a different isotherm is observed. The anionic SDS enhances the adsorption of the nonionic C_nEO_8 (Fig. 2), and the isotherms are shifted to a lower concentration region as compared to the adsorption isotherms of C_nEO_8 in the absence of any SDS (Fig. 3).

This is an indication of strong hydrophobic interaction with the co-adsorbing anionic surfactant; a schematic description of the interactions is provided in Fig. 4. When the hydrocarbon chain length of the nonionic surfactant is equal to or longer than that of the anionic SDS, the hydrocarbon chains of SDS are equally shielded from the hydrophilic environment by the hydrophobic chains of the co-adsorbing nonionic surfactant.

The identical residing environment then leads to a common isotherm for SDS adsorption on kaolinite (Fig. 1). When the hydrocarbon chain of the nonionic surfactant is shorter than that of the anionic SDS, part of the SDS hydrocarbon chain is exposed to the hydrophilic environment (aqueous solution of the hydrophilic ethylene oxide chain of the nonionic surfactant). The residing environment for SDS hydrocarbon chain is thus less hydrophobic, and therefore the isotherm is less shifted to the lower concentration region than in the previous case.

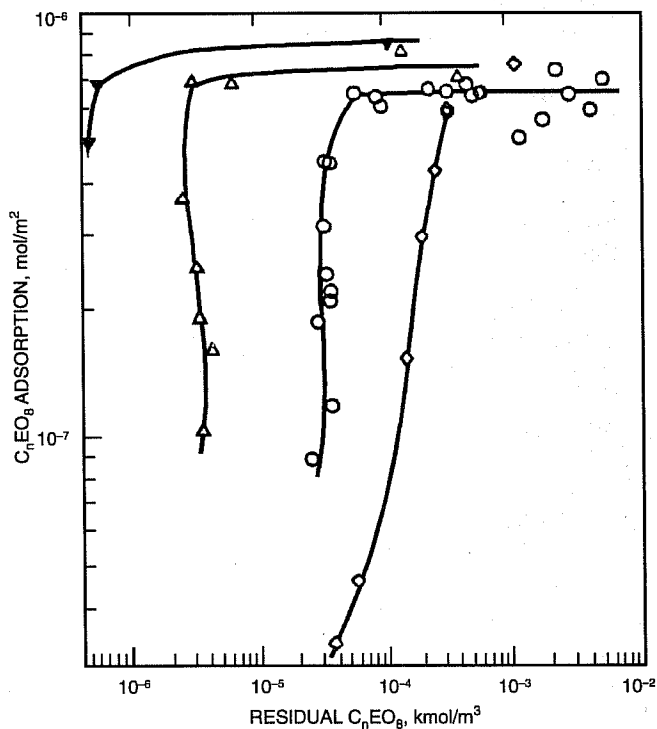


Fig. 2 Effect of nonionic surfactant hydrocarbon chain length on the adsorption of C_nEO_8 ($n=10, 12, 14, 16$) from its 1:1 mixtures with SDS, 0.03M NaCl, pH 5. ∇ , $C_{16}EO_8$; Δ , $C_{14}EO_8$; \circ , $C_{12}EO_8$; and \diamond , $C_{10}EO_8$.

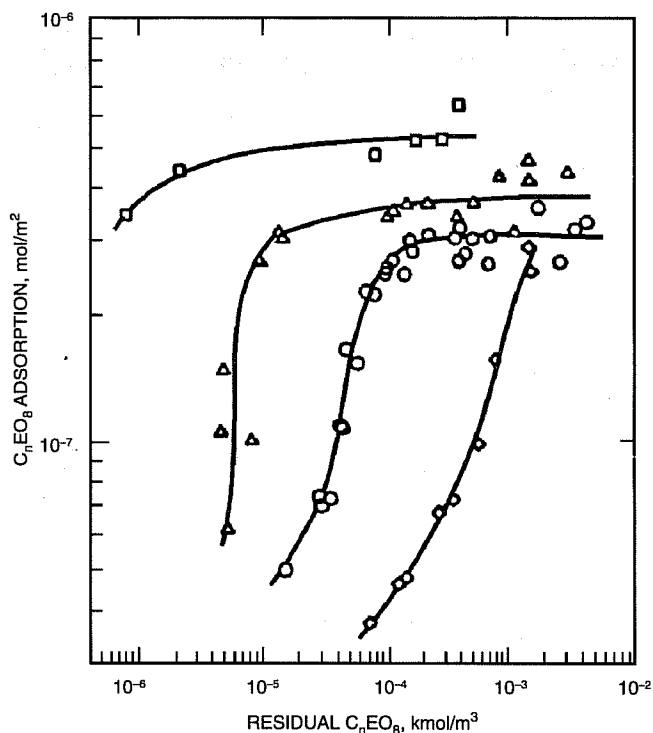


Fig. 3 Effect of hydrocarbon chain length (C_nEO_8) on the adsorption of nonionic surfactant on kaolinite, 0.03M NaCl, pH 5. \square , $C_{16}EO_8$; Δ , $C_{14}EO_8$; \circ , $C_{12}EO_8$; and \diamond , $C_{10}EO_8$.

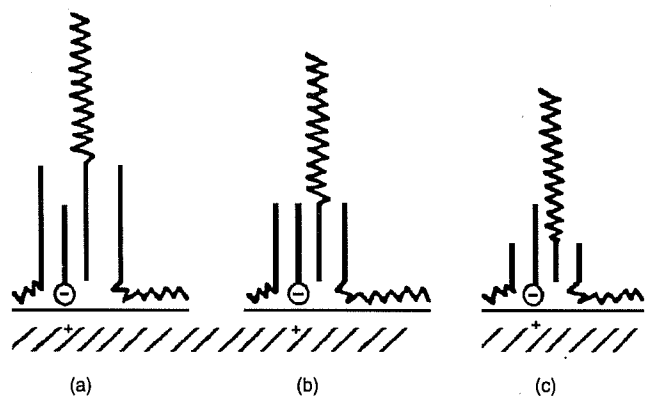


Fig. 4 Schematic presentation of the effect of nonionic surfactant hydrocarbon chain length on the adsorption of the anionic SDS: (a) Nonionic surfactant hydrocarbon chains longer than that of SDS; (b) nonionic surfactant hydrocarbon chain length equal to that of SDS; (c) nonionic surfactant hydrocarbon chain length shorter than that of the SDS, partially exposing SDS hydrocarbon chains to aqueous solution or the hydrophilic ethoxyl chains of the nonionic surfactant.

Fluorescence Probing of Mixed-Surfactant Adsorbed Layers

As reported earlier, fluorescence spectroscopy could not be conducted at the kaolinite-water interface because kaolinite quenched the fluorescence signal from pyrene. Instead, fluorescence probing of the adsorbed layer was performed for adsorption on alumina.

In earlier studies reported, pyrene monomer fluorescence was used to describe the micropolarity of the adsorbed layer. In addition to monomer fluorescence, another aspect of pyrene fluorescence (viz., excimer formation) can be exploited to determine the size of surfactant aggregates (micelles, hemimicelles, etc). An excimer is formed when a pyrene molecule in its excited state (P^*) interacts with a pyrene molecule in its ground state (P) according to the reaction



The excimer formed (PP^*) decays to the ground state by emitting a photon



In the presence of pyrene molecules in a fragmented media (such as when surfactant micelles, hemi-micelles, etc., are present), the decay of pyrene fluorescence can be fitted to the following model¹ on the basis of a Poisson distribution of probes in surfactant (or hydrophobic) aggregates:

$$I_t = I_0 \exp \{-k_o \cdot t + n [\exp(-k_e \cdot t) - 1]\} \quad (3)$$

where I_0 = fluorescence emission intensity at the desired wavelength at time $t = 0$

k_o = monomer decay rate constant

k_e = excimer formation rate constant

n = average number of pyrene molecules in a surfactant aggregate

At long times, there is no excimer formation, and the fluorescence decay profiles represent the decay caused by monomeric emission. Therefore Eq. 3 reduces to

$$\ln \left(\frac{I_t}{I_0} \right) = -n - k_o \cdot t \quad (4)$$

and extrapolation to $t=0$ gives n . With a knowledge of n , the aggregation number of the hydrophobic aggregate in which the pyrene molecules reside can be evaluated from the following:

$$N_{agg} = \frac{n \cdot [C_i - CMC]}{[Py]} \quad \text{for micelles} \quad (5)$$

$$= \frac{n \cdot [C_i - C_r]}{[Py]} \quad \text{for adsorbed layer}$$

where C_i = initial total surfactant concentration

CMC = critical micelle concentration

$[Py]$ = pyrene concentration

C_r = total residual surfactant concentration

With the use of this procedure, the aggregation number of a 1:1 SDS- $C_{12}EO_8$ -mixed adsorbed layer was determined, and the numbers so obtained are reported in Fig. 5 along the adsorption isotherms. As shown for SDS adsorption, the aggregation number initially increases and then remains relatively constant in region II. These results are similar to those obtained by Chandar et al.²

The aggregation number for the adsorption of a 1:1 SDS- $C_{12}EO_8$ mixture is larger than that for pure SDS adsorption at a similar adsorption density. As shown in Table 1, the aggregation number for a 1:1 SDS- $C_{12}EO_8$ micelle is larger than that for SDS micelles. Clearly, the reduction in electrostatic repulsion between SDS ions as the result of the presence of the nonionic $C_{12}EO_8$ is an important reason for the observed increase in the aggregation number for 1:1 SDS- $C_{12}EO_8$ mixtures in the adsorbed layer or in micelles. As a result of screening of electrostatic repulsion, the adsorption of SDS should be energetically enhanced. This is indeed seen from Fig. 6.

Because the mixed aggregates consist of both the anionic SDS and the nonionic $C_{12}EO_8$, the aggregation number for each surfactant in the mixed aggregates can be determined if the adsorption density of each component in the mixed adsorbed layer is known. As shown in Table 2, at low adsorption densities, the aggregation number of the nonionic $C_{12}EO_8$ species is lower than that of the anionic SDS. As the adsorption increases, however, the hydrophobic chain-chain interaction becomes more important, and the aggregation numbers of each surfactant become similar.

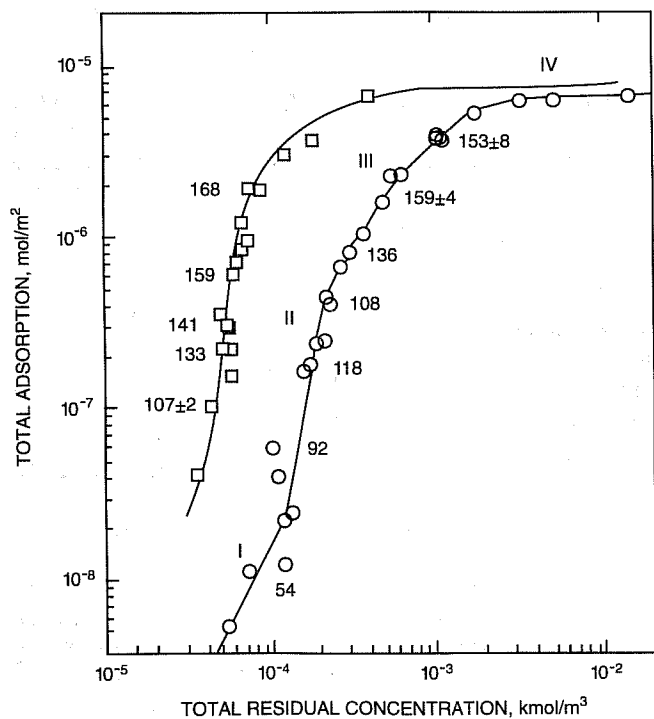


Fig. 5 Total adsorption of sodium dodecyl sulfate (SDS) and 1:1 SDS- $C_{12}EO_8$ mixtures on alumina and aggregation numbers of surfactant. Roman numerals indicate regions.

TABLE 1

Aggregation Number (N_{agg}) of Surfactant Micelles, 0.03M NaCl, 25 °C

Surfactant	Concentration, kmol/m ³	k_{d0} *, n/s	k_{e0} *, n/s	n^*	N_{agg}
Sodium dodecyl sulfate (SDS)	8.0×10^{-2}	0.0064	0.024	0.88	91
Octaethylene glycol mono <i>n</i> -decyl ether ($C_{12}EO_8$)	2×10^{-3}	0.0059	0.015	0.53	109 ± 9
1:1 SDS- $C_{12}EO_8$	8.6×10^{-3}	0.0066	0.012	0.84	165 ± 3

* k_{d0} , monomer decay rate constant; k_{e0} , excimer formation rate constant; and n , average number of pyrene molecules in a surfactant aggregate.

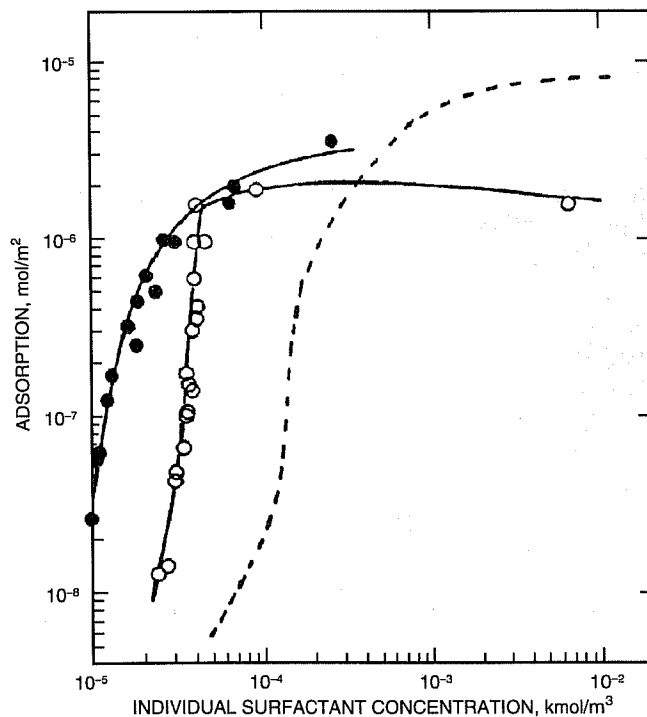


Fig. 6 Isotherms for individual surfactant adsorption on alumina from 1:1 SDS (●)- $C_{12}EO_8$ (○) mixtures. ---, 100% SDS.

Note that the aggregation number for SDS in the mixed adsorbed layer is lower than that for pure SDS adsorption. This can be explained if the surface heterogeneity is considered. Because the surface consists of energetic patches³ for SDS adsorption and the nonionic $C_{12}EO_8$ does not adsorb on alumina by itself, the aggregate size should be largely limited by the finite size of the energetic patches for SDS adsorption. In the case of 1:1 SDS- $C_{12}EO_8$ adsorption, part of the SDS ions will be displaced by the nonionic $C_{12}EO_8$ to reduce electrostatic repulsion between the SDS ions; the aggregation number of SDS is decreased.

TABLE 2

**Surfactant Aggregation Number (N_{agg}) for the Adsorption of 1:1
SDS- $C_{12}EO_8$ Mixture on Alumina, 0.03M NaCl, pH 6.5, 25 °C**

Adsorption, kmol/m ³	Surfactant- pyrene	k_o ,* n/s	k_e ,* n/s	n *	SDS	N_{agg} , $C_{12}EO_8$	Total
1.1×10^{-7}	157	0.015	0.18	0.68	61	46	107
2.3×10^{-7}	173	0.013	0.055	0.77	72	61	133
3.2×10^{-7}	179	0.01	0.015	0.79	74	67	141
6.2×10^{-7}	187	0.0079	0.011	1.60	82	77	158
1.9×10^{-6}	194	0.0071	0.0055	0.86	85	83	168

* K_o , monomer decay rate constant; k_e , excimer formation rate constant; and n , average number of pyrene molecules in a surfactant aggregate.

Adsorption-Desorption of Cationic Surfactant at the Alumina-Water Interface

Studies conducted during the first year indicated that cationic TTAC adsorbed significantly at the alumina-water interface when the alumina was negatively charged. Adsorption was found to be completely reversible at the high adsorption densities, but at lower adsorption densities, there appeared to be some hysteresis. Fluorescence spectroscopy was used during this quarter to probe the adsorbed layer and changes therein during desorption.

As mentioned in previous quarterly reports, pyrene monomer fluorescence is sensitive to the medium in which pyrene resides. The ratio of the intensities of the first and third peaks (I_3/I_1) on a pyrene emission spectrum is higher in hydrophobic environments than in a hydrophilic environment. The value for I_3/I_1 is 0.5 to 0.6 in water, 0.8 to 0.9 in surfactant micelles, and greater than 1 in nonpolar solvents. Because this ratio can be used to characterize the polarity of environments, it can be termed as the *polarity parameter*.

The adsorption isotherm of TTAC on alumina is shown in Fig. 7. Changes in the polarity parameter of pyrene at the alumina-water interface and in the supernatant are also shown in the figure. It is observed that pyrene goes to the alumina-water interface in a narrow TTAC concentration range that corresponds to a sharp increase in adsorption on the adsorption isotherm. From this, it is evident that pyrene is solubilized in TTAC aggregates at the alumina-water interface. Once TTAC micelles form in the supernatant, however, pyrene is preferentially solubilized into the micelles and does not go to the alumina-water interface in spite of the presence of TTAC hemi-micelles. This result is interesting considering that in the alumina-SDS system pyrene is preferentially solubilized in hemi-micelles at the alumina-water interface rather than SDS micelles in the supernatant.⁴ Aggregates of TTAC at the alumina-water interface are not as tightly packed, and pyrene resides in micelles once they are formed.

Supernatant solutions of varying residual concentrations along the isotherm were diluted with pyrene solution of the

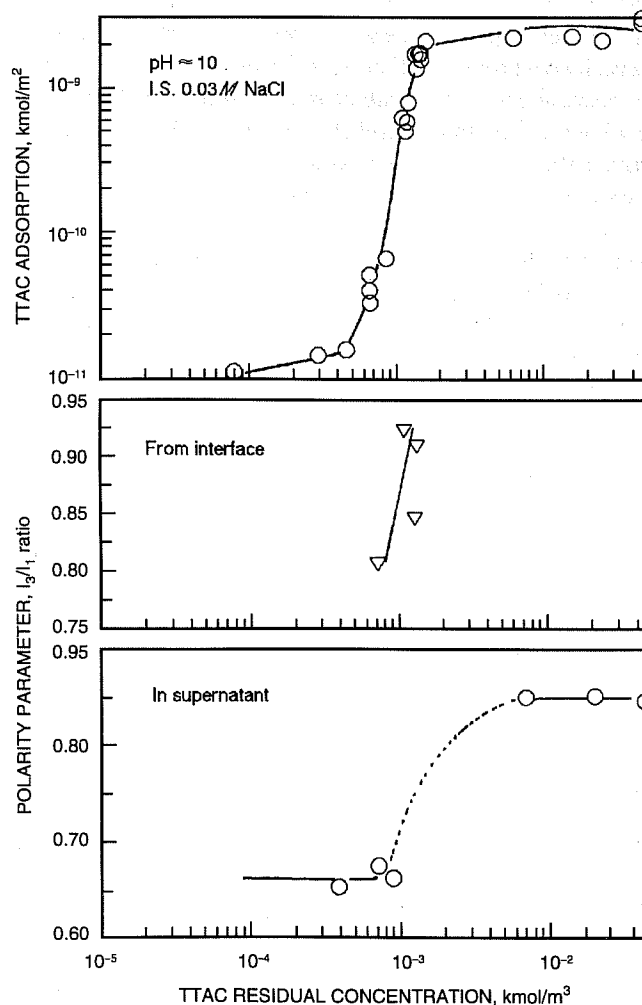


Fig. 7 Adsorption isotherm of tetradecyl trimethyl ammonium chloride (TTAC) on alumina and corresponding changes in pyrene monomer fluorescence from alumina-water interface and supernatant.

desired ionic strength and the slurry conditioned for 15 h. The procedure was repeated several times. Pyrene emission spectra were then obtained from the alumina-water interface

to gain an insight into the microstructural changes of the adsorbed layer upon dilution. The results are plotted in Fig. 8 along with the polarity parameter for pyrene dissolved in TTAC solutions of similar concentrations. Pyrene reports the presence of hydrophobic aggregate at the alumina-water interface. The value of the I_3/I_1 ratio decreases at lower concentrations, but hydrophobic aggregates are detected at concentrations lower than those detected during adsorption (see Fig. 7). Note that there will be some contribution to the spectrum obtained from the slurry by pyrene in the supernatant. For the residual concentrations studied, however, there should be no aggregates in solution, as is evidenced from the results in Fig. 8. Aggregates form in solution only above a concentration of 1.5×10^{-3} kmol/m³. Thus the hydrophobic environment reported by pyrene must be from the interface.

The adsorption of TTAC on alumina is not completely reversible, especially at the lower concentrations. The fluorescence spectroscopy studies provide support to the results from adsorption and electrokinetics reported previously. This aspect merits further investigation.

Future Work

Research in future project periods will focus on (1) adsorption of surfactant mixtures at the alumina-water interface, (2) calorimetry, and (3) effect of ethylene oxide chain length of C_nEO_n on SDS-C_nEO_n mixture adsorption.

References

1. R. Zana, in *Surfactant Solutions: New Methods of Investigation*, Surfactant Science Series, R. Zana (Ed.), Vol. 22, Marcel Dekker, New York, 1987.
2. P. Chandar, P. Somasundaran, and N. J. Turro, *J. Colloid Interface Sci.*, 117: 31 (1987).
3. J. H. Harwell, J. C. Hoskins, R. S. Schechter, and W. H. Wade, *Langmuir*, 1: 251 (1985).
4. Prem Chandar, D.E.S. Thesis, Columbia University, New York, 1987.

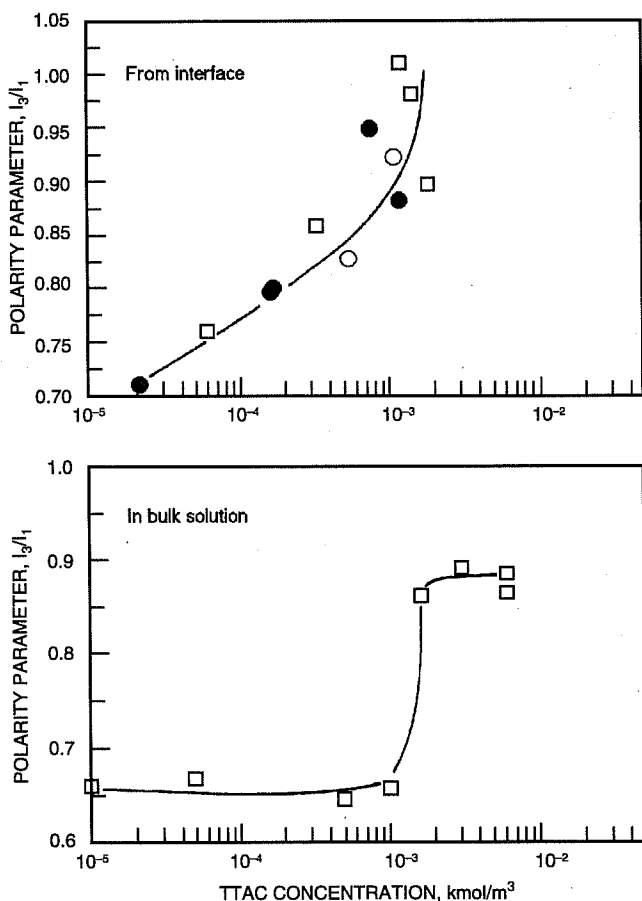


Fig. 8 Changes in pyrene polarity parameter from the tetradecyl trimethyl ammonium chloride (TTAC) adsorbed layer on alumina upon desorption from different residual concentrations (C_r) and in TTAC solutions. □, C_r , 0.0472. ●, C_r , 0.0013. ○, C_r , 0.001.

SURFACTANT-ENHANCED ALKALINE FLOODING FOR LIGHT OIL RECOVERY

Contract No. DE-AC22-92BC14883

Illinois Institute of Technology
Chicago, Ill.

Contract Date: Sept. 21, 1992
Anticipated Completion: Sept. 20, 1995
Government Award: \$150,000
(Current year)

Principal Investigator:
Darsh T. Wasan

Project Manager:
Jerry Casteel
Bartlesville Project Office

Reporting Period: Oct. 1–Dec. 31, 1993

Objective

The overall objective of this project is to develop a cost-effective method for formulating a successful surfactant-enhanced alkaline flood by appropriately choosing mixed alkalis which form inexpensive buffers to obtain the desired pH (between 8.5 and 12.0) for ultimate spontaneous emulsification and ultralow tension. In addition, the novel concept of pH gradient design to optimize floodwater conditions will be tested.

Summary of Technical Progress

The interfacial behavior of two different crude oils, one with a low acid number (Adena) and one with a high acid number (Long Beach), was previously compared.¹ The Adena crude oil has transient interfacial tensions (IFT's) on the order of 0.1 mN/m, and the minimum in IFT occurs at a short time of 100 s. The low acid number of Adena oil does not prevent sufficient interfacial activity. Sufficient interfacial activity occurs at a high pH of 13. A second minimum was found to occur at longer times. This second minimum results from the formation of middle phase.

The phase behavior and the regions wherein the middle phase occurs were investigated. Middle phase was found to go through a maximum with pH, sodium concentration, and surfactant concentration. The optimum pH is about 12.0 to 13.5, the optimum sodium concentration is about 0.513 mol/L, and the optimum surfactant concentration is about 0.2%. The effect of surfactant type was also investigated. Petrostep B-105 was found to give the most middle phase production. A white precipitate was observed in some two-phase samples.

Materials and Experiments

In this study, the crude oil (Adena) used was obtained from SURTEK from Adena field located in Morgan County, Colo. The oil is a light oil with an API gravity of 41.95, a viscosity of 3.75 cP at 25 °C, and an acid number less than 0.002. The IFT against deionized water is 39 mN/m.

The alkaline solutions are a mixture of sodium hydroxide, sodium bicarbonate, and sodium chloride. All alkalis were obtained from Fisher Scientific Co.

The preformed surfactants Petrostep B-100 (PB100), B-105 (PB105), and B-120 (PB120) were added to the alkaline solution. The surfactants were obtained from Stepan Chemical Co., and the surfactant solutions were made on a 100% basis.

The spinning-drop technique was used to measure transient (non-equilibrated) IFT. The volumetric ratio of water to oil in the spinning-drop tensiometer is about .140. An Orion microprocessor analyzer/901 with a Ross combination electrode designed for low-sodium error was used to measure the pH. All experiments were performed at 25 °C.

Throughout this study, the solutions were made by diluting an equimolar ratio of sodium bicarbonate/sodium hydroxide (NaOH) (referred to as 20/20) with either the same molarity of sodium bicarbonate plus sodium chloride (NaCl) to keep the total sodium constant or the same molarity of NaOH plus enough NaCl to keep the total sodium constant. By changing the ratio of sodium bicarbonate/NaOH, the pH is changed. Lower pH is obtained by adding the sodium bicarbonate plus NaCl solution to the 20/20 mixture, or a higher pH is obtained by adding the NaOH plus NaCl solution to the 20/20 mixture. It should be noted that 343 mol/m³ total sodium is about 2.0 wt % sodium bicarbonate/NaOH mixture.

Petrostep B-105

In the first system (0.513M with 0.1% PB105), a middle phase was observed at a pH of 11.34. The volume of middle phase increased with pH, and was a maximum at pH=12.9. In the 0.2% PB105, the middle-phase formation was observed at pHs of 12.9 and above, and was maximum at pHs of 13.13 and 13.24. The largest volume of middle phase in the whole study was observed for pH=13.13, 0.513M sodium, and 0.2% PB105. When the surfactant was increased to 0.5% PB105, only a white precipitate was observed at the interface.

At salinities lower than 0.513M sodium, a white precipitate is present at the interface. This was observed for the following systems: (1) 0.171M sodium with 0.1, 0.2, and 0.5% PB105, and (2) 0.343M sodium with 0.1% PB105 (at pH<12.9), 0.2% PB105, and 0.5% PB105. Some middle-phase formation, although of very small volume, was observed for high pH solutions (above 12.9) with 0.343M sodium and 0.1% PB105.

In general, solutions with salinities ranging from 0.171M to 0.513M exhibited cloudy aqueous phases, indicating some oil-in-water emulsions, and the cloudiness of the aqueous phase increased with pH.

At salinities higher than 0.513M sodium, the aqueous phase was clear (although of brownish color), some cloudiness appeared with increasing pH, and a precipitate was observed in most cases. The volume of precipitate increased with pH until it reached a maximum and decreased at higher pHs. For the 0.684M sodium solutions, the volume of precipitate at the interface was maximum at pH=13.31 with 0.1% PB105, between pH=13.07 and 13.27 for 0.2% PB105, and between pH=12.63 and 13.21 for 0.5% PB105. Therefore the maximum volume of precipitate occurs at lower pH when the surfactant concentration is increased.

For 1.0M sodium with 0.1% PB105, only a white precipitate was present at the interface.

Petrostep B-100

Only systems with salinities up to 0.343M sodium were equilibrated with Adena oil because the surfactant precipitated in the bulk solution (before contacting with the oil) at higher salinities.

Systems with 0.171M sodium and 0.1% PB100 exhibited a white precipitate of volume increasing with pH. Middle phase is seen at pH values from 11.07 to 12.8 with 0.2 and 0.5% PB100.

The aqueous phase was opaque but of a light yellow color. Cloudiness of the aqueous phase was found to decrease with increasing pH and became translucent at pH values above 12.7; it darkened in color with an increase in surfactant concentration.

Systems with 0.343M sodium and 0.1% PB100 have a white precipitate at the interface. The volume of this precipitate remains constant with increase in pH.

Petrostep B-120

This surfactant does not exhibit any middle-phase formation or precipitate formation. It shows no interfacial activity as seen by visual observation.

Volume of Middle Phase

Table 1 shows the volume of the middle phase as a function of sodium and surfactant concentration at a pH of 13.1 for PB105 surfactant. The volume of the middle phase goes through a maximum with both sodium concentration and surfactant concentration.

Figure 1 shows a three-dimensional (3-D) graph of the combined effects of pH and salinity on the phase behavior of the Adena oil for 0.2% PB105. The volume of the middle phase is plotted on the vertical axis. Each series of bars in the horizontal direction corresponds to a particular pH. At pH=13.1, the volume of the middle phase reaches a sharp maximum at 0.513M sodium. As the pH is decreased, less middle phase is produced, and the maximum volume is shifted to lower salinities. At 0.513M sodium, as the pH is increased from 12.6 to 13.1, the volume of the middle phase sharply increases. Little or no middle phase is found below pH of 12.6.

Figure 2 is the transient IFT as a function of pH. There is a direct one-to-one correlation between middle-phase formation and IFT. The IFT is ultralow when the middle phase is present.

TABLE 1

Volume of Middle Phase at pH=13.1

Sample	Salinity, M [Na]	PB105, wt %	Volume middle phase, mL	Middle phase, % total volume
12	0.343	0.1	0.85	5
16b	0.513	0.1	1.7	8.5
92	0.684	0.1	0.2	1
109	1.0	0.1	0.3	1.5
28	0.343	0.2	0.3	1.5
33	0.513	0.2	2.7	13.5
98	0.684	0.2	0.3	1.5
45	0.343	0.5	0	0
50	0.513	0.5	0.2	1
104	0.684	0.5	1	5

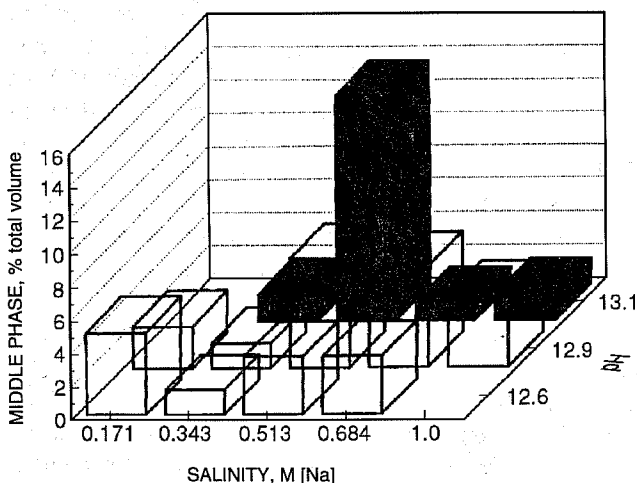


Fig. 1 Volume of middle phase at 0.2% Petrostep B-105.

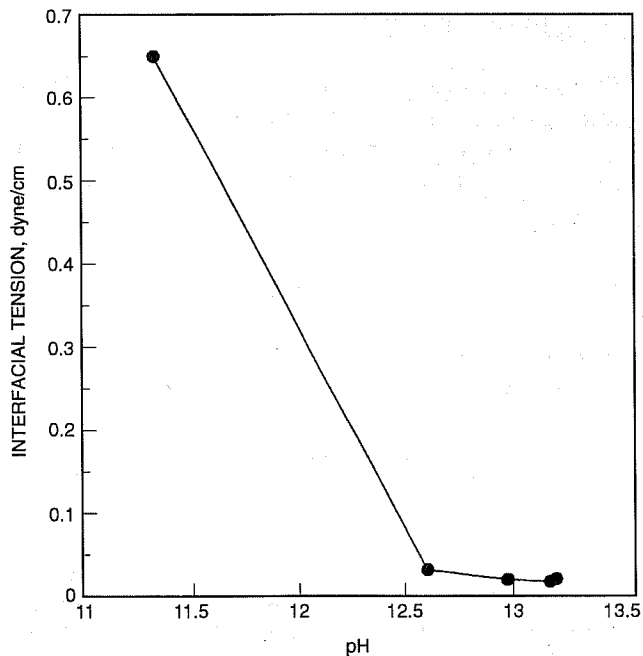


Fig. 2 Transient interfacial tension as a function of pH. 0.513M sodium, 0.2% Petrostep B-105 Adena oil.

Figure 3 is a 3-D graph showing the combined effects of sodium and surfactant concentration on the volume of the middle phase at a pH of 13.1 with PB105. Each type of shading corresponds to a particular salinity. At 0.1% PB105, a maximum occurs in the volume of the middle phase at a salinity of 0.513M sodium. A sharper maximum of the middle phase is observed at that salinity when the surfactant concentration is increased to 0.2%. As more surfactant is added, the maximum is shifted to higher salinity and is of lesser extent.

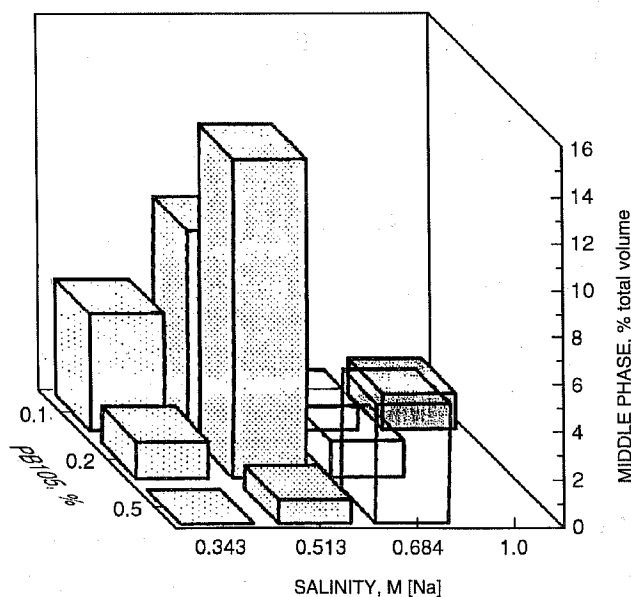


Fig. 3 Volume of middle phase at pH=13.1.

Conclusions

For a given surfactant concentration, as pH is increased, the maximum volume of the middle phase shifts to higher salinities. For a given pH, as surfactant concentration is increased, the maximum volume of the middle phase shifts to higher salinities.

Reference

1. D. T. Wasan, Surfactant-Enhanced Alkaline Flooding for Light Oil Recovery, Progress Report submitted to DOE for the Period July 1–Sept. 30, 1993.

RESPONSIVE COPOLYMERS FOR ENHANCED PETROLEUM RECOVERY

Contract No. DE-AC22-92BC14882

University of Southern Mississippi
Hattiesburg, Miss.

Contract Date: Sept. 22, 1992

Anticipated Completion: Sept. 21, 1995

Government Award: \$273,400

(Current year)

Principal Investigators:

Charles McCormick
Roger Hester

Project Manager:

Jerry Casteel
Bartlesville Project Office

Reporting Period: Oct. 1–Dec. 31, 1993

Objective

The objective of this research is the development of advanced water-soluble copolymers for use in enhanced oil recovery (EOR) that rely on reversible microheterogeneous associations for mobility control and reservoir conformance.

Summary of Technical Progress

Advanced Copolymer Synthesis

Synthetic efforts have focused on the development of ionically modified polymers based on monomers that contain an acrylamido functionality. The monomers may possess

either cationic or anionic functionality that, depending on the pH of the polymer solution, may either be ionically charged or neutral. Thus, by adjusting the pH, the degree of ionization of the polymer may be controlled, which will, in turn, influence the rheological behavior. Previous research has revealed that this behavior allows the selective synthesis of polymers operative over a wide range of conditions.^{1–5} This section describes the synthesis and solution behavior of cationic polyelectrolytes based on copolymers of acrylamide (AM) and 2-acrylamido-2-methylpropanetriethylammonium chloride (AMPTAC), and ATAM series, as well as ampholytic terpolymers of acrylamide (AM), sodium 3-acrylamido-3-methylbutanoate (NaAMB), and 2-acrylamido-2-methylpropanetriethylammonium chloride (AMPTAC), the ATABAM series. Monomers used in the ATAM and ATABAM series are shown in Fig. 1.

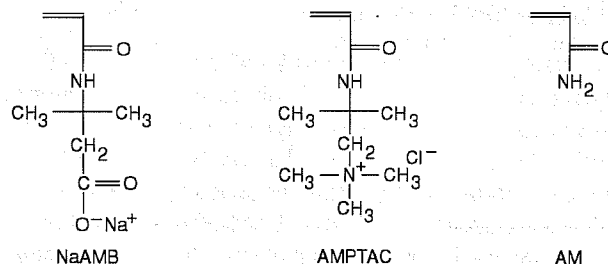


Fig. 1 Monomers used in ATAM and ATABAM series.

Monomer and Polymer Synthesis

The AMPTAC monomer was prepared by reacting 2-acrylamido-2-methylpropanedimethylamine with methyl iodide to afford [2-(acrylamido)-2-methylpropyl] trimethylammonium iodide (AMPTAI). The iodide ion was then ion-exchanged with the use of Dowex™ Cl resin to obtain the desired AMPTAC. The NaAMB monomer was synthesized via a Ritter reaction of equimolar amounts of 3,3-dimethylacrylic acid with acrylonitrile as reported by Hoke and Robins⁶ and as modified by McCormick and Blackmon.⁷ The AM from Aldrich was recrystallized from acetone. The ATAM copolymers were prepared by free radical polymerization in deionized water under nitrogen at 30 °C with the use of 0.1 mol % potassium persulfate as the initiator. The ATABAM terpolymers were prepared by free radical polymerization in a 0.5M sodium chloride (NaCl) aqueous solution under nitrogen at 30 °C with the use of 0.1 mol % potassium persulfate as the initiator. The feed ratio of AM/AMPTAC copolymers was varied from 90:10 to 50:50 mol %, whereas the feed ratio of AM/NaAMB/AMPTAC terpolymers was varied from 99:0.5:0.5 to 70:15:15 mol %. Total monomer concentration was held constant at 0.45M for all polymerizations. All polymers were dialyzed against deionized water to remove residual monomers and salts and were subsequently isolated by lyophilization.

Characterization of Molecular Structure

Elemental analyses for carbon, hydrogen, nitrogen, and sulfur were conducted by M-H-W Laboratories of Phoenix, Ariz., on the low-conversion copolymer samples. Copolymer compositions were confirmed with ^{13}C nuclear magnetic resonance (NMR) by integration of the amide carbonyl peaks. Molecular-weight studies were performed on a Chromatix KMX-6 low-angle laser-light-scattering instrument. A Chromatix KMX-16 laser differential refractometer was used to obtain refractive index increments. For quasielastic light scattering, a Langley-Ford Model LF1-64 channel digital correlator was used in conjunction with the KMX-6. All measurements were conducted at 25 °C in 1M NaCl. Polymer stock solutions were made by dissolving a specified amount of polymer in solvent and allowing it to age for 2 to 3 weeks before analyzing it with a Contraves LS-30 rheometer.

Polymer Solution Behavior

AM/AMPTAC copolymers (ATAM series). The ATAM polymers act as cationic polyelectrolytes with the reduction of intrinsic viscosities when electrolytes are added (Fig. 2). For a further demonstration of this behavior, the intrinsic viscosities were plotted as a function of the reciprocal square root of the ionic strength (Fig. 3). Only ATAM-30 exhibits the linear dependence that is typical of polyelectrolytes. The curvature of the data indicates an enhanced sensitivity to ionic strength relative to other polyelectrolytes. This may be the result of the hydrophobicity of the cationic monomer AMPTAC and the resulting site electrostatic binding of the chloride counterion (decreased dielectric constant).

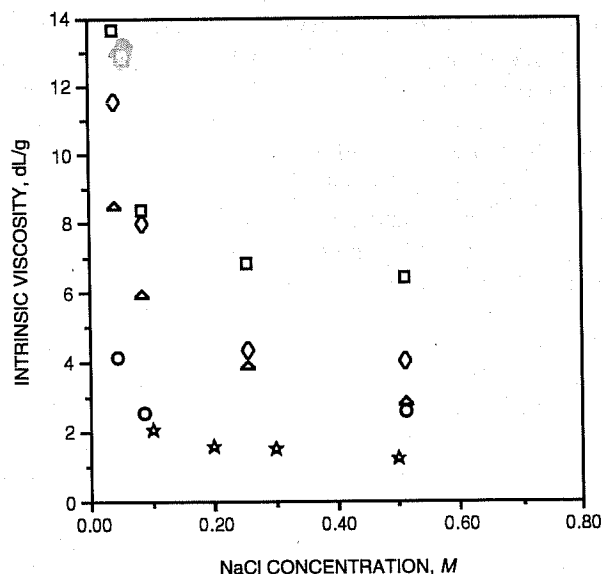


Fig. 2 Intrinsic viscosities for the ATAM copolymer series plotted as a function of NaCl concentration determined at a shear rate of 5.96 s^{-1} at 30 °C. \circ , ATAM-9. \square , ATAM-20. Δ , ATAM-30. \diamond , ATAM-50. \star , ATAM-100.

Turbidimetry. AMPTAC is designed to be a cationic monomer stable to changes in pH. An added benefit is superior phase stability. Aqueous solutions of the ATAM copolymers remain soluble to 100 °C in the presence of 3.5% sodium carbonate (Na_2CO_3). Because of the cationic nature of the ATAM polymers, divalent cations such as calcium chloride (CaCl_2) have little effect on phase behavior.

AM/NaAMB/AMPTAC terpolymers (ATABAM series). Figure 4 shows the intrinsic viscosity of a number of the terpolymers as a function of NaCl concentration. The data are indicative of classic antipolyelectrolyte behavior. Increases in solution ionic strength disrupt intramolecular ionic associations and thus produce increases in polymer hydrodynamic volume. ATABAM 10-10 undergoes a 700% increase in intrinsic viscosity, going from 0.05M to 1M NaCl. ATABAM 10-10 and 15-15, which have similar molecular weights, attain the same intrinsic viscosity in 1M NaCl.

Effects of pH. The reduced viscosities for ATABAM 10-10 obtained in neutral and acidic pH values are shown in Fig. 5. Above pH 7.5, the polymers behave as polyampholytes because all NaAMB units possess a negative charge. Intramolecular charge-charge interactions initially constrict the coils but disappear as solvent ionic strength is increased. At pH 3, the polymers behave as polyelectrolytes. The NaAMB units are protonated so that only the cationic charge of AMPTAC remains. Like typical polyelectrolytes, the coils expand in the absence of added electrolytes but collapse in their presence.

It is interesting that the dimensions of the polyelectrolyte form of ATABAM 10-10 in 1M NaCl are smaller than those of the polyampholyte form. This may be due to the relative

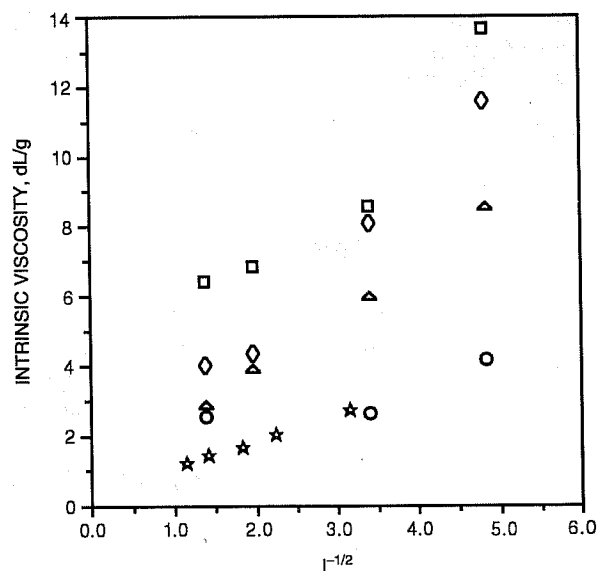


Fig. 3 Intrinsic viscosities for the ATAM copolymers plotted as a function of the inverse square root of ionic strength. \circ , ATAM-9. \square , ATAM-20. Δ , ATAM-30. \diamond , ATAM-50. \star , ATAM-100.

Characterization of Water-Soluble Polymers in Aqueous Solution by Dynamic Light Scattering

Dynamic light scattering (DLS) is a rapid and accurate method for characterizing the motions of molecules in solution. The DLS technique (sometimes referred to as intensity-fluctuation spectroscopy, Rayleigh-Brillouin spectroscopy, or quasielastic light scattering) depends on the analysis of the spectrum of light scattered from a sample solution. In a typical experiment, scattered light is frequency (Doppler) shifted from the incident laser light frequency as a result of the rotational, translational, and internal motion of the scattering species. The scattered light spectral intensity fluctuations that are monitored by photon counting are used to compute a time-based autocorrelation function. The Brookhaven Instruments Corporation DLS instrument or spectrometer used in this research is shown schematically in Fig. 6.

The autocorrelation function can yield information on macromolecular motions. These motions include translational diffusion of the polymer coil and internal chain distortions, such as chain rotation and vibration. The scattered light intensity fluctuations depend on the time scales characterizing the motions of the macromolecule. The DLS instrument can be adjusted to measure specific molecular motions by adjusting the scattering field vector.

Scattering Field Vector

The scattering field vector, q , is defined by Eq. 1:

$$q = 4 \pi n \sin\left(\frac{\theta}{2}\right) / \lambda_0 \quad (1)$$

In Eq. 1, n is the refractive index of the solution, θ is the scattering angle, and λ_0 is the radiation wavelength in vacuum. The response of the molecular chain to the scattering vector depends on the size and mobility of the polymer coils and the number of coils per volume of solution.

Too many coils per unit volume will lead to coil-coil interactions, which then scatter radiation at time scales lower than single coils. Thus the polymer concentrations in the solutions used in DLS are less than the critical concentrations characteristic of the transition from the dilute to the semi-concentrated.

Scattering Spectrum

In what is referred to as the low q region, the size of the molecular coil (the radius of gyration, R_g), is very small in comparison with distance q^{-1} , the reciprocal of the scattering vector.

$$R_g q < 1 \quad (2)$$

DLS fluctuations in this region are due to polymer coil center-of-mass motion caused by translational diffusion or undesired

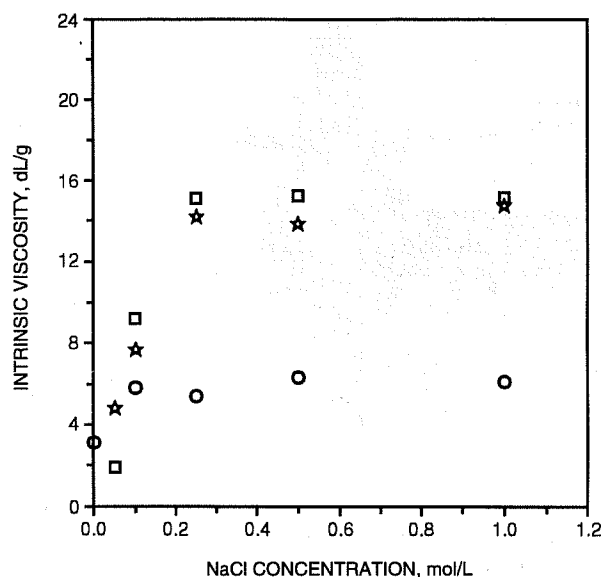


Fig. 4 Intrinsic viscosities of ATABAM 5-5, 10-10, and 15-15 plotted as a function of NaCl concentration determined at 25 °C at a shear rate of 5.96 s⁻¹. ○, ATABAM 5-5. □, ATABAM 10-10. ☆, ATABAM 15-15.

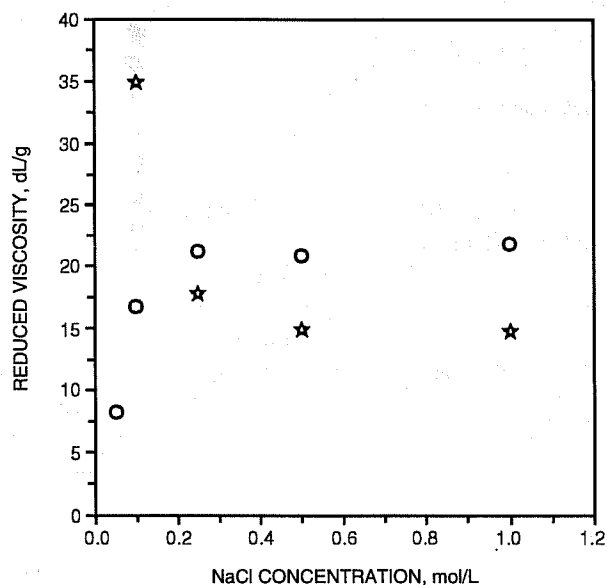


Fig. 5 Reduced viscosity for ATABAM 10-10 in the polyampholyte form (pH = 7.5) and in the polyelectrolyte form (pH = 3.0) determined with a polymer concentration of 0.10 g/dL at 25 °C at a shear rate of 5.96 s⁻¹. ○, pH 7.5. ☆, pH 3.0.

hydrophobicity of the acid form of NaAMB. For example, copolymers of NaAMB with AM precipitate from aqueous solution below pH 5. The presence of this relatively hydrophobic monomer may constrict the polymer to dimensions smaller than those of a random coil and thus produce the effect observed in Fig. 5. Also, the extent of counterion condensation may differ for the two forms at high NaCl concentrations.

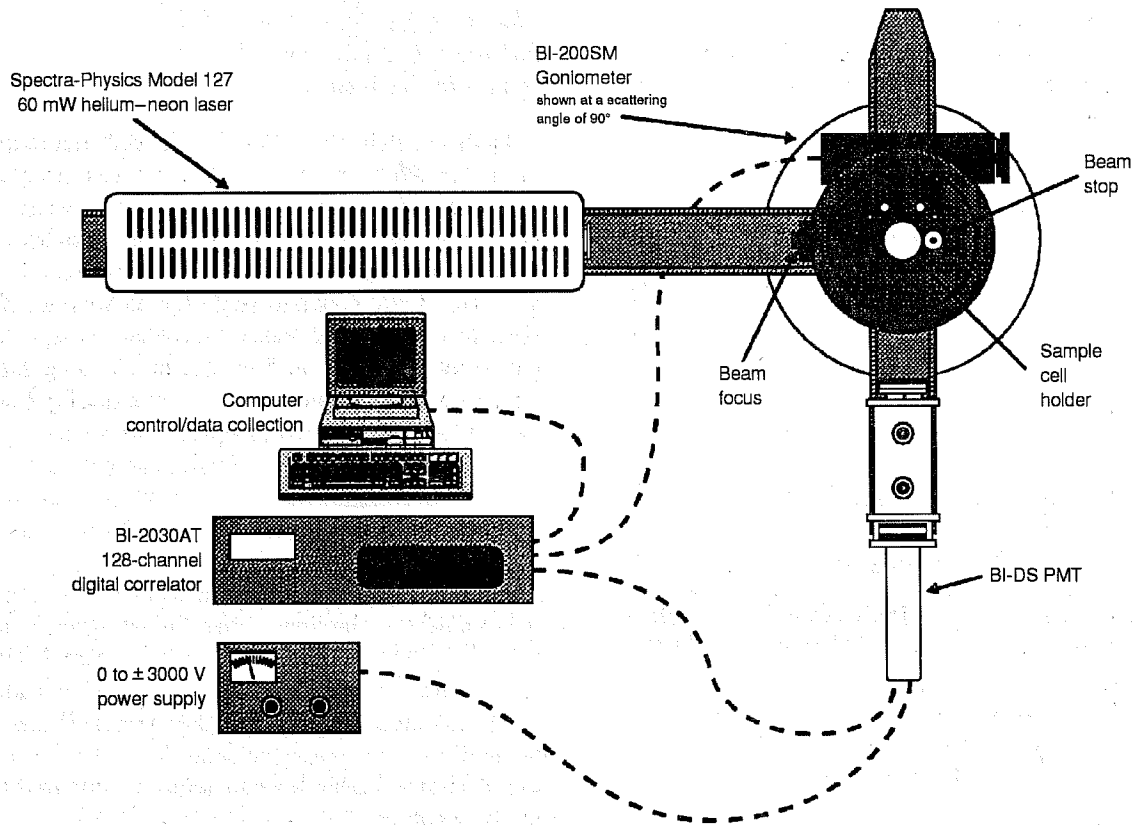


Fig. 6 Brookhaven Instruments Corporation dynamic/classical light-scattering apparatus.

bulk-fluid flow. Chain motion in this region is related to the longest molecular relaxation times, which are caused by the Brownian motions of macromolecular coils.

As the value of q is increased, additional molecular relaxation times enter into the scattering spectrum. In this region

$$R_g q > 1 \quad (3)$$

and intermolecular and intramolecular movements enter into the DLS spectrum. Fluctuations are due to internal chain distortions such as chain rotation. These motions are much faster than those caused by translational diffusion.

Fluctuation Theory

In these experiments DLS measurements are made in the low q region. These measurements can be used to find the macromolecular coil translational diffusion coefficient and coil hydrodynamic size.

An autocorrelation technique is used to analyze the small fluctuations in the scattered radiation. Mathematically, an autocorrelation function that depends upon the delay time, τ , is defined as

$$G(\tau) = \lim_{T \rightarrow \infty} \frac{1}{2T} \int_{-T}^T I(t) I(t + \tau) dt \quad (4)$$

In this relation, $I(t)$ and $I(t + \tau)$ are scattered light intensity signals that depend upon sample time, t , and the delay time between samples, τ . The autocorrelation function is a measure of the similarity between two intensities measured at time t and time $t + \tau$. Equation 4 can be approximated by measuring the instantaneous scattering intensity, n , at time intervals that are separated by an increment of time, $\Delta\tau$, and storing these data in memory channels. Thereafter these data can be summed such that the j channel at time interval i is related to the autocorrelation function as shown by Eq. 5.

$$G(\tau = j \Delta \tau) \approx \sum_{i=0}^j n_i n_{i+j} \quad (5)$$

The preceding finite sum equation, which is generated by a correlator with j channels, numerically approximates the autocorrelation function. A typical measured autocorrelation function is shown in Fig. 7.

For a system of monodispersed scattering species, the autocorrelation function is defined by a single exponential equation:

$$G(\tau) = A [\exp(-\Gamma\tau)]^2 + B \quad (6a)$$

where A = machine constant

B = signal noise or baseline correlation contribution

Γ = decay constant resulting from macromolecular motions

τ = delay time

$$R_h = \frac{\kappa T}{6\pi\eta_0 D_t^0} \quad (9)$$

In the preceding equation, κ is the Boltzman constant, T is the absolute temperature, and η_0 is the zero shear viscosity of the solvent used to make the solution of scattering species. The preceding relationship is for spherical particles but can be applied for polymer coils that are nondraining.

For random coil polymers, the hydrodynamic radius can be used to estimate the mean square radius of gyration R_g . Kirkwood and Riseman⁹ used a nondraining random coil under the condition of thermodynamic ideality (theta conditions) to develop the following equation:

$$R_g = \left(\frac{\pi (6)^{1/2}}{P} \right) R_h \quad (10)$$

An empirical relationship can be used to estimate the polymer coil draining parameter, P, at non-theta conditions.¹⁰

$$P = 5.11 [1 - 0.083(2a - 1)] \quad (11)$$

In Eq. 11, a is the Mark-Houwink equation exponent, which relates molecular weight to intrinsic viscosity.

DLS Samples Having a Distribution of Particle Sizes

When the scattering species are polydisperse in coil sizes, the autocorrelation function is defined by a distribution of exponentials. Consequently analysis of DLS scattering data must be treated with the use of a probability distribution of decay constants, $F(\Gamma)$, which is used to describe the size distribution of scattering particles. For a distribution of particles undergoing only translational diffusion, the normalized autocorrelation function, $g(\tau)$, is related to the sum of exponents by a Fredholm integral equation of the first kind.

$$g(\tau) = \int_0^\infty F(\Gamma) \exp(-\Gamma\tau) d\Gamma \quad (12)$$

The discrete form of this integral is

$$g(\tau) = \sum a_i \exp(-\Gamma_i\tau) \quad (13)$$

where $g(\tau)$ can be obtained from the DLS measured autocorrelation function $G(\tau)$.

$$g(\tau) = \frac{[G(\tau) - B]^{1/2}}{(AB)^{1/2}} \quad (14)$$

In the preceding relationships, $F(\Gamma)$ is the normalized probability distribution function of scattering particle decay constants such that

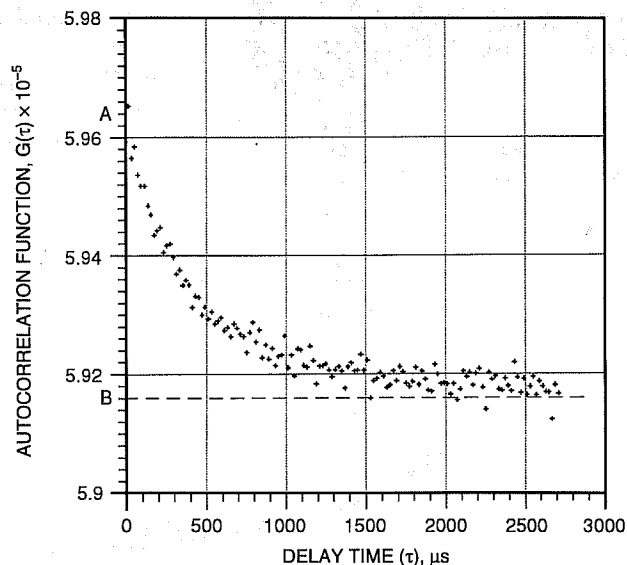


Fig. 7 Autocorrelation function for Am/AMB 85/15 copolymer in 0.514M NaCl solution.

In the low q region, the decay constant is a measure of the translational mobility of the scattering species.

Rearrangement and linearization of Eq. 6a gives

$$\ln [G(\tau) - B] = \ln [A] - 2\Gamma\tau \quad (6b)$$

Therefore the quantity of interest, Γ , can be extracted from the slope of a linear regression of $\ln [G(\tau) - B]$ vs. τ .

The translational diffusion coefficient and the decay constant Γ are related through the scattering vector.

$$D_t = q^2\Gamma \quad (7)$$

The translational diffusion coefficient in the limit of infinite sample dilution, D_t^0 , can be estimated from the measured diffusional coefficient D_t at sample concentration C with the use of relationship developed by Jamisson.⁸

$$D_t^0 = \frac{D_t}{1 + 0.58 [\eta]C} \quad (8)$$

where $[\eta]$ is the intrinsic viscosity of the sample using the same solvent as used in the DLS analysis. The samples are usually so dilute that the correction is very small.

The limiting translational diffusion coefficient, D_t^0 , is related to the hydrodynamic radius, R_h , of the scattering species. The Stoker-Einstein relationship can be used to find R_h .

$$\int_0^{\infty} F(\Gamma) d\Gamma = 1 \quad (15)$$

and a_i is the probability of particles with decay constant Γ_i .

Equation 12 was derived under the conditions that (1) no interactions exist between scatters, (2) intramolecular motions have not been measured by the autocorrelation function, and (3) the polarizability per unit scattering mass is independent of the total scattering mass.

The Fredholm integral or finite sum equation must be solved for the probability distribution of decay constants. This solution is not trivial.

Solution of the Fredholm Integral

The Fredholm integral or sum equation is ill-conditioned. Solutions to ill-conditioned equations are difficult to obtain because, in general, many solutions are possible within the constraints of the system. Thus, for even small noise in the scattering data, a large set of solutions exist within the noise level. In addition, the solutions in this set can significantly differ from each other.

The principle of parsimony is used to find a solution to an ill-conditioned equation. The principle of parsimony states that, of all the distribution solutions that have not been eliminated by constraints, choose the simplest one. The simplest distribution solution is the one that reveals the least amount of detail or information that was not already known or expected.

The most parsimonious distribution solutions in order of simplicity are monodisperse, smooth and unimodal, unimodal but with shoulder, smooth and bimodal, etc. The simplest solution is almost certainly not the true solution but probably contains the least artifacts. Several methods have been used to find a distribution solution to the autocorrelation function. The most used numerical solutions of the Fredholm integral equation include the cumulants method and the Laplace transformation method using data filtering and smoothing.

Cumulants Method

The method of cumulants provides a measure of the distribution width for polydisperse scattering systems.¹¹ The logarithm of the normalized autocorrelation function can be expressed as a power series in delay time

$$\ln [(AB)^{1/2} g(\tau)] = \ln (AB)^{1/2} - \mu_1 \tau + \frac{1}{2} \mu_2 \tau^2 - \frac{1}{6} \mu_3 \tau^3 + \dots \quad (16)$$

where $\mu_1, \mu_2, \mu_3, \dots$ = 1st, 2nd, and 3rd cumulants
 μ_1 = mean decay constant of the $F(\Gamma)$ distribution
 μ_2 = variance of $F(\Gamma)$ distribution function
 $\mu_3/\mu^{3/2}$ = skewness of $F(\Gamma)$ distribution

The series can be rearranged to give

$$\ln \left[\frac{G(\tau)}{B} - 1 \right] = \ln A - 2\mu_1 \tau + \mu_2 \tau^2 - 1/3 \mu_3 \tau^3 \dots \quad (17)$$

If only the first two right terms of Eq. 17 are used, then a linear regression of $\ln \{ [G(\tau)/B] - 1 \}$ vs. τ data can be used to find an average Γ . Figure 8 shows a typical plot of these data and the multilinear regression fit line to the data. The average gamma value can be used to find the sample average diffusional coefficient (see Eq. 7) and the sample average hydrodynamic size, R_h (see Eq. 9).

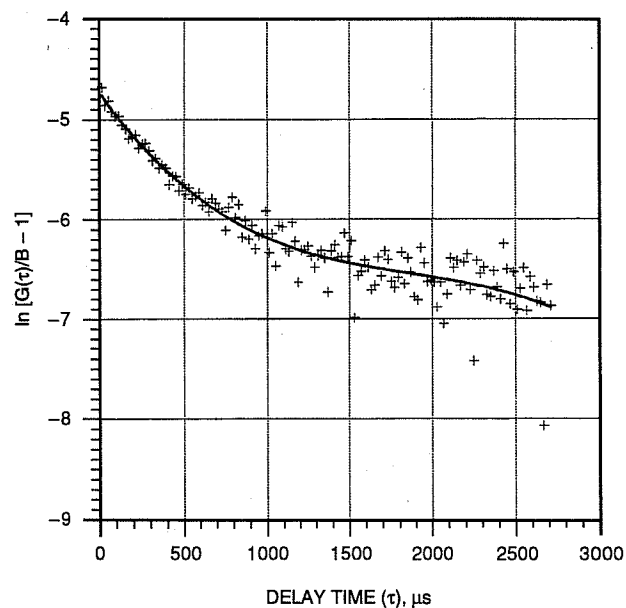


Fig. 8 Cumulants analysis of the polymer system DLS data shown in Fig. 7. Instrument constant, 8.74×10^{-3} ; mean gamma, 1.185×10^{-3} ; standard deviation, 1.062×10^{-3} (1/ μ s); and skewness, 5.03×10^{-3} .

Contin Method

In this method a histogram distribution of scattering species is generated which best fits the measured Fredholm integral equation with the use of reasonable restrictions. Provencher used a smoothness of species distribution restriction together with a non-negative constraint to generate an estimated histogram of the expected sample size distribution.¹² This analysis is often referred to as the Contin method. Smoothness is assured by forcing the solution to have a species distribution that has a minimum third derivative of species concentration with respect to species size. Also, the solution is forced to have no negative concentration of species. The Contin method is routinely used to estimate the size distribution of polymer samples analyzed by DLS. Figure 9 shows a bimodal distribution solution generated by Contin technique.

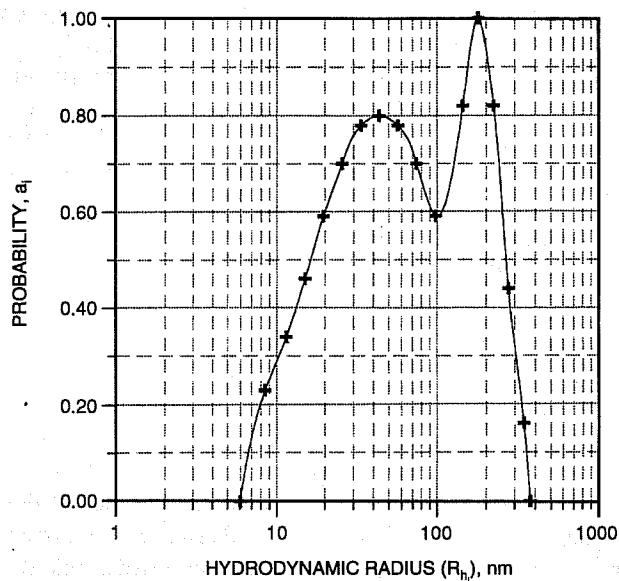


Fig. 9 Contin analysis of DLS data shown in Fig. 7.

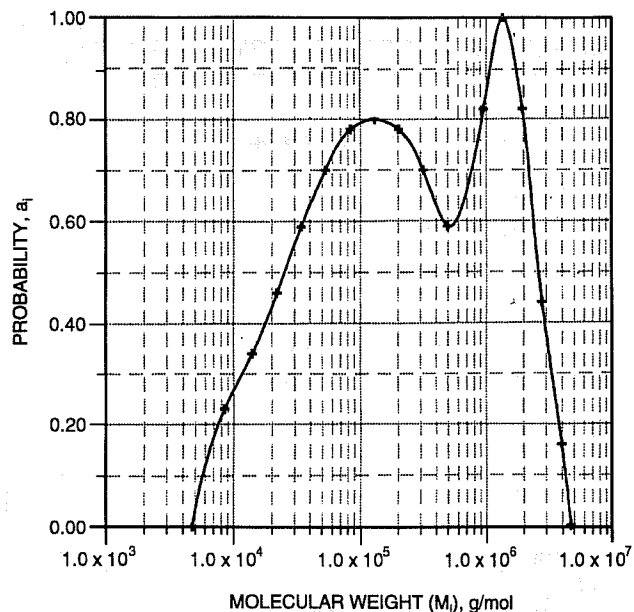


Fig. 10 Molecular-weight analysis of the data shown in Fig. 9. η , KM^a ; K , $6.31 \times 10^{-5} \text{ dL/g}$; $a = 0.80$; M_n , 0.73×10^6 (number average molecular weight); M_w , 1.90×10^6 (weight average molecular weight).

Molecular Weight from DLS Hydrodynamic Diameter Measurements

The hydrodynamic radius, R_h , is related to polymer coil molecular weight, M , by the following relationship:

$$M = \Phi \left(\frac{6\pi}{P} \right)^3 \frac{R_h^3}{[\eta]} \quad (18)$$

where P is the dimensionless draining parameter (see Eq. 11), $[\eta]$ is the intrinsic viscosity of the polymer, and Φ is the Flory constant equal to $2.07 \times 10^{21} \text{ mol}^{-1}$. Because R_h is a Z average radius, then the molecular weight calculated would also be close to the Z average molecular weight of a polydispersed polymer sample. Equation 18 can be used to estimate a sample molecular-weight distribution from the gamma probability distribution $F(\Gamma)$ generated by the Contin analysis of the DLS data.¹³ To perform this operation, the variation of intrinsic viscosity with respect to molecular weight must be used with Eq. 18. Usually the relationship is expressed by a Mark-Houwink equation

$$[\eta] = KM^a \quad (19)$$

where K and a values are parameters that depend upon polymer and solvent.

Equations 18 and 19 can be used to show that the molecular weight of the i th distribution element, M_i , having probability a_i is given by

$$M_i = \left[\left(\frac{\Phi}{K} \right) \left(\frac{\kappa T}{P\eta_0 q^2} \right)^3 \frac{1}{\Gamma_i^3} \right]^{1/1+a} \quad (20)$$

A typical plot of a_i vs. M_i is shown in Fig. 10.

References

1. C. L. McCormick and C. B. Johnson, *Macromolecules*, 21: 686 (1988).
2. C. L. McCormick and C. B. Johnson, *Macromolecules*, 21: 694 (1988).
3. C. L. McCormick and C. B. Johnson, *Polymer*, 31: 1100 (1990).
4. C. L. McCormick and C. B. Johnson, *Macromol. Sci., Chem.*, A27(5): 539 (1990).
5. C. L. McCormick and C. B. Johnson, *Polymer*, 31: 1100 (1990).
6. D. Hoke and R. Robins, *J. Polym. Sci.*, 10: 3311 (1971).
7. C. L. McCormick and K. P. Blackmon, *J. Polym. Sci., Part A: Polym. Chem.*, 24: 2635 (1986).
8. M. P. Patricia and A. M. Jamisson, Molecular Weight Scaling of the Transport Properties of Polyacrylamide in Water, *Macromolecules*, 18(2): 266-272 (1985).
9. J. G. Kirkwood and J. Riseman, *J. Chem. Phys.*, 16: 565 (1948).
10. O. B. Pitsyn and Y. E. Eizner, *Zh. Teth. Giz.*, 29: 117 (1959).
11. D. E. Koppel, Analysis of Macromolecular Polydispersity in Intensity Correlation Spectroscopy: The Method of Cumulants, *J. Chem. Phys.*, 57(11): 4814-4820 (1972).
12. S. W. Provencher, A Constrained Regularization Method for Inverting Data Represented by Linear Algebraic or Integral Equations, *Comput. Phys. Commun.*, 27: 213-227 (1982).
13. J. C. Selser, A Determination of Polymer Number-Averaged and Weight-Averaged Molecular Weight Using Photon Correlation Spectroscopy, *Macromolecules*, 12(5): 909-916 (1979).

IMPROVING RESERVOIR CONFORMANCE USING GELLED POLYMER SYSTEMS

Contract No. DE-AC22-92BC14881

University of Kansas
Center for Research
Lawrence, Kans.

Contract Date: Sept. 25, 1992
Anticipated Completion: Sept. 24, 1995
Government Award: \$707,123

Principal Investigator:
Don W. Green
G. Paul Willhite

Project Manager:
Jerry Casteel
Bartlesville Project Office

Reporting Period: Oct. 1–Dec. 31, 1993

Objectives

The general objectives are to (1) identify and develop gelled polymer systems that have potential to improve reservoir conformance of fluid displacement processes, (2) determine the performance of these systems in bulk and in porous media, and (3) develop methods to predict the capability of these systems to recover oil from petroleum reservoirs.

This work focuses on three types of gel systems—an aqueous polysaccharide (KUSP1) system that gels as a function of pH, the chromium(III)–polyacrylamide system, and the aluminum citrate–polyacrylamide system. Laboratory research is directed at the fundamental understanding of the physics and chemistry of the gelation process in bulk form and in porous media. This knowledge will be used to develop conceptual and mathematical models of the gelation process. Mathematical models will then be extended to predict the performance of gelled polymer treatments in oil reservoirs.

Summary of Technical Progress

Development and Selection of Gelled Polymer Systems

Development of KUSP1 and Derivatives

The degree of polymerization of KUSP1 was determined previously by a modification of a colorimetric arsenomolybdate method.¹ This method was limited by the insolubility of KUSP1. An alternate method was identified

for determination of the number of reducing groups on KUSP1, which is used to determine the degree of polymerization. This new method, which was developed for protein assays and employs the Pierce BCA reagent, can be performed at alkaline conditions where KUSP1 is soluble. This method is being used to reexamine the effects of growth conditions of *Cellulomonas flavigena* upon the synthesis of KUSP1 and further to investigate whether alkaline extraction of the polymer from encapsulated cells results in chemical modification of KUSP1.

Physical and Chemical Characterization of Gel Systems

Rheological Characterization

A study was initiated on the effect of shear on the gelation of a polyacrylamide–chromium(III) system. The gel system was subjected to steady shear with a superimposed oscillatory shear on a Weissenberg rheometer. This parallel superimposition experiment allows for the determination of the storage modulus (and other linear viscoelastic properties) concurrently with the shear viscosity.

Results of two experiments conducted at a net steady shear rate of 7.47 s^{-1} and at an oscillatory frequency of 1.0 Hz and an oscillatory strain of 0.5 are shown in Fig. 1. Included in Fig. 1 are the moduli-time data for the same experiment using only oscillatory shear (zero steady shear). For the samples subjected to a steady shear of 7.47 s^{-1} , the data appear curious but are reproducible. Application of steady shear significantly affects the gelation as characterized by the development of the storage modulus (G') with time. Future plans include the acquisition of data at other selected steady shear rates and analyzing and interpreting the data.

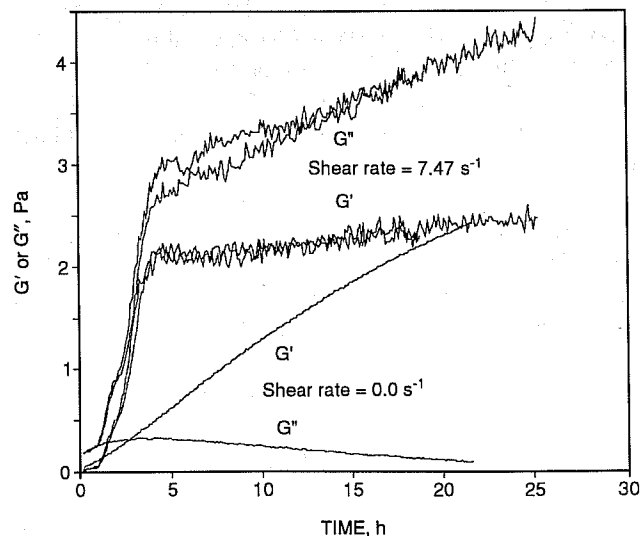


Fig. 1 Development of storage modulus and loss modulus with time with and without steady shear.

Mechanisms of In Situ Gelation

Experiments were conducted to determine if fluid-rock interactions would reduce the pH of a KUSP1 solution to the extent to cause gelation. Two pore volumes of a solution containing 1.0% KUSP1, 0.1N sodium hydroxide (NaOH), and 2.0% sodium chloride (NaCl) was passed through a 1-ft-long sandpack initially saturated with 0.1N NaOH and 2.0% NaCl. Development of increased flow resistance in only the front section of the sandpack indicated a possible problem concerning the injectivity of KUSP1 solutions in the porous matrix.

Small volumes of polymer solution that were injected subsequently into the sandpack showed that fluid-rock interactions had not triggered in situ gelation. Flow resistance in the sandpack as well as the pH of the effluent were unchanged after 6 and 21 d of shut-in time.

The experiment described was repeated, except the injected polymer solution was filtered through a 5.0- μm filter to determine if filtration would improve the injectivity of the polymer solution. Increased flow resistance in the first section of the sandpack was again observed but not to the extent that occurred when using the unfiltered solution. Work is in progress to improve the injectivity of KUSP1 solutions and to determine the effect of fluid-rock interactions using Berea sandstone cores.

Mathematical Modeling of Gel Systems

Development of Mathematical Model(s) of Laboratory In Situ Gelation

Fluid-rock interactions can play a key role in determining the efficacy of gelled polymer treatments. Effects of dissolution reactions and ion-exchange reactions were examined individually by simulating coreflood experiments. A set of simulations was conducted to study the simultaneous effects of sodium-hydrogen ion exchange and silica dissolution on high-pH brine solutions. These simulations correspond to coreflood experiments reported by Bunge and Radke² with a Huntington Beach sand core at four different flow rates.

Figure 2 shows a comparison of predicted profiles of the reduced hydroxide-ion concentration in the effluent with experimental results. The hydroxide-ion concentration is normalized by its injected value of 0.046 mol/L. Simulated profiles show good agreement with the experimental data.

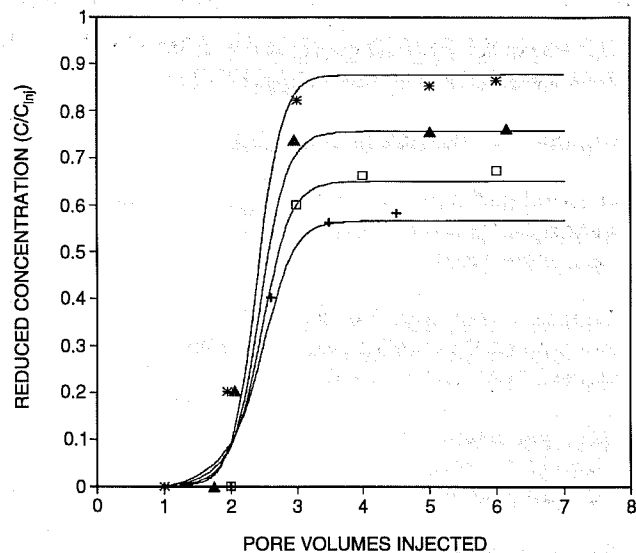


Fig. 2 Simulated profiles of the effluent hydroxide concentration compared with experimental results of Bunge and Radke.² —, simulation. *, 1 PV/d. ▲, 2 PV/d. □, 3 PV/d. +, 4 PV/d.

As the flow rate is reduced, the contact time between the injected solution and the rock matrix is increased. The kinetic nature of the silica-dissolution reaction produces progressively larger drops in the hydroxide-ion concentration. Sodium-hydrogen ion-exchange results in a delay of about 2.5 pore volumes (PV) before the breakthrough of the injected hydroxide concentrations. This delay is independent of the flow rate, which suggests the validity of the assumption of local equilibrium for the ion-exchange reaction.

The physical and reaction parameters characterizing the experiment were not known a priori. A set of typical parameters was adopted for the simulations, and this set was used for all four simulations. The model describes all the essential features shown by experimental data. These results establish the validity of the assumptions in the proposed model and the underlying mechanisms for silica dissolution and sodium-hydrogen ion exchange.

References

1. N. Nelson, A Photometric Adaption of the Somogyi Method for the Determination of Glucose, *J. Biol. Chem.*, 153: 374-380 (1944).
2. A. J. Bunge and C. J. Radke, Migration of Alkaline Pulses in Reservoir Sands, *Soc. Pet. Eng. J.*, 22(6): 998-1012 (December 1982).

IMPROVED TECHNIQUES FOR FLUID DIVERSION IN OIL RECOVERY

Contract No. DE-AC22-92BC14880

New Mexico Institute of Mining and Technology
Petroleum Recovery Research Center
Socorro, N. Mex.

Contract Date: Sept. 17, 1992
Anticipated Completion: Sept. 30, 1995
Government Award: \$192,590

Principal Investigators:

Randall S. Seright
F. David Martin

Program Manager:

Jerry Casteel
Bartlesville Project Office

Reporting Period: Oct. 1–Dec. 31, 1993

Objectives

This project has two general objectives. The first objective is to compare the effectiveness of gels in fluid diversion with those of other types of processes. Several different types of fluid-diversion processes will be compared, including those using gels, foams, emulsions, and particulates. The ultimate goals of these comparisons are to (1) establish which of these processes are most effective in a given application and (2) determine whether aspects of one process can be combined with those of other processes to improve performance. Analyses will be performed to assess where the various diverting agents will be most effective (e.g., in fractured vs. unfractured wells, in deep vs. near-wellbore applications, in reservoirs with vs. without crossflow, or in injection wells vs. production wells). Experiments will be performed to verify which materials are the most effective in entering and blocking high-permeability zones. Another objective of the project is to identify the mechanisms by which materials (particularly gels) selectively reduce permeability to water more than to oil. In addition to establishing why this occurs, the research will attempt to identify materials and conditions that maximize this phenomenon.

Summary of Technical Progress

Tracer results from previous experiments suggest that in fractured systems superior diversion may be obtained by injecting gels rather than gelants.¹ Before accepting this suggestion, however, it must be determined whether gels can be injected into fractures without screening out or developing excessive pressure gradients. Therefore several experiments

were conducted in which large volumes of gels were injected into fractured Berea cores. All these experiments were performed at 41 °C. The cylindrical cores were 14 cm long with a cross-sectional area of 10 cm². Before fracturing, the nominal permeability to brine for these cores was 650 mD. These cores were fractured lengthwise with a core splitter. The two halves of the core were repositioned and cast in epoxy. Properties of the cores are summarized in Table 1. Details of the core preparation can be found in the first annual project report.¹

A gel containing 5000-ppm HPAM (Allied Colloids Alcoflood 935®), 417-ppm chromium triacetate [Cr(III)-acetate], and 1% sodium chloride (NaCl) (pH=6) was used in several experiments. With the use of fractured Core 7, 17 pore volumes (PV) of brine was injected, followed by 17 PV of Cr(III)-acetate-HPAM gel (24 h after preparation) and then followed by 17 PV of brine (see Fig. 1). During these steps, the injection rate was 200 mL/h. During the first brine injection, the apparent brine mobility was 30 darcys/cP. During the subsequent injection of gel, the apparent gel mobility stabilized at 0.01 darcy/cP. Thus the gel was injected without

TABLE 1

Core and Fracture Permeabilities

Core	Nominal k_m ,* darcy	k_{av} , darcys	k_{fw} ,* darcy-cm	Relative flow capacity, $k_{fw}h_f/A_m k_m$
7	0.65	19.9	53.8	29.6
8	0.65	67.7	187	103
9	0.65	70.6	196	108
10	0.65	13.6	36.2	13.0
12	0.65	24.1	65.5	36.1

*Subscripts f and m refer to fracture and matrix properties, respectively.

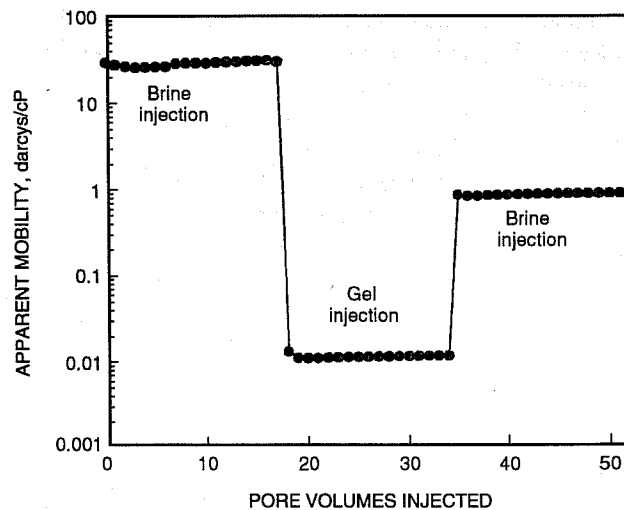


Fig. 1 Effect of brine and gel throughput on apparent mobility in fractured Core 7. Gel: 5000-ppm HPAM, 417-ppm chromium acetate, 1% NaCl, 24-h injection delay.

plugging or screening out in the fracture. Because the apparent brine and gel mobilities are known (30 and 0.01 darcys/cP, respectively) and because these values are associated almost exclusively with flow through the fracture, a resistance factor for gel in the fracture can be calculated. This value was 3000. Thus the effective viscosity for gel in the fracture was 3000 times as great as that for water.

After the gel was injected, the core was shut in for several days and gel was removed from the flow lines and the inlet and outlet core faces. Then 17 PV of brine was injected (Fig. 1). The apparent brine mobility was stable at 0.85 darcy/cP. This value was close to that expected for an unfractured core. Tracer results confirmed that the gel effectively healed the fracture (Table 2). The experiments revealed that the permeability reduction or residual resistance factor in the fracture averaged 35 (30/0.85) and was insensitive to velocity or pressure-gradient changes. In contrast, previous work demonstrated that Cr(III)-acetate-HPAM gels in unfractured cores (i.e., in porous rock) exhibit a strong apparent shear thinning behavior during brine injection.²

With the use of fractured Core 8, the apparent rheology of the Cr(III)-acetate-HPAM gel in a fracture was examined. One day after the gelant was prepared, gel was injected into the fractured core at a rate of 400 mL/h. During gel injection at this rate, the pressure gradient stabilized at about 75 psi/ft and the resistance factor in the fracture was 1500. After these data were obtained, the injection rate was decreased in stages. The results are shown by the solid circles in Figs. 2 and 3. At each successively lower rate down to 40 mL/h, stabilized pressure drops were achieved and the resistance factors increased with decreasing flow rate (Fig. 2). Also, the pressure gradient remained fairly constant between 60 and 75 psi/ft (Fig. 3). This result suggests that some minimum pressure gradient was needed to keep the gel mobilized.

When the gel injection rate was reduced to 10 mL/h (2 h after gel injection started and 26 h after the gelant was prepared), the resistance factor increased to 200,000 and the pressure gradient increased to 250 psi/ft (Figs. 2 and 3). This deviation from the previous trend may have resulted from an increased degree of gelation, from the decreased injection rate, or from a combination of both effects. At lower injection rates, the average pressure gradients were lower and the

resistance factors were erratic. The low-injection-rate data points in Figs. 2 and 3 show averages of these erratic values.

After a low gel injection rate of 0.64 mL/h was reached, the injection rate was increased in stages. Results from this portion of the experiment are illustrated by the open triangles in Figs. 2 and 3. When the gel injection rate was increased to 10 mL/h (6 h after gel injection started and 30 h after the gelant was prepared), the resistance factor was 222,000 and the pressure gradient was 280 psi/ft. These values are similar to those mentioned previously (associated with an injection rate of 10 mL/h).

At higher injection rates, the resistance factors quickly stabilized at each new rate and the pressure gradients were fairly constant around 300 psi/ft (Fig. 3). Again, this behavior suggests that some minimum pressure gradient was needed to keep the gel mobilized. At this point, however, the pressure gradient was four to six times as great as that noted earlier in the experiment. This experiment was completed 8 h after gel injection started and 32 h after the gelant was prepared.

A concern raised by the data in Fig. 3 is that pressure gradients between 40 and 300 psi/ft were necessary to force the gel through the fracture. This requirement may limit the ability of this particular gel to propagate through a fracture system. Perhaps gel propagation would be easier earlier in the gelation process or if a different gelant composition were used.

Table 2 summarizes results from experiments performed in which gels were injected into fractured cores. In all cases, 1 d elapsed between gelant preparation and gel injection into the fractured cores. The resorcinol-formaldehyde gel contained 3% resorcinol, 3% formaldehyde, 0.5% potassium chloride (KCl), and 0.42% sodium bicarbonate (NaHCO₃) at pH=9. The Cr(III)-xanthan gel contained 0.4% xanthan (Pfizer Flocon 4800®), 469-ppm chromium chloride (CrCl₃), and 0.5% KCl at pH=4. The Cr(III)-acetate-PAM/AMPS gel contained 0.3% PAM/AMPS (Drilling Specialties HE-100®), 440-ppm chromium triacetate, and 2% KCl.

The first two listings in Table 2 provide data for unfractured and fractured cores. The ideal gel treatment would heal the fracture so that tracer results matched those associated with the unfractured core. The ideal gel would also exhibit low resistance factors so that the gel could be placed without developing excessive pressure gradients. It would also

TABLE 2
Properties in Fractured Cores with One-Day-Old Gels

Core	Gel	Fracture resistance factor	Residual resistance factor	Tracer results, PV @	
				Breakthrough	C/C ₀ = 0.5
No fracture	None	—	—	0.81	1.00
7	None	1	1	0.05	0.12
7	Cr(III)-acetate-HPAM	3000	35	0.82	1.03
9	Resorcinol-formaldehyde	Plugged	70	0.36	0.54
10	Cr(III)-xanthan	8600	19	0.46	0.88
12	Cr(III)-acetate-PAM/AMPS	12.5	130	0.25	0.35

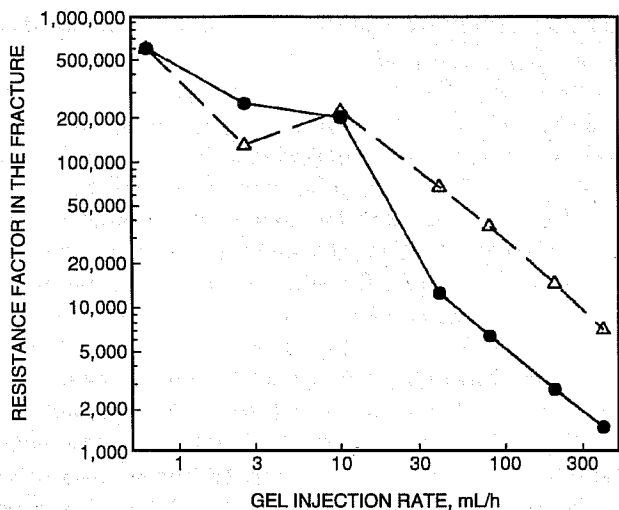


Fig. 2 Resistance factor in the fracture during placement of a Cr(III)-acetate-HPAM gel. Gel: 5000-ppm HPAM, 417-ppm chromium acetate, 1% NaCl, 24- to 32-h injection delay. —●—, successively decreasing rates. —△—, successively increasing rates.

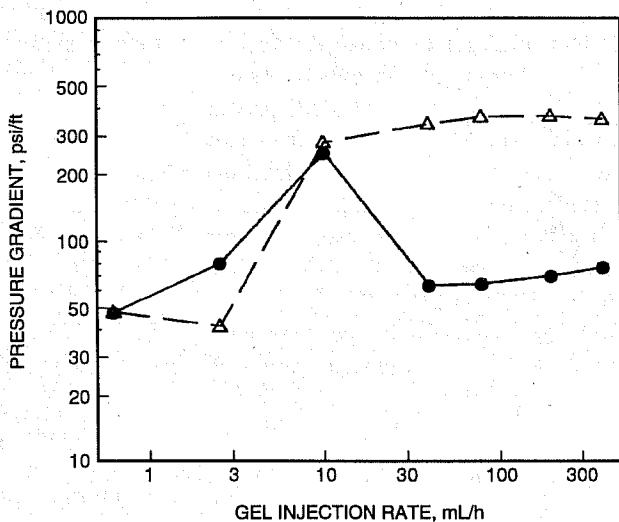


Fig. 3 Pressure gradient during placement of a Cr(III)-acetate-HPAM gel. Gel: 5000-ppm HPAM, 417-ppm chromium acetate, 1% NaCl, 24- to 32-h injection delay. —●—, successively decreasing rates. —△—, successively increasing rates.

provide a residual resistance factor that was approximately equal to the corresponding relative flow capacity value given in Table 1. (The latter property would indicate that the gel had plugged the fracture but not the rock matrix.)

The tracer results and residual resistance factors suggest that, for the gels examined, the Cr(III)-acetate-HPAM gel most effectively healed the fracture. However, the high resistance factor (3000) raises concern about the ability to propagate this gel deep into a fracture system. This concern also applies to the Cr(III)-xanthan gel and the resorcinol-formaldehyde gel. For the latter gel, severe plugging was apparent during gel injection (resistance factors exceeded 35,000 after injecting less than 1 PV of gel). After completion of the resorcinol-formaldehyde experiment, the core was disassembled to reveal that the gel had only penetrated 7 cm into the fracture (total length was 14 cm). This observation confirmed that the gel was screening out during injection into the fracture.

The Cr(III)-acetate-PAM/AMPS formulation exhibited a low resistance factor in the fracture during placement. However, the tracer results did not indicate much improvement in sweep efficiency for the core. Also, because the residual resistance factor (130) was much greater than the corresponding relative flow capacity in Table 1 (36.1), it is suspected that the gel was not sufficiently formed before injection to prevent substantial leakoff into the porous rock.

The ability of a given gel to propagate effectively through a fracture is suspected to depend on (1) the composition of the gelant, (2) the degree of gelation or gel curing, (3) the fluid velocity (or pressure gradient) in the fracture, and (4) the width, conductivity, and tortuosity of the fracture. Thus, at this point it is unknown whether one gel is necessarily better than other gels for fracture applications. More work will be needed to establish the best circumstances for propagation of gels in fractures.

References

1. R. S. Seright, Improved Techniques for Fluid Diversion in Oil Recovery, *First Annual Report*, DOE Contract No. DE-AC22-92BC14880, 95-140, October 1993.
2. R. S. Seright, *Impact of Permeability and Lithology on Gel Performance*, paper SPE/DOE 24190 presented at the 1992 SPE/DOE Enhanced Oil Recovery Symposium, Tulsa, Okla., April 21-24, 1992.

**INVESTIGATION OF OIL RECOVERY
IMPROVEMENT BY COUPLING AN
INTERFACIAL TENSION AGENT
AND A MOBILITY CONTROL
AGENT IN LIGHT OIL RESERVOIRS**

Contract No. DE-AC22-92BC14886

**Surtek, Inc.
Golden, Colo.**

**Contract Date: Sept. 28, 1992
Anticipated Completion: Sept. 30, 1995
Government Award: \$219,925
(Current year)**

**Principal Investigator:
Malcolm J. Pitts**

**Project Manager:
Jerry Casteel
Bartlesville Project Office**

Reporting Period: Oct. 1–Dec. 31, 1993

Objective

The objective of this study is to investigate two major areas concerning the coinjection of an interfacial-tension (IFT) reduction agent(s) and a mobility control agent into petroleum reservoirs. The first task will consist of defining the mechanisms of interaction of an alkaline agent, a surfactant, and a polymer on a fluid–fluid and a fluid–rock basis. The second task is the improvement of the economics of the combined technology.

This report examines the effect of cation type and of reservoir water on IFT reduction. Alkyl type and surfactant type are varied in both cases. Stability of alkaline–surfactant–polymer solutions is reported as well.

Summary of Technical Progress

A low acid number 42 °API gravity crude oil from the Adena field¹ was selected for the present study. Solutions were dissolved in 1000 mg/L sodium chloride (NaCl) except where designated.

Previously reported studies on this contract are

• *Interfacial Tension with Alkali and Surfactant.* A series of IFT measurements at 72 °F were performed to investigate how different surfactant structures and alkaline agents affect IFT reduction. Neither alkali type nor pH was a significant contributor to IFT reduction. Surfactant is the dominant contributor to the IFT reduction synergism. Olefinic character is more important than surfactant structure. As a class,

however, the alkyl aryl sulfonates are the best surfactants to achieve low IFT values.

• *Effect of Temperature on Interfacial Tension.* In the previous study, the IFT of alkaline–surfactant solutions was determined at 125 and 180 °F. No consistent trend with increasing temperature was observed for the different surfactants.

• *Effect of Polymer on Interfacial Tension of Alkaline–Surfactant Solutions.* The addition of xanthan gum, hydroxyethyl cellulose, and partially hydrolyzed polyacrylamide polymers to selected solutions of alkali and surfactant resulted in increased IFT. Polymer type was not significant. Ultralow IFTs were achieved by altering the alkali concentration.

• *Effect of Alkali and Surfactant on Polymer Solution Viscosities.* Polymer solution viscosities decreased when alkali only was added for partially hydrolyzed polyacrylamide, hydroxyethyl cellulose, and xanthan gum. The addition of surfactant to the alkaline–polymer or polymer solutions resulted in changes of solution viscosity. The change is dependent on surfactant structure and polymer type but is independent of alkali type.

• *Intrinsic Viscosity and Hydrodynamic Radius.* Changes in polymer size when alkali and surfactant were added were calculated from the apparent viscosity data. Alkali decreased intrinsic viscosity and hydrodynamic radius. When surfactant was added, both parameters initially decreased and then increased for partially hydrolyzed polyacrylamide and xanthan gum as surfactant concentrations became larger. Hydroxyethyl cellulose changes were minimal.

• *Critical Micelle Concentration.* Critical micelle concentrations (CMC) of 0.02 to 0.06 wt % active were measured for alpha olefin, linear alkyl aryl, branch alkyl aryl, and internal olefin sulfonates. When sodium carbonate (Na_2CO_3), sodium hydroxide (NaOH), sodium bicarbonate (NaHCO_3), trisodium orthophosphate (Na_3PO_4), and disodium hydrogen orthophosphate (Na_2HPO_4) were added to the surfactant solution, CMC decreased from 0.005 to 0.02 wt %. The addition of polyacrylamide and xanthan gum branched and linear alkyl aryl sulfonates increased CMC, whereas linear alkyl sulfonates decreased CMC.

• *Effect of the Addition of Sodium Chloride on Interfacial Tension, Critical Micelle Concentration, and Polymer Solution Viscosity.* When NaCl was added to the surfactant plus alkali solutions, the CMC decreased until the surfactant precipitated from solution. The IFT of alkaline plus surfactant solutions with ultralow IFTs generally showed an increase. For alkaline plus surfactant solutions with less than optimum IFT reduction and more water-soluble surfactants, the IFT often decreased. Polyacrylamide and hydroxyethyl cellulose solution viscosities, hydrodynamic radius, and intrinsic viscosity decreased with NaCl. Xanthan gum solution viscosities increased with NaCl.

• *Solution Long-Term Stability.* Various alkalis were mixed with a linear alkyl aryl sulfonate, a branched alkyl aryl sulfonate, an alpha olefin sulfonate, and partially hydrolyzed polyacrylamide and aged at 72, 92, 132, and 180 °F for 50 d. The alkaline solutions and the alkaline plus surfactant solutions were stable. The addition of polyacrylamide polymer to the linear and branched alkyl aryl sulfonates plus alkali solutions resulted in

solution instability at the higher polymer concentrations and at higher surfactant concentrations. Alpha olefin sulfonates demonstrated no solution instability at any polymer or surfactant concentration tested.

Effect of Cation on Interfacial Tension

In the present study, sodium ion was replaced with potassium and ammonium ion in the alkaline agents with sodium-based surfactants previously tested. Potassium-based and ammonium-based surfactants were also tested. When potassium or ammonium alkalis were tested, the corresponding dissolution water was either 1000 mg/L potassium chloride (KCl) or 1000 mg/L ammonium chloride (NH₄Cl). Figure 1 depicts IFT reduction as a function of alkali concentration for branched alkyl aryl sulfonates combined with sodium, potassium, and ammonium hydroxide. Petrostep B-100 is a sodium-based branched alkyl (16 to 17 carbons) aryl sulfonate, molecular weight 415; Niniate 411 is an isopropylamine-branched dodecylbenzene sulfonate; and Polystep A-7 is a sodium linear dodecylbenzene sulfonate. Interfacial tension values of the Petrostep B-100 increase with potassium hydroxide (KOH) addition. Other sodium-based surfactants that did not produce ultralow IFTs showed little change with different alkaline cations. A comparison of Polystep A-7 and Niniate 411 showed that changing the cation of the sulfonate had little effect on the IFT response.

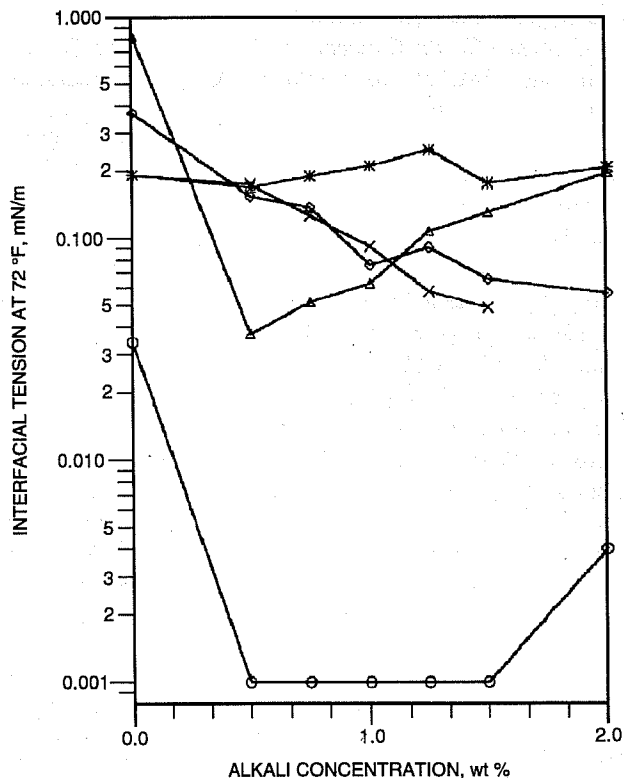


Fig. 1 Effect of potassium ion on the interfacial tension between Adena crude oil and branched alkyl aryl sulfonates. ○, 0.1 wt % Petrostep B-100 plus NaOH; △, 0.1 wt % Petrostep B-100 plus KOH; ×, 0.1 wt % Niniate 411 plus KOH; *, 0.1 wt % Niniate 411 plus NH₄OH; and ◇, 0.1 wt % Polystep A-7 plus NaOH.

Changing the cation of carbonate salts also showed little effect on the IFT response. Figure 2 depicts the data with Polystep A-7 and Polystep A-15-30K (potassium linear dodecylbenzene sulfonate). With increasing temperature, the trends did not change.

The greatest difference with alternate cations was the solution stability. The sodium solutions were considerably more stable than the potassium solutions. The ammonium cation solutions were less stable than the potassium solutions. An increase of the cation chloride concentration exacerbated the loss of solubility.

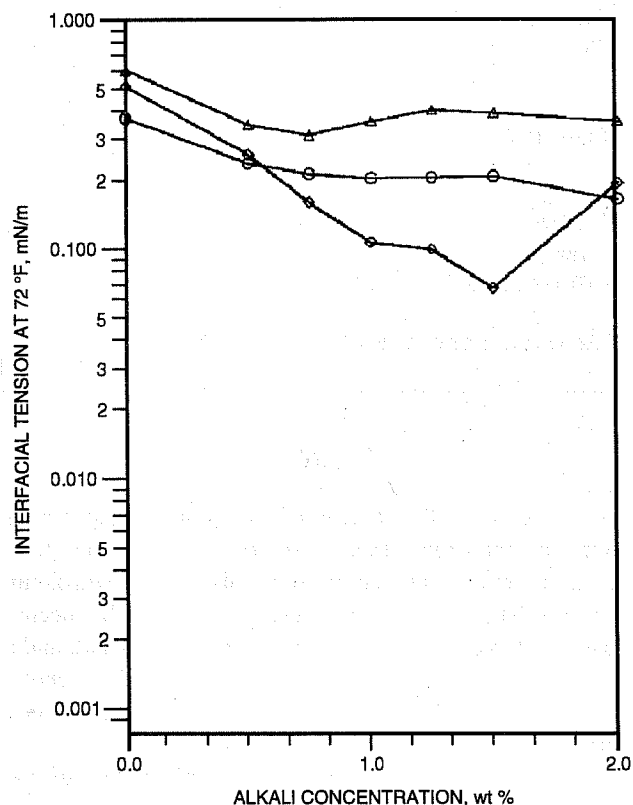


Fig. 2 Effect of ammonium ion on the interfacial tension between Adena crude oil and linear alkyl aryl sulfonates. ○, 0.1 wt % Polystep A-7 plus Na₂CO₃; ◇, 0.1 wt % Polystep A-15-30K plus K₂CO₃; and △, 0.1 wt % Polystep A-15-30K plus NH₄CO₃.

Effect of Reservoir Brine on Interfacial Tension

Four reservoir brines were blended with selected alkaline plus surfactant solutions. Two "J" sand reservoir brines and two adjacent field brines were selected. Only two "J" sand reservoir brines were selected because of the low total dissolved solids (TDS) and cation content of the "J" sand-produced waters. The ion compositions of the reservoir brines are listed in Table 1. Adena and Singleton are the "J" sand fields.

Figure 3 depicts the effect of diluting a 0.1 wt % active Petrostep B-100 plus 2.00 wt % Na₂CO₃ solution with the produced waters. The lower TDS and fresher waters resulted

in minimal increases of IFT, and the higher TDS and greater hardness resulted in significant increases of IFT. Interfacial tension increases paralleled TDS and hardness increase.

TABLE 1
Ion Composition of Reservoir Brines

Ion	Ion concentration, mg/L			
	Singleton	Adena	Sleepy Hollow	Jumper Creek
Calcium	13	18	2,230	900
Magnesium	2	8	376	150
Strontium	0	1	264	14
Barium	0	0	64	60
Sodium	111	2,700	14,200	16,400
Potassium	1	6	72	37
Chloride	18	2,750	31,750	20,100
Sulfate	8	23	10	0
Total dissolved solids	349	6,500	60,300	34,000
pH	8.0	8.5	7.0	7.6

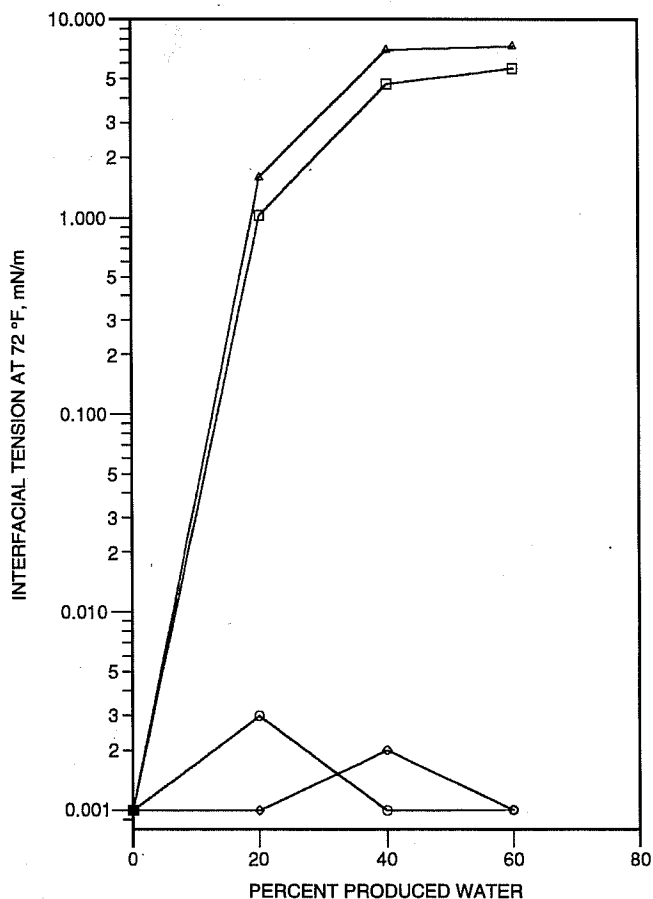


Fig. 3 Effect of produced water dilution on the interfacial tension between Adena crude oil and 0.1 wt % Petrostep B-100 plus Na_2CO_3 . ○, singleton produced water; ◇, Adena produced water; △, Sleepy Hollow produced water; and □, Jumper Creek produced water.

Figure 4 depicts the IFT increase when 0.1 wt % Petrostep B-100 combined with Na_2CO_3 , NaOH, and Na_3PO_4 is diluted with Sleepy Hollow produced water. NaOH plus surfactant solution was considerably more affected by the reservoir brine than Na_2CO_3 and Na_3PO_4 plus surfactant solutions. Sleepy Hollow produced water has the least effect on Na_3PO_4 -surfactant combinations. Other surfactant plus alkali blends demonstrated the same conclusion. Similar trends were observed at 170 °F and with other alkali plus surfactant combinations.

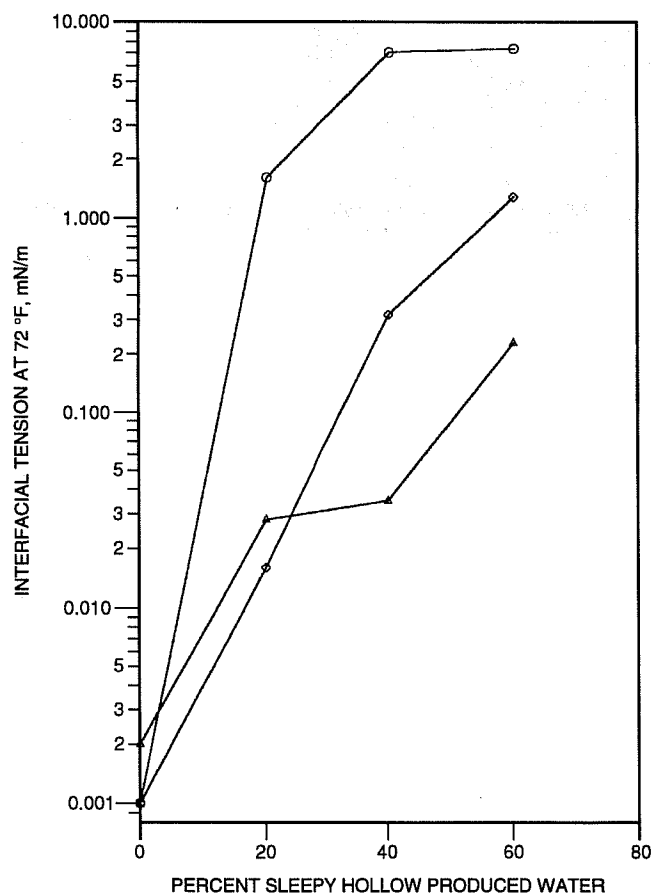


Fig. 4 Effect of alkali type on the increase of interfacial tension by Sleepy Hollow produced water dilution. 0.1 wt % Petrostep B-100 plus alkali. ◇, 2.0 wt % Na_2CO_3 ; △, 2.0 wt % Na_3PO_4 ; and ○, 1.25 wt % NaOH.

Adsorption of Surfactant

The adsorption of the various surfactants onto crushed Berea sandstone was studied. Surfactants studied were described previously.² Surfactant adsorption was lowest for the more water-soluble surfactants. Surfactants with molecular weights greater than 370 amu have the greatest adsorption. A sulfated ethoxylate alcohol (399 amu) and a branched alkyl toluene sulfonate (430 amu) are the exceptions. The effect of surfactant molecular weight on surfactant adsorption vs. time at 72 °F is shown in Fig. 5.

Continued Evaluations

Future studies will investigate the effect of alkali, cation type, temperature, and polymer on surfactant adsorption onto rock. Changes in relative permeability caused by alkali plus surfactant adsorption, oil recovery efficiency by alkali plus surfactant and alkali plus surfactant plus polymer solutions and changes to improve the economics of oil recovery will be evaluated.

References

1. L. W. Holm, Propane-Gas-Water Miscible Floods in Watered-Out Areas of the Adena Field, Colorado, *J. Pet. Technol.*, 24: 1264-1270 (October 1972).
2. Progress Report Submitted to DOE for the Period January 1-March 31, 1993.

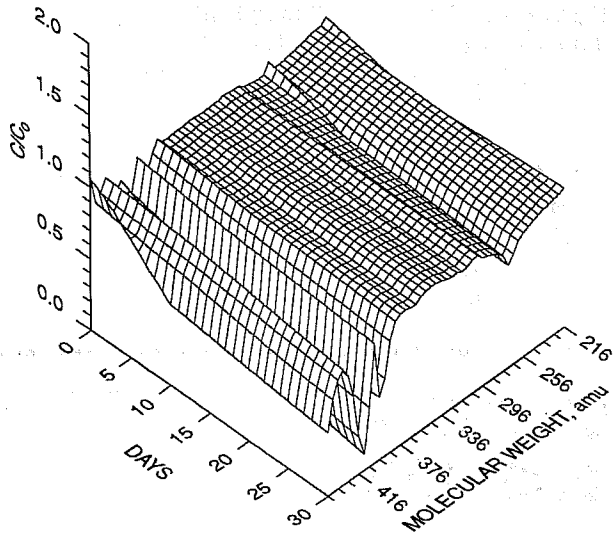


Fig. 5 Effect of surfactant molecular weight on surfactant adsorption vs. time at 72 °F. Surfactant without alkali.

GAS DISPLACEMENT— SUPPORTING RESEARCH

FIELD VERIFICATION OF CO₂-FOAM

Contract No. DE-FG21-89MC26031

**New Mexico Institute of Mining and Technology
Petroleum Research Center
Socorro, N. Mex.**

Contract Date: Sept. 16, 1992

Anticipated Completion: Sept. 16, 1995

Total Project Cost:

DOE	\$2,000,000
Contractor	2,035,000
Total	\$4,035,000

Principal Investigators:

**F. David Martin
John P. Heller
William W. Weiss**

Project Manager:

**Royal Watts
Morgantown Energy Technology Center**

Reporting Period: Oct. 1–Dec. 31, 1993

Objectives

The objectives of this cooperative industry, university, and government project are to (1) transfer promising laboratory

research to a field demonstration test, (2) provide research support to design and implement the test, and (3) evaluate the use of foam for mobility control and fluid diversion in a field CO₂ flood.

Summary of Technical Progress

The East Vacuum Grayburg/San Andres Unit (EVGSAU), operated by Phillips Petroleum Company (PPCo), is the site selected for a comprehensive evaluation of the use of foam for improving the effectiveness of a CO₂ flood. The Petroleum Recovery Research Center (PRRC), a division of the New Mexico Institute of Mining and Technology (NMIMT), is providing laboratory and research support for the project. The project is jointly funded by the EVGSAU Working Interest Owners (WIO), the U.S. Department of Energy (DOE), and the State of New Mexico. A Joint Project Advisory Team (JPAT) composed of WIO technical representatives from several major oil companies provides input, review, and guidance for the project. The four-year project began in late 1989, and in 1993 a no-cost extension of the project was granted by DOE for a period of six months.

The production responses resulting from the first foam injection test are described in previous progress reports. The favorable changes in injection profiles resulting from the first test are shown in Figs. 1 and 2 for water and CO₂, respectively. On the basis of these favorable responses, a second foam injection test was initiated in May 1993 in the same injection well that was used for the first foam test. At some period after the initiation of the second foam injection

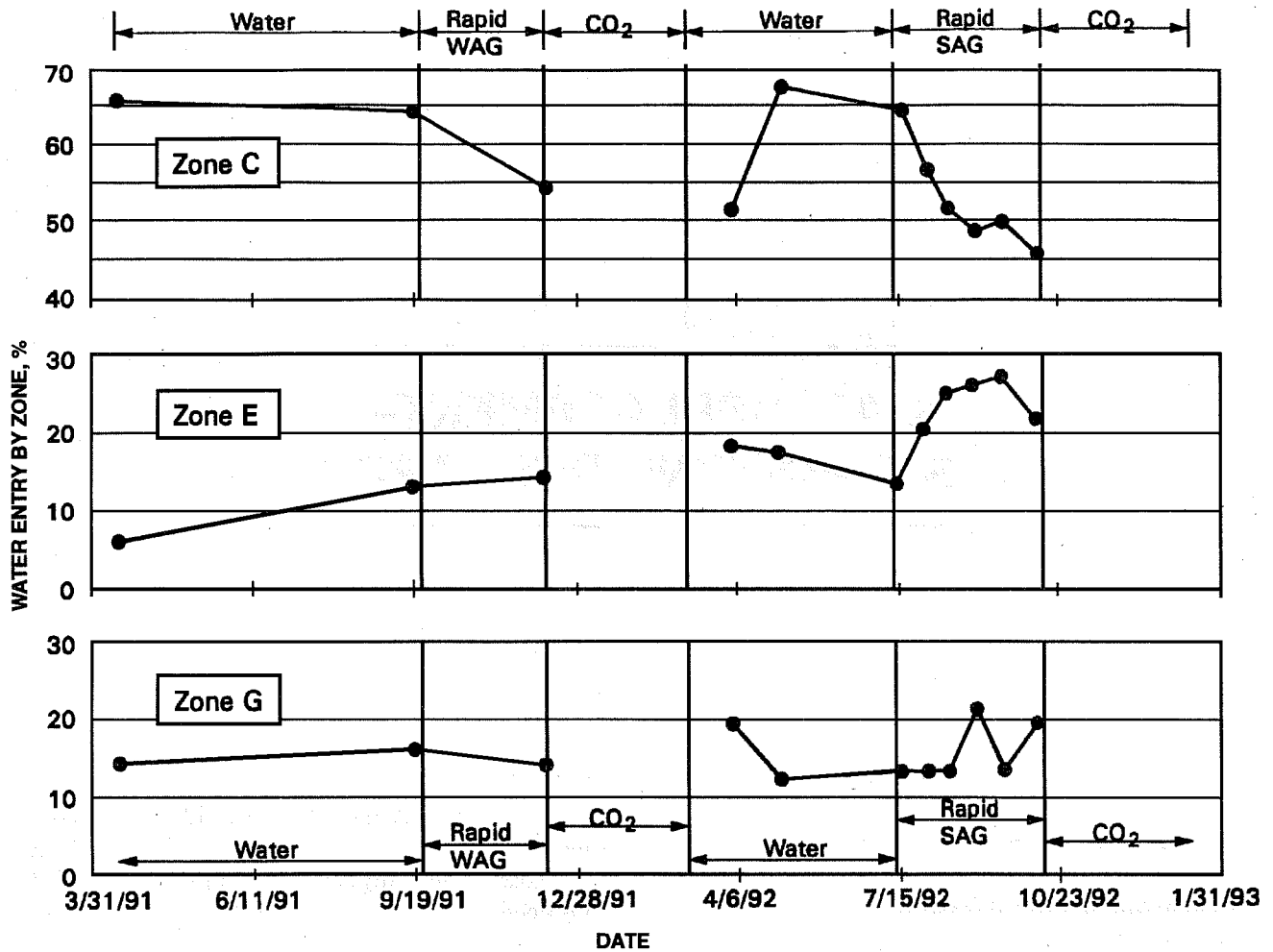


Fig. 1 Results of water injection profiles in well 3332-001. WAG, water alternating gas. SAG, surfactant alternating gas.

test, however, a facilities problem was discovered that resulted in uncertainties in the injected gas composition and the resulting bottomhole pressures. Therefore the second foam injection test was aborted, and pre-foam baseline injectivity is being reestablished. The rates and pressures in the test well are shown in Fig. 3. The second foam injection test will be reimplemented during the next quarter after the water injectivity stabilizes.

The reservoir simulation studies conducted at the University of Houston are complete. A final report on this aspect of the project is expected in January 1994.

During this quarter a detailed geological reservoir characterization study was received from PPCo that provides results of an extensive multidisciplinary study of the EVGSAU foam pilot area. Results of this study will be summarized in the final report on the project. Additionally, two papers^{1,2} were prepared for presentation at the 1994 Permian Basin Conference, Midland, Tex.

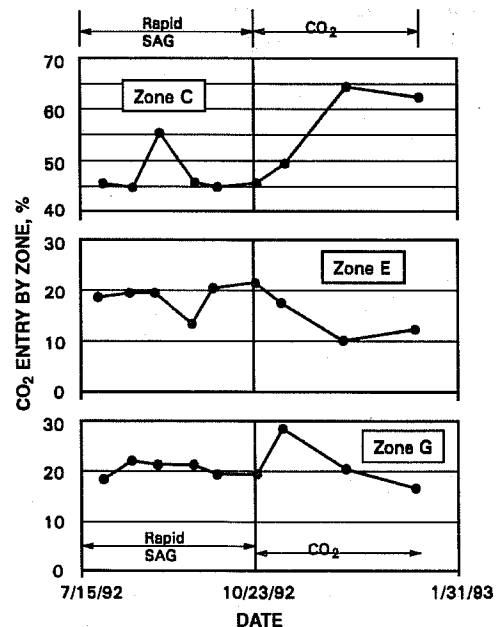


Fig. 2 Results of CO₂ injection profiles in well 3332-001. SAG, surfactant alternating gas.

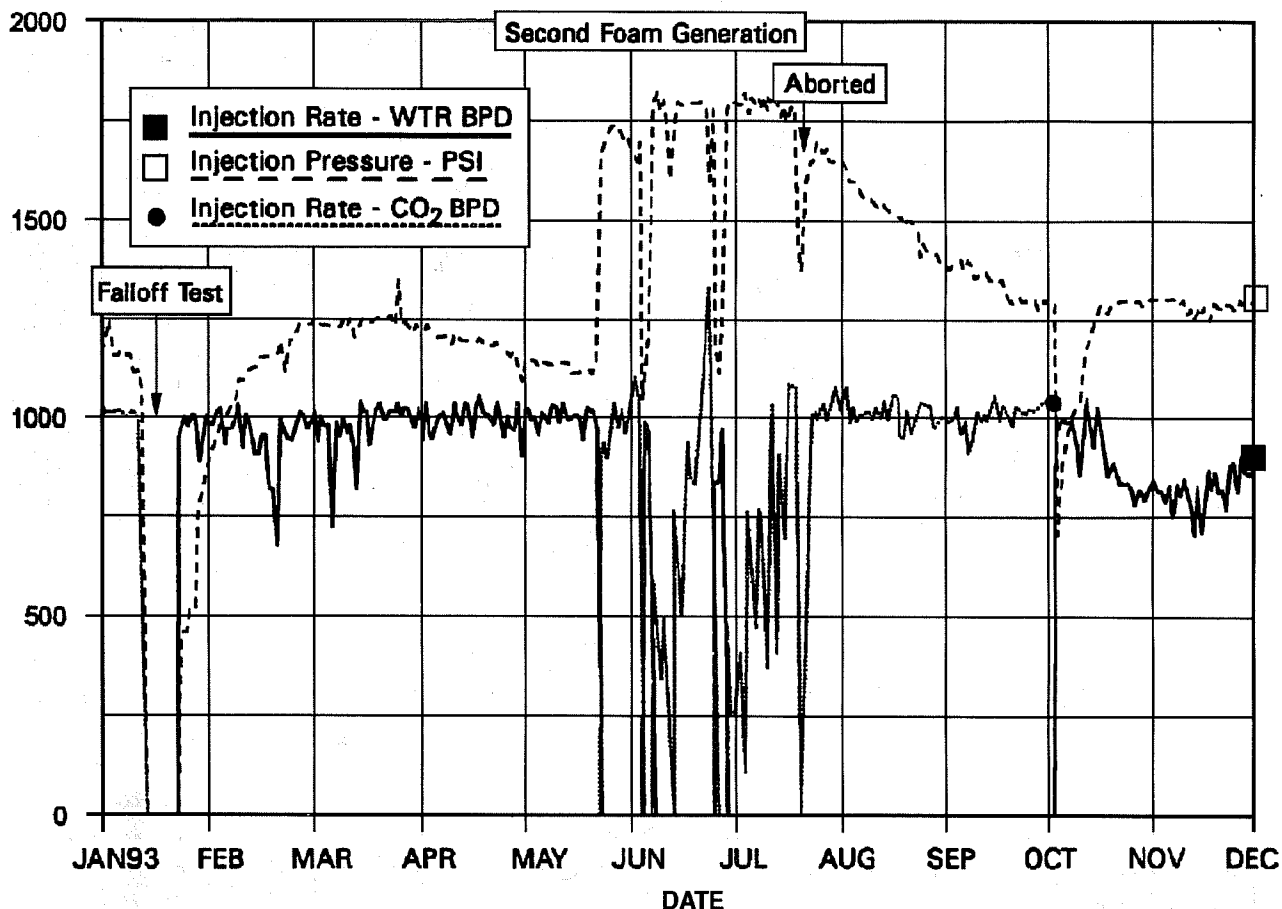


Fig. 3 Well 3332-001 injection pressure and rate during foam generation.

References

1. S. H. Chang and R. B. Grigg, *Laboratory Flow Tests Used to Determine Reservoir Simulator Foam Parameters for EVGSAU CO₂ Foam Pilot*, paper SPE 27675 to be presented at the 1994 Society of Petroleum Engineers Permian Basin Conference, Midland, Tex., March 16-18, 1994.
2. A. J. Sultan, A. Ouenes, and W. W. Weiss, *Automatic History Matching for an Integrated Reservoir Description and Improving Oil Recovery*, paper SPE 27712 to be presented at the 1994 Society of Petroleum Engineers Permian Basin Conference, Midland, Tex., March 16-18, 1994.

SCALEUP OF MISCIBLE FLOOD PROCESSES

Contract No. DE-FG22-92BC14852

**Stanford University
Stanford, Calif.**

**Contract Date: Sept. 30, 1992
Anticipated Completion: Sept. 30, 1995
Government Award: \$349,985**

**Principal Investigator:
Franklin M. Orr, Jr.**

**Project Manager:
Jerry Casteel
Bartlesville Project Office**

Reporting Period: Oct. 1-Dec. 31, 1993

Objective

The objective of this research is a systematic effort to quantify the relationships between process mechanisms that can lead to improved recovery from gas injection processes performed in heterogeneous Class 1 and Class 2 reservoirs. It will provide a rational basis for the design of displacement processes that take advantage of crossflow that results from capillary, gravity, and viscous forces to offset partially the adverse effects of heterogeneity. In effect, the high-permeability zones are used to deliver fluid by crossflow to zones that would otherwise be flooded only very slowly. The research effort is divided into five areas:

1. Development of miscibility in multicomponent systems.
2. Design estimates for nearly miscible displacements.
3. Design of miscible floods for fractured reservoirs.
4. Compositional flow visualization experiments.
5. Simulation of near-miscible flow in heterogeneous systems.

Summary of Technical Progress

Work continued in the following areas:

1. *Development of Miscibility in Multicomponent Systems.* Progress has been made on the creation of a systematic theory of miscibility development in multicomponent systems. The dispersion-free theory developed previously at Stanford shows that in any multicomponent displacement the recovery behavior is determined by a small number of key tie lines that include the tie lines that extend through the initial and injection compositions and one or more crossover tie lines. If any of those tie lines is a critical tie line, then the displacement is multicontact miscible. Thus the key to determining minimum miscibility pressure (or minimum enrichment for miscibility) is to find which tie line approaches the critical locus first as pressure (or enrichment) is increased. Efficient algorithms for calculation of the critical locus are being investigated. The next step is to develop an algorithm to determine which tie line lies closest to the critical locus. Once the key tie line for miscibility is so identified, it should be possible to develop an efficient algorithm to determine minimum miscibility pressure for a multicomponent system.

2. *Design Estimates for Nearly Miscible Displacements.* The scaling theory developed previously has been extended to include the effects of layer ordering in scaling nearly miscible displacements in layered reservoirs. It was found that gravity forces can offset the adverse effects of high-permeability channels in some layered reservoirs if adequate vertical communication exists.

3. *Design of Miscible Flood for Fractured Reservoirs.* Significant progress has been made in modifying the existing high-pressure pressure-volume-temperature (PVT) equipment to conduct high-pressure gravity drainage. It will soon be possible to conduct high-pressure gravity drainage in the presence of carbon dioxide (CO₂) in cores up to 2 ft in length.

Progress has also been made in developing the theory of three-phase gravity drainage. Recent experimental and theoretical results suggest that it will soon be possible to predict oil drainage rate and final recovery for a given system with good agreement between experiment and theory.

4. *Flow Visualization Experiments.* To understand more fully the visualization experimental results that have been obtained, a compositional simulator code is being modified to simulate the observations. A subroutine for calculating the phase behaviors of the fluid system used in the experiments is to be completed. The oil-water-alcohol systems used in the low-pressure experiments are not modeled accurately by cubic equations of state, and hence an approach based on excess free-energy models is being used.

5. *Simulation of Flow in Heterogeneous Reservoirs.* The streamtube approach is being investigated as a numerical alternative to conventional finite-difference simulators to be used in predicting near-miscible gas injection in heterogeneous reservoirs. The streamtube approach is applied to the two-phase immiscible case, which is assumed to be well understood and for which many reliable numerical methods have been developed. Results have provided new insight on the applicability of the streamtube approach and, particularly, on the novel idea that proposes to map a one-dimensional (1-D) analytical solution (Riemann solution) along the streamtubes to obtain a two-dimensional (2-D) solution for a heterogeneous reservoir.

Streamtube Approach

Previous research using streamtubes focused almost exclusively on the immiscible two-phase problem with an areal geometry. Principally, it is the weak nonlinearity of the immiscible two-phase problem (waterflood) that allows for the assumption of constant streamtube geometries, which are almost universally applied in the published literature. A notable exception is found in Renard's work.¹ Here the streamtubes are recalculated periodically, and the fluid is assigned to the new streamtubes using a much finer mesh than that upon which the tubes are calculated. In general, though, the assumption of a fixed streamtube geometry is widely used and reinforced by the areal geometry because, by continuity, a streamline must start and end at a source. In the areal plane sources are points, which leaves little room for the streamtubes to change their shape during the displacement. Furthermore, except for Hewett and Behrens,² all studies in the literature consider a homogeneous reservoir to generate the streamtubes.

The physical and geometrical constraints imposed on the governing partial differential equations (PDE) are such that the geometry of the streamtubes becomes a weak function of the total mobility distribution. In light of this, the good matches reported by Higgins and Leighton,³ Higgins, Boley, and Leighton,⁴ Martin and Wegner,⁵ and Hewett and Behrens² are not surprising. Another way of accounting for the weak nonlinearities was proposed by Martin and Wegner.⁵ They show that, instead of updating the geometries of the

streamtubes, the total volume of fluid injected can be made a function of the resistance of each tube. The change in volume of a streamtube is traded for a varying volume of fluid going down each tube while keeping the actual streamtube geometry constant. Although the approaches differ slightly, all show convincingly that streamtubes can be used to successfully and inexpensively predict recovery for 2-D areal waterflood problems.

In this work, the waterflood problem is approached differently and used to demonstrate the applicability of a Riemann method. Detailed descriptions of techniques for construction of solutions for multicomponent, two-phase flow problems have been presented previously.⁶ The domain is considered to be heterogeneous and the geometry to be cross-sectional. The streamlines are now no longer pinned down by two points in the domain as in the areal case. This makes them freer to move and conform to the flow field, which allows the nonlinearities to become more noticeable. But the real difference is in the mapping of the 1-D solution along each streamtube. In this work, the 1-D solution is treated as a solution to a Riemann problem. This means that at the new time level the solution is not given by an integration from t_D to $t_D + \Delta t_D$, as in conventional time-stepping algorithms, but rather from t_D to $0 + t_D + \Delta t_D$, where the initial condition at time $t_D = 0$ is characterized by a discontinuity at $x_D = 0$. This is the well-known initial condition for the Buckley–Leverett solution. Treating the 1-D solution as a Riemann solution means that each streamtube is treated as a true 1-D system on which the Buckley–Leverett solution is simply mapped repeatedly for different times.

In this approach, the underlying assumption is that the solution is indeed scalable by x_D/t_D along each tube. In other words, the fluid entering a tube remains in the tube and can exit only by the outlet end. The validity of this assumption is considered in detail in the section that follows.

Validation of the Riemann Approach

The Riemann approach was tested by the following numerical experiment. With the use of a standard finite-difference simulator (ECLIPSE), the velocity fields were stored for regular increments of dimensionless time. From each velocity field, the corresponding streamtubes were then calculated and used to find the saturation profiles by mapping a Riemann solution along the streamtubes. The saturation profiles obtained by this method were then compared with the saturation profiles obtained by the direct Riemann approach proposed in this research, with the underlying assumption that the velocity fields obtained from the finite-difference simulator are indeed correct.

The data used to test the Riemann approach are shown in Fig. 1. Although the end-point mobility ratio is 10, the frontal mobility ratio is, in fact, only 1.36, which results in a more stable displacement than that suggested by the end-point value alone. A similar statement can be made for many waterfloods with reasonable relative permeability curves: the frontal mobility ratio is usually of the order of 1, even though the end point can be of the order of 10 or 100. The weak nonlinear

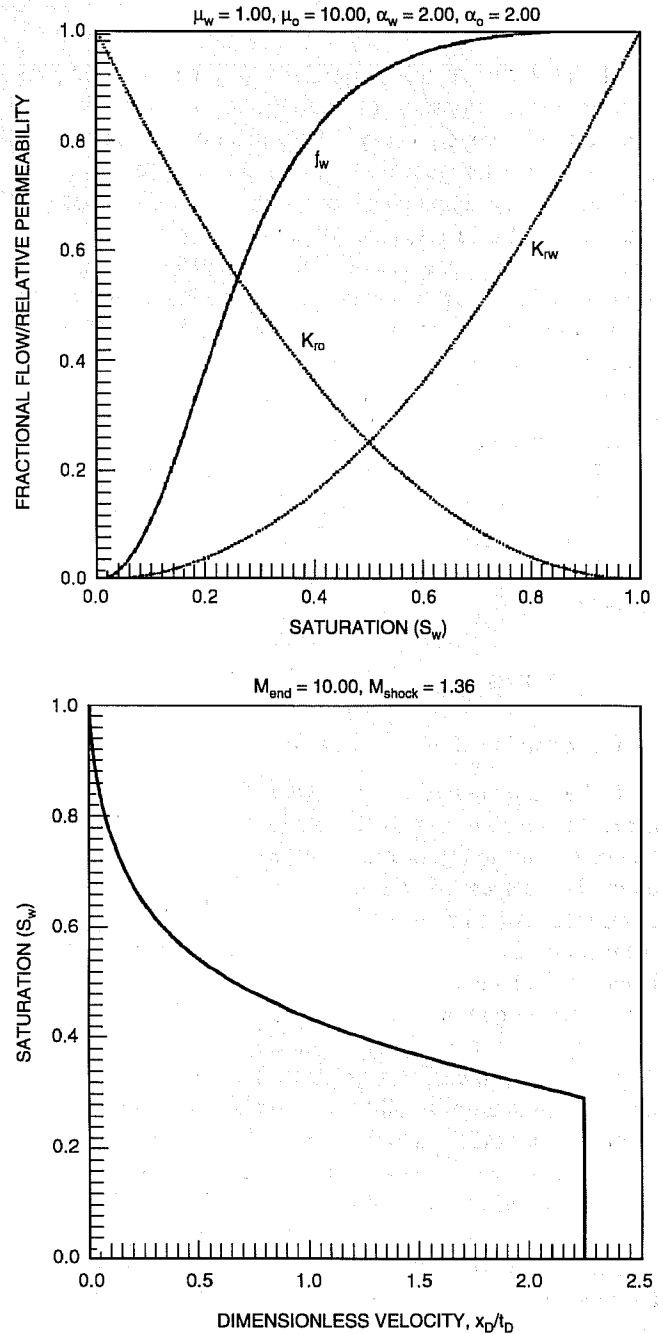


Fig. 1 Relative permeability curves ($k_{rw} = S_w^2$, $K_{ro} = S_o^2$), corresponding fractional flow function for a viscosity ratio of 10 ($\mu_o = 10.00$; $\mu_w = 1.00$), and Buckley–Leverett analytical solution used for testing the Riemann approach. The mobility ratio at the shock front is $M_{shock} = 1.36$.

behavior of the two-phase immiscible problem results from the relatively mild adverse mobility ratio.

The absolute permeability field is shown in Fig. 2. This field was derived from a finer 250×100 permeability field by taking a geometric average of each set of four blocks on the fine grid that equal one block in the 125×50 grid used here.

As is shown in Fig. 3, the pure Riemann approach agrees well with the mixed method (ECLIPSE velocity field +

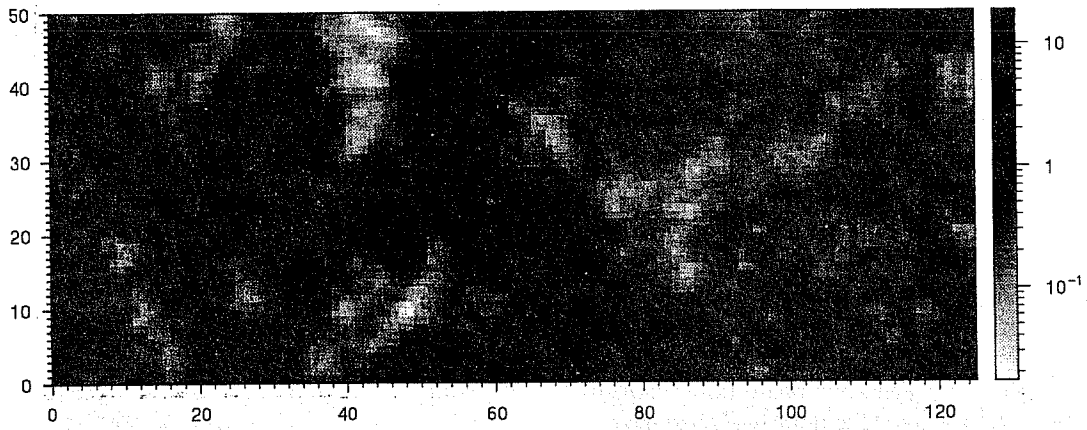


Fig. 2 Permeability map with logarithmic scaling (125 × 50 grid).

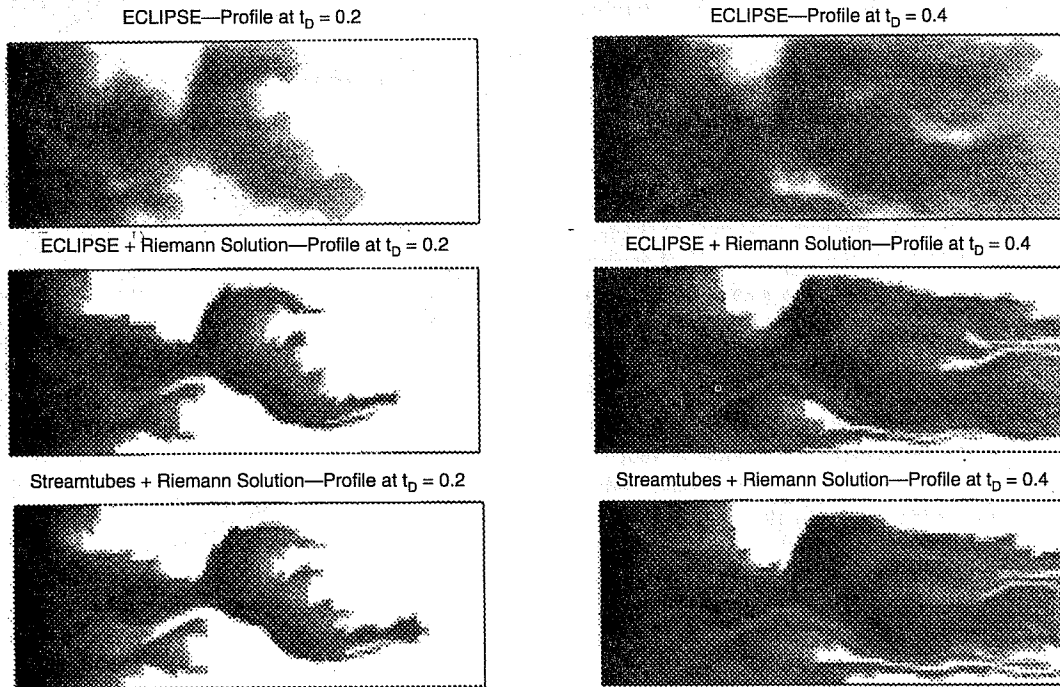


Fig. 3 Saturation profiles at times $t_D = 0.2$ and $t_D = 0.4$. From top to bottom: profiles obtained directly from ECLIPSE, profiles obtained by using the velocity field from ECLIPSE but mapping a Riemann solution along streamtubes, and profiles obtained by the method proposed in this work.

Riemann solution). Both are seen to be devoid of numerical dispersion, as expected, compared with the saturation profiles obtained directly from ECLIPSE. Figure 3 displays profiles for dimensionless times $t_D = 0.2$ and $t_D = 0.4$. The upper row shows saturation profiles obtained directly from ECLIPSE. The middle row shows profiles obtained using the velocity from ECLIPSE (and consequently the streamtubes) but mapping the solution as a Riemann solution. The last row shows profiles obtained by using the Riemann approach only to solve the entire nonlinear problem.

The difference between the two methods is small, which suggests that the nonlinearity of the velocity field is captured correctly by the direct Riemann approach. It is interesting to note that numerical dispersion causes a larger difference in

recovery than the direct Riemann solution method. Figure 4 shows the differences in recovery performance for the three methods. The recovery curve obtained from the mixed method (ECLIPSE velocity field + Riemann solution) lies above the recovery curve obtained directly from ECLIPSE. Because the velocity fields for these two recovery curves are identical, the difference must be attributed to numerical dispersion and the way in which the 1-D solution is mapped along the streamtubes. That numerical dispersion may have the upper hand is suggested by the saturation profiles shown in Fig. 5.

Although this numerical experiment does not prove that the 2-D solution is scalable by x_D/t_D along streamtubes, it suggests that the differences in the velocity field compared with a traditional finite-difference approach are small and

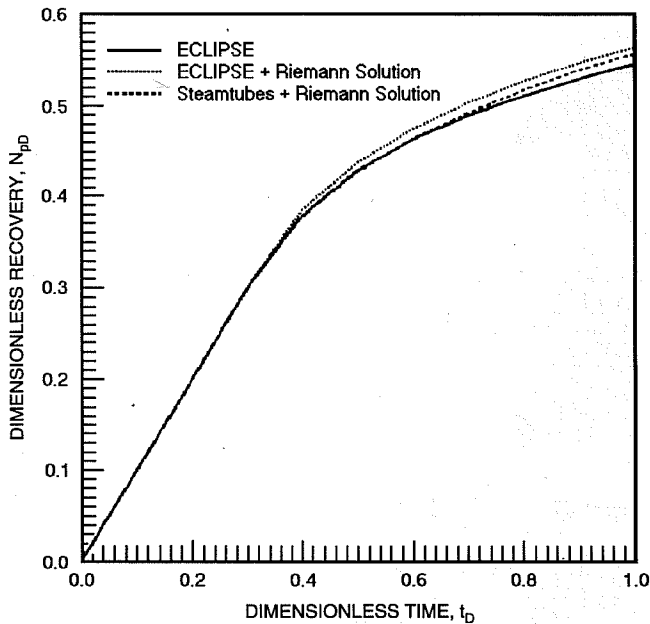


Fig. 4 Recovery curves for the three different solution methods used to generate the profiles in Fig. 3.

that numerical dispersion can lead to larger deviations than those caused by assuming a Riemann solution along streamtubes.

Convergence of the Riemann Approach

Before using the Riemann approach to investigate other immiscible cases, the issue of convergence is addressed. In other words, at what rate must the streamtubes be recalculated in order to consider the solution converged? If the two-phase immiscible problem is weakly nonlinear, then it may require fewer updates of the pressure (or Ψ -field) than currently used in finite-difference simulators and thus lead to a substantial speedup. Finite-difference simulators usually use a CFL (Courant, Friedrichs, and Lewy⁷) type stability criterion for the discretized hyperbolic conservation equation to determine when to resolve for the pressure field. In such methods the pressure field is recalculated at every time step.

In the streamtube approach, the conservation equation is not discretized, and therefore there is no CFL condition. The question that arises, instead, is how many times the streamtubes must be updated to consider the solution converged? This question is addressed by solving the previous problem repeatedly while increasing the number of streamtube updates over 2 pore volumes (PV) injected. Recovery curves for 1, 10, 20, 40, and 100 streamtube updates are shown in Fig. 6.

It is surprising to find that 20 updates are sufficient to consider the problem converged over a range of 2 PV. With only 20 updates, the new approach represents a reduction in computation time by two orders of magnitude compared with the thousands of updates needed by a traditional finite-difference simulator like ECLIPSE.

Thus two important points can be made:

1. The displacement is only weakly nonlinear. Although the end-point mobility ratio is 10, it is the shock-front mobility ratio of 1.36 that dictates the severity of the nonlinearity. Far fewer updates of the pressure field are required than used by traditional finite-difference simulators, which leads to a two-orders-of-magnitude speedup.

2. The dominating factor in the displacement is not the viscous instability caused by the difference in viscosity of the fluids but rather the reservoir heterogeneity and preferential flow channels. Because viscous instability is the more difficult problem to solve, this is an encouraging result.

Other Immiscible Solutions

This section considers other immiscible cases intended to verify further the streamtube method as well as to gain some physical insight. Many parameters affect the displacement efficiency, and an exhaustive investigation would have to consider them all. Because the scope of this research is to understand miscible displacements, only two parameters are investigated: (1) the end-point mobility ratio and (2) the correlation length of the reservoir. Except where noted, the relative permeabilities are assumed fixed and given by $k_{rw} = S_w^2$, $k_{ro} = S_o^2$.

End-Point Mobility Ratio. The end-point mobility is simply varied by increasing the resident fluid viscosity, in this case that of the oil. The end-point mobility is defined as

$$M_{\text{end}} = \frac{\lambda_J}{\lambda_I} = \left(\frac{k_r}{\mu} \right)_J \left(\frac{\mu}{k_r} \right)_I = \frac{\mu_o k_{rw}}{\mu_w k_{ro}} \quad (1)$$

where the subscript I refers to initial conditions and J refers to injected conditions. As is shown in Figs. 7 and 8, the changing end-point mobility ratio seems to affect the rate of convergence only, with the $M_{\text{end}} = 1$ case requiring one update, the $M_{\text{end}} = 3$ less than 10, the $M_{\text{end}} = 5$ approximately 10, and the $M_{\text{end}} = 10$ to 20 updates mentioned earlier. The converged recovery curves all compare in the same way with the recovery curves obtained from ECLIPSE. As discussed previously, the differences can be attributed to numerical dispersion caused by the finite-difference formulation in ECLIPSE. ECLIPSE consistently underestimates recoveries compared with the recoveries obtained from the streamtube approach; this is surprising because it is usually assumed that numerical dispersion increases recovery because it mitigates viscous instability and thereby reduces viscous fingering and early breakthrough. One possible explanation in this case is that numerical dispersion smears the shock front and thus reduces its effectiveness in recovering the oil ahead of it. Because the streamtube actually uses an analytical solution along each streamtube, the piston-like recovery mechanism remains intact and predicts a higher oil recovery from the reservoir. In fact, the true physical answer may lie somewhere between the two, but these results are significant because, for

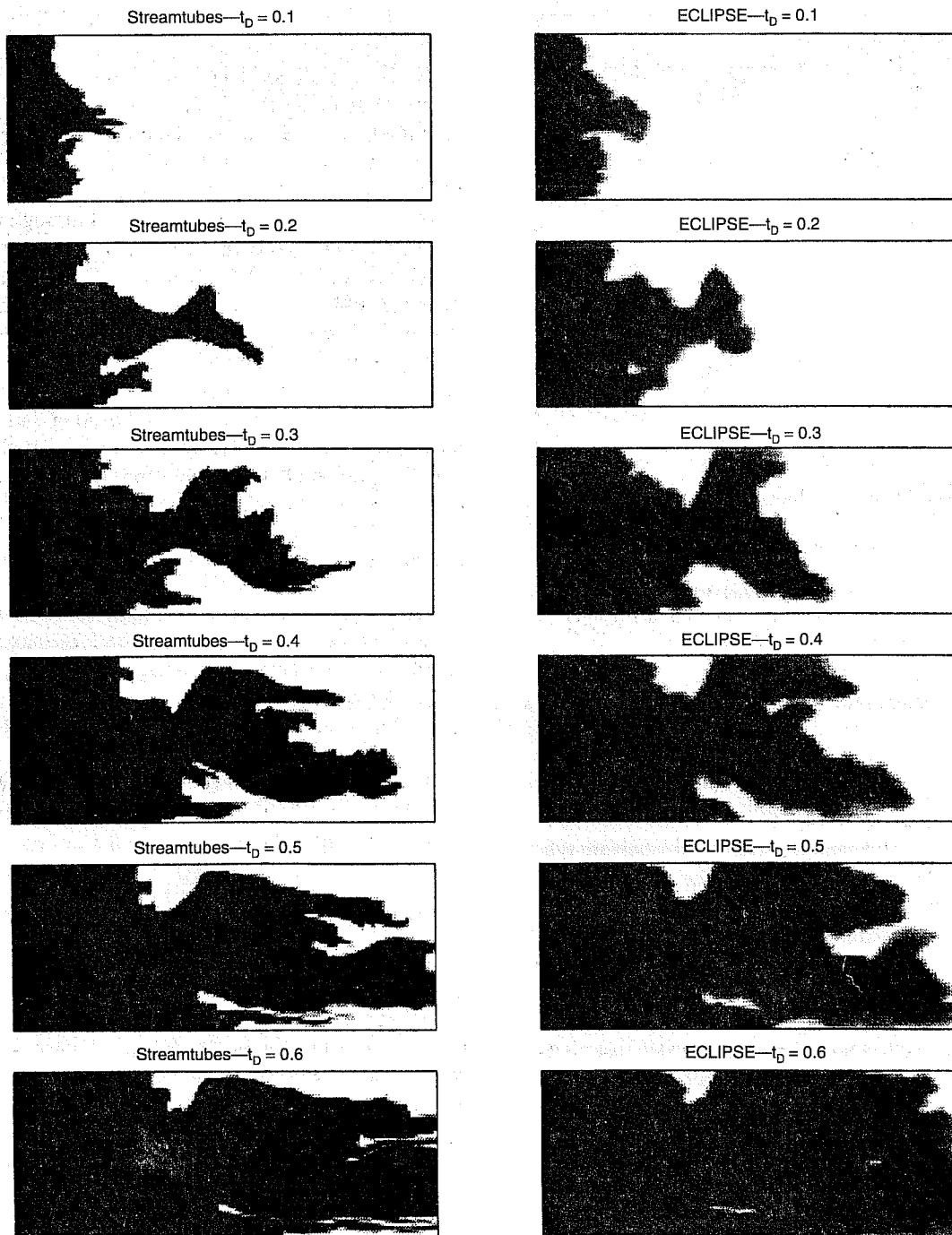


Fig. 5 Displacement history at $\Delta t_D = 0.05$ intervals for a Buckley-Leverett problem with a fractional flow given by Fig. 1.

the first time, the effects of numerical dispersion on recovery are quantifiable.

Data for another example are shown in Fig. 9. In this case the end-point relative permeability of the oil phase is $k_{ro}|_{S_o=1} = 0.25$. Keeping the same exponents as before and assuming an oil-to-water viscosity ratio of 10 ($\mu_o = 10, \mu_w = 1$) leads to an end-point mobility ratio of $M_{end} = 40$. But even in this case, as the recovery curve in Fig. 10 demonstrates, the

streamtube method is able to capture the nonlinearity within 20 updates.

Reservoir Heterogeneity. To understand the impact of reservoir heterogeneity on recovery, the $M_{end} = 10$ 1-D solution of Fig. 1 was used to find recoveries up to 2 PV injected for the three permeability fields shown in Fig. 11. All three permeability fields have a four-orders-of-magnitude variation in absolute permeability and differ only

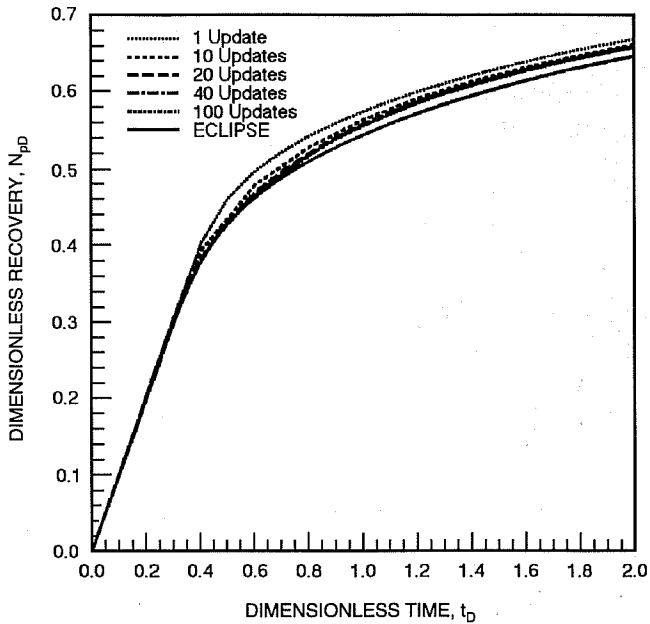


Fig. 6 Recovery curves for 1, 10, 20, 40, and 100 streamtube updates over 2 pore volumes injected ($t_D = 2$) showing that the problem can be considered converged if more than 20 updates are used.

in the correlation length. The recoveries are shown in Fig. 12.

As in the end-point mobility case, the streamtube method is able to give some interesting insight that may not have been observable with a standard finite-difference simulator. For example, the recovery curves suggest that the degree of the nonlinearity of the problem is actually dependent on the reservoir heterogeneity present. A permeability field with a very short correlation length tends to mitigate the nonlinearity (see case with $\lambda_c = 0.02$), whereas longer correlation lengths allow for a stronger nonlinear behavior (see case with $\lambda_c = 0.6$). Short correlation lengths promote the growth of many fingers, but no single finger is able to grow into a dominant flow channel that will characterize the recovery curve. As soon as a finger begins to grow beyond the field's correlation scale, there is a high probability that it will encounter a low-permeability region and slow down. Therefore the nonlinearity is not as noticeable in the geometry of the streamtubes because all streamtubes expand and contract many times over the duration of the displacement and end up, on average, to behave like streamtubes from the unit mobility case. The correct recovery curve can be obtained by simply solving for the streamtubes once and mapping the appropriate Buckley–Leverett solution. The success of that approach is clearly shown by the recovery curves for

$\lambda_c = 0.02$ in Fig. 12, which practically fall on top of each other.

As the correlation length increases, the nonlinearity becomes more noticeable; in fact, for a $\lambda_c = 0.6$, the converged solution is reached at about 40 updates. The long correlation length produces a clear path of least resistance between the inlet and outlet, which the fluid enters readily. A dominant flow channel is created and early breakthrough occurs. As a result, the nonlinearity of the problem is accentuated, which means that the injected phase increases its total velocity along the path until it reaches the outlet end (this increasing total velocity is the nonlinearity). Capturing this continuous increase in total velocity is what requires the more updates of the streamtubes compared with the shorter correlation length cases. It should be emphasized at this point that “more” is to be understood within the context of streamtubes but still compares favorably to the thousands of updates a traditional finite-difference simulator would require.

Conclusions

1. Two-phase problems for 2-D heterogeneous reservoirs can be solved efficiently by mapping a 1-D Buckley–Leverett solution onto streamtubes.
2. The combination of Riemann solutions and streamtubes leads to solutions that are devoid of numerical dispersion.
3. Computations with the Riemann streamtube approach are orders of magnitude faster than comparable finite-difference computations.

Nomenclature

t_D	dimensionless time
x_D	dimensionless length
k_{rw}	relative permeability of water
k_{ro}	relative permeability of oil
S_w	water saturation
S_o	oil saturation
M_{end}	end-point mobility ratio
M_{shock}	shock-point mobility ratio
λ_T	initial mobility
λ_j	injected mobility
λ_l	injected length
λ_c	correlation length
μ_w	water viscosity
μ_o	oil viscosity
N_{PD}	dimensionless recovery
HI	Heterogeneity Index

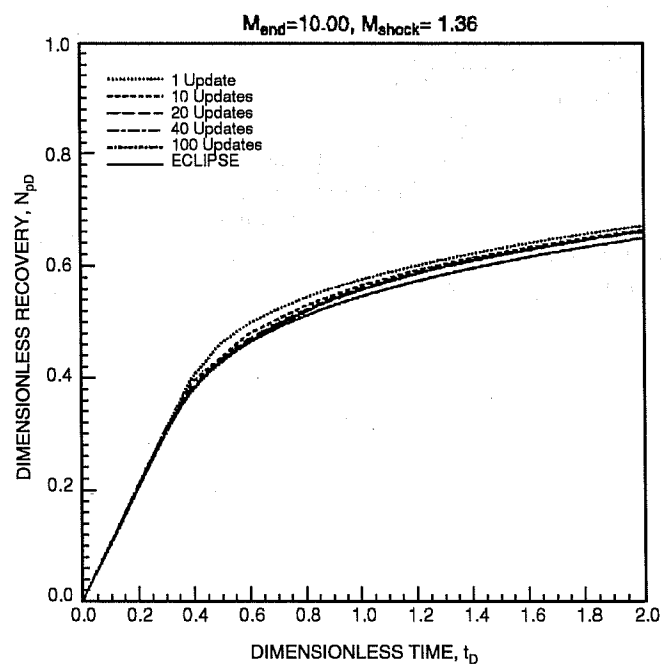
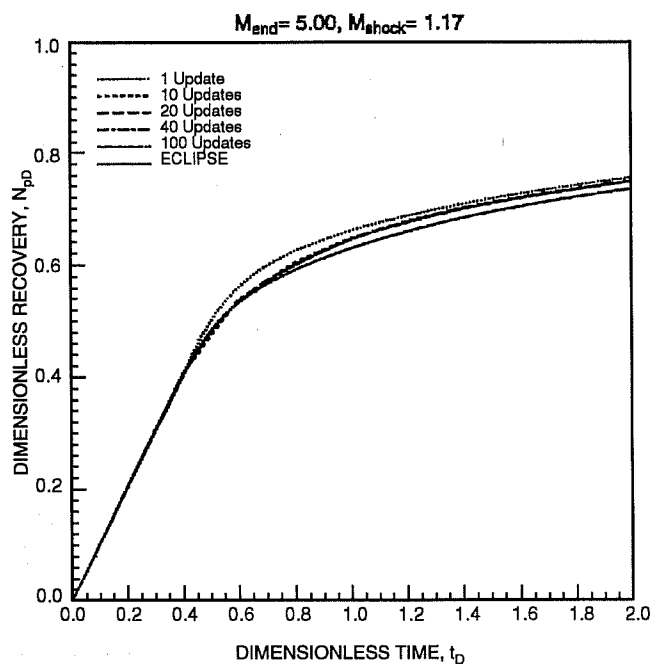
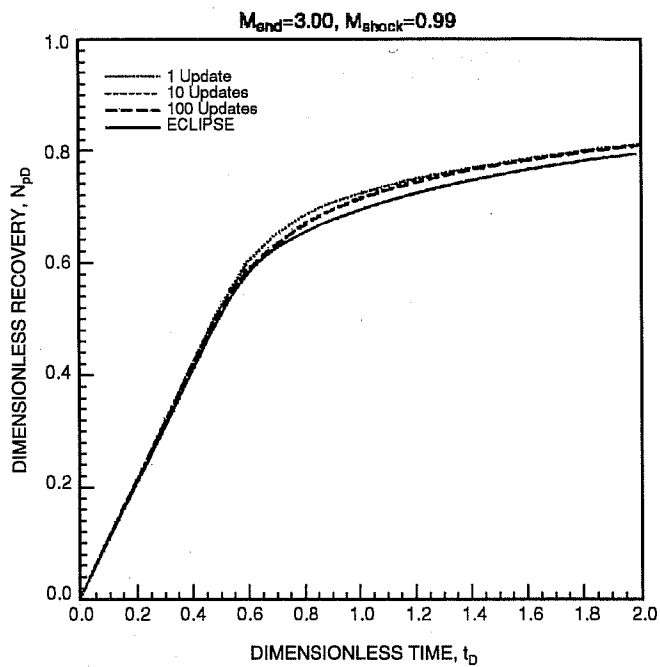
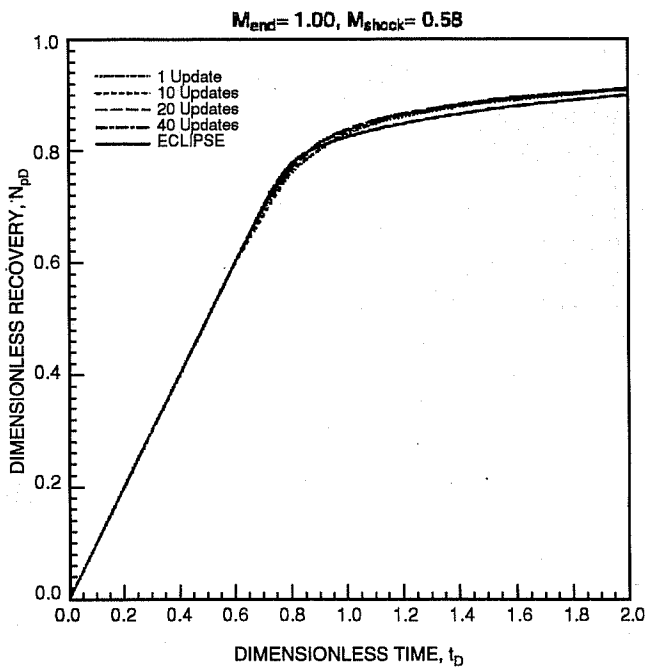


Fig. 7 Recovery curves showing convergence of the streamtube approach and comparison with recovery curves obtained from ECLIPSE.

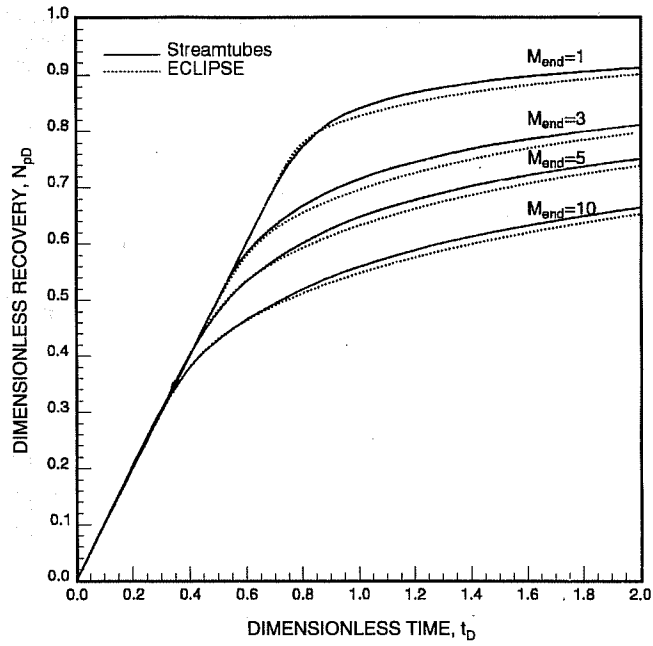


Fig. 8 Summary of converged recovery curves.

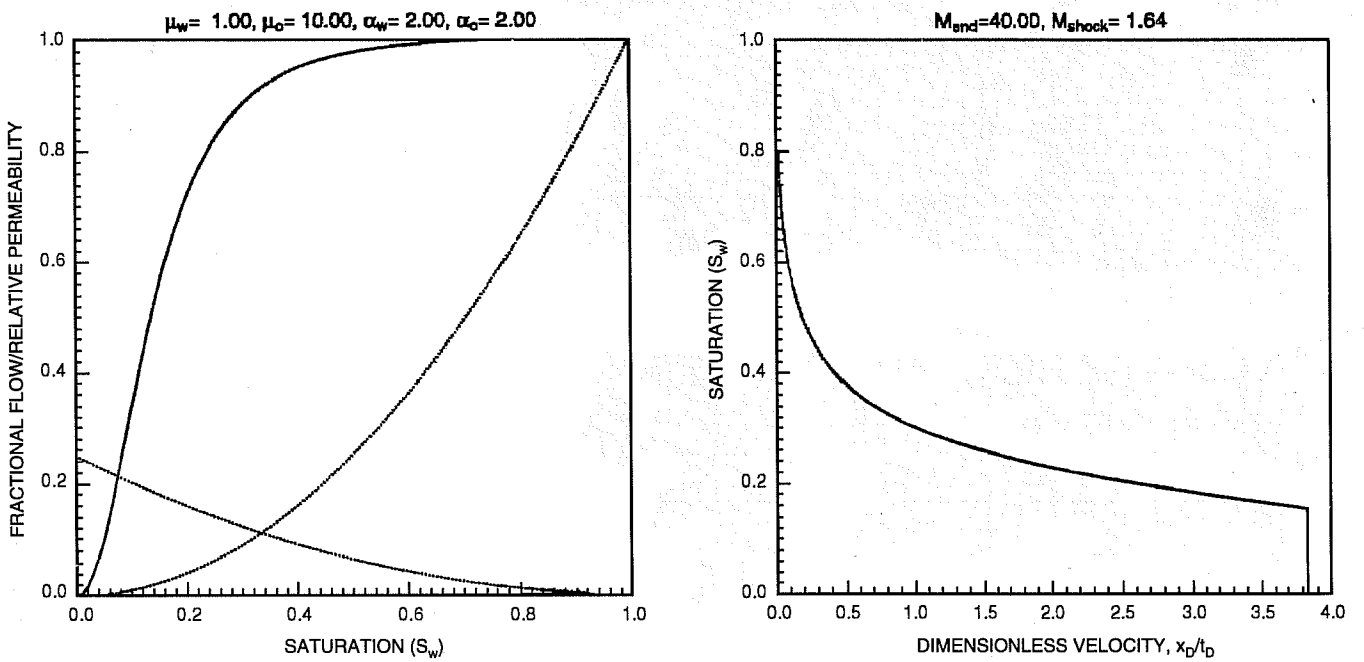


Fig. 9 Relative permeabilities, fractional flow, and one-dimensional saturation profile for $M_{end} = 40$. The shock-front mobility ratio is $M_{shock} = 1.64$. ($k_{rw} = S_w^2$, $k_{ro} = S_o^2$, $\mu_o = 10$, $\mu_w = 1$).

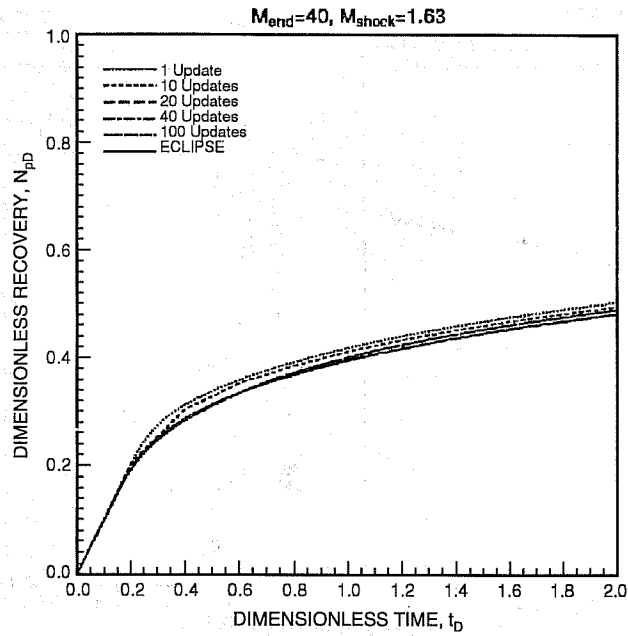


Fig. 10 Recovery curves for the data shown in Fig. 9.

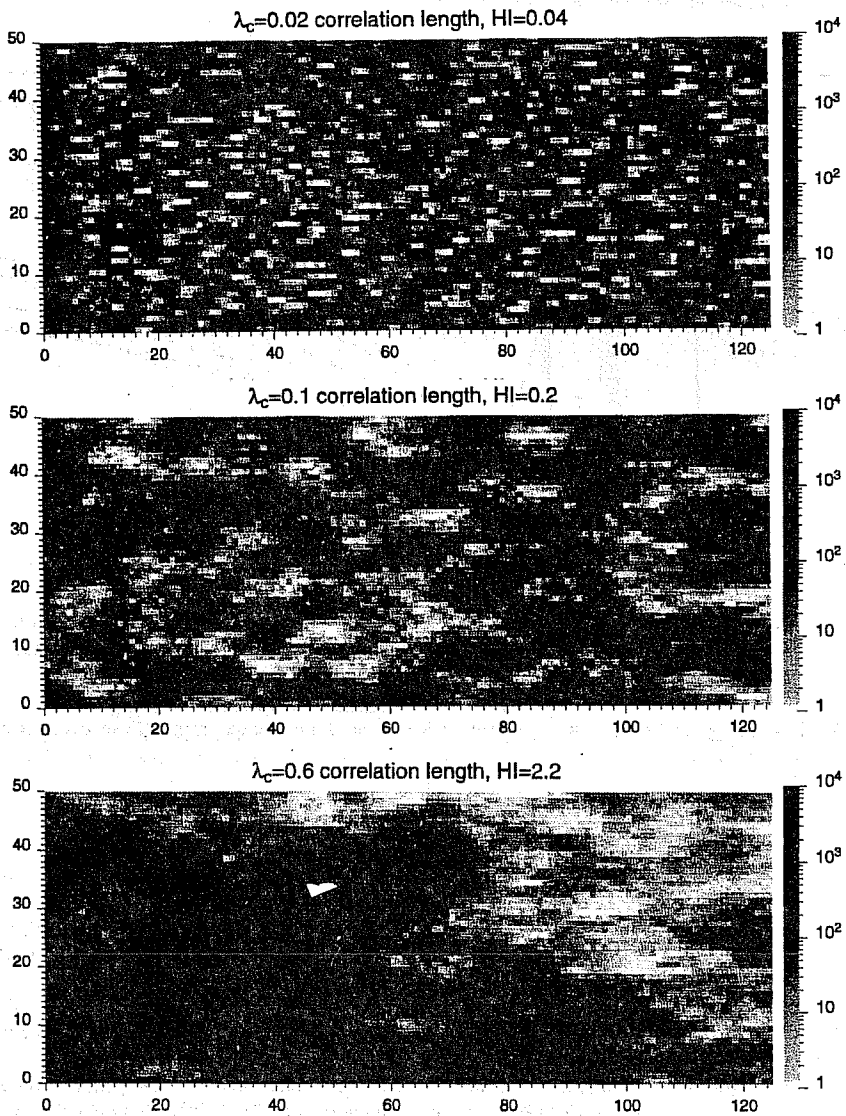


Fig. 11 Permeability fields differing only in correlation length. Correlation lengths from top to bottom: 0.02 [Heterogeneity Index ($HI = 0.04$)], 0.1 ($HI = 0.2$), and 0.6 ($HI = 2.2$) of reservoir dimensions.

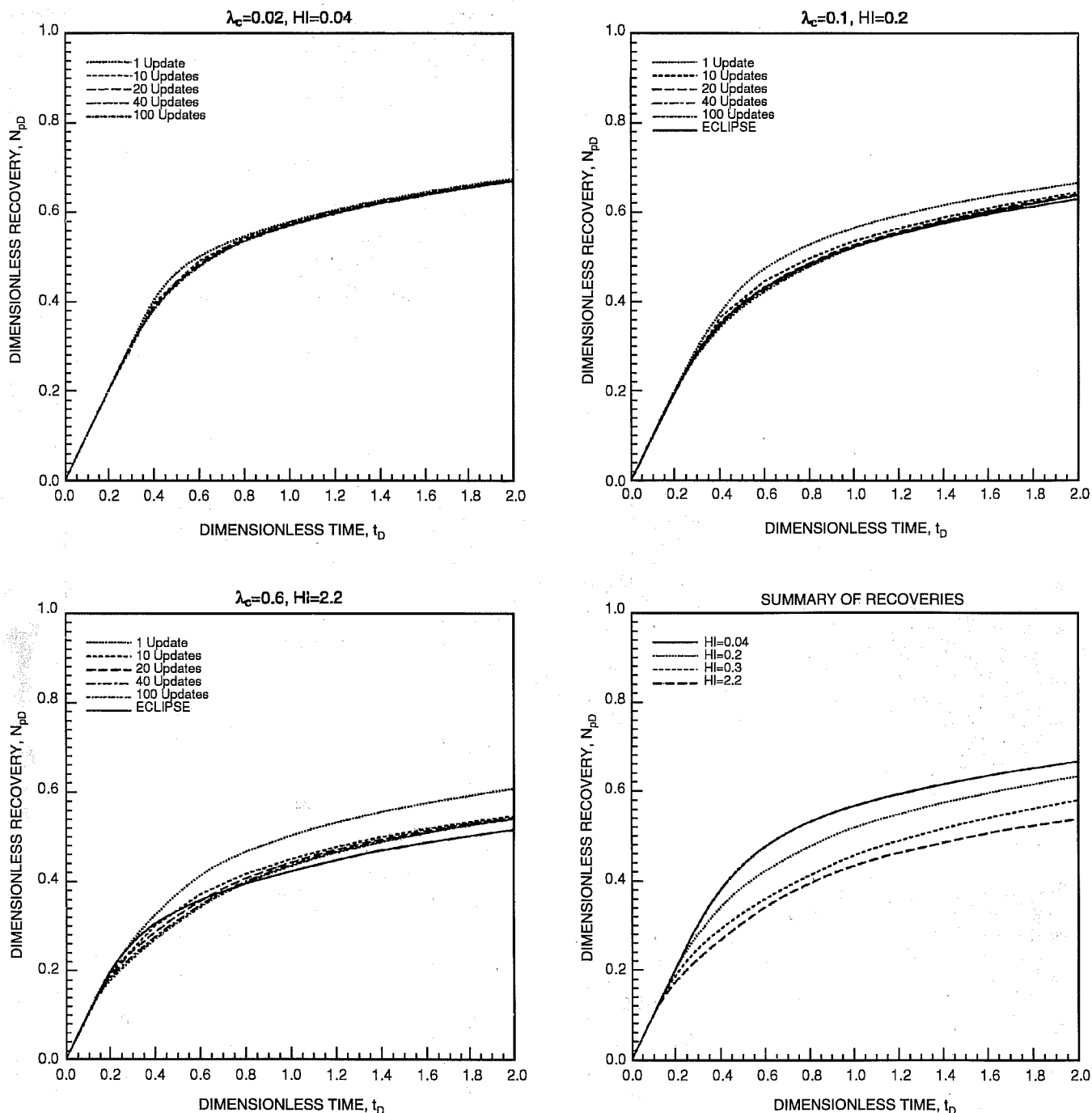


Fig. 12 Recovery curves for permeability fields of Fig. 11 showing convergence of the streamtube approach and comparison with recovery curves obtained from ECLIPSE.

References

1. G. Renard, A 2D Reservoir Streamtube EOR Model with Periodical Automatic Regeneration of Streamlines, *In Situ*, 14(2): 175-200 (1990).
2. T. Hewett and R. Behrens, Scaling Laws in Reservoir Simulation and Their Use in a Hybrid Finite Difference/Streamtube Approach to Simulation of the Effects of Permeability Heterogeneity, *Reservoir Characterization, II*, L. Lake and J. Carroll (Eds.), Academic Press Inc., London, 1991.
3. R. V. Higgins and A. J. Leighton, A Computer Method to Calculate Two-Phase Flow in Any Irregularly Bounded Porous Medium, *J. Pet. Technol.*, 679-683 (June 1962).
4. R. V. Higgins, D. W. Boley, and A. J. Leighton, Aids to Forecasting the Performance of Water Floods, *J. Pet. Technol.*, 19: 1076-1082 (September 1964).
5. J. C. Martin and R. E. Wegner, Numerical Solution of Multiphase, Two-Dimensional Incompressible Flow Using Streamtube Relationships, *SPEJ, Soc. Pet. Eng. J.*, 19: 313-323 (October 1979).
6. M. Thiele and M. Blunt, Predicting Flow in Heterogeneous Systems Using Streamtubes, *Annual Report (1993)*, DOE Grant No. DE-FG22-

92BC14852, U.S. Department of Energy, Bartlesville, Okla. (October 1993).

7. R. Courant, K. O. Friedrichs, and H. Lewy, Ueber die partiellen Differenzgleichungen der mathematischen Physik, *Math. Ann.*, 100: 32-74 (1928).



THERMAL RECOVERY— SUPPORTING RESEARCH

HORIZONTAL OIL WELL APPLICATIONS AND OIL RECOVERY ASSESSMENTS

Contract No. DE-AC22-93BC14861

**Maurer Engineering Inc.
Houston, Tex.**

**Contract Date: June 3, 1993
Anticipated Completion: June 2, 1994
Government Award: \$124,119**

**Principal Investigator:
William J. McDonald**

**Project Manager:
Thomas Reid
Bartlesville Project Office**

Reporting Period: Oct. 1–Dec. 31, 1993

Objective

The primary objective of this project is to examine factors affecting technical and economic successes of horizontal well applications. The goals of the project will be accomplished through five tasks designed to evaluate the technical and economic successes of horizontal drilling, highlight current

limitations, and outline technical needs to overcome these limitations. Data describing experiences of the operators throughout the domestic oil and gas industry will be gathered and organized. Maurer Engineering Inc. (MEI) databases containing detailed horizontal case histories will also be used. All data will be categorized and analyzed to assess the status of horizontal well technology and to estimate the impact of horizontal wells on present and future domestic oil recovery and reserves.

Summary of Technical Progress

Information Base on Horizontal Wells

A spreadsheet data file was constructed from well data describing 3885 domestic horizontal wells, the total as of summer 1993. Three principal formations are the focus of the majority of this activity: the Austin Chalk in Texas, the Bakken Shale in North Dakota, and the Niobrara in Colorado and Wyoming. Results from these fields are well known, and a large volume of published results is available. Given the objective of the present study, it was decided to limit the analyses to formations other than these three fractured carbonates. On the basis of domestic well data, 431 horizontal wells have been completed in other formations.

About 180 operators drilled these other wells in a total of 112 formations. Contacts were located for 150 of these companies, who were telephoned about the project and sent a

questionnaire. Questionnaires covering over 60% of the wells have been returned.

An extensive review of the literature was conducted on these other applications. Over 70 technical articles were reviewed and analyzed for data pertinent to the study. Information from these articles is being compiled into a comprehensive discussion of horizontal applications to be included as a section of the final report.

Specialized Database for Horizontal Well Forecasting

A database for the questionnaire formation data was constructed in dBASE IV. Questionnaires have been received from several sources, including operators listed in the original well data file, participant companies in the DEA-44 Horizontal Well Technology joint-industry project, attendees of the Horizontal Technology Forum held in Calgary during July 1993, and attendees of the Horizontal Technology Forum held in Houston, Tex., during September 1993.

Over 160 records (1 for each returned questionnaire) have been generated. A few questionnaires describing formations outside the scope of this study, including Austin Chalk wells and wells outside the United States, have been returned. These data may be evaluated at a later date.

Economic and Technical Trend Analysis

Multiple analyses have been performed on the database. Overview analyses were designed to determine the types and frequencies of the various applications of horizontal technology. Results are shown for 58 formations in Fig. 1. Applications reported include (1) intersect natural fractures, (2) target thin formations, (3) layered or heterogeneous formation(s), (4) water or gas coning, (5) surface restrictions, (6) water drive–water injection, (7) low permeability, (8) gravity drainage, (9) enhanced oil recovery (EOR), and (10) favorable economics. Multiple responses were typical; therefore the results shown in the figure total more than 100%. The three most common applications include intersecting fractures (53%), delaying coning (33%), and economics (35%). Least-used applications include surface restrictions (7%) and water drive and EOR (both with less than 9%).

Operators were asked whether their horizontal applications in each field were technical and/or economic successes. Not unexpectedly, most programs were indicated as technically successful. Of 57 responses, 54 were technically successful, which represents a 95% success rate. This high rate of success suggests that horizontal technology has advanced to the point that the majority of technical barriers to placing a well in the ground can be overcome.

Economic success has not been as widespread as technical success. Of 56 responding formations, 28 were economic successes (50%) and 24 were economically unsuccessful (43%). An additional 4 formations (7%) had mixed eco-

nomic results (i.e., multiple operators in a particular field reported both successful and unsuccessful projects). Economic success can be negatively affected by several factors not related to horizontal technology per se, including poor choice of well location and improper application. A played-out field may also not yield enough flow to rate economic success, although horizontal implementation was successful.

Technical and economic successes of the formations in the survey are summarized by lithology in Fig. 2. When lithology is considered, the data suggest that carbonate applications have been slightly more technically successful than clastic: 100% vs. 91%. This difference may reflect the lack of experience with the larger variety of clastic formation types and applications rather than indicate inherent technical difficulties. Conversely, clastic applications reported more economic success than carbonates: 59% vs. 45%, respectively.

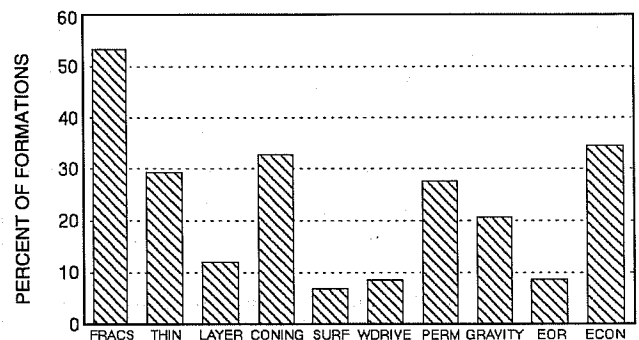


Fig. 1 Horizontal technology applications (58 formations). FRACS, intersect natural fractures; THIN, target thin formations; LAYER, layered or heterogeneous formations; CONING, water or gas coning; SURF, surface restrictions; WDRIVE, water drive–water injection; PERM, low permeability; GRAVITY, gravity drainage; EOR, extended oil recovery; and ECON, favorable economics.

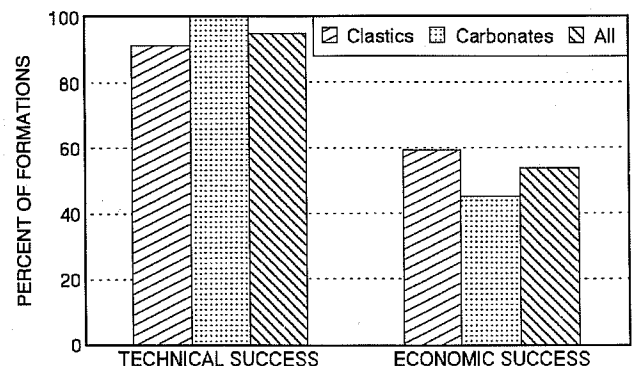


Fig. 2 Technical and economic successes.

Horizontal Well Application Forecast

Another key parameter in the project data is the estimated increase in reserves as a result of implementing horizontal

technology. Results from 47 formations (Fig. 3) show that over half the operators have seen an increase of greater than 5%. Horizontal wells are expected to increase recoverable reserves through, for example, delaying the onset of water coning or accessing oil not economically recoverable with vertical wells.

According to the Tertiary Oil Recovery Information System (TORIS), proven U.S. oil reserves amount to about 27 billion bbl. This volume represents 5% of the total domestic original oil in place of 513 billion bbl. Increases in these reserves, as reported by survey respondents, ranged from 0 to 300%. The overall average increase is 24.6%. Extrapolated to the total U.S. reserves base, this represents an additional 6.6 billion bbl of reserves as the result of widespread and appropriate application of horizontal technology. Forecasts of the number of horizontal wells to be drilled over the next decade in various drilling environments and applications will be analyzed.

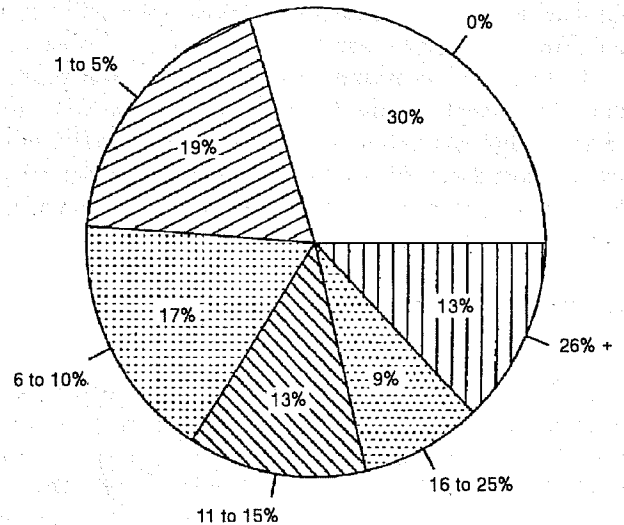


Fig. 3 Chart showing reserves increase with horizontal wells (average increase, 24.6%).

STUDY OF HYDROCARBON MISCIBLE SOLVENT SLUG INJECTION PROCESS FOR IMPROVED RECOVERY OF HEAVY OIL FROM SCHRADER BLUFF POOL, MILNE POINT UNIT, ALASKA

Contract No. DE-FG22-93BC14864

University of Alaska
Fairbanks, Alaska

Contract Date: Dec. 1, 1992

Anticipated Completion: June 30, 1996

Total Project Cost:

DOE Funding for FY93	\$200,000
Contractor	<u>129,726</u>
Total	\$329,726

Principal Investigator:
G. D. Sharma

Project Manager:
Thomas Reid
Bartlesville Project Office

Reporting Period: Oct. 1–Dec. 31, 1993

Objectives

The ultimate objective of this 3-yr research project is to evaluate the performance of the hydrocarbon miscible sol-

vent slug process and to assess the feasibility of this process for improving recovery of heavy oil from Schrader Bluff reservoir. This will be accomplished through measurement of pressure-volume-temperature (PVT) and fluid properties of Schrader Bluff oil, determination of phase behavior of Schrader Bluff oil solvent mixtures, asphaltene precipitation tests, slim-tube displacement tests, coreflood experiments, and reservoir simulation studies. The expected results from this project include determination of optimum hydrocarbon solvent composition suitable for hydrocarbon miscible solvent slug displacement process, optimum slug sizes of solvent needed, solvent recovery factor, solvent requirements, extent and timing of solvent recycle, displacement and sweep efficiency to be achieved, and oil recovery.

Summary of Technical Progress

During this quarter calibration and testing of the miscible coreflood apparatus were completed. Displacement experiments using this apparatus began. Displacement experiments in the slim tube have been started to verify the previously conducted slim-tube simulation results.

Coreflood Experiments

An unsteady-state waterflood experiment was performed with live Schrader Bluff crude oil. In this experiment, the core holder was packed with Oklahoma No. 1 sand. The porosity and absolute permeability of the core were 33.8% and 5.1 darcys, respectively. The core was first saturated with water and an initial water saturation was established

by displacement of the water with live Schrader Bluff crude oil. The oil was then displaced by injection of water at a constant rate of 4 cm³/min. Oil production, water production, and pressure drop across the core were monitored. Figure 1 shows the oil recovery and water/oil ratio (WOR) as functions of pore volumes (PV) of water injected. The breakthrough oil recovery was about 30%, but oil production continued beyond breakthrough, and the recovery was 61% at 1.8 PV injection. Such behavior can be expected when water displaces a high-viscosity oil.

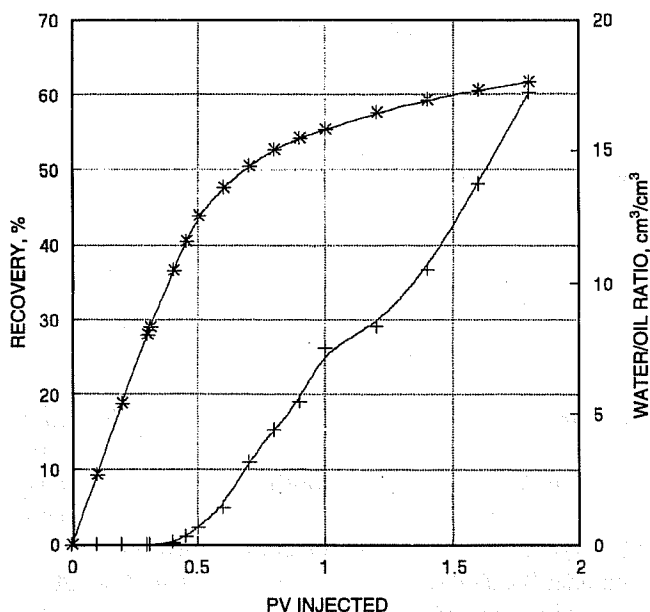


Fig. 1 Oil recovery (+) and water/oil ratio (*) for unsteady-state water-flood experiment.

Slim-Tube Experiments

The slim tube is composed of a 12-m section of 6.4-mm-outside-diameter high-pressure stainless steel tubing, which is packed with Ottawa sand and coiled to a diameter of approximately 1 ft. The porosity of the slim tube is 35.2%, and permeability was calculated to be 5.0 darcys with the use of pure toluene as the test fluid of known viscosity. Two runs were completed during this quarter.

100% Kuparuk-Schrader Bluff Gas at 1300 psia and 72 °F

This was the first run conducted in the slim-tube apparatus with pure Kuparuk-Schrader Bluff gas as solvent at 1300 psia and 72 °F. This run resulted in recovery of 37.8% at 1.2 PV injection (Fig. 2). This shows that there is no development of miscibility. Also, sight glass observations showed two separate phases. Figure 3 shows that solvent break occurred at around 57% PV injection.

100% Prudhoe Bay Gas at 1300 psia and 72 °F

This run was conducted with 100% Prudhoe Bay Gas as solvent at 1300 psia and 72 °F. This run resulted in recovery of 45% at 1.2 PV injection (Fig. 4). This clearly shows that there is no development of miscibility. Sight glass observations also showed the presence of two separate phases. Figure 5 shows that solvent break occurred around 59% PV injection.

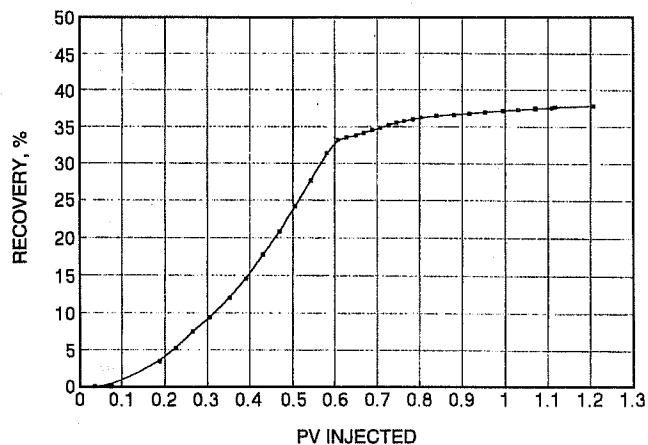


Fig. 2 Recovery vs. pore volume injected. Solvent, 100% Kuparuk Bluff gas.

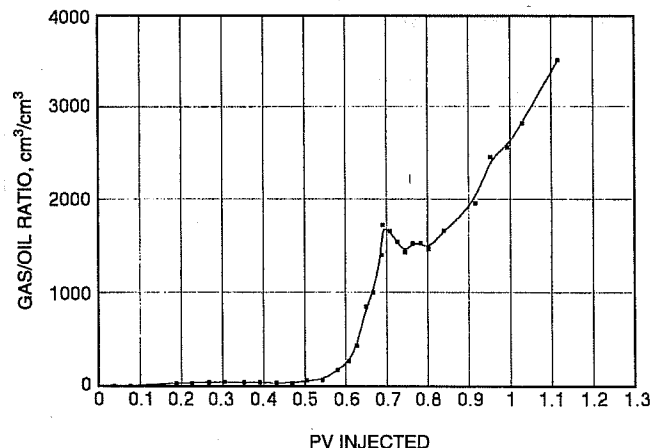


Fig. 3 Gas/oil ratio vs. pore volume injected. Solvent, 100% Kuparuk-Schrader Bluff gas.

Future Work Plan

Coreflood experiments with live Schrader Bluff oil and miscible solvents will continue. With injection of miscible solvents, effects of slug size and water-alternating-gas (WAG) ratio will be examined. Slim-tube experiments will also continue with solvents such as CO₂ and natural gas with various enrichments with natural gas liquids.

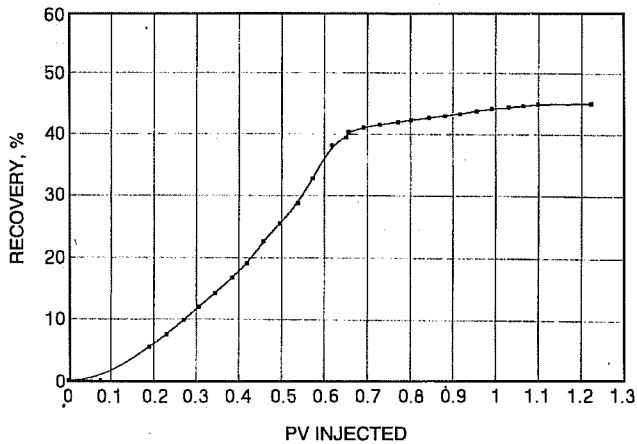


Fig. 4 Recovery vs. pore volume injected. Solvent, 100% Prudhoe Bay gas.

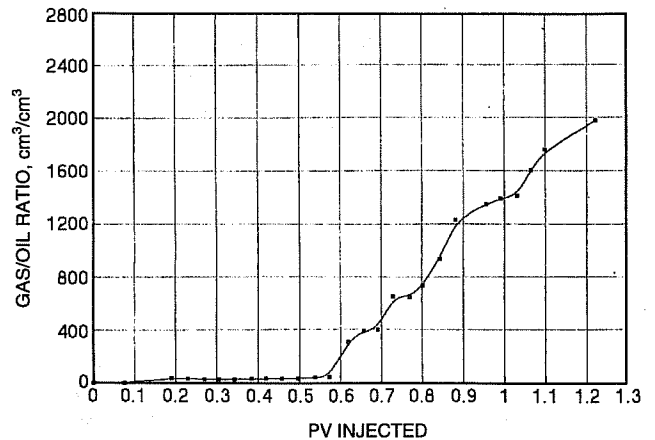


Fig. 5 Gas/oil ratio vs. pore volume injected. Solvent, 100% Prudhoe Bay gas.

**MODIFICATION OF RESERVOIR
CHEMICAL AND PHYSICAL FACTORS
IN STEAMFLOODS TO INCREASE
HEAVY OIL RECOVERY**

Contract No. DE-FG22-90BC14899

University of Southern California
Los Angeles, Calif.

Contract Date: Feb. 22, 1993
Anticipated Completion: Feb. 21, 1996
Government Award: \$150,000
(Current year)

Principal Investigator:
Yanis C. Yortsos

Project Manager:
Thomas Reid
Bartlesville Project Office

Reporting Period: Oct. 1–Dec. 31, 1993

Objectives

The objectives of this research are to continue previous work and to conduct new studies in the following fundamental areas of interest to thermal recovery: displacement and flow properties of fluids involving phase change (condensation–evaporation) in porous media, flow properties of mobility-control fluids (such as foam), and the effect of reservoir heterogeneity on thermal recovery. The specific projects address the need to improve heavy oil recovery from typical

reservoirs as well as from less conventional fractured reservoirs producing from vertical or horizontal wells.

Thermal methods, particularly steam injection, are currently recognized as the most promising for the efficient recovery of heavy oil. Despite significant progress, however, important technical issues remain unresolved. Specifically, knowledge of the complex interaction between porous media and the various fluids of thermal recovery (steam, water, heavy oil, gases, and chemicals) is still inadequate. Also, the interplay of heat transfer and fluid flow with pore- and macro-scale heterogeneity is largely unexplored.

Summary of Technical Progress

Vapor–Liquid Flow

Work has continued on the modeling of vapor–liquid flow in porous media. During the last quarter a Ph.D. Thesis was completed on this subject.¹ Currently a pore network simulator exists that accounts for the growth of the vapor phase by heat transfer in a single-component system. Various effects, such as the heat conduction rate and the importance of solid conductivity and heat convection, were analyzed. The work in progress involves extension to a three-phase system involving oil, water vapor, and water liquid under conditions that simulate steam displacement of oil.

The bubble-growth problem analyzed has an important application to thermal methods for the recovery of crude oils containing volatile components, where a natural solution gas-drive mechanism may develop at a certain temperature. Experiments conducted with sample crude oils in uniformly heated etched-glass micromodels showed that this process does actually occur after a certain temperature is reached. The growth of the vapor clusters can be modeled by a combination

of heat and mass transfer, a phenomenon examined in detail^{1,2} and also summarized.^{3,4} This natural solution gas drive may be important for the recovery of oil from naturally fractured systems. Still in progress is the analysis of the mechanisms of gravity drainage and film flow, which influence significantly the magnitude of the residual oil saturation.

Heterogeneity

Visualization experiments of steam displacement of various oils (natural and synthetic) in micromodel geometries mimicking a naturally fractured system were conducted. The objectives of this study were to identify the mechanisms operating during steam injection in naturally fractured systems. It was found that displacement occurs mostly by the imbibition of the condensed water. Penetration of the vapor phase into the matrix is also possible at higher rates, as reported in the analogous drainage experiments.⁵ However, it was found that in natural oils two additional mechanisms also operate, one involving a solution gas-drive mechanism and another involving the formation of stable lamellae, stabilized by natural surfactants, which act in a foam-like manner. Both of these mechanisms help to improve the displacement efficiency. Similar phenomena also apply to systems involving strongly correlated heterogeneities (such as permeability streaks).

Additional work on heterogeneities addressed effects of anisotropy, correlations, and permeability gradients in immiscible displacement. The effect of anisotropy on capillary pressure curves during invasion percolation was studied to relate capillary pressure to the direction of displacement.⁶ Effects of pore size correlations on drainage were investigated theoretically, with particular emphasis placed on the correlation of the saturation profile and the possibility of identification of the correlation of permeability from saturation measurements. This study is still in progress. Effects of permeability gradients were discussed in a technical paper.⁷ Finally, a study is in progress to investigate the applicability of conventional relative permeabilities to displacements in heterogeneous media.

In parallel, further progress has been made in the approximation of displacement processes by using the concept of vertical equilibrium (VE). A boundary effect associated with viscous fingering under these conditions has been identified. The relation of VE to empirical viscous fingering models is also being investigated. Finally, work has begun on the optimization of recovery processes with the use of optimal control methods.

Chemical Additives

In the area of chemical additives, work on the behavior of non-Newtonian fluid flow and displacement in porous media has continued. Experiments are being conducted to study displacement processes involving power-law fluids to test theoretical results previously obtained. Further work involving displacements of Bingham plastics has also been performed.

In the area of foam flow, efforts were focused on the development of a mechanistic pore-network simulator for gas displacement of a wetting phase in the presence of a surfactant. The simulator contains as a parameter the probability of snap-off in pore throats. A key rule in the simulation is the advancement of interfaces following a path of minimum resistance. The simulator predicts that a stable front develops, the propagation of which requires a minimum pressure gradient. The dependence of the latter on the porous media properties is being investigated.

References

1. C. Satik, Ph.D. Thesis, University of Southern California, December 1993.
2. X. Li, Ph.D. Thesis, University of Southern California, April 1993.
3. X. Li and Y. C. Yortsos, Bubble Growth in Porous Media, submitted to *Chem. Eng. Sci.*, 1993.
4. G. Satic, X. Li, and Y. C. Yortsos, Scaling of Bubble Growth in Porous Media, submitted to *Phys. Rev. Lett.*, 1993.
5. M. Haghighi, B. Xu, and Y. C. Yortsos, Visualization and Simulation of Immiscible Displacement in Fractured Systems Using Micromodels: 1. Drainage, *J. Colloid. Interface Sci.*, in press (1994).
6. B. Xu and Y. C. Yortsos, in preparation, 1994.
7. M. Chauouche, N. Rakotomalala, D. Salin, B. Xu, and Y. C. Yortsos, paper SPE 26658 presented at the 1993 SPE Annual Technical Conference and Exhibition, Houston, Tex., Oct. 3-6, 1993.

DETAILED EVALUATION OF THE WEST KIEHL ALKALINE-SURFACTANT-POLYMER FIELD PROJECT AND ITS APPLICATION TO MATURE MINNELUSA WATERFLOODS

Contract No. DE-AC22-93BC14860

**Surtek, Inc.
Golden, Colo.**

**Contract Date: Jan. 7, 1993
Anticipated Completion: Sept. 30, 1994
Government Award for FY93: \$165,148**

**Principal Investigator:
Malcolm J. Pitts**

**Project Manager:
Thomas Reid
Bartlesville Project Office**

Reporting Period: Oct. 1-Dec. 31, 1993

Objectives

The objectives of this research are to (1) quantify the incremental oil produced from the West Kiehl alkaline-surfactant-polymer (ASP) project by classical engineering and numerical simulation techniques, (2) quantify the effect of chemical slug volume injection on incremental oil in the two swept areas of the field, (3) determine the economic ramifications of the application of the ASP technology, (4) forecast the results of injecting an ASP solution to mature waterfloods and polymer floods, and (5) provide the basis for independent operators to book additional oil reserves by using the ASP technology.

This report documents the geological and reservoir engineering data developed. In addition, some laboratory results are discussed. Some evaluation of the West Kiehl has been published.^{1,2} The numerical simulation coreflood history match and the initial West Kiehl history match also are discussed.

Summary of Technical Progress

Geological and Reservoir Engineering Evaluation

A geological study of 72 fields surrounding the West Kiehl is complete. Of the 72 fields, 35 were studied in detail. Decline curve analysis was used to develop current and estimated ultimate oil recovery data for each of the 35 fields. From this list of 35 fields, 2 were selected for numerical simulation (polymer flood, Simpson Ranch; and waterflood, Prairie Creek South).

A series of geologic maps and cross sections were prepared for Prairie Creek South and Simpson Ranch. Reservoir simulation models will be run on both of these fields.

The remaining 33 fields were also subjected to reservoir analysis. Each of these fields has been mapped in a slightly less rigorous manner than West Kiehl, Prairie Creek South, and Simpson Ranch. Pore volumes (PV) and oil saturations were calculated. The production histories were subjected to decline analysis to determine ultimate primary and secondary oil recoveries. From the primary performance characteristics, reservoirs with a water drive, a partial water drive, and no water drive were defined. A table of information about each field, an isopach map, and a plot of the oil production, oil cut, and injection rate was developed for each of the 35 fields.

Laboratory Study

Two linear corefloods and seven radial corefloods were completed. Relative permeability analysis indicated that the Minnelusa Lower B sand is water-wet and the mobility ratio for water-displacing West Kiehl oil averages 2.2. Oil saturation shifts were from 0.788 to 0.343 PV for a recovery of 56.5% of the initial oil saturation by coreflooding. After the injection of polymer (Pusher 700) after the waterflood, no additional oil was recovered. After the injection of 0.8 wt % sodium carbonate (Na_2CO_3) plus 0.1 wt % Pestrostep B-100 plus Pusher 700, the oil saturation was reduced to 0.207 PV for an additional recovery of

0.136 PV of incremental oil or 39.7% of the waterflood residual oil. The dynamic retention of chemical from the linear corefloods averaged 72,966 lb/acre-ft for Na_2CO_3 , 5,123 lb/acre-ft for Pestrostep B-100, 723 lb/acre-ft for Pusher 700 injected with Na_2CO_3 plus Pestrostep B-100, and 314 lb/acre-ft when dissolved in Fox Hills injection water before injection with ASP solution. When Pusher 700 dissolved in injection water was injected after the ASP solution, an additional 49 lb/acre-ft was retained by the Minnelusa sand. On the basis of resistance factor and chemical retention data of these linear corefloods, the injection concentration of 1,050 mg/L Pusher 700 is sufficient for mobility control if 1 PV of polymer were injected.

Chemical oil recoveries of the radial corefloods with 4-in. radial disks are summarized in Table 1. The chemical floods were performed with no waterflood before chemical injection with the exception of two corefloods.

The average polymer flood performed no better than the average waterflood, 42.8% S_{oi} vs. 46.6% S_{oi} , respectively. However, after the injection of 0.8 wt % Na_2CO_3 plus 0.1 wt % Pestrostep B-100 plus 1050 mg/L Pusher 700, 15% S_{oi} was recovered. Additional oil was recovered when 30% PV or more of ASP slug was injected. Reducing the volume of ASP slug injected to 13% PV lowered the incremental oil production to 6.2% S_{oi} .

TABLE 1

Chemical Oil Recoveries of the Radial Corefloods with 4-in. Radial Disks

Chemical injected	Waterflood recovery, % S_{oi} *	Chemical flood recovery, % S_{oi} *	Combined recovery, % S_{oi} *
Waterflood followed by 37% PV ASP	45.4	12.6	58.0
Waterflood followed by 13% PV ASP	47.7	5.5	53.2
29% PV ASP-10% PV polymer	-	61.2	-
13% PV ASP-26% PV polymer	-	52.7	-
94% ASP-no polymer	-	65.9	-
43% polymer	-	40.0	-
35% polymer	-	45.7	-

* S_{oi} , initial oil saturation.

Numerical Simulation of the West Kiehl Field

Three radial corefloods were history matched to calibrate the chemical option of the numerical simulator. These included waterflood to residual oil saturation followed by Na_2CO_3 plus Pestrostep B-100 plus Pusher solution injection; Na_2CO_3 plus Pestrostep B-100 plus Pusher 700 injection; and Pusher 700 injection. The cumulative oil recovery, oil cut, and chemical production vs. produced fluids history matches are depicted in Fig. 1 for the ASP coreflood.

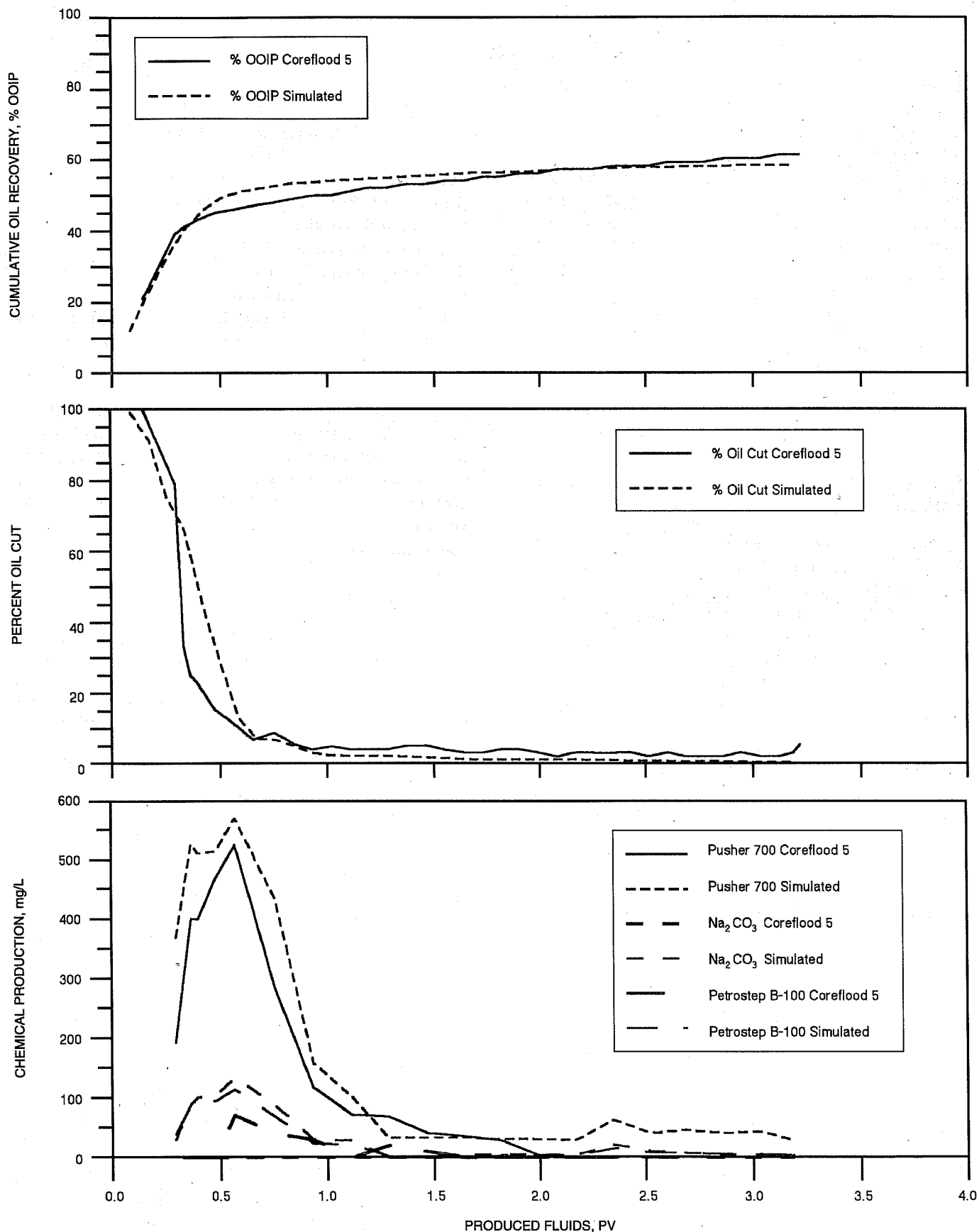


Fig. 1 West Kiehl cumulative oil recovery, oil cut, and chemical production vs. produced fluids. OOIP, original oil in place.

The initial West Kiehl reservoir model has been designed. The chemical flood model parameters defined in the coreflood history matches have been incorporated into the numerical simulator. A history match has not been achieved.

Simulation Analyses Application to Waterflooded Minnelusa Fields

The grid systems have been designed and the initial reservoir properties interpolated for the Prairie Creek South and the Simpson Ranch reservoir models. History matches have not been started.

References

1. S. R. Clark, M. J. Pitts, and S. M. Smith, Design and Application of an Alkaline-Surfactant-Polymer Recovery System to the West Kiehl Field, *SPE Advanced Technology Series*, 1(1): 172-179 (April 1993).
2. J. J. Meyers, M. J. Pitts, and K. Wyatt, *Alkaline-Surfactant-Polymer Flood of the West Kiehl, Minnelusa Unit*, paper SPE/DOE 24144 presented at the Eighth SPE/DOE Symposium on Enhanced Oil Recovery, Tulsa, Okla., April 1992.

Objectives

The project objectives include the following:

- *Modeling horizontal wells*—Establish detailed three-dimensional (3-D) methods of calculation that will successfully predict horizontal well performance under a range of reservoir and flow conditions, review both commercial simulators and simple inflow performance relationships used by the industry, investigate the sensitivity of various parameters on the performance of horizontal wells, and develop modeling techniques and computer codes based on generalized 3-D flexible gridding techniques that can be incorporated into reservoir simulators.

- *Reservoir characterization*—Investigate reservoir heterogeneity descriptions of interest to applications of horizontal wells, develop averaging techniques in three dimensions that will adequately compute effective single-phase and two-phase directional permeabilities within the variable gridding characteristics of the model developed in task 1, and perform sensitivity studies of the averaging technique to uncertainties in the heterogeneity distribution.

- *Experimental planning and interpretation*—Critically review technical literature on two-phase flow in pipes and the correlation of these results in terms of their relevance to horizontal wells; perform sensitivity studies to choose parameter spaces of interest for some typical field conditions using the advice of oil companies; plan key experiments to investigate sensitivity to parameter variation, including inflow distribution, completion variations, void fractions, etc.; perform data analysis, including flow pattern distribution, scaling, dependence on perforation intervals, confidence levels, etc.; revise two-phase pressure drop in horizontal wells; and incorporate this capability in the modeling horizontal wells task.

PRODUCTIVITY AND INJECTIVITY OF HORIZONTAL WELLS

Contract No. DE-FG22-93BC14862

**Stanford University
Stanford, Calif.**

**Contract Date: Mar. 10, 1993
Anticipated Completion: Mar. 10, 1998
Government Award: \$359,000
(Current year)**

**Principal Investigators:
F. John Fayers
Khalid Aziz
Thomas A. Hewett**

**Project Manager:
Thomas Reid
Bartlesville Project Office**

Reporting Period: Oct. 1–Dec. 31, 1993

Summary of Technical Progress

A number of activities have been carried out in the last three months. Brief descriptions of each activity are given in the subsequent sections of this report.

Progress is being made on the development of a black oil three-phase simulator that will allow the use of a generalized Voronoi grid in the plane perpendicular to a horizontal well. The available analytical solutions in the literature for calculating productivity indexes (inflow performance) of horizontal wells have been reviewed. The pseudo-steady-state analytic model of Goode and Kuchuk has been applied to an example problem. A general mechanistic two-phase flow model is under development. The model is capable of predicting flow transition boundaries for a horizontal pipe at any inclination angle. It also has the capability of determining pressure drops and holdups for all the flow regimes. A large code incorporating all the features of the model has been programmed and is being tested. The experimental data on the single-phase oil

and water have been analyzed in more detail for all the measured flow rates. The variation of the wellbore diameter along the flow direction has been considered. The apparent roughness of the wellbore model has been determined. The two-phase flow experiments of oil with air and nitrogen are being completed at the Marathon Oil Co.

The first review meeting of the Horizontal Well Industrial Affiliates Program was held Oct. 7–8, 1993, at Stanford University. A presentation of this project was given at the Second Japan National Oil Corp.–Technical Research Center International Symposium, Nov. 1–7, 1993, Chiba, Japan.

Development of a Simulator Based on Voronoi Gridding

The major objective of this facet of the project is to develop a three-phase black oil reservoir simulator that uses Voronoi gridding features. In the first version under development, Voronoi grids can be selected in the plane perpendicular to the well, with Cartesian spacing of layers along the well. Thus the simulator should be able to honor local radial flow geometry, faults, major heterogeneities, boundaries, anisotropy, etc., in the plane perpendicular to a horizontal well. The solution approach is based on control volume finite difference (CVFD) formulation, which is particularly appropriate for Voronoi grids because they are locally orthogonal. The development methodology includes such topics as coupling flow inside the well with fluid flow in the reservoir, grid-generation algorithms, grid visualization, property allocation, well models, reservoir initialization, and numerical solution methods. The simulator is being written with the use of object-oriented programming in C++. Work is nearing completion on the first stage of the simulator, which will give the 3-D generation capability described previously for modeling horizontal wells.

Analytic Solutions for Well Productivity

A number of analytic expressions are available for calculating the steady-state productivity index of a horizontal well with finite length, of which one of the earlier results is that of Giger.¹ These solutions require a constant-pressure condition on the outer surfaces of a drainage volume encompassing the well. Since a horizontal well, because of its usually long length, occupies a significant portion of the drainage volume, the constant-pressure boundary condition is rarely satisfied. Therefore the steady-state productivity should be looked upon only as a rough estimate of the actual productivity for a horizontal well.

Usually the no-flow condition is the more appropriate boundary condition on all the outer surfaces of the drainage volume containing a horizontal well. The pseudo-steady-state solutions for the productivity of a horizontal well incorporating the no-flow outer boundary condition are more complex than their steady-state counterparts but generally are more realistic and practical for a horizontal well. Babu and Odeh²

have given a derivation of complicated analytic expressions for the pseudo-steady-state productivity of a horizontal well in a finite box-shaped drainage volume of a 3-D reservoir. The well is assumed to have finite length at an arbitrary location, with alignment along the y axis of the box. Some slightly simplified approximations for these solutions are then illustrated by these authors in a summary paper.³ A simpler analytic solution for the pseudo-steady-state productivity of a horizontal well has been derived by Goode and Kuchuk,⁴ which includes anisotropy in k_x, k_y, k_z . They have considered a horizontal well parallel to the x direction producing from a rectangular region of dimensions $x_e \times y_e$ with uniform thickness. The well of length L is located at x_w, y_w , and z_w . Under the reasonable assumption that the thickness of the reservoir is small compared with the distance from the well to any of the boundaries in the x or y direction, the well is treated as an infinitely conductive fracture that fully penetrates the formation. The partial penetration in the z direction is accounted for by a geometric skin factor. The dimensionless pressure is derived as

$$P_{wD} = \frac{2\pi y_e}{y_w} \left(\frac{k_x}{k_y} \right)^{1/2} \left(\frac{1}{3} - \frac{y_w}{y_e} + \frac{y_w^2}{y_e^2} \right) + \frac{8x_e^2}{\pi^2 L^2} \sum_{n=1}^{\infty} \frac{1}{n} E_x^2(1 + \xi) + S_{zD} \quad (1)$$

where E_x, ξ , and S_{zD} are functions of the dimensions of the system.⁴

The productivity index (PI) can then be calculated from

$$PI = \frac{2\pi (k_x k_y)^{1/2} h}{\mu_o B_o (P_{wD} + S_m^*)} \quad (2)$$

in which

$$S_m^* = (h/L) (k_x/k_z)^{1/2} S_m \quad (3)$$

and S_m is the mechanical skin.

This method has been used to compute PIs for a numerical example. A reservoir with dimensions of $x_e = 5000$ ft, $y_e = 5500$ ft, $h = 120$ ft with $\mu_o = 2$ cP and $B_o = 1.22$ RB/STB is being produced by a single horizontal well of length $L = 4000$ ft with $r_w = 0.26$ ft located at $x_w = 2500$ ft, $y_w = 2750$ ft, and $z_w = 30$ ft. Permeabilities in the x and y directions are taken as $k_h = 100$ mD, whereas the vertical permeability k_v in the z direction is varied. Variation of the PI with the length of the well is calculated for three values of $k_v/k_h = 1.0, 0.1$, and 0.01 with $S_m = 0$. Results are shown in Fig. 1. It can be seen that the productivity increases almost linearly with the length of the well for a fixed ratio of k_v/k_h . The PI also increases, as expected, with an increase in the vertical permeability. The effect of a change in the wellbore

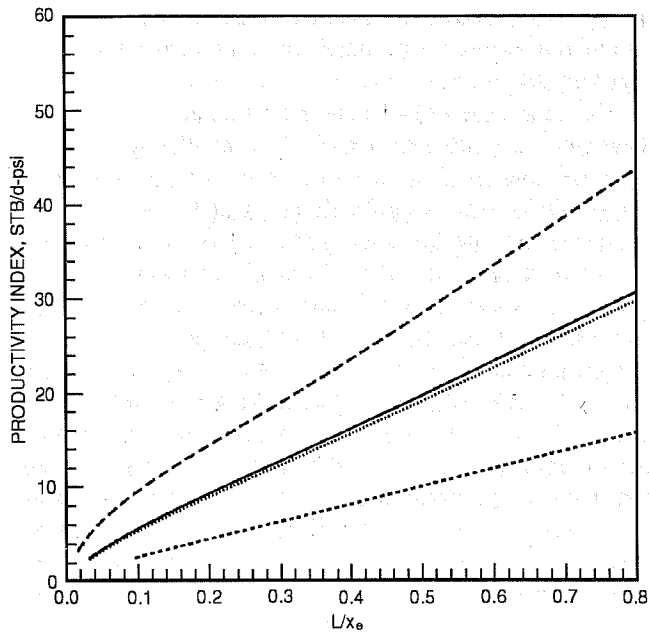


Fig. 1 Variations of productivity index for the example problem. ---, $k_v/k_h=0.01$, $r_w=0.26$ ft. —, $k_v/k_h=0.1$, $r_w=0.26$ ft. ———, $k_v/k_h=1.0$, $r_w=0.26$ ft. ·····, $k_v/k_h=0.1$, $r_w=0.18$ ft.

radius on the PI is also studied. Results with a smaller wellbore radius of 0.18 ft and $k_v/k_h=0.1$ are shown in Fig. 1, where a weak dependence of PI on the wellbore radius is obtained for this example. Simulation results are being used to confirm this analysis and the shift of results if non-uniformities in permeabilities are introduced, etc.

Development of a General Mechanistic Two-Phase Flow Model

Besides the uncertainty of the applicability of two-phase flow correlations to the horizontal well problems, there is also considerable uncertainty about the accuracy of these correlations even for standard pipe-flow calculations. Furthermore, many of the well-known correlations have sharp discontinuities in holdup and pressure drop across flow-pattern boundaries. A general mechanistic model is being developed for modeling two-phase flow in pipes. This model, which is an extension of the work of Barnea,⁵ is also capable of calculating pressure drops and holdups for all flow regimes. The flow-pattern predictions by this method are sensitive to changes in the angle of inclination and fluid properties, with significant differences between up-flow and down-flow in tilted pipes. Figure 2 shows flow pattern

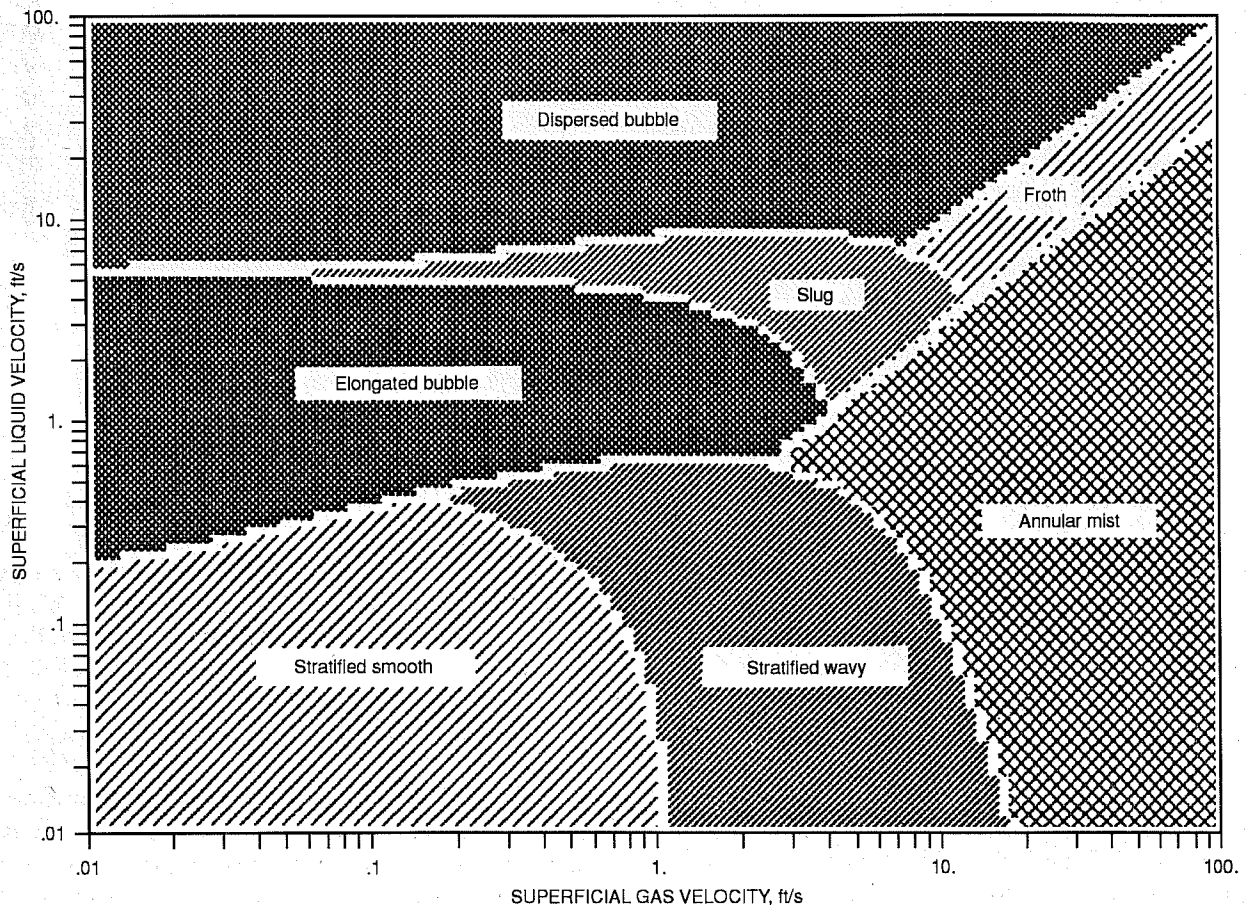


Fig. 2 Prediction of flow regimes from the general mechanistic model under development.

transitions predicted by this model for a two-phase oil-gas flow in a horizontal pipe with an internal diameter (ID) of 6.18 in. and an absolute roughness of 0.01 ft. The oil and gas viscosities were taken as 2.8 and 0.018 cP, respectively. The oil density was 52.53 lb-m/scf and that of gas was 8.139 lb-m/scf. Figure 3 shows the flow pattern transitions predicted by a modification of the Beggs and Brill method⁶ by Brown⁷ for the same case. Significant differences in the location of transition boundaries are seen from the log scales of the axes. Moreover, the Beggs and Brill method uses the same flow-pattern prediction method for all angles of inclination.

The mechanistic flow model is currently being tested and the two-phase flow experiments are under way. The flow model will then be used to predict the experimental data. The results will then be used to verify and refine the flow model.

**Experiments at the Marathon Oil Company:
Data Analyses**

The reported data for the single-phase flow experiments have been analyzed. Only the core flow data with no influx of water or oil are considered in this first analysis. The wellbore

model has also been characterized (i.e., selected the appropriate roughness of the pipe) with the single-phase flow calculations.

The water core flow data were analyzed first. Data with water core flow rates of $Q = 400, 500, \text{ and } 580$ gpm, in both forward and reverse directions, were considered. In the computation of the pressure drops, the measured variations of the wellbore diameter along the length of the model were taken into account. For each 10-ft section of the wellbore, an average diameter was calculated from the reported ultrasonic measurements of the diameter along the model. With the use of the smooth pipe assumption, the pressure drops were calculated per 10-ft length of pipe. Next a match of a single data point was attempted. (The data for the 60- to 70-ft section with $Q = 580$ gpm was used.) A good match was obtained with a small absolute roughness of $\epsilon = 8 \times 10^{-5}$ ft. The pressure drop computations were then performed with this value of roughness for all the cases. The data and results are shown in Fig. 4. The data points are placed at the middle of the sections to which they apply in the figure.

As shown in Fig. 4, the calculated rough case predicts the pressure drop data better than the calculated smooth case. In general, the agreement between the data and the calculated

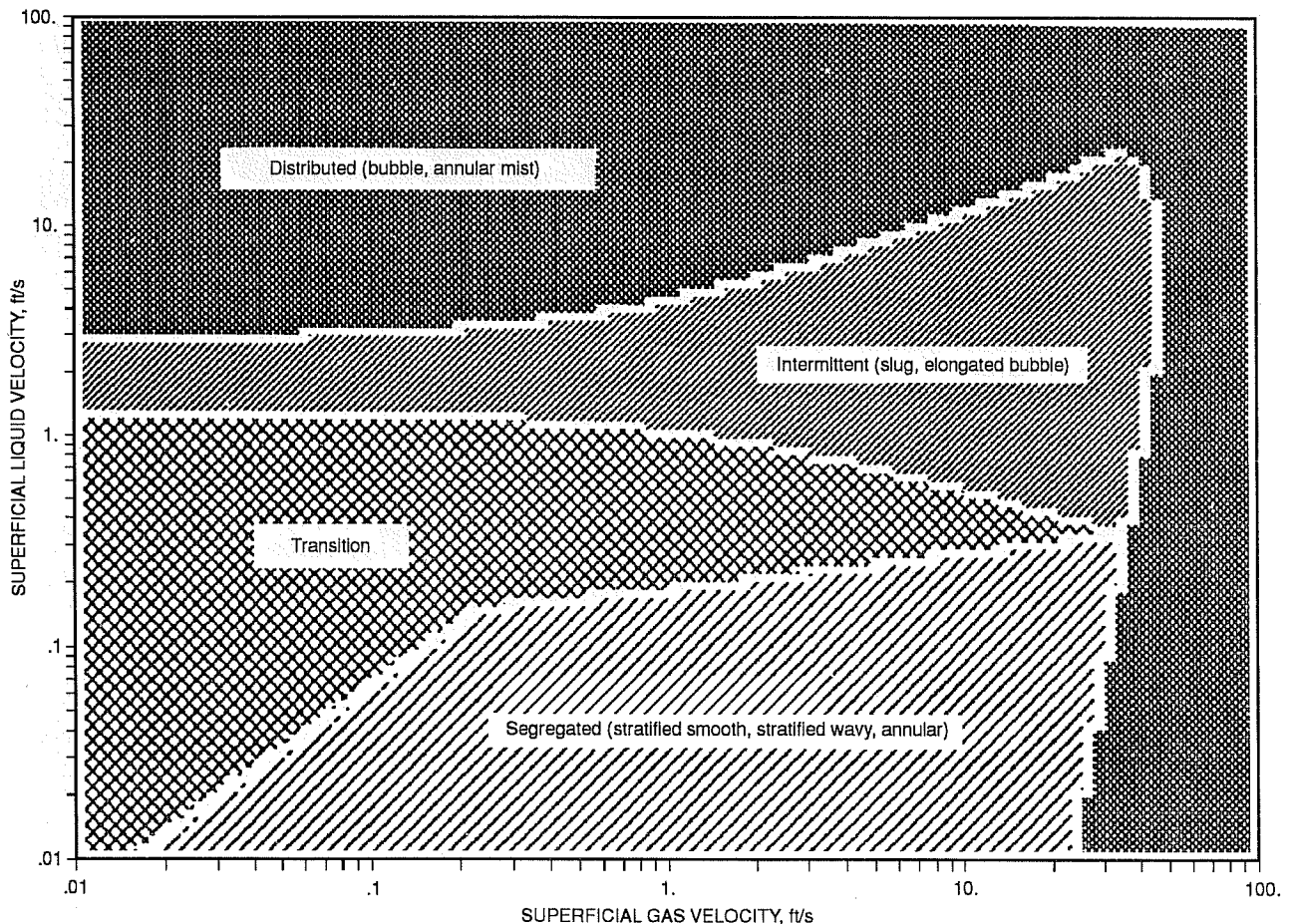


Fig. 3 Prediction of flow regimes for a horizontal pipe from a modification of the Beggs and Brill method.

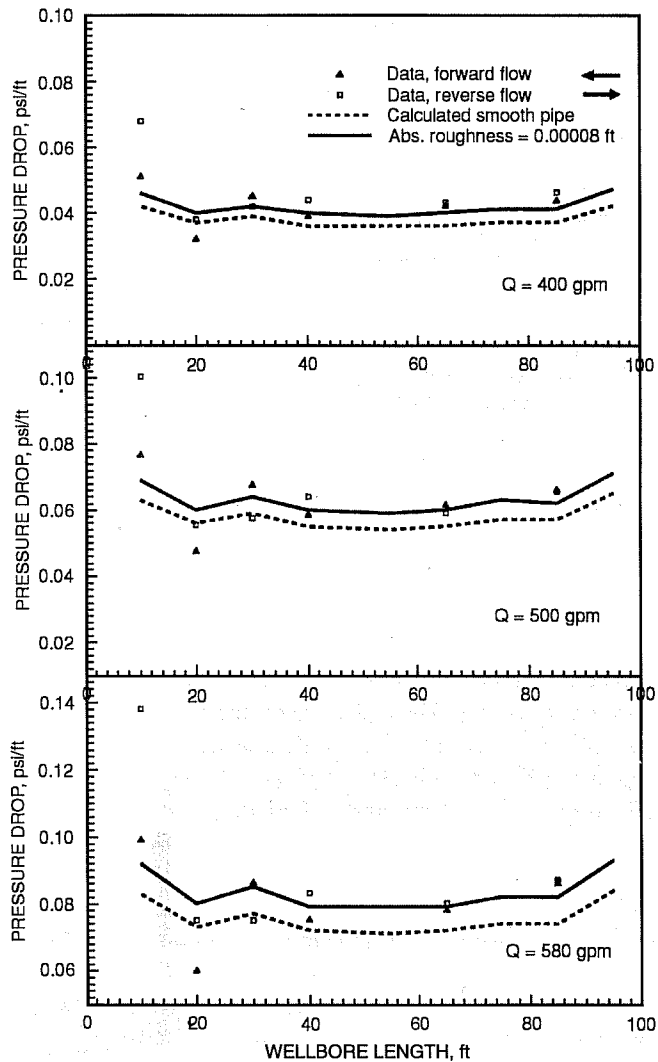


Fig. 4 Data analysis of single-phase water core flow experiments.

values is good except for the last two sections in the forward flow direction (i.e., the 15- to 25-ft section and the 5- to 15-ft section). The 15- to 25-ft section reads low in both directions for all flow rates, whereas the 5- to 15-ft section reads very high, especially for the reverse flow. The pressure drop in the 5- to 15-ft section is possibly influenced by the end or entrance effects in the forward or reverse flow directions, respectively. An important feature is the observed consistency in the data. For instance, the same section reads low for all the flow rates in both directions. The sensitivity to flow direction that appears for the 5- to 15-ft section is not seen at the opposite end (80 to 90 ft), even though the connection arrangements at each end are similar (i.e., 4-in. pipe joined to 6-in. test section). The reasons for this sensitivity at only one end are under investigation. Next, the oil core flow data for flow rates of $Q = 311$, 400, and 493 gpm were examined. These were performed in only one direction. Pressure drop calculations were made for the smooth pipe and the rough cases with the same roughness as

that used in the water case. Figure 5 displays the pressure drop data and the predictions. The higher oil viscosity results in lower Reynolds numbers than those of water ($Re \approx 4 \times 10^4$ for oil vs $\approx 2 \times 10^5$ for water with $Q = 400$ gpm). Therefore the pipe roughness and the variations of the diameter have a smaller effect on the pressure drops in oil runs in comparison with the water experiments as shown in Fig. 5. The ASA software package was used for all the computations.⁸

Various changes are being made to the rig to give better conditions for two-phase flow experiments of oil-air or nitrogen. A number of experimental runs with oil-water core flow and air influx have been conducted. Higher gas flow rates are achieved by vaporizing liquid nitrogen, which is then supplied, instead of air, to the wellbore model through the perforations. The higher gas inflow rate causes a larger pressure drop in the wellbore and changes the flow patterns, which are recorded on a television scanning system.

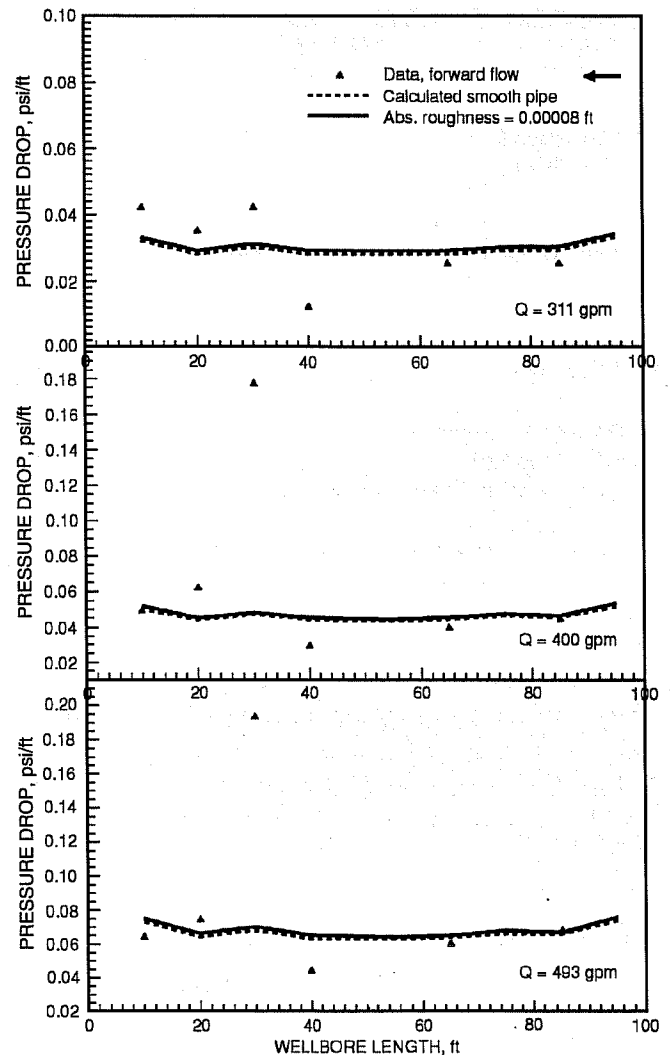


Fig. 5 Data analysis of single-phase oil core flow experiments.

Nomenclature

B_o	Oil formation volume factor
h	Oil column thickness
k_i	Permeability in the i th direction
P_w	Well pressure
P_D	Dimensionless pressure
r_w	Well radius
S_m	Skin factor
x_e	Longitudinal well spacing
x_w	x coordinate location of the well
y_e	Transverse well spacing
y_w	y coordinate location of the well
z_w	Height of well above the bottom of pay zone
μ_o	Oil viscosity

References

1. F. Giger, Reduction du Nombre de Puits par l'Utilisation de Forages Horizontaux, *Rev. Inst. Francais du Petrole*, 38(3): 351-360 (May-June 1983).
2. D. K. Babu and A. S. Odeh, Productivity of a Horizontal Well: Appendices A and B, paper SPE 18334 available from SPE Book Order Dept., Richardson, Tex.
3. D. K. Babu and A. S. Odeh, Productivity of a Horizontal Well, *SPE Reserv. Eng.*, 4(4): 417-421 (November 1989).
4. P. A. Goode and F. J. Kuchuk, Inflow Performance of Horizontal Wells, *SPE Reserv. Eng.*, 319-323 (August 1991).
5. D. Barnea, A Unified Model for Predicting Flow-Pattern Transitions for the Whole Range of Pipe Inclinations, *Int. J. Multiphase Flow*, 13: 1-12 (January-February 1987).
6. H. D. Beggs and J. P. Brill, A Study of Two Phase Flow in Inclined Pipes, *J. Pet. Technol.*, 1417-1425 (November 1987).
7. K. E. Brown, *The Technology of Artificial Lift Methods*, Petroleum Publishing Company, Tulsa, Okla., 1: 134-138 (1977).
8. *ASA Multiphase Flow Software Systems User Guide*, Aziz, Spencer & Associates, Inc., 1993.

OIL FIELD CHARACTERIZATION AND PROCESS MONITORING USING ELECTROMAGNETIC METHODS

Lawrence Livermore National Laboratory
Livermore, Calif.

Contract Date: Oct. 1, 1984

Anticipated Completion: Oct. 1, 1994

Government Award: \$350,000

Principal Investigator:

Mike Wilt

Project Manager:

Thomas Reid

Bartlesville Project Office

Reporting Period: Oct. 1-Dec. 31, 1993

Objective

The objective of this project is to develop practical tools for geophysical characterization of oil strata and monitoring of enhanced oil recovery (EOR) processes in a developed field. Crosshole and surface-to-borehole electromagnetic (EM) methods are being applied to map oil field structure and to provide images of subsurface electrical conductivity changes associated with EOR operations.

Summary of Technical Progress

The primary activity during this quarter was a field experiment at the Lost Hills oil field. Both crosshole and surface-to-

borehole EM data sets were collected at the onset of steam injection activities. These data were interpreted during this quarter, and the results are described. Analysis of these data together with data collected in May 1993 indicates that the crosshole measurement error is between 1 and 3% and the surface-to-borehole data measurement error is between 1 and 10%. The image derived from inverting the crosshole measurements compares well with the borehole induction logs, which suggests that it is a good representation of the subsurface between the observation boreholes.

Most of the field measurements associated with a saltwater injection experiment at the University of California (UC) Richmond Field Station have been completed. Multicomponent borehole-to-surface and crosshole EM data were collected before and after saltwater injection, and the results are included in this report. Comparison of data collected before and after injection indicates that the majority of the measurements are accurate to within 1%, but some of the surface-to-borehole data collected near the injection borehole were contaminated by current leakage to instrument grounds and show errors greater than 20%.

EM Monitoring at Lost Hills

After some remedial work to increase the injectivity, Mobil began injecting significant quantities of steam in borehole 5035 at the Lost Hills site. This well and an adjacent well have been completed for steam injection into two separate zones at 60 and 90 m depth, respectively. Steam injection will continue for the next several years.

During October and November 1993, a set of crosshole and surface-to-borehole EM data was collected to establish a new baseline set. These data were compared with earlier data collected in May 1993 to assess the long-term system errors. On the basis of the rate of steam supply and some numerical

model calculation, it is not expected that the 1 month of steam injection will have a large effect on the subsurface resistivity; therefore these data can be used as baseline measurements. Significant subsurface resistivity changes in this region are expected to occur within 6 months.

Surface-to-borehole data were collected with 10-m² surface loop antennas with the use of borehole receivers in well O35E (Fig. 1). The data were collected at frequencies of 1 and 5 kHz using eight surface loops spaced at 10- and 20-m increments along a profile connecting the two observation holes. The vertical magnetic field was measured in borehole O35E at 3- and 6-m increments at depths from 10 to 150 m. Crosshole EM data were collected at a frequency of 5.5 kHz with the use of 15 receivers in well O35E coupled with continuous transmitter coverage from 30 to 130 m in depth in well O35W.

Figure 2 displays the 1-kHz vertical field amplitude vs. depth measured with a surface transmitter located 105 m from borehole O35E. The plot also displays the observed differences between the data set collected in November 1993 and one collected in May 1993. The amplitude plot shows a monotonically decreasing field with depth with a repeatability error ranging from 0 to 2% except for the bottom 20 m, where errors are as high as 5%. This error level is typical of the 1-kHz data collected at Lost Hills. The 5-kHz repeatability error was much worse because of a combination of lower signal levels and increased sensitivity to surface cultural features. Some of the data collected near surface steam pipes, for example, were clearly contaminated and may not be used in subsurface interpretations. Much of the good data repeat at about the 10% level, which is too high for imaging subsurface resistivity changes.

Both crosshole and surface-to-borehole data will continue to be collected every 3 to 6 months at both low and higher

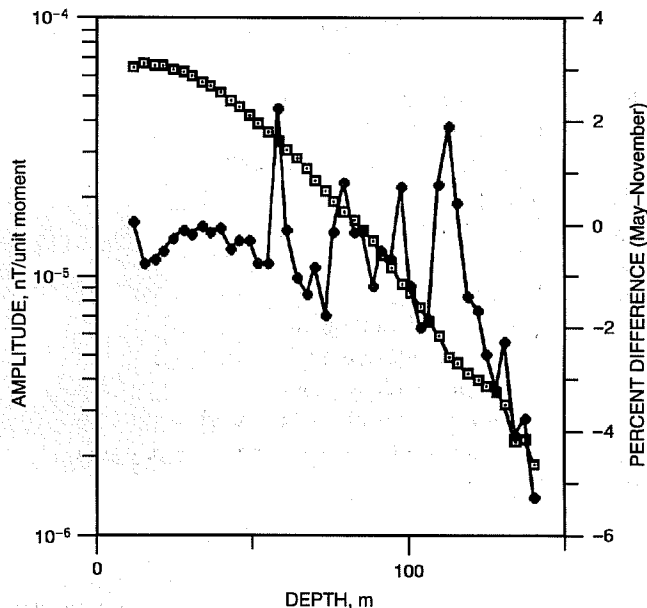


Fig. 2 Comparison of surface-to-borehole data sets collected 6 months apart. ●, May 1993. □, November 1993.

frequencies. Researchers are presently seeking to reduce the sensitivity of the high-frequency surface-to-borehole data to external noise and cultural features. This is important because the higher frequency data have a much greater sensitivity to subsurface changes and are therefore important for the resolution of the changes in subsurface resistivities. Note that the crosshole 5-kHz data are much less affected by surface culture and typically repeat to 2 to 3% or better.

Inversion of Crosshole EM Data at Lost Hills

In December 1993, researchers visited the Schlumberger-Doll Research (SDR) facilities in Ridgefield, Conn., to apply the SDR's new imaging code to the newly collected crosshole EM data set at Lost Hills. The EM data, with spurious points removed, were formatted so that the data could be accessed by the SDR code. This code was then applied to the data set, and the data were fitted to this model to within 2%.

This code, based on a formulation developed by Torres-Verdin and Habashy,¹ provides much more accurate solutions in regions of high resistivity contrast than Alumbaugh's code.² It is therefore more suitable for application to oil fields where resistivity contrasts of 100 or more are typical. In addition, the code is a rectangular two-dimensional formulation, which is more suitable for crosshole EM data than the earlier cylindrical-symmetry codes.

The inversion of the Lost Hills crosshole EM profiles is shown on a gray-scale plot in Fig. 3. The darker shades are regions of higher resistivity, typically associated with oil-saturated sands; the lighter shades indicate lower resistivities associated with confining shales and silts. The figure indicates that there are at least two distinct high-resistivity zones, an

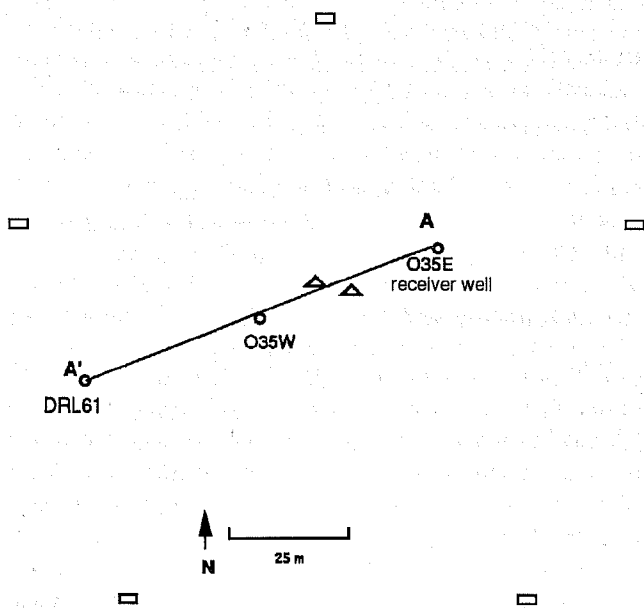


Fig. 1 Base map for electromagnetic field activities at the Lost Hills No. 3 site. A-A', surface-to-borehole profile. △, steam injection well. ○, fiberglass observation well. □, production well.

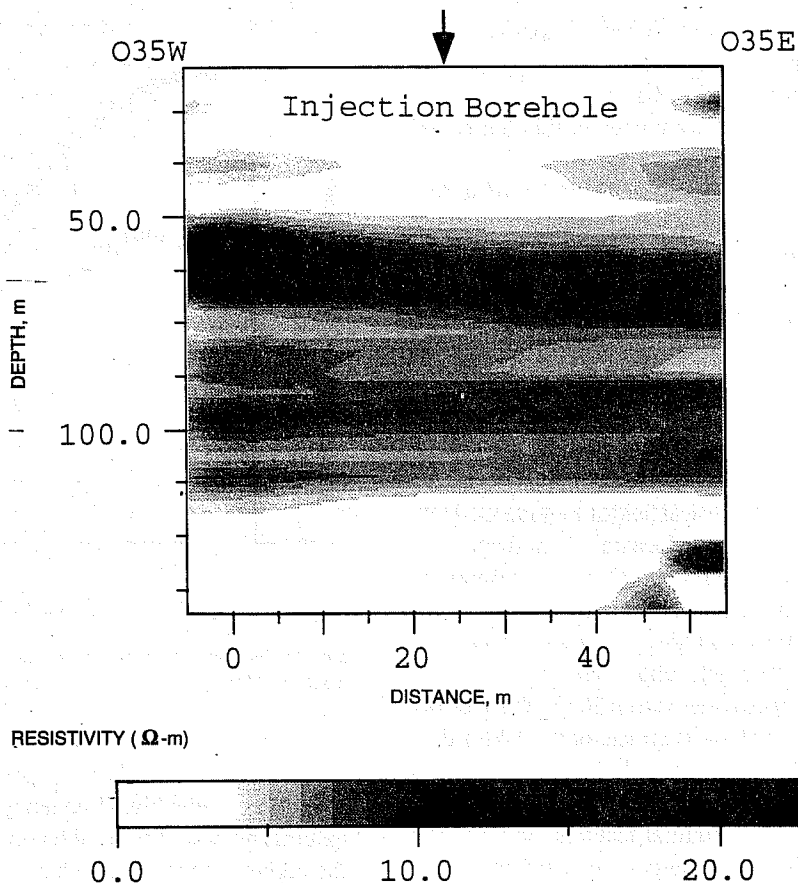


Fig. 3 Resistivity cross section at Lost Hills from two-dimensional inversion of 5.5-kHz crosshole electromagnetic data. Inversion was done by Dr. C. Torres-Verdin of Schlumberger-Doll Research.

upper zone at a depth of 55 m with an eastward dip of approximately 10 degrees and a less-clear lower zone at between 85 and 100 m, which seems to be dipping at approximately the same angle. The upper, higher resistivity zone correlates well with the borehole induction logs and corresponds to the upper Tulare sands.³ This layer is the primary target for steamflood activities at this site. The lower sands, which are not as well defined by the EM data, are also shown to be laterally discontinuous on the borehole logs. The lower resolution at these depths may be the result of the greater geological complexity, the lower sampling density (twice the sampling density was used in the upper sands), or a combination of both.

The resolution achieved by this inversion is a hopeful sign that successful imaging of the resistivity changes during the steam injection at Lost Hills as well as definition of the reservoir heterogeneity is possible.

Surface-to-Borehole Experiment at Richmond Field Station

As part of the Lawrence Berkeley Laboratory (LBL)/Lawrence Livermore National Laboratory (LLNL)/industrial sponsors electromagnetic consortium, a field exercise at

University of California (UC) Richmond Field Station was undertaken beginning in December 1993. This experiment consists of saltwater injection monitoring with a variation of the borehole-to-surface EM technique. The experimental plan calls for high-density multistation and multicomponent surface measurements along two crossing profiles over the saltwater injection borehole. A borehole transmitter is used as a source and is deployed in the injection well.

A significant departure from earlier surveys is that four channels of surface data are measured simultaneously. In addition to much faster data acquisition, this allows for the determination of magnetic field gradients in addition to the fields themselves. Both the vertical magnetic field and the radially directed horizontal field components are measured. Recent theoretical work at UC Berkeley has shown that use of multicomponent magnetic fields and field gradients can markedly improve the resolution of subsurface features. Crosshole EM measurements will also be collected so that the borehole-to-surface and crosshole methods can be compared on the same profile.

The baseline data for this experiment were collected and the saltwater was injected in December 1993. Postinjection data were collected during the last week of December and early January 1994. Early analysis of these data shows that

whereas more than 70% of the data are very high quality, there seems to be persistent errors for surface-to-borehole stations located near the injection (and transmitter) well. Differences of up to 25% have been observed between pre-injection and postinjection data sets, which are more than three times as great as the maximum expected changes. These may be partially the result of current leakage along the surface grounding point of the transmitter. The magnitude of this problem is being determined. There may be a need to remeasure about 30% of the data.

References

1. C. Torres-Verdin and T. Habashy, *An Approach to Nonlinear Inversion with Application to Crosswell EM Tomography*, paper presented at the 1993 Society of Exploration Geophysicists Annual Meeting, Washington, D.C., Sept. 26–30, 1993.
2. D. L. Alumbaugh, *Iterative Electromagnetic Born Inversion Applied to Earth Conductivity Imaging*, Ph.D. Dissertation, University of California, Berkeley, 1993.
3. M. J. Wilt, Quarterly Progress Report for Project FEW6038, in *Activities of the Oil Implementation Task Force*, DOE Report DOE/BC-93/3, 1993.

Objectives

The goal of this project at the Stanford University Petroleum Research Institute (SUPRI) is to conduct research directed toward increasing the recovery of heavy oils. Presently SUPRI is working in five main areas:

1. Flow properties studies—to assess the influence of different reservoir conditions (temperature and pressure) on the absolute and relative permeability to oil and water and on capillary pressure.
2. In situ combustion—to evaluate the effect of different reservoir parameters on the in situ combustion process; this project includes the study of the kinetics of the reactions.
3. Steam injection with additives—to develop and understand the mechanisms of the process using commercially available surfactants for reduction of gravity override and channeling of steam.
4. Formation evaluation—to develop and improve techniques of formation evaluation, such as tracer tests and pressure transient tests.
5. Field support services—to provide technical support for design and monitoring of U.S. Department of Energy (DOE)-sponsored or industry-initiated field projects.

Summary of Technical Progress

Flow Properties Studies

After completion of the displacement experiments with cyclohexane and brine, the cyclohexane was displaced from the core by a mixture of decane and mineral oil. The purpose of this run was to study the influence of oil viscosity on the end effects. The new mixture viscosity is 5 cP compared with 1 cP for cyclohexane. Imbibition and drainage displacements were performed at flow rates of 1, 4, and 8 cm³/min. Results showed a more severe nonlinearity of the flow paths near the end than in the 1-cP runs.

Software was developed to calculate relative permeabilities with history matching of the displacement data. Either one- or two-dimensional numerical models can be used for this work. Another use of the model will be to study the sensitivity of calculated relative permeability curves to possible errors in the capillary pressure data. Capillary pressure curve measurement for the core used in the experiment is still in progress.

The CATSOFT image visualization software is almost ready. A three-dimensional (3-D) construction module allowing interpolation between the computerized tomography (CT) slices was added. The calculation routines have been verified and errors corrected. A user manual is being written.

A new researcher is working on two-phase flow in fractured media at isothermal conditions. Fine-grind simulations performed by Guzman and Aziz¹ will be used to guide the design of an experiment to study matrix-to-fracture transfer in oil-water systems. The literature review is almost complete,

RESEARCH ON OIL RECOVERY MECHANISMS IN HEAVY OIL RESERVOIRS

Contract No. DE-FG22-93BC14899

**Stanford University
Petroleum Research Institute
Stanford, Calif.**

**Contract Date: Feb. 8, 1993
Anticipated Completion: Feb. 7, 1997
Government Award: \$800,000
(Current year)**

**Principal Investigators:
W. E. Brigham
H. J. Ramey, Jr.**

**Project Manager:
Thomas Reid
Bartlesville Project Office**

Reporting Period: Oct. 1–Dec. 31, 1993

and a new core holder is being built. Better epoxy resins are still being sought.

In Situ Combustion

The effect of metallic additives on in situ combustion will be studied. Emphasis has been on literature review, organization of the laboratory, and calibration and verification of the equipment. Repeat runs of previous tests with iron and tin as additives will be performed first. The concentration of additive will then be decreased to try to find the lower limit of effectiveness. In parallel, the mechanisms of the additive action will be studied by visual and scanning electron microscope (SEM) observations.

Steam Injection with Additives

New micromodels have been built to study oil-foam interaction at the pore level. Following the method developed by Hornbrook,² a new set of models representing Berea sandstone networks was delivered in December 1993. A better optical system will be purchased in January 1994. Future tasks include calibration of the pump and the pressure transducers and connection of the new microscope to a video digitizer for quantitative data analysis.

The plumbing of the model for steam injection in fractures is complete. Three test runs were interrupted by leaks caused by a defective gasket and bad thermocouple fittings. Despite these problems, part of the data can be analyzed to determine proper steam injection rates. No new runs are planned until the new CT scanner becomes available.

The 3-D steam injection experiment with CT scanning is being calibrated for a new series of runs at residual oil saturation. The results obtained by numerical simulation with

STARS or THERM will be compared with those obtained by the experiments. Future work on this equipment will include investigating the effect of oil on foaming additives with steam.

Two papers relating to foam additives were presented during this quarter.³⁻⁴

Formation Evaluation

A paper based on SUPRI TR 61 has been accepted for publication by the Society of Petroleum Engineers after certain revisions are made.⁵

Field Support Services

An attempt is being made to optimize injection-production rates in a steam drive. As a first step, a Marx-Langenheim type model is being combined with a multivariable optimization program to try to maximize profit. The program will be tested against field data for reservoirs with extensive steam-drive data. The steam injection model will later be refined to address specific problems, such as multilayers, dip, and/or gravity override.

References

1. R. E. Guzman and K. Aziz,
2. Hornbrook,
3. L. M. Castanier and W. E. Brigham, *Critique of a Steam Foam Field Pilot*, paper presented at the International Energy Agency Symposium on Salzburg, Austria, Oct. 18-20, 1993.
4. W. E. Brigham and L. M. Castanier, *Foams as Mobility Control Agents*, paper presented at the International Energy Agency Symposium on Salzburg, Austria, Oct. 18-20, 1993.
5. M. Riley and W. E. Brigham, *Detecting Linear Barriers by Type Curve Analysis*, accepted for publication by the Society of Petroleum Engineers.

GEOSCIENCE TECHNOLOGY

**INTEGRATION OF ADVANCED GEOSCIENCE
AND ENGINEERING TECHNIQUES TO
QUANTIFY INTERWELL HETEROGENEITY**

Contract No. DE-AC22-93BC14893

**New Mexico Institute of Mining and Technology
Petroleum Recovery Research Center
Socorro, N. Mex.**

**Contract Date: Sept. 29, 1993
Anticipated Completion: Sept. 30, 1996
Government Award: \$249,850**

**Principal Investigator:
F. David Martin**

**Project Manager:
Robert Lemmon
Bartlesville Project Office**

Reporting Period: Oct. 1–Dec. 31, 1993

Objectives

This interdisciplinary effort will integrate engineering and petrophysical results with geological and geophysical data through reservoir simulation to quantify reservoir architec-

ture and the dynamics of fluid–rock and fluid–fluid interactions. The reservoir characterization will include geological methods (outcrop and reservoir rock studies), geophysical methods (interwell acoustic techniques), and other reservoir–hydrologic methodologies, including analyses of pressure transient data, field tracer tests, and laboratory core studies. The field testing will be conducted at the Sulimar Queen Unit with related laboratory testing at the Petroleum Recovery Research Center (PRRC) on samples from the Sulimar site and Queen sandstone outcrops. Research methods will involve the acquisition and integration of data obtained at a wide variety of different scales and the quantitative development of interrelationships based on scale definition as it relates to the reservoir.

The aim is to (1) characterize lithologic heterogeneity, (2) quantify changes in heterogeneity at various scales, (3) integrate the wide variety of data into a model that is jointly constrained by the interdisciplinary interpretive effort, and (4) achieve greater accuracy and confidence during simulation and modeling as steps toward optimizing recovery efficiency from existing petroleum reservoirs.

Subcontractors from Stanford University and the University of Texas at Austin (UT) will collaborate on the project. At Stanford, crosswell reflection imaging and interwell transmission tomography will be coupled in a procedure not previously attempted on field data. The UT will conduct further research, design, and interpret a single-well wettability tracer test developed in their laboratories but not yet field

tested. Several members of the PRRC staff will participate in the development of improved reservoir description by integration of the field and laboratory data as well as in the development of quantitative reservoir models to aid performance predictions. The results of the research will be transferred to other petroleum producers through seminars, workshops, and professional publications.

Summary of Technical Progress

During the first quarter of the project, initial activities and planning for the 3-yr effort began. Subcontractor agreements with UT and Stanford University were submitted, modified, and executed. Pecos Petroleum Engineering Inc., Roswell, N. Mex., was retained as the field site agent. An industrial liaison committee will also be formed.

The state production tapes for the Sulimar Queen Unit were reformatted into a personal computer (PC)-based relational database. An AutoCAD basemap of the field was constructed. A Quattro[®] Pro production file for each well in the field and

for the whole field was completed. The following plots are attached to each file: total fluid vs. time, oil cut vs. time, oil rate vs. time, oil cut vs. cumulative oil, and oil rate vs. cumulative oil. All the plots were copied and converted to AutoCAD format and were incorporated with the basemap for viewing and plotting purposes. Copies of logs for each well in the field were obtained from the Roswell Geological Society log library. The logs will be converted to AutoCAD format and incorporated with the basemap.

Preserved reservoir core material is available from well 1-16 that the PRRC drilled in 1990. Thin sections were made from this core material to investigate diagenesis in the cored interval of this well. Results of this study will be provided during the next quarter of the project. In addition, a fresh crude oil sample from the field site was obtained for the petrophysical research that will begin in the next quarter.

Requests for proposals to measure current static reservoir pressure throughout the field were distributed by Pecos Petroleum Engineering Inc. This pressure testing is scheduled for completion in January 1994.

APPLICATION OF ARTIFICIAL INTELLIGENCE TO RESERVOIR CHARACTERIZATION: AN INTERDISCIPLINARY APPROACH

Contract No. DE-AC22-93BC14894

**University of Tulsa
Tulsa, Okla.**

**Contract Date: Oct. 1, 1993
Anticipated Completion: Sept. 30, 1996
Government Award: \$312,407**

**Principal Investigator:
B. G. Kelkar**

**Project Manager:
Robert Lemmon
Bartlesville Project Office**

Reporting Period: Oct. 1–Dec. 31, 1993

goal is to design and implement a single, powerful expert system for use by small producers and independents to exploit reservoirs efficiently.

The development of expert systems is perhaps the most significant and tangible outcome of AI research. An expert system is a computer program that demonstrates expert-level competence in a small restricted domain of human endeavor. Such a system typically embodies diverse knowledge about its domain and effectively engages this knowledge to solve complex real-world problems within the domain. Techniques have been developed to acquire knowledge from an expert and represent it in a computer-usable form through the practice of *knowledge engineering*. In addition, methodologies have been designed to *validate* and *verify* an expert system. Validating an expert system is the process of showing that the system reflects the knowledge and problem-solving abilities (i.e., the right system was built) of the expert. Verifying an expert system is the process of showing that the expert system produces correct and consistent answers.

The main challenge of the proposed research is to generate detailed reservoir descriptions honoring all available soft and hard data, which range from qualitative and semiquantitative geological interpretations to numeric data obtained from cores, well tests, well logs, and production statistics. In this sense, the proposed research is truly multidisciplinary. It involves a significant amount of information exchange between researchers in geology, geostatistics, and petroleum engineering. Computer science and AI provide the means to effectively acquire, integrate, and automate key areas of expertise in the various disciplines represented in a reservoir

Objectives

The basic objective of this research is to use novel techniques from artificial intelligence (AI) and expert systems to capture, integrate, and articulate key knowledge from geology, geostatistics, and petroleum engineering to develop accurate descriptions of petroleum reservoirs. The ultimate

characterization expert system. Additional challenges are the verification and validation of the expert system because much of the interpretation of the experts is based on extended experience in reservoir characterization.

The overall project plan to design the system to create integrated reservoir descriptions begins by initially developing an AI-based methodology for producing large-scale reservoir descriptions generated interactively from geology and well test data. Parallel to this task is a second task that develops an AI-based methodology that uses facies-biased information to generate small-scale descriptions of reservoir properties such as permeability and porosity. The third task involves consolidation and integration of the large-scale and small-scale methodologies to produce reservoir descriptions honoring all available data. The final task will be technology transfer. This research plan allocates and sequences the activities involved in each of the tasks to promote concurrent progress toward the research objectives. Moreover, the project duties are divided among the faculty member participants, and graduate students will work in teams with faculty members.

The results of the integration are not limited merely to obtaining better characterizations of individual reservoirs. They have the potential to significantly impact and advance the discipline of reservoir characterization itself.

Summary of Technical Progress

The first task under each of the concurrent phases of developing large-scale and small-scale reservoir descriptions is to identify the main knowledge sources. This task involves the identification of the critical variables that have an impact on large-scale heterogeneities. Because of the interdisciplinary nature of the project, a common vocabulary has been developed among the researchers to accomplish this identification task of Phases I and II. The computer science faculty and students had to familiarize themselves with the information processed in geology, geostatistics, and petroleum engineering. In addition, the geology and petroleum engineering researchers required instruction in the process of building expert systems.

To this end, tutorials consisting of a presentation by a faculty member or student on topics related to the project, such as geostatistics, well testing, knowledge engineering and expert systems, and ProKappa (the software chosen for implementing the expert system) were conducted. The students of

the project have also begun presentations that attempt to integrate the information learned so that the experts can comment on and correct the overall understanding of the project and its components. These presentations have been vital in determining the key information needed to build a successful expert system for this domain and in planning the next step of building small prototypes for integration.

As part of the simulation task of Phases I and II, the design of the expert system has been decomposed into smaller component parts to get a clearer picture of what expert knowledge is needed. This decomposition facilitates the validation and verification of a complex expert system. Concurrently, three small prototype systems will be developed that will interface with a central repository of reservoir descriptions. The three component systems will be representative of how each of the experts in geology, geostatistics, and engineering characterizes the reservoir. The repository will hold all descriptions that are consistent with the currently known information. The system as a whole will operate in a manner similar to the *blackboard system* technology in AI, in which information is centrally located (i.e., on a blackboard), and experts take their turn to update, change, and correct the information on the blackboard. This system will serve as an initial prototype and will not contain all necessary information. However, it will help determine the necessary knowledge and an appropriate representation for that knowledge such that it is consistent with numeric and nonnumeric information.

The empirical nature of the project requires a great deal of flexibility in the system. The necessary rules for each of the components of the expert system (geostatistical, well test, and geological information) and the rules to integrate the components must be thoroughly investigated before a complete system can be built. During this investigation, however, small prototypes will be built that are representative of each expert's knowledge and method of reservoir description to enhance understanding of the entire system. The use of prototypes is in contrast to building a single large system that would be difficult to verify and validate. Building these prototypes requires investigating the inputs and outputs of each information component. Therefore an interface between large-scale and small-scale descriptions will be developed concurrently as part of the reservoir description repository such that the reservoir descriptions produced can be easily exchanged and updated later.

**GEOSCIENCE/ENGINEERING
CHARACTERIZATION OF THE
INTERWELL ENVIRONMENT IN
CARBONATE RESERVOIRS BASED
ON OUTCROP ANALOGS, PERMIAN
BASIN, WEST TEXAS AND NEW MEXICO**

Contract No. DE-AC22-93BC14895

**University of Texas
Austin, Tex.**

**Contract Date: Sept. 29, 1993
Anticipated Completion: Sept. 28, 1996
Government Award: \$354,400**

Principal Investigators:

**F. J. Lucia
C. Kerans**

Project Manager:

**Robert Lemmon
Bartlesville Project Office**

Reporting Period: Oct. 1–Dec. 31, 1993

Objectives

The primary objective of this project is to investigate styles of reservoir heterogeneity found in low-permeability pelleted wackestone–packstone facies and mixed carbonate–clastic facies found in Permian Basin reservoirs by studying similar facies exposed in the Guadalupe Mountains. Specific objectives for the outcrop study include construction of a stratigraphic framework, petrophysical quantification of the framework, and testing the outcrop reservoir model for effects of reservoir heterogeneity on production performance. Specific objectives for the subsurface study parallel objectives for the outcrop study.

Summary of Technical Progress

Outcrop Activities

During the fall of 1993, an outcrop characterization study of the Grayburg formation on Plowman Ridge, west of Carlsbad, N. Mex., was initiated. This 4-mile-long, north–south striking ridge is subparallel to depositional dip and provides excellent exposures of the Grayburg formation from the basal contact overlying the San Andres formation to the uppermost Grayburg interval. Eight stratigraphic sections were measured and described in detail. These sections attain a maximum thickness of 600 ft on the outer platform and thin to less than 300 ft in the more proximal sections, 3.5 miles to the north. The measured sections are 800 to 4000 ft apart and have been physically correlated by walking out a key marker bed and by using aerial photographs of the laterally continuous strata. More than 140 core plugs were collected from a distal measured section, 550 ft in thickness, which was vertically sampled at every lithologically distinct unit and/or at 5-ft intervals, whichever was closer. The core-plug porosity and permeability data indicate excellent reservoir quality in some ooid grainstones ($f = 10$ to 20% and $K = 50$ to 1500 mD) and some sandstones ($f = 0$ to 15% and $K = 1$ to 10 mD). These reservoir-quality units are bounded by relatively impermeable (<0.01 mD) mud-dominated lithologies. Core-plug data also indicate that the upper one-third of the Grayburg formation has poor reservoir quality ($k = 0.01$ mD). This preliminary work established a framework for ongoing, detailed outcrop studies directed toward characterization of reservoir architecture and resolution of interwell-scale reservoir heterogeneity to provide an analog to the subsurface productive Grayburg formation.

Subsurface Activities

The South Cowden field, Ector County, Tex., has been selected as an analog field, and characterization activities have begun. The South Cowden field produces from the Grayburg–San Andres formations at a depth of about 4500 ft. The collection of data has begun, and 12 cores from the field have been described for construction of a stratigraphic framework. Rock fabric and petrophysical studies have also begun.

**INTERDISCIPLINARY STUDY OF
RESERVOIR COMPARTMENTS**

Contract No. DE-AC22-93BC14891

**Colorado School of Mines
Golden, Colo.**

**Contract Date: Sept. 29, 1993
Anticipated Completion: Sept. 30, 1996
Government Award: \$753,266**

**Principal Investigator:
Craig W. Van Kirk**

**Project Manager:
Robert Lemmon
Bartlesville Project Office**

Reporting Period: Oct. 1–Dec. 31, 1993

Objective

The objective of this research project is to document the integrated team approach for solving reservoir engineering problems. A field study integrating the disciplines of geology, geophysics, and petroleum engineering will be the mechanism for documenting the integrated approach. The goal will be to provide tools and approaches that can be used to detect reservoir compartments, reach a better reserve estimate, and improve profits early in the life of a field.

Summary of Technical Progress

The first task of the project team was to select a field and gather data. Initial team meetings focused discussions on the team process, project goals, and methods of approach. Each team member proposed candidate fields for consideration in the selection process. Attributes of each candidate field were compared with the ideal characteristics deemed important for achieving project goals. Nine candidate fields were presented and discussed. Several fields that lacked critical data were eliminated.

Emphasis was placed on selecting a field where the integration of each discipline could be demonstrated. Thus a field with components from geology, geophysics, and petroleum engineering was needed. The availability of three-dimensional seismic data was given high priority to achieve the goal of demonstrating and documenting the process of integration. The selected field also needed to meet requirements for access to geologic and petroleum engineering data.

The South Casper Creek field located in Natrona County, approximately 25 miles west of Casper, Wyo., was selected and submitted to the U.S. Department of Energy (DOE) for approval.

Because the eolian depositional environment of the selected field did not fit within the DOE research objectives, DOE rejected the South Casper Creek proposal.

The project team proposed as its second choice the Lambert field. This field has many of the desirable attributes with some compromises when compared with the South Casper Creek field. This proposal is currently under review by DOE. On approval of a field for study, the data-gathering portion of the task will commence.

**ANISOTROPY AND SPATIAL VARIATION
OF RELATIVE PERMEABILITY AND
LITHOLOGIC CHARACTERIZATION OF
TENSLEEP SANDSTONE RESERVOIRS
IN THE BIGHORN AND WIND RIVER
BASINS, WYOMING**

Contract No. DE-AC22-93BC14897

**University of Wyoming
Laramie, Wyo.**

**Contract Date: Sept. 15, 1993
Anticipated Completion: Sept. 14, 1996
Government Award: \$258,359**

**Principal Investigator:
Thomas L. Dunn**

**Project Manager:
Robert Lemmon
Bartlesville Project Office**

Reporting Period: Oct. 1–Dec. 31, 1993

Objectives

The objectives of this multidisciplinary study are designed to provide improvements in advanced reservoir characterization techniques. The objectives are to be accomplished through (1) an examination of the spatial variation and anisotropy of relative permeability in the Tensleep sandstone reservoirs of Wyoming; (2) the placement of that variation and anisotropy into paleogeographic, depositional, and diagenetic frameworks; (3) the development of pore-system imagery techniques for the calculation of relative permeability; and (4) reservoir simulations testing the impact of relative permeability anisotropy and spatial variation on Tensleep sandstone reservoir enhanced oil recovery (EOR).

Concurrent efforts are aimed at understanding the spatial and dynamic alterations in sandstone reservoirs that are caused by rock–fluid interaction during carbon dioxide (CO₂) EOR processes. The work focuses on quantifying the interrelationship of fluid–rock interaction with lithologic characterization in terms of changes in relative permeability, wettability, and pore structure and with fluid characterization in terms of changes in chemical composition and fluid properties. This work will establish new criteria for the susceptibility of Tensleep sandstone reservoirs to formation alteration that results in a change in relative permeability and wellbore scale damage. This task will be accomplished by flow experiments with the use of core material, examination of regional trends in water chemistry, examination of local water chemistry trends on the scale of a field, and chemical modeling of the reservoir and experimental systems to scale up the experiments to reservoir conditions.

Summary of Technical Progress

Work has begun on each of the three technical tasks and the administrative task, Project Management. The effort has focused on acquisition of the necessary databases, acquisition and construction of the relative permeability apparatus, initial development of the design for the CO₂ flood experiments, and assembly of the necessary scientific and administrative staff. The contract effort has been strengthened by the creation of the Institute for Energy Research (IER) at the University of Wyoming in October 1993. The IER is a research and instructional organization devoted to basic and applied research in oil and gas exploration and production. The IER will provide administrative infrastructure and office space for the project staff in an advanced working environment for engineers, geologists, geochemists, and mathematicians.

Regional Frameworks

This research will associate spatial distributions and anisotropy of relative permeability with the depositional subfacies and zones of diagenetic alteration found within the Tensleep sandstone. The associations between depositional lithofacies, diagenetic alteration, and pore geometry will strongly link relative permeability with the distinct and measurable dimensions of lithofacies and authigenic mineral facies. Effects of the depositional processes and burial diagenesis will be investigated.

The IER has obtained the Dwight's historical database for the Bighorn and Wind River Basins. This information serves as a basis for base maps of the Tensleep sandstone. A decision to purchase the production database is pending. Sorting and loading the relevant data into OGCI's PRODUCTION ANALYST software are in progress. This will be one of the principal systems used to analyze and output the regional frameworks. Both the program and the database are in place. Partial listings of Tensleep formation cores from two core repositories have been obtained. Core examination will begin after the first of the year, and extensive field work will begin in early summer 1994. A reconnaissance of the western side of the Bighorn Mountains and the northeastern Owl Creek Mountains was performed. The Tensleep sandstone is extensively exposed along the ranges, typically in steeply dipping hogbacks and excised canyons along the Bighorn Mountains and as barrier cliffs in the Owl Creek Mountains. In anticipation of the summer field sampling program, a gasoline-powered, small-diameter coring device was constructed. This device will be used in conjunction with other IER projects.

Relative Permeability Measurements

The focus of this task is to obtain quantitative laboratory data on the magnitude and variability of relative permeability anisotropy and spatial variation of the dominant reservoir and boundary surface lithologies of the Tensleep sandstone. Existing data will be collected, compiled, and placed within the regional frameworks. Laboratory measurements will be performed in

the Petroleum Engineering Department at the University of Wyoming. The unsteady-state technique will be used to measure the relative permeability. An additional objective of this study is to provide algorithms for calculating relative permeability from quantitative pore imagery data.

The major engineering effort has been the configuration of a laboratory apparatus capable of making the necessary measurements. Published material on relative permeability determination has been reviewed, and the technique to be used in this study has been selected.

For relative permeability laboratory experiments, the unsteady-state technique, commonly referred to as the Johnson-Bossler-Naumann (JBN) method, will be used.¹ Graphical techniques for extrapolating both saturation and relative permeability from the same linear displacement curve have been presented,² and these techniques have been incorporated into a textbook on waterflooding.³ The use of JBN allows the comparison of laboratory measurements with previously published work. In particular, impressive quantities of two-phase flow experiments have been recorded.^{4,5} The effects of wettability on relative permeability measurements are particularly important.⁶

The necessary equipment for building a new relative permeability measuring apparatus has been ordered. Also on order is an assortment of tubing, valves, and connections and a constant-rate fluid pump (a critical item). Past experience with unsteady-state relative permeability tests has indicated that the flow rate must be maintained at a precisely constant level irrespective of pressure and temperature. The pump ordered has a temperature control confinement and is specified to maintain a constant flow rate to 0.1% up to 10,000 psi on a single syringe displacement piston. Construction of the measuring apparatus will begin in the second quarter of this contract.

The investigation of anisotropy will not necessarily require actual relative permeability calculations. Laboratory data directly provide measurements of fractional (water-cut) flow only, which can then be interpreted to yield relative permeability data. Use of the JBN technique in this investigation will allow anisotropy effects to be detected with more than just relative permeability. Raw laboratory data will be given in terms of pore volume injected vs. average core saturation. It can be shown that variations in relative permeability are necessarily a result of variations in the first derivative of a pore-volume-vs.-saturation curve. In this way a minimum number of assumptions and calculations will be needed to examine relative permeability anisotropy.

CO₂ Flood—Formation Alteration and Wellbore Damage

The work of this task is to establish criteria for the susceptibility of Tensleep sandstone reservoirs to formation alteration, which will result in a change in absolute or relative permeability and/or possible wellbore scale damage during CO₂ EOR. This advanced reservoir characterization technology will be used to optimize recovery efficiencies. This task includes (1) flow

experiments on core material to examine the effects of CO₂ flooding on the alteration of the fluid and rock system, (2) examination of regional trends in water chemistry, (3) examination of local water chemistry trends on the scale of a field, and (4) chemical modeling of both the reservoir and experimental systems to scale up the experiments to reservoir conditions.

The first experiment of the experimental design phase is scheduled to commence in May 1994. The design is being iteratively constructed and reviewed by the task leader, advisor-mentors, and the Marathon Oil Co. research staff. Data available through the Wyoming Geological Survey are initially being used to construct the regional water database.

Project Management and Technical Transfer

This task incorporates the efforts to achieve a high level of success in this interdisciplinary project. This administrative task provides for effective coordination and integration of the project's research tasks. The program manager is responsible for ensuring that the task workers meet on a frequent and regular basis to exchange information and discuss results. The program manager is responsible for the coordination and timely reporting of results to its industry advisor-mentors, the Department of Energy (DOE), and the scientific and engineering communities.

Administrative duties performed include the preparation of the Once After Award documents required by the DOE (Management Plan, Cost Plan, Work Plan, Travel Plan, Milestone Schedule Log and Plan, etc.) and the creation of an Associate Research Scientist position. An engineering undergraduate has been hired to help assemble, test, and run the relative permeability apparatus. An engineering graduate student will arrive before the beginning of the 1994 fall semester to work on the relative permeability measurements. An undergraduate geology student will be hired to help assemble the data for the regional frameworks. An office technician has been hired to perform accounting and general office duties. This administrative staff will be in place by Dec. 28, 1993. The project director has been in contact with each of the industry advisor-mentors.

References

1. E. F. Johnson, D. P. Bossler, and V. O. Naumann, Calculation of Relative Permeability from Displacement Experiments, *Trans. Am. Inst. Min. Eng.*, 216: 370-372 (1959).
2. S. C. Jones and W. O. Roszelle, Graphical Techniques for Determining Relative Permeability from Displacement Experiments, *J. Pet. Technol.*, 30: 807-817 (1978).
3. G. P. Willhite, *Waterflooding*, SPE Textbook Series, Vol. 3, 1986.
4. N. R. Morrow, P. J. Cram, and F. G. McCaffery, Displacement Studies in Dolomite with Wettability Control by Octanoic Acid, *Trans. Soc. Pet. Eng. AIME*, 255: 221-232 (1973).
5. N. R. Morrow and P. Jadhunandan, *Effect of Wettability on Waterflood Recovery for Crude Oil/Brine/Rock Systems*, paper SPE 22597 presented at the 66th Society of Petroleum Engineers Annual Technical Conference and Exhibition, Dallas, Tex., Oct. 6-9, 1991.
6. W. G. Anderson, The Effects of Wettability on Relative Permeability, *J. Pet. Technol.*, 39(11): 1453-1468 (1987).

RESOURCE ASSESSMENT TECHNOLOGY

**CONTINUED SUPPORT OF THE
NATURAL RESOURCES INFORMATION
SYSTEM FOR THE STATE OF
OKLAHOMA**

Contract No. DE-FG22-92BC14853

**Oklahoma Geological Survey
University of Oklahoma
Norman, Okla.**

**Contract Date: May 18, 1992
Anticipated Completion: May 17, 1994
Government Award: \$350,000
(Current year)**

**Principal Investigators:
Charles J. Mankin
Terry P. Rizzuti**

**Project Manager:
R. Michael Ray
Bartlesville Project Office**

Reporting Period: Oct. 1-Dec. 31, 1993

Objective

The objective of this research program is to continue developing, editing, maintaining, using, and making publicly available the Oil and Gas Well History File portion of the Natural Resources Information System (NRIS) for the state of Oklahoma. This contract funds the ongoing development work as a continuation of earlier contract numbers DE-FG19-88BC14233 and DE-FG22-89BC14483. The Oklahoma Geological Survey (OGS), working with Geological Information Systems at the University of Oklahoma Sarkeys Energy Center, has undertaken the construction of this information system in response to the need for a computerized, centrally located library containing accurate, detailed information on the state's natural resources. Particular emphasis during this phase of NRIS development is being placed on computerizing information related to the energy needs of the nation, specifically oil and gas.

Summary of Technical Progress

The NRIS Well History File contains historical and recent completion records for oil and gas wells reported to the Oklahoma Corporation Commission (OCC) on Form 1002-A. At the start of this quarter, the Well History File contained

348,996 records, providing geographical coverage for most of Oklahoma (all but the northeast part of the state). Data elements on this file include American Petroleum Institute (API) well number, lease name and well number, location information, elevations, dates of significant activities for the well, and formation items (e.g., formation names, completion and test data, depths, and perforations). In addition to the standard Well History File processing, special projects are undertaken to add supplemental data to the file from well logs, scout tickets, and core and sample documentation.

A large portion of the Well History File work involves photocopying the completion reports for use in coding before data entry. The historical completion reports are checked out of the OGS's Archive Library and copied at an average rate of about 1500 forms per week. All new completion reports are copied as soon as they are received from the OCC. More than 384,000 completion reports had been copied by the end of the quarter, which represents all the 1002-A completion reports available in-house and approximately 5000 completion reports obtained from Sooner Well Log.

Processing of the OCC's oil and gas well completion reports (Form 1002-A) is proceeding smoothly. Well records are being prescanned, keyed, and edited for Osage County. Approximately 6900 well records were keyed and added to the file this quarter. Thus, as of December 1993, the database contained 355,873 records. Table 1 uses NRIS regional divisions to report Well History File progress. The current status of county coverage and the total record counts by county are shown in Figs. 1 and 2, respectively.

TABLE 1

Well History File Progress by Regional Division

Area of coverage	Start of grant	Start of quarter	Current
Southeast region	65,712	66,954	67,006
Southwest region	69,453	71,669	71,682
Northeast region	23,467	117,181	122,409
Northwest region	32,507	33,355	33,360
North-central region	40,883	59,837	61,416
Total	232,022	348,996	355,873

Both general and specialized edit procedures were continued on the well data. Search strategies are used to research well records with incorrect township-range-section (TRS) or county location data and well records that should be cross-referenced. Oklahoma Tax Commission (OTC) lease numbers are being assigned to well records through a combined machine and manual matching process between the lease and well files. The statewide Lease File/Well File match used to identify sections with significant discrepancies in the lease and well counts has been facilitated by cooperation from NRIS users and from Sooner Well Log Service, Oklahoma City, Okla. Since the start of the contract, efforts to locate missing 1002-A forms for areas identified through these methods have been successful.

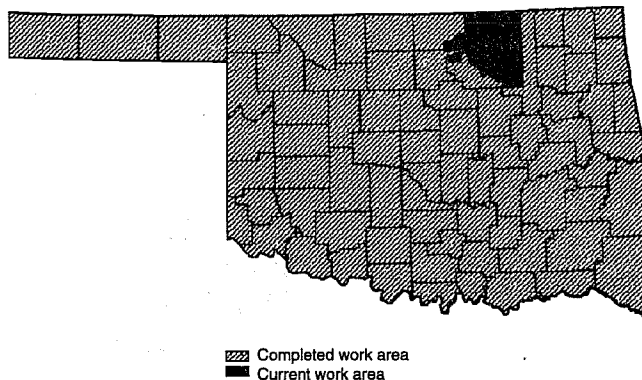


Fig. 1 Status of well history database project by county coverage as of December 1993.

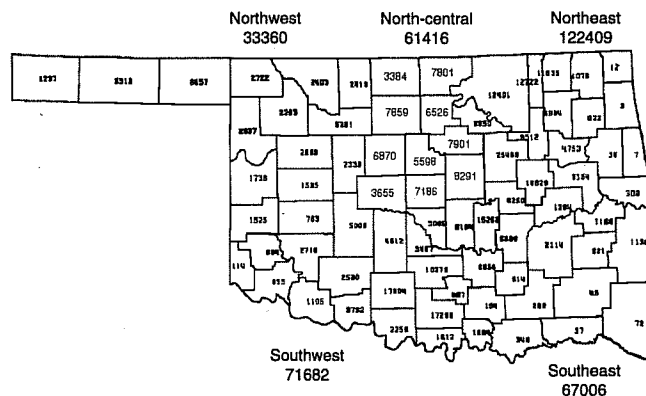


Fig. 2 Status of well history database project. Total well records, 355,873.

Early last quarter all the completion reports available in house had been processed, which resulted in approximately 350,000 forms on the file. Work efforts then emphasized three areas of research to obtain the remaining records, estimated at that time to be an additional 50,000 forms. For example, the Lease File/Well File matching efforts continued as a means of identifying areas with missing 1002-A forms. Another method involved implementing research efforts, whereby well records currently on file were matched against hard-copy scout tickets available through the Lawrence Youngblood Energy Library at the University of Oklahoma. Initial efforts concentrated in the northeastern part of the state on a township-by-township basis. Scout tickets identified for wells not on the Well History File were sent to Sooner Well Log Service, and any missing 1002-A forms available through their collection were obtained and added to the File. Those scout tickets for which no corresponding 1002-A records could be identified were added to the Well History File to ensure a more complete file.

Additionally, efforts were finalized and procedures were established to obtain access to Osage County records available through the Osage Tribal Agency. By the close of the quarter, records for the western half of the county had been copied and received to be coded, keyed, and entered into the

Well History File. Forms from the first shipment of Osage records were reviewed to ascertain how many different form layouts were used to report well completions. It was determined that five layouts would require new keying formats, reformatter programs, and processing job streams. The five layouts were reviewed to identify what data elements were unique to the Osage forms. As a result of this review, 62 labels were identified and added to the data dictionary. Coding procedures for these data elements and formats were established, and coding began. Data-entry keying formats, reformatter programs, and processing job streams were developed and tested. Data entry will begin next quarter.

It is expected that 400,000 forms will be on file by the close of the contract. However, discussions with the Bureau of Indian Affairs (BIA) staff at the Osage Tribal Agency have revealed that there may be as many as 50,000 to 100,000 more forms for Osage County than originally estimated. If so, discussions will be initiated with DOE to identify funding options for completing Osage County coverage.

Efforts to standardize the formation names on the Well History File are continuing. A personal computer (PC)-based program uses a conversion table to standardize spellings and allows the user to build interactively new entries for the conversion table as new spelling variations are encountered. In the southeast, southwest, and northwest regions, over 99% of the reported names have been standardized. Efforts to standardize formation names in the northeast region are complete with 97% standardized. Efforts on the north-central region were resumed with 95% of the region standardized. This formations-editing process is further enhanced by the addition of a table to determine the standard Franklinized abbreviation for each reported name following the convention with which industry users are familiar.

One goal of the NRIS system involves efforts to assign leases and wells to fields on the basis of the official field outlines as designated by the Midcontinent Oil and Gas Association's Oklahoma Nomenclature Committee (ONC). Some areas exist in which significant field extension drilling has taken place, but the ONC has had insufficient resources to update the field boundaries accordingly. To assist the ONC in updating their field outlines, information packages are produced from the NRIS system for selected areas; these packages include well data listings and well spot maps. On the basis of this input, the ONC began by first updating several gas-field boundaries; emphasis has shifted to oil-field boundaries as work proceeds on a separate Department of Energy (DOE) project involving the identification and evaluation of Oklahoma's fluvial-dominated deltaic reservoirs. Overall, unassigned gas production comprises 13% of the annual average production and unassigned oil production comprises 20%.

Twenty-eight new data elements were added to accommodate the new 1002-A completion report forms for 1992. A new reformatter program was written as well as a processing job stream. Keying of the new forms will begin next quarter. Initial efforts for the January 1994 data release began this

quarter also, and all new data elements (definitions and coding instructions) will be documented in the NRIS Data Manual next quarter. It is anticipated that the 92 new data elements for the 1992 forms and the Osage County records will be included in the July 1994 data release.

Public Data Release

Since early 1991 efforts have been made to disseminate NRIS information through meetings, workshops, OGS annual reports, and mass mailings to numerous individuals, companies, and organizations. As a result, a dramatic response to the release of NRIS data began during the summer of 1991 and has continued. Feedback from the public continues to reflect excitement about this new resource for the oil and gas industry in Oklahoma. Data and analyses have been provided that would not have been feasible before construction of the NRIS system.

One commercial firm subscribes to the Well History File, and several inquiries are received each quarter from small companies and independents who typically acquire NRIS subsets to evaluate within their specific computer systems before committing to larger data acquisitions.

Also, as previously reported, NRIS well data have been made available through the Oklahoma City Geological Society Library with positive results. The high level of interest by library members has led to the acquisition of several thousand records by several members as well as constructive feedback on user-detected data anomalies. Also, the Library, which is cataloging its extensive well-log collection and tying each log to the corresponding NRIS well record, will be able to provide a listing of logs for which no NRIS records are on file. This should greatly enhance efforts to locate missing well records.

The OGS is establishing a computing facility to promote user access to the NRIS data, initially by OGS staff and eventually by the public. A PC-level relational database management system called Advanced Revelations is being used to develop a menu-driven retrieval system customized to NRIS data. A large digitizer, large plotter, and desk-top scanning equipment enhance the capabilities available through GeoGraphix and Radian CPS/PC contour mapping software as well as through ARC/INFO, a geographical information system (GIS) spatial analysis tool.

The NRIS data factor significantly in several projects. One such project, under way in conjunction with the Geography Department, involves the creation of a GIS database of oil and gas pipelines for the Oklahoma Ad Valorem Task Force in which four Oklahoma counties are used as a pilot study. The NRIS well data were included as related data layers. Another project, a DOE project, involves the study of Oklahoma's fluvial-dominated deltaic reservoirs. A third project, which involves cooperative research with the School of Civil Engineering and Environmental Science, is the creation of a GIS database (with a wellhead protection component) containing current and potential waste sites located on Oklahoma's Cheyenne/Arapaho tribal lands.

ASSIST IN THE RECOVERY OF BYPASSED OIL FROM RESERVOIRS IN THE GULF OF MEXICO

Contract No. DE-AC22-92BC14831

**Louisiana State University
Baton Rouge, La.**

**Contract Date: Feb. 18, 1992
Anticipated Completion: Mar. 18, 1994
Government Award: \$2,025,755**

**Principal Investigator:
Philip A. Schenewerk**

**Project Manager:
Gene Pauling
Metairie Site Office**

Reporting Period: Oct. 1–Dec. 31, 1993

Objective

The objective of this research is to assist the recovery of noncontacted oil from known reservoirs on the Outer Continental Shelf (OCS) in the Gulf of Mexico. Mature offshore reservoirs, declining oil reserves, declining production, and other natural forces are accelerating the abandonment of offshore oil resources and production platforms. As these offshore wells are plugged and the platforms are abandoned, an enormous volume of remaining oil will be permanently abandoned. Significant quantities of this oil could be recovered with advanced technologies now available if the resource can be identified. Project research will proceed under three broad phases: data analysis, supporting research, and technology transfer.

The Tertiary Oil Recovery Information System (TORIS)-level data will be collected on the major fields located in the piercement salt dome province of the Gulf of Mexico OCS. Representative reservoirs will be studied in detail to evaluate undeveloped and attic oil reserve potential. These detailed investigations will be used to calibrate the TORIS-level predictive models. The recovery potential of advanced secondary and enhanced oil recovery (EOR) processes and the exploitation of undeveloped and attic oil zones for salt dome reservoirs in the Gulf of Mexico will be assessed.

Supporting research will focus on the modification of public domain reservoir simulation models to accurately simulate the conditions encountered in the piercement salt dome province of the Gulf of Mexico. Laboratory research will focus on the development of fluid relationships that will be used in the simulation of miscible and immiscible processes in the project area.

A significant effort is planned to transfer the results of this project to potential users of the technology. Technology transfer activities will also provide feedback channels that will help keep the analysis and supporting research focused on the most important problems associated with this project.

Summary of Technical Progress

Data Validation and Map Measurements

Maps collected at the Minerals Management Service (MMS) office in New Orleans were planimeted and measured in order to verify and cross-check data in the Field and Reservoir Reserve Estimate (FRRE) database and to obtain reservoir size, shape, dip, and relative well-position data for use in TORIS process models. Measurements of estimated salt diameter and updip areas are also being derived. Production data were read from the tapes obtained in New Orleans and reformatted for use in TORIS. There were errors in some of the tapes that will be corrected.

Model Development

Conceptual work began on the development of the models required to assess unrecovered oil, continued primary recovery of existing mapped oil, updip attic oil recovery, and miscible and immiscible carbon dioxide (CO₂) injection recovery. Preliminary model designs have been tested against subsets of the data, and the models are being refined. When this work is complete, coding will begin. This effort included a literature search on topics related to EOR in offshore Gulf of Mexico reservoirs.

Supporting Cost Data Collection

Efforts began to supplement existing TORIS data with drilling, workover, and facility costs related to past EOR programs in the offshore Gulf of Mexico area. Data on CO₂ sources were collected, and by-product CO₂ costs were estimated for use in the economic model.

Detailed Reservoir Studies

Louisiana State University (LSU) continued the analysis of data obtained from Taylor Energy on the South Marsh Island (SMI) Block 73 field in the Gulf of Mexico.

Reservoir 3, Field 2

Data analysis continued on Reservoir 3 in Field 2. Simulations are being run on BOAST III as well as on the operator's in-house proprietary simulator. A similar data set is being used to enable calibrations and comparisons to be made. The history match made by BOAST III matched well with the history match made by the operator's simulator.

B-65-G Sand Reservoir

Material balance and computer simulation studies of the B-65-G sand reservoir in the SMI Block 73 field also continued. Work on refining the match for use in predictive runs is in progress. The B-65-G sand reservoir was chosen as a model for calibration studies because of its numerous gas injection cycles from different locales, longevity of its production, and access to data. Actual production from this reservoir was more than 6 million bbl of oil, 4.1 Bcf of gas, and 820 million stock tank barrels of water. On the basis of material balance and the computer simulation, the reservoir is estimated to have originally contained more than 12 million bbl of oil and a gas cap containing 1.8 Bcf.

Critical Process Parameter Laboratory Experiments

The apparatus for experiments on attic oil recovery techniques is being tested.

BOAST II Radial Grid Modification

Tests of the two-dimensional (2-D) adaptive finite element model are simulating oil-water flow through porous media. Although coning traces similar to those in the Lance Hebert thesis¹ are being produced, oscillations are still a problem. Testing on much simpler hypothetical problems produces oscillation-free results but at the expense of heavy mesh refinement along the oil-water interface. It is believed that extensive mesh refinement in the Hebert problem would also

produce oscillation-free results, but more work is needed to speed up the calculations and reduce the memory requirements. Distribution of the workload and memory across a cluster of RS6000s has been accomplished with the use of a parallel virtual machine (PVM) for interprocess communication. On an unloaded system, the speed-ups have been excellent. However, the system is currently limited to four nodes on the cluster at a time, usually sharing the nodes with other users, so it is difficult to achieve any speed-up under these conditions. The code will be ported to a 128-node Cray T3D for testing in a massively parallel processing (MPP) environment. The parallel version of the code is suitable for one-, two-, and three-dimensional problems using static meshes. Currently, the implementation of dynamic mesh routines on the parallel architectures is being studied; the fact that efficient load balancing will become a major issue is recognized. Much of this work is being written up as a doctoral dissertation with the intention of publishing parts of it—particularly the parallel implementation. Testing of this method on areal sweep efficiencies is continuing.

MASTER Modification

The MASTER modification has been completed and is undergoing testing.

Reference

1. L. Hebert, *An Experimental Study of the Effects of Water Coning on a Horizontal Well in a Bottom Water Drive Reservoir*, thesis, Louisiana State University, Baton Rouge, La.

FIELD DEMONSTRATIONS

DYNAMIC ENHANCED RECOVERY TECHNOLOGIES

Contract No. DE-FC22-93BC14961

**Columbia University
New York, N.Y.**

**Contract Date: July 5, 1993
Anticipated Completion: Oct. 30, 1995
Government Award: \$7,742,000**

**Principal Investigator:
Roger N. Anderson**

**Project Manager:
Edith Allison
Bartlesville Project Office**

Reporting Period: Oct. 1–Dec. 31, 1993

Objective

The objective of this project is to test the concept that the growth faults in a Gulf of Mexico field are conduits through which the producing reservoirs are charged and that enhanced production can be developed by producing from the fault

zone. The field demonstration will be accomplished by drilling and production testing of growth fault systems associated with the Eugene Island Block 330 operated by Pennzoil in federal waters off Louisiana.

Summary of Technical Progress

Management Start-Up

The 1994 American Association of Petroleum Geologists (AAPG) Annual Meeting will be held in Denver, Colo., June 12–15, 1994. At this meeting, there will be a special poster session entitled “DOE/GBRN-Sponsored Gulf of Mexico drilling program—Eugene Island 330.” Eighteen abstracts have been accepted for the poster session.

Database Management

Geological Analyses of Industry Three-Dimensional Seismic Surveys

Landmark Graphics has completed its task of comparing the traditional interpretation of the horizons and faults and the reinterpreted reflector horizons and faults as discussed in the previous quarterly report.

The computer algorithm for correlating well logs from Eugene Island has entered the second phase of development. In the first phase, success was achieved in devising a

technique for automatic, high-resolution correlation of any two related time series (at this stage isotope records and simulated well logs). Although refinement of the technique will continue, correlations are now defined in terms of a mapping function, a point-by-point relation that establishes how one time series maps into the time-space domain of another. Deviations in this function from a one-to-one correlation reveal mismatches between time series as a result of time-space distortions (e.g., differences in sedimentation rates) or missing sections (e.g., unconformities). Mapping functions are determined through a forward comparison of the relative amplitude and shape at each pair of points in the two time series. The global comparison results in not one but multiple correlations. The second phase in the development of the algorithm is to devise a routine for the bookkeeping of all the possible mapping functions. This routine, which is simple in concept but which will be computer intensive, is being developed and tested. Once implemented, the third phase and the testing of several different methods for statistically ranking the mapping functions will begin.

Real-Time Visualization of Database

The real-time database is online. Currently, the Lamont-Doherty Earth Observatory (LDEO), Louisiana State University (LSU), Pennsylvania State University (PSU), and Cornell University have the capability of sharing data and results. Plans are to store and make accessible on this system all the field demonstration experiment data.

Field Demonstration Experiment

The Pathfinder well spudded on Nov. 2, 1993. Pennzoil drilled the first portion of the hole and set 9⁵/₈-in. casing at a depth of 7035 ft measured. At this depth, the Global Basins Research Network/U.S. Department of Energy (GBRN/DOE) well extension began on Nov. 23, 1993, and ended on Dec. 16, 1993, at which time Pennzoil again took over financial responsibility of the well. The field demonstration experiment actually ended on Dec. 25, 1993, because of the generosity of Pennzoil in providing financial support to complete the third stage of the field demonstration experiment.

In the final preparation for the field demonstration experiment, letters were mailed to vendors, and final vendor and Pennzoil meetings occurred before the initial GBRN rig activity. A substantial effort was made in the planning of these experiments to anticipate and eliminate any foreseeable problems during the field demonstration experiment.

Field Demonstration Experiment—Stage I

The objective is to take over financial responsibility for the well from Pennzoil, whole core, and complete drilling to 8000 ft true vertical depth (TVD) or through fault zone.

Pennzoil agreed to log while drilling the well extension from the 9⁵/₈-in. casing to the point where GBRN begins to core. The LWD operation helped to predict the location of the first whole core. The bit used for the whole coring project was

an experimental anti-whirl bit developed by Amoco and Baker Hughes Inteq and had never been in a real coring situation before. A 60-ft core barrel was chosen over the usual 30-ft barrel normally used in the oil industry because the core could be obtained twice with every trip in the hole. A total of 343 ft of whole core was obtained from an attempted 360 ft (95% recovery).

The first whole core, taken from 7650 to 7710 ft, was acquired and back on the rig floor within 12 h, a coring speed never before experienced in 16.2 ppg mud weight. The first whole core recovery was 53 ft out of 60 ft attempted. Core Labs sectioned the core for shipment and cut 1-in. disks every 6 ft. From these disks, fractures cutting the bedding, dipping 20° to the well, could be seen. Steeper dipping fractures are cross-cutting the bedding with a prominent one dipping at 45° and striking about 30° to the bedding strike. A slab was separated along the fracture plane, and slickensides were clearly visible on the fracture. Several small stringers of Pennzoil's OI-5 pay sands were luminescent and oil bearing, but most of the section was a dark-gray shale. Mud filtrate had invaded the fracture during the coring operation. The core sections are being refrigerated and frozen, alternately, every 3 ft and shipped to Core Labs in Houston for quick analysis and photography.

Whole core No. 2, taken from 7710 to 7770 ft (100% recovery), contained near-vertical fracturing, and increasingly more shattered shales were encountered from the fault zone in core No. 2 to core No. 3, taken from 7770 to 7830 ft (100% recovery) with the bedding tilting to steeper angles and the fractures offsetting the bedding. In one slab, a series of 20 microfractures, all 70°, offset the bedding in the neat stair-stepping pattern of miniature growth faults. These fractures are easy to separate, and many are filtrate filled, in other words, permeable. No slickensides were found, but some of the fractures seemed to be healed. Near the bottom of core No. 3, about 10 ft of solid shale was encountered with only a couple of fractures, one of which looked healed.

Six feet of oil-bearing silty shale was encountered at the top of core No. 4, taken from 7830 to 7890 ft (100% recovery). The lithology became more sandy, and again there were pervasive, steeply dipping fractures; however, the rock was fluorescent throughout and especially on the planes of the easily opened fractures. The petroleum aroma was strong. This was followed by 20 ft of solid shale. Upon opening the lower 30-ft barrel, a strong gas odor was apparent. Chevron gas bags were used to capture some of the gas for analysis. The rock was silty-sandy, although extremely fine grained and very dry looking, which was likely a dry gas zone.

The base of the fault was found in core No. 5, taken from 7890 to 7950 ft (83% recovery) at 7511 ft TVD by a return of shallower dipping fractures, some of which were slickensided and had features like worm burrows and cross-cutting laminations. These features were more apparent because of far fewer fractures. The slabs alternate between massive shale and friable, silty shale with some slickensides. This pattern continues into the top of core No. 6, taken from 7950 to 8010 ft (100% recovery). In core No. 6, more 20°

dipping slickensided fractures were seen as the depth increased. With the hole inclined 20° to vertical, the surfaces are either horizontal or they are dipping 45° to the southwest, just as the fault system does. If so, another splay of the fault system was encountered.

Field Demonstration Experiment—Stage II

The objective is to wireline log, sidewall core and acquire several pressure readings throughout the well extension with a formation tester.

On Nov. 27, 1993, GBRN began the second stage of the GBRN/DOE field demonstration experiment. Logs were made from 8360 to 7035 ft MD with several logging tools to obtain as complete a picture of the fault zone as possible with the newest logging equipment available. Table 1 lists all logs obtained from the well extension.

TABLE 1
Eugene Island 330 A-20ST Well
GBRN/DOE Project Listing of Log Data

Resistivity Logs
1. Array Induction Log-TVD, 1 in., Run #2
2. Array Induction Correlation Log, 1 in., Run #2
3. Array Induction/GR/Cali/AMS, 5 in., Run #2
4. Array Induction/GR/Cali/AMS-TVD, 5 in., Run #2
Acoustic Logs
1. Dipole Shear Imager-TVD, 1 in., Run #2
2. Dipole Shear Imager/GR/AMS, 1 in., Run #2
3. Dipole Shear Imager/GR/AMS-TVD, 5 in., Run #2
4. Dipole Shear Imager/GR/AMS, 5 in., Run #2
Porosity Logs
1. LithoDensity/Comp Neutron/GR/AMS, 5 in., Run #1
2. HNGS Log, 5 in., Run #2
3. LDS/APS Porosity Log, 5 in., Run #2
4. LDS/APS Porosity Log-TVD, 5 in., Run #2
Geochemical Logs
1. ECS Yields, Experimental, 5 in., Run #2
2. GRA Elemental Yield Experimental, 5 in., Run #2
3. ELAN
Formation Micro-Imager Logs
1. FMI monitor log/GR/AMS, 5 in., Run #2
2. Mean Square Dip Log/FMI/GR/AMS
3. FMI Image Log wrapped by P1AZ, Run #2
4. Borehole Ovality Log
Other Logs
1. Modular Formation Dynamics Tester, Run #2
2. AMS/Mud Temp/Mud Resistivity Log, 5 in.
3. Borehole Profile Log/GR/AMS, Run #2
4. Sand Strength Analysis Log
5. Frac-Height Log
6. Mechanical Properties Log

Because of the hole conditions, while attempting to obtain the first pressure, the modular formation dynamics tester (MDT) got stuck. As a result of this and the previous fishing job, it was decided not to pursue additional pressures. The stage II budget was depleted at this point. Pennzoil agreed to pay for sidewall cores and rig time for the well extension. Pennzoil acquired 75 sidewall cores from 7157 to 7661 ft in three coring runs in the hole.

Field Demonstration Experiment—Stage III

The objective is to case the well extension, perform a stress test below the fault zone test interval, frac-pack the fault zone test interval, flow fluids to surface in a production test, and shut the well in for a pressure transient limits test.

Stage III of the experiment began on Dec. 2, 1993, with the running of a 7 $\frac{7}{8}$ -in. liner into the well extension. The cement job on the liner was apparently a failure according to the CBL/VDL/CET log, which shows cement bonding logs. As a result of the poor cement job, it was necessary to squeeze cement into the intervals directly above and below the test zones to ensure isolation of the test zone. Two squeeze jobs were performed, one at 7726 to 7730 ft MD and the other at 7573 to 7577 ft MD. A stress test was performed below the fault at 7726 to 7730 ft MD and at 7573 to 7577 ft MD to obtain formation fracture pressure at different points within the fault zone.

Because of the costly completion fluid at this depth and the costs associated with the squeeze jobs, GBRN was at the point of shutting the stage III experiment down when Pennzoil agreed to pick up any costs associated with the remainder of the experiment.

The pressure data obtained revealed two separate permeability networks: a high-permeability fracture network and a lower permeability, far-field network. Because the single fracture design must address both networks, a dual permeability model was used to design the pumping rates. The fracture was performed by driving a vertical fracture 40 ft away from the wellbore and extending 20 ft on either side of the perforations. The downhole pressure readings showed that the formation permeability increased from 3 to 84 mD, and the producibility increased from 135 mD/ft to 3.5 D/ft. The well was then shut in to clear the sand from the wellbore, and the well began to flow again at 400 psi against a 16.3-ppg completion fluid. The well began to flow at 2 bbl/h; however, the completion fluid weight was increased to stop the flow and retrieve the fracture assembly.

The testing assembly was then tripped in the hole to flow test the fault-zone interval. The flow test began with a rate of 192 bbl/d and within 2 h dropped down to the same rate previously flowed. All data indicate that the formation should maintain a substantial flow rate, so Pennzoil called out a coiled tubing unit to jet the well with nitrogen. Once this procedure began, the flow rate increased to 200 bbl/d but would not sustain itself. It was possible, however, to get oil to the surface and to obtain fluid and oil samples within the fault-zone

interval. As the jetting got deeper, the formation flowed less and less until it completely stopped at 5000 ft MD. In other words, the more underbalanced it was, the less the formation flowed. The conclusion drawn from this behavior is that the permeability in the fault zone is pressure dependent, and, as the pressure in the wellbore is drawn down, the fracture network supplying the permeability within the fault zone shuts down tighter and tighter. Additional efforts to flow the formation failed. However, 15 gal of oil from the fault-zone interval was sampled for geochemical analysis.

Pennzoil abandoned the fault-zone interval and will complete in their economic target the OI-4 formation, which is only 120 ft above the fault zone. The OI-4 may be connected to the fault zone by several of the natural vertical fractures, so the plan is to monitor production closely.

Reservoir Characterization

At this point almost all the significant well data for the Eugene Island Area have been obtained. Data from 3 seismic surveys and well data for over 460 wells have been obtained. Eugene Island Blocks 314, 330, 331, 337, 338, and 339 contain extensive directional and wireline data as well as some sidewall core data and well event picks. Many of the wells outside this nine-block area contain velocity, mud logger, and directional data.

All the new data acquired during the drilling of the Pathfinder well will be added to the database as soon as the equipment returns to PSU. This includes Formation Micro-Imager (FMI), AIT, DSI, MDT, and geochemical test results as well as mud logger, wireline, and core data.

Four-Block, Three-Dimensional Analysis (Pennsylvania State University)

Work on reservoir characterization is being undertaken with the use of Landmark software for interpretation of three-dimensional (3-D) seismic data and Mincom/Geolog software for wireline data. Two 3-D seismic data sets, a Pennzoil-donated survey centered on Block 330 and a Texaco-donated survey centered on Blocks 338/339, are currently being analyzed.

The major faults have been identified and mapped in the Pennzoil seismic data set. The main features include

- A prominent NW-SE trending down to the southwest growth fault (the "A" Fault or "Red" Fault), which extends from the SE corner of Block 330 to the NW limit of the data in Block 314. Vertically, the fault extends from over 3 sec. TWT to the sea floor. This fault has several splays toward the NW and SE margins and a prominent E-W trending antithetic fault, which splays off the Red Fault near the center of Block 330.

- A series of NW-SE trending down to the southwest normal faults located to the north of the Red Fault (principally Block 315) and running subparallel to it.

- A series of NE-SW trending down to the southeast normal faults to the north of the Red Fault located principally in Block 316. A domed rollover structure located in Block 330 forms the principal structural trap. Structural mapping is in its

initial phases for the Texaco seismic data set. There, south of Block 330, a prominent counter-regional growth fault (down to the north) bounds the southern flank of the rollover structure, which peaks in Block 330.

Wireline logs are being used to pick specific sand units. At present, the focus is on the GA sand and neighboring units. The tops of the GA, FA, and HB sands and the base of the GA sand have been picked and entered into Geolog for all wells with gamma-ray curves and deviation surveys (approximately 200 wells in Blocks 314, 315, 329, 330, 331, 337, 338, and 339). The GA sand body forms (stratigraphically) the highest reservoir in Block 330. The production history from this sand indicates that it has significantly overproduced with respect to initial reserve estimates.

For integration of the wireline and seismic data sets, synthetic seismograms have been generated in Geolog for holes that have sonic and density wireline logs. The results of the synthetic seismogram construction have been used to repick the GA sand top throughout the entire Pennzoil and Texaco 3-D seismic data sets.

The work done by PSU on the GA sand is being integrated with the results of work by Chevron in Lafayette on correlative strata (4500-ft sands) in Blocks 338 and 339. From an examination of seismic facies configuration on seismic profiles and correlation of these observations with wireline data, a detailed sequence stratigraphic interpretation is being developed. Relative sea-level rise terminated deposition of the HB delta front sands. This was accompanied by, or followed shortly by, large-scale mass wasting of the continental margin. Slump scars thus generated have previously been interpreted as channels at the base of the GA sand, which incised into the top of the HB sand. The GA sand itself records a basin-ward transition from thick (locally over 400 ft) channelized sand bodies near the Red Fault in Block 330 to prograding clinoforms (representing a delta slope environment) to the south, toward and into Block 338. The effects of smaller scale mass wasting events can be seen in places as base of slope turbidities and, possibly, as some disruption of the clinoform geometry.

Pressure Mapping

Effective stress, porosity, and abnormal pressure in the E.I. 330 field. The objective was to test the hypothesis that abnormal fluid pressures were mainly the result of sediment undercompaction. A north-south section across a pressure-sealing growth fault was chosen, and the porosity-depth profiles were investigated. The gamma-ray log was used to pick shale intervals and the sonic log was used to determine porosities. Assuming that porosity of shales is an exponential function of effective stress (overburden-fluid pressure) in the E.I. 330 field, fluid pressure was predicted from sonic-log-derived porosities. The porosity-stress relationship in the hydrostatic pressure zone is calibrated to determine the parameters ϕ_0 and λ that characterize normal compaction:

$$\phi = \phi_0 e^{-\lambda \sigma}$$

where ϕ_0 equals 0.51, λ is approximately $5.8 \times 10^{-5} \text{ psi}^{-1}$, and σ is the effective stress (psi).

The normal pressure gradients predicted from porosity data are approximately 10% lower than those predicted from mud-weight data. These data are at a much higher resolution than mud-weight data, although there is some noise in the vicinity of oil-bearing sands.

The E.I. 330 field is found on the downthrown and low-pressure side of a pressure-sealing growth fault. The porosity profiles on the upthrown (footwall) side of the fault actually increase with depth as thick, shallow shales are penetrated. In contrast, geopressures in the hanging wall are much deeper, and, although the same mud-weight gradients are reached, the porosity profile reverses (increases) only slightly in the geopressured zone. In the hanging wall, the transition from hydrostatic to geopressures occurs in the two phases. The major reservoir interval is found in the transition from 12 to 14 lb/gal; beneath this interval hard geopressure is marked by an abrupt jump to almost 16 lb/gal as a thick shale is penetrated.

These results suggest that the primary cause of geopressures in this region is undercompaction. The association of the transition to geopressure with the transition to a shale-prone stratigraphic section reveals that the pressure seals are stratigraphic; regional, low-permeability shales seal pressures in this basin. In addition, the abrupt jump in fluid pressures across the fault plane implies that the fault itself is also sealing.

Modeling

The integration of preprocessing and finite-element modeling into a single user-friendly AKCESS.BASIN modeling system has been successfully completed and will be demonstrated to the corporate affiliates in January. New functions for inferring salt movement from the pattern of sedimentation have been written and used to define the history of salt movement in the South Eugene Island Minibasin and regionally in a 400×200 km portion of the Louisiana shelf. The modeling capability has been expanded to include (in a separate preprocessor) deformation defined by horizontal extension along nonvertical faults and a detachment surface. Hydrocarbon maturation has been added to AKCESS.BASIN. The preprocessor is menu driven, and AKCESS.BASIN execution is greatly streamlined.

FORTRAN Algorithms

Diapirism and compaction (80% completed). The algorithms for modeling diapirism and compaction have been modified on the basis of the recognition that volume is not conserved in cases of uneven sedimentation in which the pseudo-wells are nonvertical and the recognition that robust correction will be difficult. The solution adapted is to separate modeling into two basic types. In the first type of model, deformation and vertical faulting are driven by sedimentation, and diapirism and compaction are taken into account. All pseudo-wells are vertical, and no horizontal extension is allowed. The second type of model allows nonhorizontal

wells and extensional faulting as well as diapirism but assumes that there is no compaction. The first type of model is directly extendible to 3D and will be the basis for the initial realistic modeling in the South Eugene Island minibasin. The first type is the basis for the two-dimensional AKCESS.BASIN package released in January 1994. The second type of modeling (faulting) will be the basis for a future preprocessor release.

Fault movement (70% completed). A major advance was achieved this quarter with the development of a fault preprocessor. The fault preprocessor uses stratigraphic gaps on nonvertical fault surfaces to define the horizontal extension that has occurred. The gaps can normally read from seismic reflection profiles. The horizontal faulting processor incorporates the horizontal extension into the geologic history of the area and writes a file of node movement (both horizontal and vertical) for the use of AKCESS.BASIN. Diapirism can be simulated along with the faulting. Compaction is not taken into account in the horizontal faulting type of model. Derivative effects of compaction, such as increased thermal conductivity, however, can be taken into account by AKCESS.BASIN.

Physical property algorithms (70% completed). Testing of algorithms describing heat transport only around salt structures is complete. The results of AKCESS.BASIN simulations have been verified for simple free thermal convection with a variety of Rayleigh numbers. In addition, AKCESS.BASIN reproduced results computed from the U.S. Geological Survey's program SUTRA for an onshore salt dome in south Louisiana.¹

Chemical Models

Gas solubility and gas generation kinetics (75% completed). The hydrocarbon maturation model of Burnham has been incorporated into AKCESS.BASIN. This C program model was coded under funding from the Gas Research Institute (GRI). The model has the potential to simulate oil and gas compositions in considerable detail. It will be used to calculate oil and gas compositions in the SEI minibasin, with the hope that this will prove to be an effective way to determine the past history of fluid flow in the area.

In a related area, jointly funded by GRI and this DOE project, considerable progress has been made in calculating the compositions of coexisting oil and gas as a function of P and T. The procedure was used to generate the C maturation code discussed previously. The C hydrocarbon composition code is being combined with one-dimensional finite-difference models of sedimentation and maturation and will be combined next quarter with hydrocarbon fluxes to obtain a predictive model of hydrocarbon maturation that can be applied to the SEI minibasin.

Reports and Abstracts

Eight abstracts were submitted to the AAPG from the Modeling Group. One abstract was submitted to the Hedberg

Research Conference that precedes the AAPG meeting. One paper was completed for publication.²

Geochemistry

Inorganic Geochemistry

The core was oriented for slabbing at Core Labs by use of X-ray fluoroscopy. After slabbing, the core was logged at a scale of 1:5. Description revealed a variety of fault features: fault deformation in shales was noted in the first 150 ft of core, followed by a less-faulted, rotated block containing shaly silts and sands about 90 ft thick (cumulative fluorescent sand thickness in this interval is about 16 in.), followed by a second fault zone in the lower 120 ft, with the most intense deformation within a 30-ft-wide zone within that interval. Although observed fluorescence in faults and fractures in the upper fault zone was scarce, there was considerable fluorescence in faults of the lower zone. Faults in the core are of two distinct styles: single discrete slickensided planes (many containing drilling mud) and gouge or gouge breccia zones up to several inches thick. High-angle faults (angle is measured relative to a plane that cuts across the core, and that would be horizontal if the core were stood on end) are typically planar to curvilinear and are narrow zones to hairline fractures, whereas nearly all the gouge and gouge breccia zones (with one notable exception) are low angle. In most cases, the low-angle structures truncate the high-angle ones.

Copies of the preliminary core description have been sent to Shell, Exxon, Pennzoil, and Conoco as well as to the Woods Hole Oceanographic Institution (WHOI) and LDEO. On the basis of these logs, Shell and Exxon plan to sample at selected intervals: Shell for rock property, diagenesis, and geochemical studies and Exxon for density measurements and computerized axial tomography scanning of fault zones. Samples of cuttings and core are being analyzed for paleontological dating by Pennzoil. Project scientists from WHOI also sampled the core in Houston. Schlumberger has taken 50 plugs for bulk geochemical analysis to compare with the output from the geochemical log. Two plugs have been taken for overburden porosity measurements. In addition, discussions have been held with Cornell University, who intends to study the cored fault in terms of strain history, deformation mechanisms, and rock properties. Work is ongoing at Cornell to integrate the remaining structural data from X-ray fluoroscopy and log data from the core and downhole gamma-ray logs and the FMI log for the purpose of orienting the core in space. When this is done, structures in the core will be placed in a larger context, and a priority will be established for sampling for geochemical work at Cornell and Michigan Technological University.

Organic Geochemistry

During drilling of the pathfinder well excellent gas and oil samples were obtained. The gas samples were obtained with a new gas sampler that is used extensively at Chevron. These samples have been shipped to Chevron, where they will be

analyzed for structural and isotopic composition. Several oil samples from various other wells that have been drilled from the same platform were also collected. These samples are now in analysis.

Plan for Core Storage

The cores are being stored at Core Labs in Houston, Tex. Eventually, they must be shipped to one of the GBRN institutions for permanent storage. The tentative plan is to keep all the samples together, which means storage at Penn State. However, there is evidently no money in the Penn State budget at the present time for this purpose. This means that Woods Hole will probably have to purchase the four or five freezers required for permanent storage of the frozen cores.

References

1. Ranganathan, J. *Geophys. Res.* (1992).
2. R. A. Manning, P. D. Manhardt, J. A. Orzechowski, L. M. Cathles, and A. J. Baker, *A Parallel 3-D Finite Element Geologic Basin Modeling Code*, paper prepared for SIAM Conference on Mathematical and Computational Issues in the Geosciences, Houston, Tex., April 19-21, 1993.

WEST HACKBERRY TERTIARY PROJECT

Contract No. DE-FC22-93BC14963

**Amoco Production Company
Houston, Tex.**

**Contract Date: Sept. 3, 1993
Anticipated Completion: April 2, 1997
Government Award: \$6,017,500**

**Principal Investigator:
Travis H. Gillham**

**Project Manager:
Gene Pauling
Metairie Site Office**

Reporting Period: Oct. 1-Dec. 31, 1993

Objective

The objective of this project is to demonstrate the technical and economic feasibility of combining air injection with the double displacement process (DDP) for tertiary oil recovery. The DDP is the gas displacement of a water-invaded oil column for the recovery of oil through gravity drainage. The novel

aspect of this project is the use of air as the injection fluid. The target reservoirs for the project are the Camerina C-1,2,3 sands located on the west flank of West Hackberry field in Cameron Parish, La. If successful, this project will demonstrate that the use of air injection in the DDP can economically recover oil in reservoirs where tertiary oil recovery is uneconomical.

Summary of Technical Progress

During the first quarter, areas of progress included construction of surface facilities, workovers of existing wells, technology transfer, and laboratory tests.

Construction of Surface Facilities

The first major goal of this project is to initiate air injection during the second quarter of FY 1994. To accomplish this goal, work has gone forward on issues relating to the air compressors, compressor foundation, electric utilities, and permitting.

Air Compressors

An evaluation was completed to determine the optimum pressure crossover point for air flow from the screw compressors to the reciprocating compressor. The purpose of the evaluation was to determine if the number of screw compressors could be reduced from two to one (total compressors from three to two). This would simplify the installation, operation, and maintenance of the compressor facility. From the evaluation, it was determined that lowering the crossover pressure from 200 to 100 psi could reduce the number of screw compressors required from two to one. Although an additional compression stage and a larger engine would be required for the reciprocating compressor, the overall cost would not increase. On the basis of the revised design, updated compressor bid specifications were prepared and sent to vendors. Returned bids were evaluated, vendors were chosen, and purchase orders were completed for the air compressors. The vendors have ordered major equipment.

Compressor Foundation

With the number of compressors reduced from three to two, the compressors can be installed on an abandoned compressor foundation that exists in the field; this will eliminate the need for the concrete compressor barge that was included in the original design and will reduce the environmental impact of the project by doing away with the need for additional dredging or the preparation of a shell pad for the barge. The existing compressor foundation is being studied to determine what modifications are required and to verify that the foundation will accept the loading.

Electric Utilities

A meeting was held with Gulf States Utilities in West Hackberry field to outline the electrical services that will be required. Gulf States Utilities is preparing the work order.

Permitting

An air permit revision was submitted to the Louisiana Department of Environmental Quality for the addition of the two air compressors to the West Hackberry field. The permit revision was approved on Nov. 15, 1993.

Planned Surface Facilities Work

The following facilities work is planned for the second quarter of FY 1994:

- Finish evaluation of using the existing foundation for the air compressors.
- Review and approve final design drawings from compressor vendors.
- Submit revised permits to the Corps of Engineers for any construction changes.
- Purchase materials for injection lines and water purge system.

Workovers of Existing Wells

Two injection wells and nine producing-monitoring wells will be involved in the project. Two workovers of existing wells are planned for the upcoming quarter. During the final week of November 1993, a workover rig will be moved onto the site of the Gulf Land D R/A A No. 13. This well, which was plugged and abandoned during 1983, will be reentered and completed to serve as a future producing well in the air injection project. As per the state regulations, the well's name will be changed to the WH Cam C RI SU; Gulf Land D R/A A No. 56. During the month of December 1993, a rig will be moved to the Watkins No. 16, which will be converted from a shut-in (watered-out) well in the Cam C-3 sand to an air injection well in the Cam C-1,2,3 sands.

Technology Transfer

Two significant events occurred during this quarter. A talk entitled "Air Injection for Tertiary Oil Displacement at W. Hackberry, La., a DOE Co-Sponsored Project" was presented to the Improved Recovery Study Group of the Society of Petroleum Engineers (SPE) Gulf Coast Section in Houston, Tex., on Sept. 8, 1993.¹ Also, a paper was presented at the 1993 SPE Annual Technical Conference and Exhibition entitled "The Use of Air Injection to Improve the Double Displacement Process."²

Additional technology transfer activities are planned for the next two quarters. A paper entitled "An Introduction to the West Hackberry Air Injection Project" will be presented at the monthly meeting of the New Orleans Section of the SPE on Feb. 8, 1994.³ An abstract has also been submitted to the 1994 National Institute of Petroleum Engineers/Department of Energy (NIPER/DOE) Symposium: In Situ Combustion Practices—Past, Present and Future Applications, scheduled for Apr. 21–22, 1994, in Tulsa, Okla.

Also during this quarter a contract was negotiated between Amoco Production Company and Louisiana State University (LSU). The contract provides for LSU's independent study of the project along with technology transfer activities. The DOE approved the contract, and the contract was signed during November 1993.

Laboratory Tests

During 1992 Amoco Production Research used a numerical thermal model (THERM) to conduct scoping studies for estimating oil recovery performance as the result of air injection in West Hackberry. The results of this study were used to assess the economic feasibility of the air injection project. Although all available data on this reservoir were used in this study, several key data on fluid and rock properties were not available. New laboratory tests were proposed to obtain the necessary data. The status of these tests and a summary of the results are included in this report. The final objective of this study is to use these data in a comprehensive numerical model to get a better prediction of the oil recovery performance in this field. These data will also be used in the final history matching of the field performance.

Combustion Tube Runs

For the understanding of the oil behavior in the presence of air under nonisothermal conditions, combustion tube tests are required. Plans were to conduct two combustion tube tests in reservoir sand with reservoir fluids at pressures of 2000 and 3500 psi (corresponding to planned injection pressures in Fault Blocks II and IV, respectively). Several pounds of dry and crushed Hackberry cores were shipped to Tulsa to be packed in the tube. Then the packed sand was saturated with the field stock tank oil. The first test was conducted at 2000 psi. A duplicate test at 2000 psi was also conducted to compare the results. On the basis of the results of these two tests, the contribution of the generated in situ flue gas to the oil displacement appears to be very important. Also, a steady burning front can be established at reservoir conditions under the tested air fluxes in the laboratory. Quantitative analysis of these tube runs is under way. Preparations are being made for the second test at 3500 psi.

Exothermic Behavior of Crude Oil

The accelerating rate calorimeter (ARC) can be used to assess the exothermic behavior of crude oil at different conditions. Two ARC tests were planned during 1993. In these tests, West Hackberry oil and formation sand were placed inside the ARC at 3500 psig air pressure. The corresponding tests at 2000 psi were completed previously. Two runs were made with the system operating in a closed mode (static conditions) and an open mode (under a continuously replenished stream of air). The collected data were used to obtain the Arrhenius activation energy, order of reaction, and preexponential factor. The exotherm continuity (under closed and open mode

conditions) will also be studied to obtain insight into the maximum process temperature. Additionally, the ARC was used to test the effectiveness of the core cleaning procedure. Crushed core samples were tested before being cleaned with air at reservoir temperature. The temperature was increased in steps, and the exothermic activity was noted. The cleaned and dried samples were run under the same conditions, and no exothermic activity was observed, which signifies acceptable cleaning of the core material before combustion tube testing.

Oil-Flue Gas Interaction

The oil-flue gas (nominally 85% nitrogen and 15% carbon dioxide) interaction has a significant effect on the stripping of the light ends as well as on the swelling of the oil at reservoir conditions. A detailed procedure for measuring such interactions was prepared. The corresponding tests were conducted at the Western Atlas Core Lab facility in Dallas, Tex. All the planned tests have been completed. In these tests the differential vaporization analysis (DVA) of the oil and the oil-flue gas mixtures at 200 and 400 °F was studied. There was excellent agreement between these data and the results of a 1955 DVA study of a live oil sample from this field. However, the new analysis showed the oil to be less viscous (by about 15%) than the results obtained with the old sample. The source of this discrepancy is not clear.

Multicontact Displacement Tests

The core lab tests described previously measured only a single contact between the oil and the flue gas. Coreflood tests in which oil-saturated rock is subjected to a gas flood are needed to arrive at the dynamic displacement behavior of the gas front. Two coreflood tests (at 2000 and 3500 psi) were planned in 1993. Both tests have been completed.

In each case a horizontal 8-ft-by-2-in.-diameter Berea core was saturated with live Hackberry oil and then displaced with synthetic flue gas. The first coreflood was conducted at 3500 psig and 200 °F with a Hackberry separator oil sample recombined to a bubble point of 3290 psig (200 °F). The composition of the recombined oil sample was formulated to match an earlier (1955) analysis available from a downhole fluid sample from the Gulf Land D R/A A No. 9. The Gulf Land D R/A A No. 9 was completed in the project's Cam C reservoir at the time of sampling. A sample of this oil was shipped to Western Atlas Core Laboratory in Dallas, Tex., for their tests.

Gas breakthrough was at 16% pore volumes of gas injected, and recovery after 78% pore volumes of gas injected was 28%. The second coreflood was conducted at 2200 psig and 190 °F. The same fluids were used in the second coreflood with the exception that the recombined oil was first differentially depleted to 2000 psig (190 °F). Breakthrough in the second coreflood was at 15% pore volumes of gas injected, and oil recovery at 82% pore volumes of gas injected was 27% pore volumes. The composition of the produced gas and oil samples is under analysis.

References

1. M.R. Fassihi, *Air Injection for Tertiary Oil Displacement at W. Hackberry, La.: A DOE Co-Sponsored Project*, paper presented to the Improved Recovery Study Group, SPE Gulf Coast Section, Houston, Tex., Sept. 8, 1993.
2. M. R. Fassihi, *The Use of Air Injection to Improve the Double Displacement Process*, paper SPE 26374 presented at the 68th Annual Society of Petroleum Engineers Technical Conference, Houston, Tex., Oct. 3-6, 1993.
3. *An Introduction to the West Hackberry Air Injection Project*, paper to be presented at New Orleans Section, Society of Petroleum Engineers, New Orleans, La., Feb. 8, 1994.

INCREASED OIL PRODUCTION AND RESERVES FROM IMPROVED COMPLETION TECHNIQUES IN THE BLUEBELL FIELD, UINTA BASIN, UTAH

Contract No. DE-FC22-92BC14953

**Utah Geological Survey
Salt Lake City, Utah**

**Contract Date: Sept. 30, 1993
Anticipated Completion: Sept. 29, 1998
Government Award: \$412,890**

**Principal Investigator:
M. Lee Allison**

**Project Manager:
Edith Allison
Bartlesville Project Office**

Reporting Period: Oct. 1-Dec. 31, 1993

Objective

The objective of this project is to increase the oil production and reserves in the Uinta Basin, Utah, by demonstration of improved completion techniques in the Bluebell field. Low productivity is attributed to gross production intervals of several thousand feet that contain perforated thief zones, water-bearing zones, and unperforated oil-bearing intervals. Geologic and engineering characterization and computer simulation of the Tertiary Green River and Wasatch formations in the Bluebell field will determine reservoir heterogeneities related to fractures and depositional trends. This phase will be followed by drilling and recompletion of several wells to demonstrate improved completion techniques based on the reservoir characterization. Technology transfer of the project results will be an ongoing component of the project.

Summary of Technical Progress

Outcrop Studies

Outcrops of the Green River formation are being investigated to better understand reservoir quality and distribution. The study includes describing depositional environments, facies distributions, petrophysical properties, and fracture susceptibility. A 2713-ft (827-m) stratigraphic section in the Willow Creek Canyon area of Carbon and Duchesne Counties, Utah, was described. The section was divided into 719 units. Petrographic classification indicates a minimum of 18 major rock types, which were analyzed for plug porosity and permeability. Porosity values range from 0.2 to 27.2% and permeabilities range from <0.01 to 1342 mD. Interpreted depositional environments range from paralic fluvial to open-lacustrine. Samples were collected for fracture-inducement studies to determine the potential fracture type and density for each significant potential reservoir facies. The individual facies will be correlated with geophysical logs from wells near the outcrop to determine the log characteristics. These will be used in combination with petrophysical properties of drill cuttings and core to identify and correlate important reservoirs in the Bluebell field.

Subsurface Studies

Digitizing of geophysical well logs from the Bluebell field is 14% complete (34 logs digitized of the 240 planned). The digital data will be used for field-wide correlation and determination of porosity trends, sandstone/shale ratios, oil saturation, and clay content of the various reservoir types. Detailed correlation and analyses of the primary reservoir facies are being done in the eastern portion of the field where the demonstration phase of the project is tentatively located.

Imaging logs and dip logs from the Bluebell field are being examined to determine fracture orientation, density, distribution, and principle stress direction in the various reservoirs within the productive interval. Borehole imaging logs are not part of the normal logging suite in the Bluebell field. Therefore, to encourage their use and to gather the needed imaging data, the program is offering to pay a portion of the logging cost associated with running such logs. Bluebell field operators and logging companies have been notified of this offer.

Oil and gas cumulative production, flush-oil production, initial potential, and gas/oil ratios for both the initial and cumulative production were contoured for the Bluebell field.¹ The cumulative production from individual wells in the Bluebell field typically ranges from <100,000 to 500,000 bbl of oil per well in the eastern portion of the field. In contrast, many of the wells in the west-central portion of the field have produced 1,000,000 to 3,000,000 bbl of oil per well. A typical well in the Bluebell field produces one- to two-thirds of its cumulative volume of oil during its first 5 yr of production. The gas/oil ratio is typically 500 to 1,000 ft³ (14 to 28 m³) of gas per bbl of oil during the initial production and rarely

changes significantly during the life of the well. The wells in the Bluebell field are commonly perforated over a gross interval of 1,000 to 2,500 ft (300 to 760 m) (Fig. 1) with 20 to 40 separate reservoirs open to the wellbore.

A well database for the Bluebell field was developed, which includes current operator name, well name, location, elevation, status, spud and completion dates, current status, and monthly production history since 1984. Input tables were generated for age information, formation top data, completion history, oil and gas analyses, and logs, cuttings, and core that are available at the Utah Geological Survey.

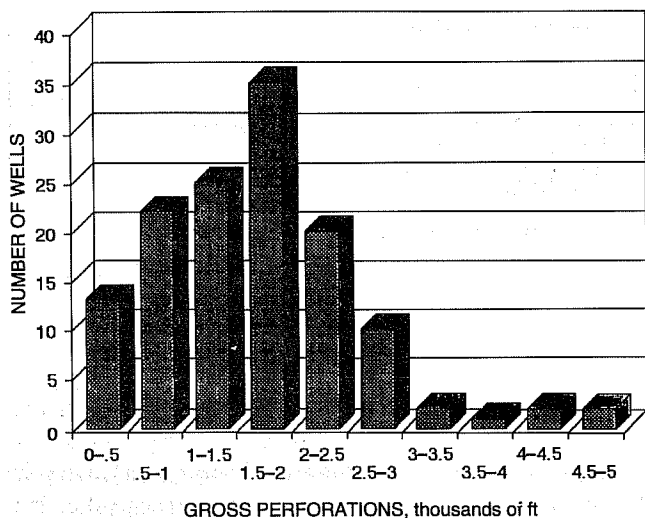


Fig. 1 Histogram of gross perforated interval of wells (132 total) completed in the Lower Green River and Wasatch formations in a portion of the Bluebell field (T. 1 S., R. 1 E., R. 1 W. and 2 W., Uinta Base Line).

Engineering Studies

Oils from the Bluebell field are generally characterized as either black or yellow wax crude. The black wax crude is produced from the shallower, lower Green River formation. The yellow wax is a slightly higher gravity, more mature crude that is produced from the deeper Wasatch formation. Short- and long-column compositional analyses were conducted on both crudes. The long-column analysis provided the carbon number distribution from C_5 to C_{44} and a $C_{44} +$ fraction. The yellow wax crude had a $C_{44} +$ fraction of 0.28 and the black wax crude $C_{44} +$ fraction was 0.48 (Fig. 2). These data are consistent with the API gravities of these crude oils, which were reported to be 39° API and 33° API, respectively. Analysis of the lighter yellow wax showed a lower percentage of residual high-boiling fraction. The short-column analysis revealed that all the yellow wax crude oil eluted before the residence time for carbon number C_{90} . Thus all the $C_{44} +$ fraction had a carbon number distribution between C_{44} and C_{90} .

Preliminary investigation of the reservoir and hydrocarbon parameters determined the oil bubble point to be about 3,200 psi (22,000 kPa). The oil formation factor is 1.45 to 1.50 at a

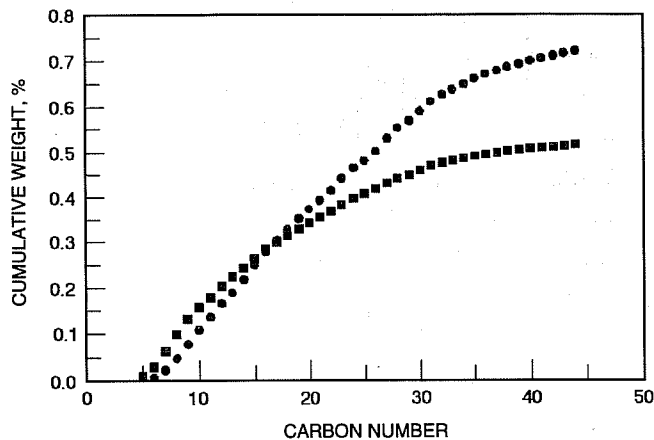


Fig. 2 Long-column compositional analysis of a yellow (●) and black (■) wax crude from the Bluebell field.

gas/oil ratio of 800 to 900 ft^3 (22.7 to 25.5 m^3) of gas per bbl of oil. The initial reservoir pressure was estimated to have been approximately 4,000 psi (27,000 kPa) at an average depth range of 10,000 to 12,000 ft (3,000 to 3,700 m).

Initial reservoir pressure is difficult to determine accurately in most wells in the Bluebell field. Reservoirs in the lower Green River formation and the upper portion of the Wasatch formation are typically at normal pressure with a gradient of 0.40 to 0.50 psi/ft (9.2 to 11.2 kPa/m). Reservoirs in the lower portion of the Wasatch are commonly overpressured with gradients as high as 60 to 70 psi/ft (13.5 to 15.7 kPa/m). Drill stem tests that can provide a shut-in pressure are rarely conducted in the Bluebell field. As a result, the few tests that have been run do not provide sufficient data to evaluate or predict reservoir pressure for the field or vertically through the section. An attempt to identify the top of the high-pressure zone in the lower Green River and Wasatch formations by plotting the mud-weight gradient was inconclusive. Although operators typically built the mud weight from 9 lb/gal to 14 lb/gal (1079 to 1679 kg/m^3) within a 50- to 100-ft (15- to 30-m) interval, many did so prior to encountering the high-pressure zone and drilled to total depth overbalanced. Shut-in pressures determined during the completion of the wells represent the lowest pressure in the perforated interval. The perforated interval is typically 1000 to 2000 ft (300 to 600 m) and may include both normal-pressured and overpressured zones (Fig. 3).

The Quinex Energy 1-7 Michelle Ute (sec. 7, T. 1 S., R. 1 E., Uinta Base Line) and 1-17 Malnar Pike (sec. 17, T. 1 S., R. 1 E.) wells are being considered for recompletion as part of the demonstration phase of the project. The Michelle Ute has produced 102,200 bbl of oil in 9 yr, and the Malnar Pike has produced 89,687 bbl of oil in 6 yr (as of Sept. 30, 1993). A decline curve analysis indicates the Michelle Ute would produce 156,000 bbl of oil and the Malnar Pike would produce 123,000 bbl of oil if they produced for 20 yr. The wells are currently near their economic limit and cannot be produced for the calculated 20 yr without additional recompletion

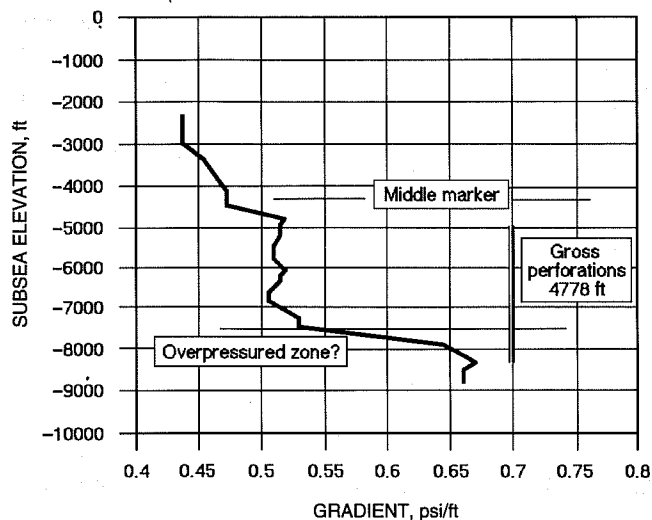


Fig. 3 Mud-weight pressure gradient calculated from the mud weights reported on the mud log of the 1-17 Malnar Pike well. The actual formation fluid pressure (unknown) is less than the mud-weight fluid pressure. The gross perforated interval includes both apparent normal-pressured and overpressured zones.

work. Preliminary original-oil-in-place (OOIP) calculations of the perforated intervals in the Michelle Ute and Malnar Pike wells indicate 3.65 million and 6.5 million stock tank bbl of oil, respectively (assumed is a 30% water saturation and a 40-acre drainage area). The preliminary calculations show that the wells may only recover 1 to 3% of OOIP.

Completion information from the digitized wells is being entered into a database in order to evaluate the effectiveness of the various completion techniques used.

Reference

1. C. D. Morgan, *Oil and Gas Production Maps of the Bluebell Field, Duchesne and Uintah Counties, Utah*, Utah Geological Survey Oil and Gas Field Study 15, 1994.

VISUAL DISPLAY OF RESERVOIR PARAMETERS AFFECTING ENHANCED OIL RESERVOIRS

Contract No. DE-AC22-93BC14892

Michigan Technological University
Houghton, Mich.

Contract Date: Sept. 29, 1993

Anticipated Completion: Sept. 30, 1996

Government Award: \$272,827

Principal Investigator:

James R. Wood

Project Manager:

Robert Lemmon

Bartlesville Project Office

Reporting Period: Oct. 1–Dec. 31, 1994

Objectives

The principal objective of this project is to provide the small- to medium-sized oil-field operator with the tools necessary to undertake an enhanced oil recovery (EOR) reservoir characterization and evaluation of quality and sophistication similar to those performed by large oil companies. The techniques will be demonstrated in a field trial on Pioneer Anticline in the southern San Joaquin Valley. The study will include collection, visualization, and manipulation of well-log and borehole-sample data. Physical and chemical property data gathered from laboratory measurements of conventional core and cuttings will be used to develop algorithms relating geological and engineering parameters to log responses. Digitized logs calibrated in this fashion will be used to characterize the reservoirs in fields on the Pioneer Anticline. Core, well-log, and production data will be assembled in a commercial personal computer (PC)-based database manager. The database manager will be used to provide data input to commercial visualization software to produce two-dimensional (2-D) and three-dimensional (3-D) representations of reservoir geometry, facies and subfacies stratigraphy, and distribution of remaining oil in place as well as spatial displays of measured and calculated reservoir parameters. These database and visualization tools will be used to evaluate the reservoirs for EOR. In addition, rock alteration caused by interaction with hot fluids will be modeled quantitatively and used to predict reservoir response to thermal EOR. Many of these tasks are being performed on expensive computer workstations by major oil companies. A primary goal of this project is to transfer this workstation technology to PCs, where programs can be run for a tenth of the cost by small independent operators.

The Michigan Technological University (MTU) team will be responsible for reservoir characterization, database construction, and rock-water modeling.

Digital Petrophysics Inc., Bakersfield, Calif. (DPI), which specializes in formation evaluation and development geology, with special expertise in the San Joaquin Basin, will head the industrial arm of the group; they will be responsible for well-log acquisition, calibration, and interpretation.

Summary of Technical Progress

Project Administration and Management

The Spatial Database Manager

Commercial PC-based database management systems are being tested and evaluated to choose one that is best for the project and for the small- to medium-sized producers who will ultimately use the results of the project. Database managers fall into two general categories: those which are simple and user friendly (e.g., Access and Approach) but may lack some features desirable for dealing with geological data sets and those which are more flexible but also more complex (e.g., FoxPro and Paradox) and may therefore be more difficult to operate. The advantages of ease of operation vs. flexibility will be carefully weighed before a final decision is reached. In the interim, all data are being collected in Quattro Pro spreadsheets, from which they can be transferred easily to the database management system of choice.

Both 2-D and 3-D visualization software packages available for PC systems will be tested and evaluated. Many 3-D geological-geophysical visualization programs are designed to run on workstations. Simplified versions of some are available for the PC. These programs are specifically designed to receive and manipulate geologic data, but the amount of flexibility sacrificed in adapting workstation programs to the PC is unknown. Visualization software packages, including Autocad and Geographic Information Systems (GIS), will be tested on sample data sets to choose the package that will best fit the needs of the smaller independent producer.

On Dec. 9, 1993, members of the MTU team met with members of the Computer Visualization Working Group at Chevron Petroleum Technology Co. (CPTC) to discuss the advantages of different commercial hardware and software configurations.

Database initialization. Log and core data from all 13 wells that penetrate the Monterey formation in Pioneer field and immediately adjacent areas were recovered and inventoried. The DPI is performing a database search to identify additional wells that penetrate the Monterey formation on the Pioneer Anticline west and north of Pioneer field. About 120 additional wells have been identified to date.

The DPI technical staff set up a Quattro Pro spreadsheet to collect well location and depth, well-log, and sample data during the interim period until a database management pro-

gram is chosen. The information collected during this initial search is being compiled in a Quattro Pro spreadsheet and will be transferred to the project database as soon as possible.

Database management. Every manager and site will need a high-end PC (e.g., a 486-based computer or better) to access the database and use the visualization applications programs. The computers will be networked and linked to a common server at MTU.

Organization and Management

Organization and management were discussed in detail at the Oct. 27, 1993, meeting in Bakersfield, Calif., and the organizational structure was agreed on.

Data Collection

Well Logs and Well Data

Structural data on the entire Pioneer Anticline will be input to the database management and visualization software programs so that Pioneer field can be viewed within a broader structural context and data from outside the immediate vicinity of Pioneer field can easily be included in the study at a later date if so desired. The Pioneer field covers a small area relative to the structure. Numerous small fields are spread across the structure. Surface geology of the area to the immediate south and west of Pioneer field will be recovered from existing maps and included on the basemap.

The reservoir interval to be characterized in detail will be confined to a zone of principal interest which extends from about 300 ft above the top of the Miocene to the base of the Monterey reservoir facies. Although reservoir characterization studies will focus on the Monterey reservoir, this interval includes the Etchegoin sandstone reservoir as well. There is evidence that most of the Pioneer Anticline structure outside the Pioneer field limits contains heavy oil in the Monterey.

Log database management. The DPI staff constructed a Quattro Pro spreadsheet to collect well location and depth, well-log, and sample data during the interim period until a database management system is chosen. Data can be easily exported from this Quattro Pro inventory file to the database manager of choice. Once the well logs are digitized, well-log data will be input, managed, and analyzed at DPI with the use of the PC-based version of Crocker Data Processing's Petrolog program. The petrophysical parameters calculated by this program will be input to the database management system and used in visualization applications.

Log digitization. DPI has begun to digitize the basemap and the zone of principal interest on well logs from the initial 13 wells. Digitization of these first 13 wells should be completed in the second quarter of FY94, at which time they will be ready for analysis with the use of the Crocker Petrolog program. As more logs are collected from elsewhere on the Pioneer Anticline, tops and bases of the formations of interest will be picked to improve control on the structure of the

anticline for use in the visualization package, and additional wells will be chosen for digitization and input to the Crocker Petrolog program.

Core and Sample Acquisition

Sidewall core and cuttings samples were recovered from one of the initial 13 wells and were shipped to MTU in December 1993 for petrographic, petrophysical, and geochemical analysis. Core and cuttings samples should be recovered from many of the other wells on Pioneer Anticline that are being inventoried.

Project members will approach ARCO Oil and Gas Co., Bakersfield, Calif., to attempt to acquire additional core and cuttings samples from several ARCO wells in the vicinity of Pioneer field. As wells located elsewhere on the Pioneer Anticline are inventoried, other operators will be contacted as well. The DPI will approach ARCO and/or Western Geophysical Co. to request access to several seismic lines shot over the Pioneer Anticline. If access can be arranged, picks on the top of the Miocene and on other stratigraphic markers will be used to further improve control on the structure of the anticline for the visualization package.

Data Analysis and Measurement

Petrophysics

The petrophysics subtask is not scheduled to begin until the second half of FY94; however, the Institute of Mineral Processing (IMP) has purchased a condenser lens.

Petrology

The petrology subtask is not scheduled to begin until the second half of FY94; however, image analysis work on cuttings from one of the Pioneer wells began. Also, IMP has paid \$1000 toward this year's maintenance contract on the scanning electron microscope (SEM) from project funds.

Log Calibration

Acquisition of the modern log suite and conventional core data from a well through the Monterey in nearby Cymric field, which has been promised to the project by UNOCAL, is being completed. This information will be used to calibrate well-log data to rock properties in Pioneer field. The core is currently stored in the UNOCAL Research Center in Brea, Calif., and will be sampled when final permission is granted.

During the second and third quarters of FY94, well-log data for the initial 13 wells in the Crocker Petrolog program will be entered, all depths will be corrected for well deviation, all logs will be printed out at the same scale, and the reservoir intervals between wells will be correlated.

After calibration of these logs to the Cymric core, the Crocker Petrolog program will be used to calculate additional parameters, such as porosity, S_o , percent clays, and matrix properties, from the Pioneer well-log suite. These parameters are critical to reservoir evaluation. This work will continue

through the third and fourth quarters of FY94 and will result in logs of calculated parameters that will be adjusted to the same scale and used to zone the reservoir. This information will be primary input to the reservoir visualization program.

Modeling

Geochemical Modeling

The geochemical modeling program CHILLER will be used to model fluid-rock interaction. This has practical significance because of active steamflooding of the Monterey and Etchegoin formations elsewhere in the southern San Joaquin Valley. Geochemical modeling is scheduled to begin in late FY95.

Basin Modeling

This subtask is not scheduled to begin until the last quarter of FY95.

Technology Transfer

Since the goal of this project is to provide smaller operators with the tools necessary to do sophisticated EOR evaluation, the first act of technology transfer was to announce the program to operators in the southern San Joaquin Valley through a press release. The article described the project and encouraged interested parties to contact project members to obtain further information.

Reports

Each task manager will prepare a quarterly summary of individual efforts, all relevant activity by subordinates, and all trips. Financial reports will be prepared by MTU staff and will be transmitted directly from MTU to DOE.

The regional and national meetings of the American Association of Petroleum Geologists (AAPG) and the Society of Petroleum Engineers (SPE) are the preferred venues for presentation of project results. Professional papers will be submitted to the *AAPG Bulletin*, to SPE journals (e.g., *Formation Evaluation*), and to other publications deemed appropriate for communicating results to the petroleum industry.

Workshops

Short courses and workshops will be run through the AAPG because SPE has no mechanism for this type of communication. The possibility of additional workshops being conducted in the Bakersfield area has been discussed. These may be scheduled in conjunction with a local geological or engineering society meeting or may be independent of either. A list of potential clients will be prepared and publicity will be generated to make them aware of workshops. The DPI will coordinate local workshops with MTU. Suggested format includes 4 h of prepared discussions followed by an informal examination of the database, maps, logs, and other materials.

A representative from MTU will coordinate the database aspects of the workshops.

Arrangements have been made to present preliminary results of the project at an academic booth in the exhibition hall at the 1994 AAPG National Meeting, Denver, Colo., June 12–15, 1994.

GEOLOGICAL AND PETROPHYSICAL CHARACTERIZATION OF THE FERRON SANDSTONE FOR THREE-DIMENSIONAL SIMULATION OF A FLUVIAL-DELTAIC RESERVOIR

Contract No. DE-AC22-93BC14896

Utah Geological Survey
Salt Lake City, Utah

Contract Date: Sept. 29, 1993
Anticipated Completion: Sept. 29, 1996
Government Award: \$321,042

Principal Investigator:
M. Lee Allison

Project Manager:
Robert Lemmon
Bartlesville Project Office

Reporting Period: Oct. 1–Dec. 31, 1993

Objective

The objective of this project is to develop a comprehensive, interdisciplinary, quantitative characterization of a fluvial-deltaic reservoir that will allow realistic interwell and reservoir-scale modeling to be used for improved oil-field development in similar reservoirs worldwide. The geological and petrophysical properties of the Cretaceous Ferron sandstone in east-central Utah (Fig. 1) will be quantitatively determined. Both new and existing data will be integrated into a three-dimensional representation of spatial variations in porosity, storativity, and tensorial rock permeability at a scale appropriate for interwell to regional-scale reservoir simulation. Results could improve reservoir management through proper infill and extension drilling strategies, reduce economic risks, increase recovery from existing oil fields, and provide more reliable reserve calculations. Transfer of the

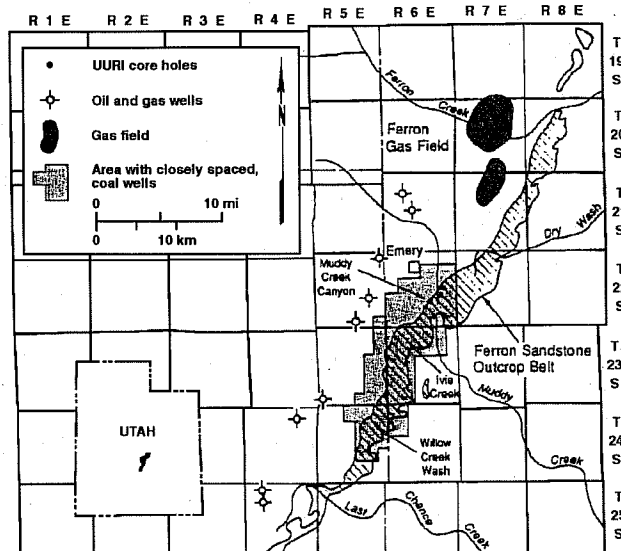


Fig. 1 Location map of the Ferron sandstone study area (cross-hatched) showing potential detailed case study sites. UURI, University of Utah Research Institute.

project results to the petroleum industry will be an integral component of the project.

Summary of Technical Progress

The technical progress is divided into several sections corresponding to subtasks outlined in the Regional Stratigraphy Task of the original proposal. Other tasks are dependent on field work that will begin in April 1994. The primary objective of the Regional Stratigraphy Task is to provide a more detailed interpretation of the stratigraphy of the Ferron sandstone outcrop belt from Last Chance Creek to Ferron Creek (Fig. 1). This regional study will include determination of the dimensions of each sandstone body, depositional environment, and the nature of its contacts with adjacent rocks or flow units. The study will provide a basis for selecting optimal outcrops for detailed case studies of the major reservoir types (meander belt, mouth-bar complex, wave-dominated delta front, bar-finger sands, distributary channel, and tidal channels). The morphological framework established from the case studies will be used to generate subsequent flow models.

Surface Mapping/Interpretation of the Outcrop Belt

Most of the Ferron sandstone outcrop belt within the study area (Fig. 1) will be obliquely photographed and photomosaics will be constructed. Several techniques to determine the most cost-effective method for producing digital photomosaics without significant loss of resolution are being evaluated. Good quality air-photo coverage of the Muddy Creek area is currently available, and the Utah Geological Survey (USG) is negotiating a purchase or trade for this photography.

Collection and Interpretation of Existing Surface and Subsurface Data

Published and unpublished maps, measured sections, well log, core descriptions, minipermeameter data, reports, and other data are being collected and compiled by the UGS. Seven potential sources of basic geological and geophysical drill data on the Ferron sandstone (Table 1) have been identified. The largest data holder is the Bureau of Land Management (BLM), which has hundreds of drill records from coal exploration holes drilled by Consolidation Coal Co. (CONSOL). Lease records were checked to determine which leases had been dropped by CONSOL and what drilling data could be released for use in the study. Land records show nine federal leases have been relinquished, three preference-right lease applications have been closed, and two prospecting permit applications have not been issued. Records show 352 wells with data on the unleased federal lands in the study area. The BLM has been contacted, and permission to use these records has been obtained.

Data were obtained from two recently drilled core holes in the study area from the University of Utah Research Institute (UURI). BP Exploration (BP) has donated core and geophysical logs from five stratigraphic test holes in the study area. The UGS has compiled published records¹⁻⁵ from 39 wells drilled by the Federal Government [BLM and U.S. Geological Survey (USGS)] in the study area. These records include 14 wells with geophysical logs and 35 wells with core or cutting descriptions. The study area contains 58 oil and gas exploratory and development wells. Records of the wells that penetrate the Ferron sandstone are also being obtained.

The UGS has developed a database for this study to integrate various geologic attributes of the Ferron sandstone with point-source locations in the study area. The relational

database application has been written, and all the tables, reports, and forms are ready for data entry. Both existing and newly collected data will be entered. The database will include well, core, and outcrop location; lithology; porosity; minipermeameter values; core plug permeability data; and unit tops, as well as other information.

Potential Case Study Sites

Three potential case study sites were delineated during a reconnaissance trip in October 1993: Muddy Creek Canyon, Ivie Creek, and Willow Creek Wash in the north, central, and southern parts, respectively, of the study area (Fig. 1).

Muddy Creek Canyon Site

Unlike the other potential study sites, where the focus will be entirely on delta-front units in the basal part of the Ferron, the Muddy Creek site will involve analyses of the entire Ferron section. The nearly continuous outcrops, the three-dimensional (3-D) aspect of the exposures, and the relative abundance of subsurface control facilitate 3-D mapping of individual reservoir types in the Ferron sandstone in this area. Initial plans are to create a 3-D field-scale reservoir model of several sandstone units representing an area measuring about 3 miles (4.8 km) in the north-south direction, 2 miles (3.2 km) in the east-west direction, and 450 to 500 ft (140 to 150 m) vertically. The Ferron sandstone is composed of seven deltaic units in the Muddy Creek Canyon area. Some of these units are stratigraphically simple; others include a variety of facies and display abrupt lateral facies variations.

Ivie Creek Site

The Ivie Creek site was selected for examination of the abrupt facies changes in the No. 1 delta-front unit in outcrops

TABLE 1

Summary of Well, Geophysical Log, and Core Data in the Ferron Sandstone Study Area

Source of wells	No. of wells drilled	No. of wells with geophysical logs	No. of logs obtained by the UGS*	No. of wells cored/ footage cored	Cored footage obtained by the UGS*
Oil and Gas					
UURI	2	2	2	2/800	800
ARCO	8	8	0	8/350+	0
BP	5	5	5	5/1000	1000
Other	58	58	21	0	0
Coal					
CONSOL	352	36	36	352/unknown	Descriptions only
USGS	33	14	14	29/1402	Descriptions only
BLM	6	0	0	6/1156	Descriptions only

*As of January 1, 1994.

Note: UGS, Utah Geological Survey; UURI, University of Utah Research Institute; ARCO, Atlantic Richfield Company; BP, British Petroleum; CONSOL, Consolidation Coal Company; USGS, United States Geological Survey; BLM, Bureau of Land Management.

north of Ivie Creek, east of the mouth of Ivie Creek Canyon. The basal unit is a thick, sandy, river-dominated parasequence, tentatively designated 1-Ivie-a, which pinches out to the west. Overlying the 1-Ivie-a and extending beyond it to the west is a thin, presumably river-dominated parasequence of very low-energy, tentatively designated 1-Ivie-b. Of particular interest is the interrelationship among high-angle foreset beds, hummocky, and planar laminated sandstones. Modeling will focus on the effects the various bounding surfaces would have on fluid flow in these units. How bounding surfaces can be identified from core and well-log data will be recommended, and, ultimately, how such features should be considered in field development and secondary/enhanced recovery programs.

Willow Creek Wash Site

The Willow Creek Wash site is the largest of the potential study areas. It covers an area 3.5 miles (5.6 km) long and 4 miles (6.4 km) wide (Fig. 1). The site was selected because of the excellent 3-D aspect of exposures in the Willow Springs Wash and Indian Canyon areas. The focus of work at this site will be parasequences of the No. 1 delta-front unit (Fig. 2). Reservoir modeling will concentrate on variations in fluid flow between the parasequence types and on the amount of communication between them.

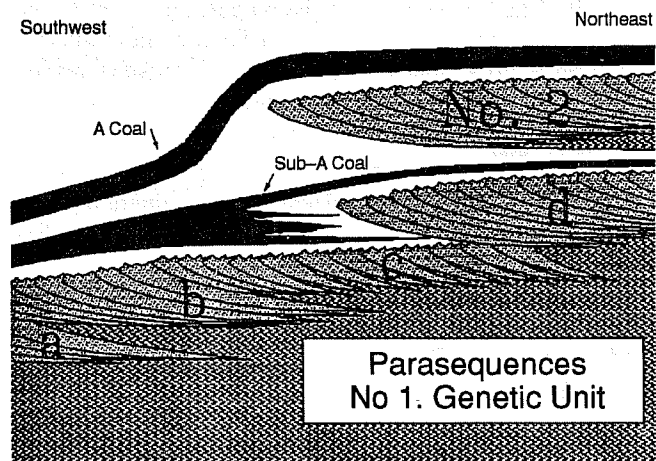


Fig. 2 Diagrammatic cross section showing arrangement of parasequences (a, b, c, and d) of the No. 1 delta-front sandstone unit at the Willow Creek Wash site.

Planned Activities

Planned activities for the next quarter are to (1) continue collecting measured sections, well logs, core descriptions, minipermeameter values, and other data and begin entering this information into the database; (2) designate areas for ground vs. air photography and obtain existing photographic coverage (if weather permits, begin aerial photography); (3) obtain software to develop a 3-D gridded database; and (4) plan the upcoming field season and select possible locations for core holes.

References

1. G. M. Edson and C. L. Barnosky, *Lithologic and Geophysical Logs of Holes Drilled in the Willow Springs Quadrangle, Emery and Sevier Counties, Utah*, U.S. Geological Survey Open-File Report 77-866, 1977.
2. G. M. Edson, *Core Drilling in 1978—Willow Springs Quadrangle, Emery and Sevier Counties, Utah*, U.S. Geological Survey Open-File Report 78-1049, 1978.
3. D. T. Hodder and R. C. Jewell (Eds.), *Reclaimability Analysis of the Emery Coal Field, Emery County, Utah*, U. S. Bureau of Land Management EMRIA Report No. 16, 1979.
4. E. G. Ellis, *Geophysical Logs and Coal Sections for Four Holes Drilled in the Emery East Quadrangle, Emery County, Utah*, U.S. Geological Survey Open-File Report 80-1027, 1980.
5. T. A. Ryer, *The Muddy and Quitcupah Projects—A Progress Report with Descriptions of Cores of the I, J, and C Coal Beds from the Emery Coal Field, Central Utah*, U.S. Geological Survey Open-File Report 81-460, 1981.

REVITALIZING A MATURE OIL PLAY: STRATEGIES FOR FINDING AND PRODUCING UNRECOVERED OIL IN FRIO FLUVIAL-DELTAIC RESERVOIRS OF SOUTH TEXAS

Contract No. DE-FC22-93BC14959

University of Texas
Bureau of Economic Geology
Austin, Tex.

Contract Date: Oct. 21, 1992
Anticipated Completion: Dec. 31, 1994
Government Award: \$817,911

Principal Investigator:
Noel Tyler

Project Manager:
Edith Allison
Bartlesville Project Office

Reporting Period: Oct. 1–Dec. 31, 1993

Objectives

Project objectives are divided into three major phases: The first phase, reservoir selection and initial framework characterization, consisted of the initial tasks of screening fields within the play to select representative reservoirs that have a large remaining oil resource and are in danger of premature abandonment and performing initial characterization studies on selected reservoirs to identify the potential in untapped,

incompletely drained, and new pool reservoirs. The second phase will involve advanced characterization of selected reservoirs to delineate incremental resource opportunities. Subtasks include the volumetric assessments of untapped and incompletely drained oil along with an analysis of specific targets for recompletion and strategic infill drilling. The third and final phase of the project will consist of a series of tasks associated with technology transfer and the extrapolation of specific results from reservoirs in this study to other heterogeneous fluvial–deltaic reservoirs within and beyond the Frio play in South Texas.

Summary of Technical Progress

Work during this project quarter consisted of continued evaluation of engineering and geologic characteristics of Frio fluvial–deltaic reservoirs from two South Texas fields. A preliminary assessment of incremental resource potential of oil reservoirs in Rincon and Tijerina–Canales–Blucher (TCB) fields was completed. Data screening for various engineering parameters of reservoirs throughout both fields was performed, and completion density, abandonment rates, and production trends for individual reservoirs were evaluated in order to assess the level of remaining potential for each productive reservoir zone. Reservoir development histories for major oil-producing zones in both fields were reconstructed in order to rank and prioritize zones with the best potential for incremental reserve growth.

Geologic data are being evaluated in order to identify interwell stratigraphic heterogeneity of individual reservoir zones and the potential for compartmentalization of significant volumes of unrecovered hydrocarbons. A regional structural and stratigraphic context has been developed for the Frio reservoir sequence, as well as preliminary facies interpretations for the productive reservoir interval in each of the two fields. Cross-section grids have been established in each of the field areas, and field-wide reservoir correlations to document lateral variations within individual reservoir intervals targeted for detailed studies are under way.

The first phase of the studies has provided a basis for the selection of a few reservoir zones for further detailed study. Important details of the play-wide stratigraphic framework of Frio fluvial–deltaic reservoirs and summaries of the reservoir stratigraphy and identification of candidate reservoirs for detailed study in Rincon and TCB fields are provided in this report.

Incremental Oil Recovery Opportunities in Frio Fluvial–Deltaic Reservoirs

The productive stratigraphic interval in the Frio fluvial–deltaic sandstone/Vicksburg Fault Zone play in South Texas is part of a sedimentary wedge that records a major depositional offlap episode of the northwestern shelf of the Gulf of Mexico Basin. Frio sedimentation represents the entry of a major extrabasinal river into the Gulf Basin along the axis of the Rio Grande Embayment in Oligocene time. This ancient fluvial–

deltaic complex has been divided into the Gueydan fluvial and Norias delta systems. Fields within the Frio fluvial–deltaic sandstone play occupy a transitional area between these two depositional systems. In general, lower Frio sands represent deltaic facies of the ancestral Norias delta system, and middle and upper Frio sands predominantly reflect deposition in fluvial channels of the Gueydan fluvial system. In early Frio time, the Norias delta system prograded rapidly seaward (southeastward) across the Vicksburg Fault Zone, which resulted in the deposition of a relatively thin lower Frio sequence of progradational fluvial-dominated deltaic depositional facies. Later stages of Frio deposition in the vicinity of the Vicksburg Fault Zone represent a return to aggradational fluvial deposition, as the Norias delta system continued to prograde farther to the east and deposit a thick sequence of massive, sandy, shoal-water, arcuate deltas and wave-modified lobate deltas that extended eastward from the Vicksburg Fault Zone to the present position of the Frio Fault Zone.

Lower Frio reservoir facies are delta-plain, distributary-channel, and delta-front channel-mouth-bar sandstones. Reservoir compartments in narrow distributary-channel sandstones isolated by low-permeability mudstone facies and channel-mouth-bar sandstones that pinch out into finer grained delta-front facies are the primary targets for additional oil recovery in the lower Frio section. Reservoir facies in middle Frio units include channel-fill, point-bar, and crevasse-splay sandstones. Low-permeability subfacies within the channel fill act as flow baffles and barriers and create isolated reservoir compartments that represent a significant opportunity for additional recovery. Crevasse-splay deposits, which are of limited areal extent and are laterally separated from channel-fill facies by low-permeability facies, are also potential targets for additional recovery of compartmentalized reserves.

The identification of facies and resulting patterns of reservoir architecture and heterogeneity of the reservoirs selected for detailed study in Rincon and TCB fields will be evaluated within the context of a well-defined regional sequence-stratigraphic framework. This will provide a critical means to predict the distribution and continuity of permeable zones in Frio reservoirs in other fields within the Vicksburg Fault Zone play and ultimately to other reservoirs deposited in analogous fluvial–deltaic settings.

Stratigraphic Framework and Reservoir Geology in Rincon Field

General Reservoir Stratigraphy

More than 50 individual productive reservoir sands within the stratigraphic interval from 3000 to 5000 ft have been identified and mapped across the Rincon field area. Oil reservoirs range in dimension from only a few acres to complex, inter-related reservoir systems that cover the entire field. Fault displacements in the productive Frio interval are generally minor, and the major cause for reservoir complexity and compartmentalization of hydrocarbons is a result of the multilateral and

multistacked nature of the Frio reservoir sands. The variability in sandstone geometries and the complex depositional architecture of these reservoirs provide excellent potential for identifying additional hydrocarbons that have been isolated in untapped and incompletely drained reservoir compartments.

The productive reservoir interval in Rincon field includes strata from both the middle and lower Frio section (Fig. 1) and is located in an aggradational to mixed aggradational and progradational setting. Preliminary evaluation of net sand isopach data on several reservoir horizons based on earlier work by Conoco indicates two patterns of sand deposition. The dominant pattern consists of deposition in dip-elongate fluvial channel systems flowing from northwest to southeast across the low-relief Oligocene gulf coastal plain toward the shoreline. These periods of aggradational channel-fill sedimentation are briefly punctuated by short intervals in which linear strike-oriented sandstone bodies are developed. These phases probably reflect periods of decreased aggradation, which allows for minor marine transgression and subsequent reworking and redistribution of the sand originally deposited in dip-elongate channels by wave action. The development of these strike-oriented bar deposits is limited, and isopach mapping indicates that they are laterally discontinuous. They do not form important oil reservoirs.

All the major productive oil reservoir zones in Rincon field appear to represent deposition in broad dip-elongate fluvial systems. Individual reservoir units occur both as narrow channel-fill sandstones isolated vertically and laterally by very low permeability overbank facies and floodplain mudstones and as large channel complexes with multiple sand lobes that combine into a single large communicating reservoir. These reservoir complexes commonly consist of multiple thin sand units that range in gross thickness between 50 and 100 ft and possess a net sand thickness of 0 to 40 ft.

Reservoir Development History

Production histories of all oil reservoir zones in Rincon field (Table 1) were compiled with data from public sources, including the Texas Railroad Commission, Dwight's Energydata, and Petroleum Information Consultants, as well as extensive well records from Conoco, the field operator. Detailed well history records and a computerized production database with completions and oil and gas production listed by individual reservoir zone and by well have been made available from Conoco.

Perforation data for individual reservoir zones in 220 wells were tabulated to provide a chronological history of completions by reservoir. In addition, cumulative oil and gas production for all oil productive reservoir zones were compiled in order to provide comparisons of oil produced by reservoir zone and to illustrate the stratigraphic distribution of oil production. This information is illustrated in Fig. 2a. The D, E, and G sand series account for 69% of all completions and 88% of the oil produced in the field area selected for study (Fig. 2b). The dramatic decline in oil production from these major reservoirs since 1968 is reflected in the significant increase in abandonments of

reservoir zones throughout the 1970's (Fig. 2c). As of 1990, there were only 27 oil wells remaining in the field that were producing or had shut-in status.

Reservoirs with High Potential for Incremental Oil Recovery

The Frio D and E sand series are the two most highly prolific reservoir zones in Rincon field. Sandstones within this combined interval have produced more than 22 MMbbl of oil since their discovery in 1940.

The main productive D sand interval consists of four units correlated as the D-3, D-4, D-5, and D-6 sands. These sand units are correlated as individual sands that combine into a complex stratigraphic channel system that covers more than 2000 acres in the northern half of the field. Pressure and production histories indicate that these sands form a single, large, communicating reservoir. Data from reservoir mapping, log correlations, and core analyses indicate significant heterogeneity within the D reservoir interval, and permeability barriers have previously been mapped within the large D-5 sand.

The E zones are individually mapped as the E-1, E-2, E-3, and E-4 sands. Stratigraphic correlation and production data indicate that the E-1 and E-2 sands are often in fluid communication, as are the E-3 and E-4 sand zones. In some cases, all of the individual reservoir sands have been interpreted to be in communication.

The stratigraphic complexity of this interval of vertically stacked and laterally coalescing sand lobes provides ideal conditions for the isolation of oil accumulations in multiple reservoir compartments, many of which are incompletely drained or completely untapped. Vertical and lateral heterogeneity of the complex D and E reservoir interval is being identified through the construction of detailed stratigraphic cross sections.

Stratigraphic Framework and Reservoir Geology in TCB Field

General Reservoir Stratigraphy

The area of study in the TCB field consists of the 3500-acre Blucher lease, which covers the southwest portion of the field. Additional data from wells in four adjacent leases have also been made available by Mobil Exploration and Production U.S.

The Frio reservoir interval in the TCB field comprises the middle and lower members of the formation and consists of a series of sandstone units that occur over the depth interval from 5500 to 7600 ft and include the Maun through Lobberecht sands. Preliminary correlations were made within the study area to group the more than 40 reservoir sands, some of which are stratigraphic equivalents, into genetic packages that share a common architectural style. The resulting stratigraphic zonation incorporates paleontologic data from recent wells and regional correlations¹ and is a revised version of the stratigraphy developed by operators during initial field development in the 1940's (Fig. 3).

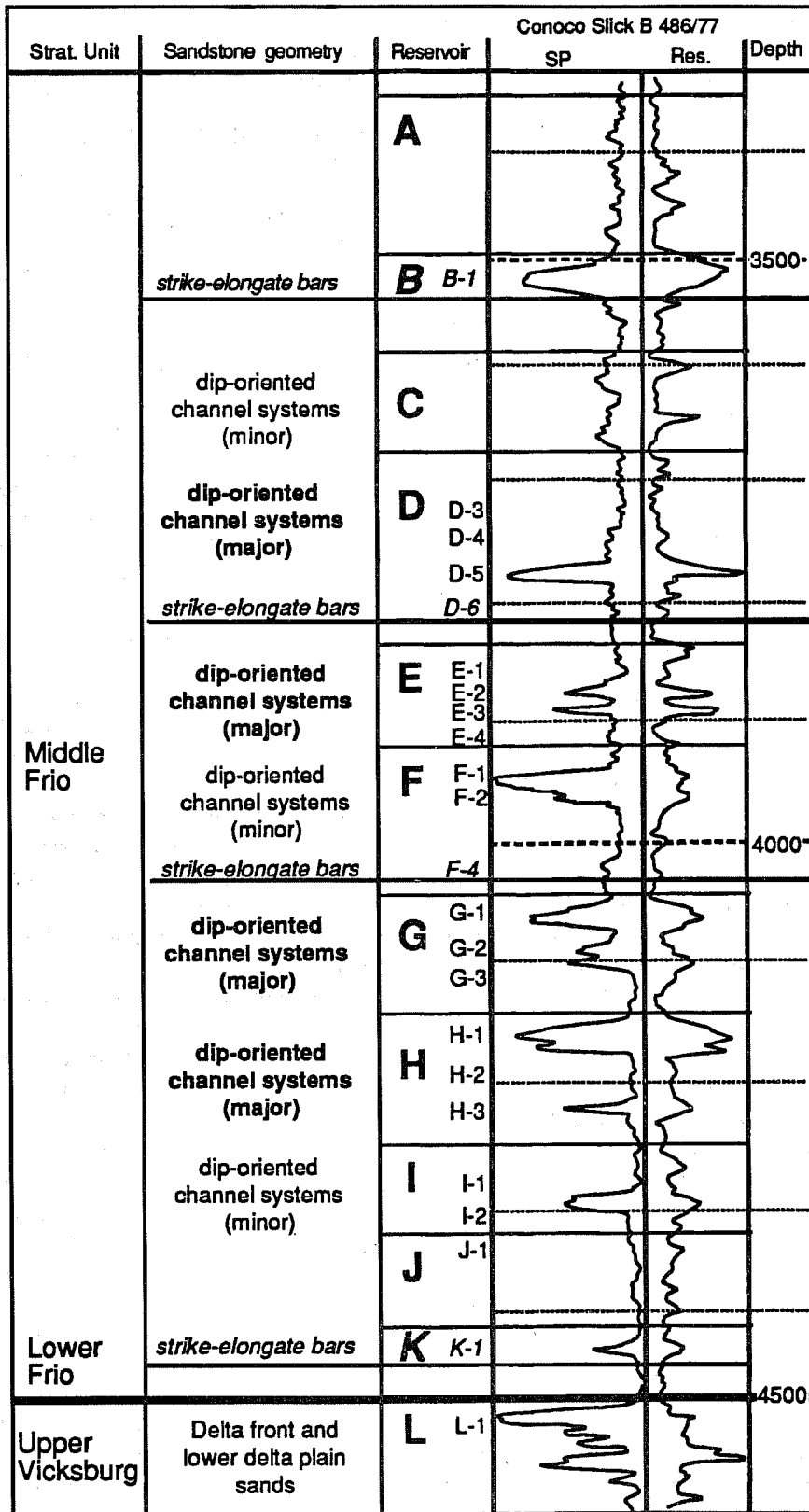


Fig. 1 Representative log from Rincon field illustrating generalized stratigraphy, reservoir nomenclature, and depositional geometry of oil-productive reservoir sands. Sandstone geometry is based on net sandstone isopach values.

TABLE 1

Development History of Major Productive Reservoir Sandstone Zones in Rincon Field*

Sand unit name	Average depth (subsea)	Reservoir acres	Completions		Abandoned zones		Completion density, acre/comp.	Total oil wells‡	Cumulative production	
			Total	Active†	Total	Total, %			Gas, Mcf	Oil, Mstb
B-1	2,947	316	31	6	25	81	10	13	12,070	138
D-3	3,240	468	18	1	17	95	26	11	1,476	749
D-4	3,248	635	5	0	5	100	127	2	70	855
D-5	3,248	2,189	81	4	77	95	27	51	12,315	7,550
D-6	3,280	687	5	0	5	100	137	2	257	301
E-1	3,390	167	25	7	18	72	7	17	8,288	1,802
E-2	3,390	1,360	46	10	36	78	30	39	14,604	6,882
E-3	3,391	931	39	0	39	100	24	35	4,408	4,721
E-4	3,520	505	9	1	8	89	56	4	1,797	661
G-1	3,586	955	33	6	27	82	29	20	10,068	3,151
G-2	3,570	1,180	18	2	16	89	66	13	5,378	1,716
G-3	3,587	280	5	0	5	100	56	3	1,950	489
I-1	3,660	532	11	1	10	91	48	11	8,729	1,315
I-2	3,655	377	5	0	5	100	75	5	3,556	742
J-1	3,708	153	7	0	7	100	22	7	3,051	645
K-1	3,782	184	10	0	10	100	18	10	5,850	420

*Reservoir acreage, completion data, and cumulative production volumes are from wells within the study area (see Fig. 2 for comparison of total field production volumes vs. study area totals).

†Active zones include presently producing completions and shut-in zones.

‡Total oil wells indicate the number of completions for oil compared to those for gas. Those bold are significant gas reservoirs.

Reservoir styles in both the middle and lower Frio intervals of TCB field provide many opportunities for uncontacted and poorly drained reservoir compartments. The lower Frio is approximately 1000 ft thick and is composed of sandstones that were deposited in delta front and delta plain settings. Lower Frio reservoirs are predominantly thin, vertically isolated sandstones of moderate lateral continuity that are further compartmentalized by faulting. The middle Frio is about 1300 ft thick and contains primarily fluvial sandstones. The architecture of middle Frio reservoir packages alternates from sand-prone intervals with laterally stacked, interconnected channel-fill and splay sandstones with individual thicknesses of 10 to 30 ft and limited lateral extent to sand-poor sections with thin vertically stacked sandstones that are isolated within a 100- to 150-ft-thick overall shaley unit. Middle Frio sandstones are less affected by faulting; the primary causes of reservoir compartmentalization are reservoir architecture and internal heterogeneity.

Reservoir Development History

Reservoir development throughout the life of TCB field was assessed to aid in the screening of reservoirs for infill potential. On the basis of data available on production since 1967, development histories, including number of known successful completions, abandonments, active completions, and cumulative production were compiled for individual reservoir intervals.

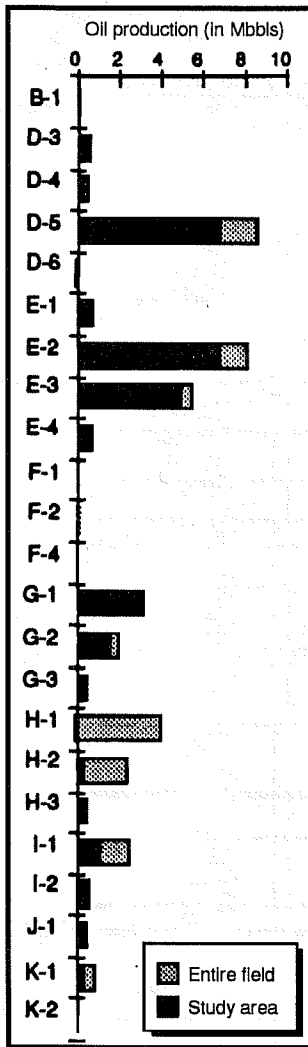
A plot of cumulative oil productions and the ratio of gas to oil produced by reservoir interval are shown in Fig. 4, which illustrate the relative importance of zones on the basis of cumulative production. High cumulative gas/oil ratios indicate reservoirs with large gas caps and thin oil rims. The greatest

number of reservoirs lies in the lower Frio, with just a few intervals in the middle Frio section. Oil and gas production are dominated by the Marie and Mary reservoirs, which are part of the prolific 21-B interval. These preliminary data indicate that the Scott and Kilmar intervals in the middle Frio and the Carl, Charles, Conrad, and Richard in the lower Frio are the other major reservoirs.

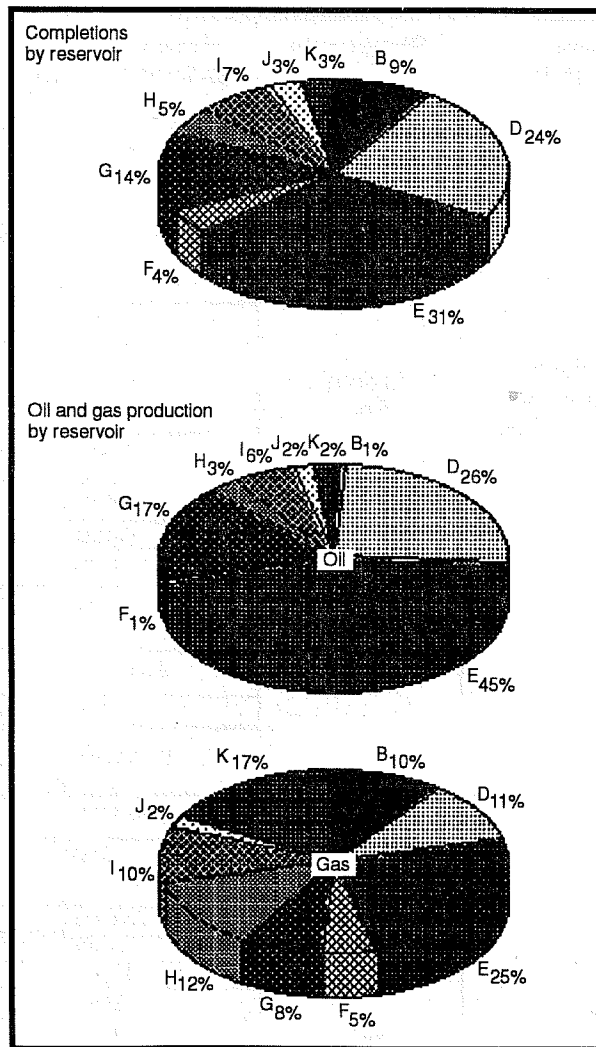
Determination of completion density was based on preliminary histories for wells in all the contiguous Mobil acreage, totaling 4800 acres. The reservoir units with highest cumulative production, the Mary and Richard zones in the deltaic lower Frio formation and the Scott and Kilmar in the more fluvially influenced middle Frio formation, have average completion densities of 400 acre/completion to more than 600 acre/completion (Table 2).

Reservoirs with High Potential for Incremental Oil Recovery

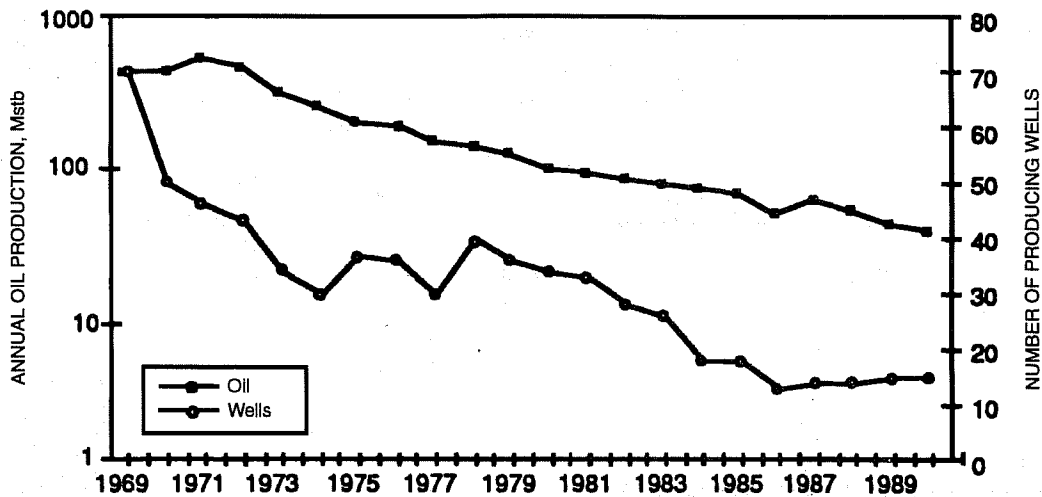
To prioritize reservoirs for detailed characterization study, the focus was placed on those intervals which have the greatest potential for untapped or incompletely drained reservoir compartments. Selection criteria emphasized volumetrically important reservoirs, based on past production, that have a low completion density, high stratigraphic heterogeneity, and low structural complexity. The last criterion was intended to avoid having to devote resources to resolving structural compartmentalization. The reservoirs in the middle Frio formation are expected to have high heterogeneity because of their fluvial setting. A dip-oriented seismic line provided by Mobil (Fig. 5) shows that reservoirs in the lower Frio formation



(a)



(b)



(c)

Fig. 2 Summary of reservoir production in Rincon field showing (a) stratigraphic distribution of oil production; (b) relative oil production, gas production, and completions by reservoir zone; and (c) declining trend of annual oil production and producing wells since 1969.

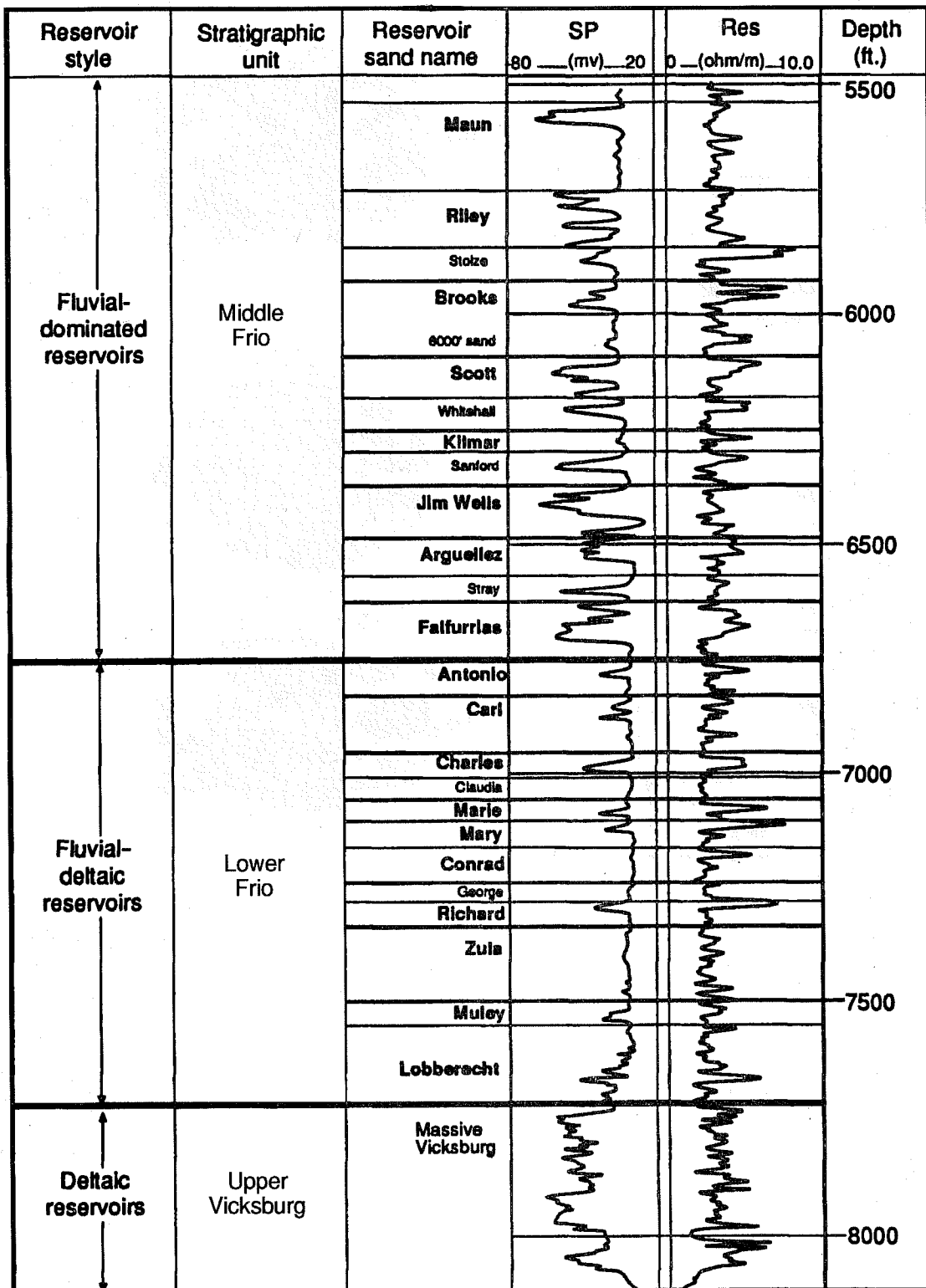


Fig. 3 Representative log from Tijerina-Canales-Blucher (TCB) field illustrating generalized stratigraphy, nomenclature of productive reservoirs, and division of lower and middle Frio intervals. Primary reservoir zones are shown in bold, and secondary names of lesser sub-units are listed in plain text. (Mobil Exploration and Production U.S., C.F.H. Blucher No. 59.)

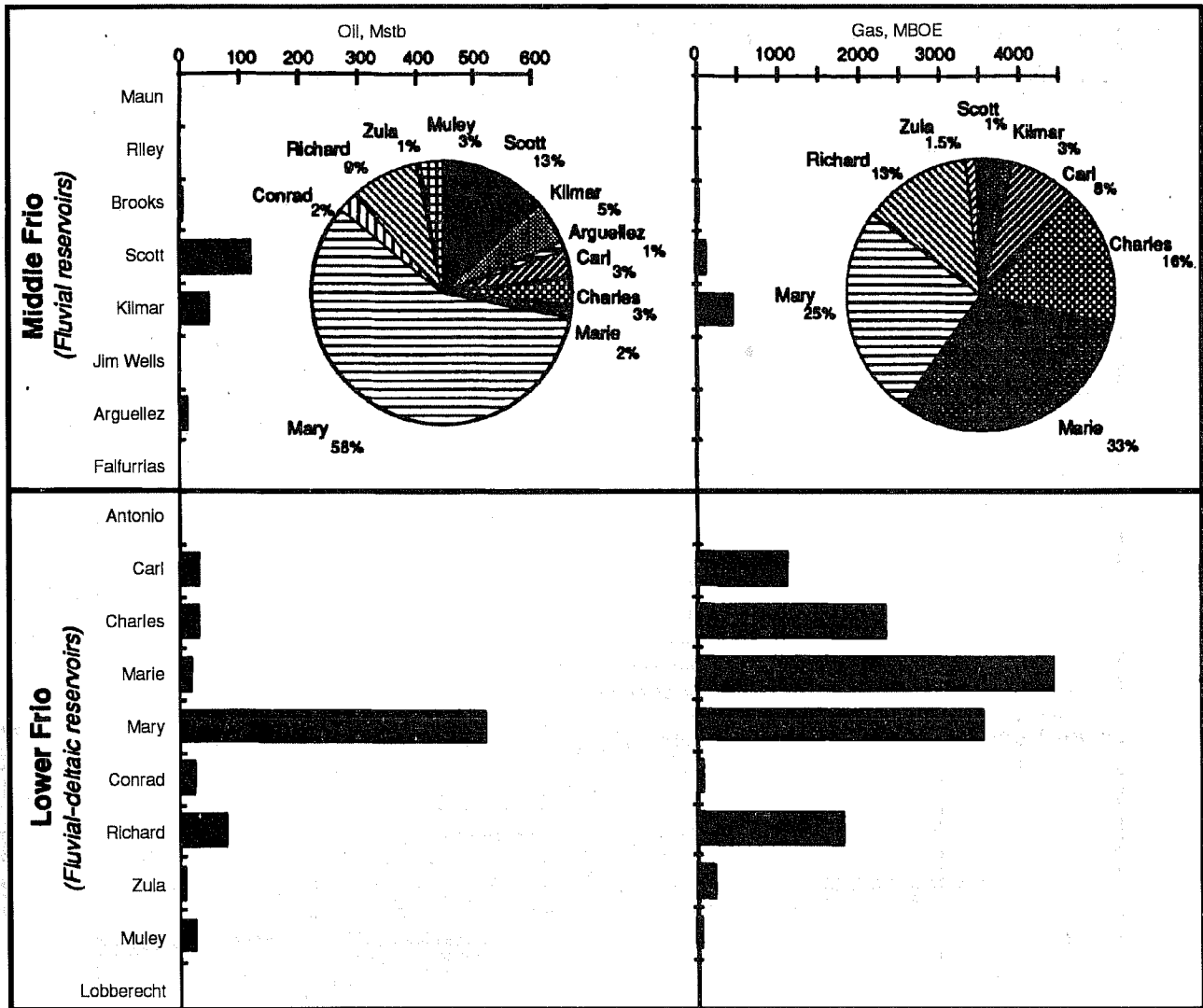


Fig. 4 Summary of cumulative oil and gas production from Mobil TCB leases from 1967 to 1992 illustrating the relative importance and stratigraphic position of Frio reservoir intervals. The Mary and Marie sands are equivalent to the prolific 21-B interval, which has produced more than 20 million bbl throughout the life of the entire TCB field area.

contain significant structural complication, whereas faulting does not continue upward into the middle Frio formation.

Additional factors investigated to prioritize reservoirs included analysis of petrophysical data to evaluate variability within the middle and lower Frio formation and in each reservoir interval because higher variability suggests higher internal heterogeneity and thus a larger potential for compartmentalization. Clay mineralogy data gathered by Mobil on recently drilled wells were also evaluated. The purpose was to examine the potential for sensitivity to drilling and completion fluids that could have resulted in abandonment of low-productivity completions as the result of unrecognized formation damage.

Preliminary work suggests that the Scott and Kilmar intervals in the more fluviably influenced middle Frio formation have the greatest potential for untapped and incompletely drained reservoir compartments while having the lowest structural complexity. They will likely receive the highest priority in detailed

studies in the second phase. Priorities could be modified if it is found that the operator has sufficiently documented the structure of the lower Frio deltaic interval to simplify the characterization of the Mary and Richard reservoirs, or if subsequent well history and production data significantly alter the cumulative production or completion density values.

Planned Activities

The second phase studies focus on delineation of incremental recovery opportunities in Rincon and TCB fields. Targeted reservoir intervals from both fields are being assessed from a geologic standpoint to identify reservoir architecture and internal heterogeneity. Work in progress that will continue into the next project quarter includes construction of field-wide cross sections and further detailed work on stratigraphic correlations of prospective reservoir zones in Rincon and TCB fields to identify the degree of lateral heterogeneity and reservoir

TABLE 2

Production History of Reservoir Sandstone Intervals in TCB Field*

Reservoir interval	Average depth (subsea)	Completions		Abandonments		Completion density, ‡ acre/comp.	Completions (1983 to present)		Post-1967 production§	
		Total	Active†	Total	Total, %		Attempt	Success	Gas, MMcf	Oil, Mstb
Brooks	6,000	4	0	4	100	1,200	1	0	113	3
Scott	6,100	8	3	5	63	600	4	3	649	120
Kilmar	6,200	9	3	6	67	533	2	1	2,654	48
Jim Wells	6,300	2	0	2	100	2,400	2	1	0	0
Arguellez	6,500	5	0	5	100	960	7	1	71	9
Falfurrias	6,650	2	0	2	100	2,400	1	0	0	0
Antonio	6,720	4	0	4	100	1,200	3	1	2	0
Carl	6,820	10	2	3	30	480	4	2	6,712	31
Charles	6,870	18	4	14	78	267	3	0	13,939	29
Marie	7,010	29	6	23	79	166	5	3	26,679	16
Mary	7,040	11	1	10	91	436	2	0	21,199	520
Conrad	7,100	13	2	11	85	369	0	0	352	22
Richard	7,150	11	7	4	36	436	7	5	10,767	77
Zula	7,180	7	0	7	100	686	1	0	1,252	5
Muley	7,220	6	0	6	100	800	0	0	266	23
Lobberecht	7,250	5	1	4	80	960	4	0	0	0

*Reservoir acreage completion data and cumulative production volumes are from within the Blucher lease study area.

†Active zones include presently producing completions and shut-in zones.

‡Completion densities calculated using 4800 acre area for the Blucher lease.

§Pre-1967 by reservoir production data are incomplete.

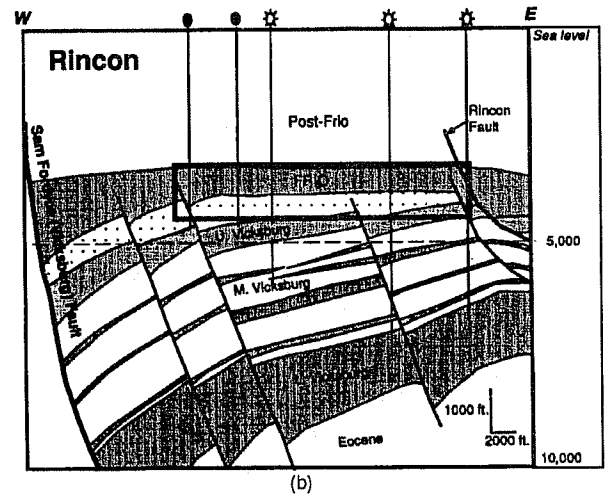
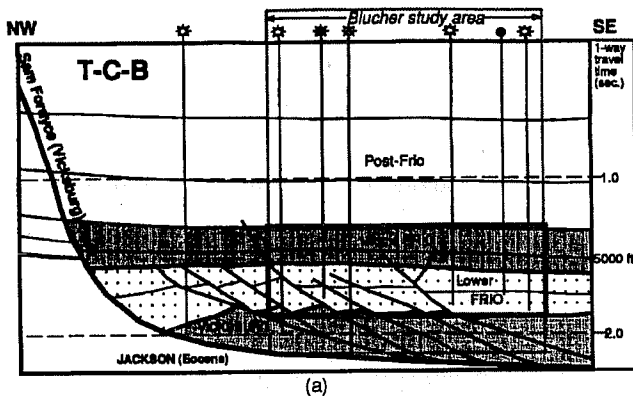


Fig. 5 (a) Geoseismic cross section of the TCB field study area based on a dip line across a portion of the field provided by Mobil Exploration and Production U.S. Note the structural complexity of the lower Frio interval, especially as compared with the equivalent reservoir section being studied in Rincon field, as illustrated in cross section. (b) Rincon cross section adapted from Ashford, 1972.

compartmentalization. The completeness of existing structural interpretations is being evaluated in TCB field to determine the suitability of structurally complicated lower Frio reservoirs for inclusion in detailed studies. Digital base databases are being developed in order to facilitate the construction of maps illustrating distribution of net sandstone thickness, percentage sand, permeability thickness, and water saturation. Detailed facies maps will be developed for selected reservoir zones using log and core data. The evaluation of digitized log data in conjunction with core analyses values for depth-adjustment purposes is also

nearing completion. Whole-core studies of D and E reservoir sands from Rincon field are also scheduled to begin during the next project quarter.

Production data in each field are still being evaluated. Additional well completion and production data are being acquired from TCB field. Volumetric estimates of produced fluids and remaining reserves in selected reservoirs in both fields will be calculated to identify and delineate the additional resource potential residing in incompletely drained and untapped reservoir compartments.

**POSTWATERFLOOD CO₂ MISCIBLE
FLOOD IN LIGHT OIL, FLUVIAL-
DOMINATED DELTAIC RESERVOIR**

Contract No. DE-FC22-93BC14960

**Texaco Exploration and Production, Inc.
New Orleans, La.**

Contract Date: June 1, 1993

Anticipated Completion: Dec. 31, 1997

**Government Award: \$3,424,258
(Current year)**

**Principal Investigator:
Darrel W. Davis**

**Project Manager:
Chandra Nautiyal
Bartlesville Project Office**

Reporting Period: Oct. 1–Dec. 31, 1993

Objectives

The objectives of research on postwaterflood carbon dioxide (CO₂) miscible flood in light oil, fluvial-dominated deltaic (FDD) reservoir during the first quarter of FY94 are to (1) complete the reservoir model, (2) raise reservoir pressure, (3) initiate production testing, (4) drill horizontal CO₂ injection well and initiate CO₂ injection, (5) develop hard data results, and (6) receive approval to delay workover on one well.

Summary of Technical Progress

Production from the Port Neches CO₂ project was initiated on Dec. 6, 1993, after having been shut in since the start of CO₂ injection on Sept. 22, 1993, to allow reservoir pressure to build. Rates were established at 236 bbl of oil per day (BOPD) from two wells in the 235-acre waterflood project area, which before project initiation had produced only 80 BOPD from the entire area. These wells are flowing large amounts of fluid as the result of the high reservoir pressure, and their oil percentages are increasing as a result of the CO₂ contacting the residual oil. One well, the H. J. Kuhn No. 15-R, is flowing 217 BOPD, 1139 bbl of water per day (BWPD), and 2500 thousand cubic feet per day (MCFPD) of CO₂ at a flowing tubing pressure (FTP) of 890 psi. The other producing well, the H. J. Kuhn No. 33, is currently flowing 19 BOPD, 614 BWPD, and 15 MCFPD at an FTP of 400 psi. Unexpectedly high rates of CO₂ production are being made from Well No. 15-R and from the W. H. Stark "B" No. 8. This No. 8 well produced 7 BOPD, 697 BWPD,

and 15 MCFPD before being shut in during September 1993 to allow for the reservoir pressure to build by injecting CO₂, but when opened on Dec. 6, 1993, the well flowed dry CO₂ at a rate of 400 MCFPD for a two-day test period. More sustained production tests will be obtained after all wells are tied into the new production facility.

Difficulties occurred in the drilling of the horizontal CO₂ injection well, but a successful completion across 250 ft of sand has been accomplished. A formation dip of 11 to 14° in the area where the well was being drilled made the proposed 1500-ft horizontal sand section too difficult to accomplish. The shale section directly above the sand caused sticking problems on two separate occasions, which resulted in two sidetracks of the well around stuck pipe. The well will be tied into the facility, and CO₂ injection into the well will begin before Feb. 1, 1994.

Technology transfer of project results will continue in 1994 in the form of technical paper presentations and topical reports. During the 9th Society of Petroleum Engineers/Department of Energy (SPE/DOE) Symposium on Improved Oil Recovery to be held in Tulsa, Okla., April 17–20, 1994, two papers will be presented on the work performed during this project: reservoir characterization and project design methods will be discussed in one paper, and the CO₂ screening model development will be addressed in another. This screening model will also be released during 1994, thus making available to industry a very useful CO₂ design program. A topical report discussing the environmental regulations and constraints of these types of projects will also be completed during 1994.

Reservoir Model

The FDD reservoir model was planned to incorporate (1) relative permeability curves obtained from conventional core analysis, (2) improved geological interpretation where center fault controls contours and fluid flow in reservoir, (3) permeability grid developed by geostatistics program, and (4) water-alternating-gas (WAG) scenarios.

The new relative permeability curves were incorporated into the FDD reservoir model, and runs were made to determine the effects of a higher residual oil saturation. The geologic grid using the central fault was built, and contours were redrawn for the waterflooded fault block; however, the new grid has not yet been incorporated into the model. Preliminary work with Texaco's geostatistics program Gridstat failed to yield favorable approximations of permeability data because of binary data being used in a program that uses averaging methods. Reservoir simulation runs evaluating the WAG process were made, which resulted in approval by Texaco management of a modified WAG injection approach. Water injection into the Kuhn No. 17 during the first 3 yr of the project will allow for higher withdrawal rates to be obtained from wells in the northern portion of the reservoir, where pure CO₂ is being injected.

Reservoir Pressure

The reservoir pressure has been raised with CO₂ and/or water to 3335 psia, 25 psia above the minimum miscibility pressure (MMP) of 3310 psia. The objective goal is 3400 psia.

Production Testing

Production testing of wells began as soon as pressure was raised to acceptable levels. Production was initiated from the project on Dec. 6, 1993, from the H. J. Kuhn Nos. 15-R, 33, and 38 and from the W. H. Stark "B" No. 8.

Horizontal Injection Well

The Port Neches (Marginulina Area 1) Well No. 1-H horizontal CO₂ injection well has been drilled to a measured depth (MD) of 6902 ft true vertical depth (TVD) of 5958 ft and is currently being completed across a 250-ft horizontal sand section. CO₂ injection should begin by Feb. 1, 1994.

Hard Data Results

Hard data results of the Louisiana State University (LSU) study of FDD reservoirs were developed. The information developed and future work requirements are provided in this report.

Delay Well Workover

The DOE approval to delay workover on Polk "B" No. 2 was requested because of the limited benefits this well will serve in the project.

Results—Phase II (Field Implementation)

CO₂ injection continued during the first quarter of FY94 at an average rate of 4.3 MMCFPD into the Port Neches (Marginulina Area 1) project area. This injection volume was distributed to Well Nos. 7, 10, 17, and 36 (Fig. 1) as wellhead pressures allowed. To accelerate the reservoir pressure buildup, CO₂ injection was discontinued in the No. 17 well during November 1993, and water was injected at a rate of 2000 BWPD. This increased injection reduced the amount of time necessary for the reservoir to achieve its MMP of 3310 psia and thus allowed the producing wells to be opened one month sooner. As shown in Fig. 2, continued injection of water into this well for the first 3 yr of the project allowed accelerated oil recovery while maintaining reservoir pressure. CO₂ must then be injected into the well to recover the surrounding oil reserves. The early tests of the producing wells suggest that CO₂ may be injected into the No. 17 well much sooner because of the higher CO₂ volumes available.

Early production tests from the project indicate that CO₂ breakthrough has already taken place in the producing wells. The Stark B No. 8 was shut in during September 1993, while making 7 BOPD, 697 BWPD, and 15 MCFPD, to allow for the reservoir pressure to be increased above the MMP. When opened on Dec. 6, 1993, the well flowed dry CO₂ at a rate of 400 MCFPD for a 2-d period before being shut in. Because

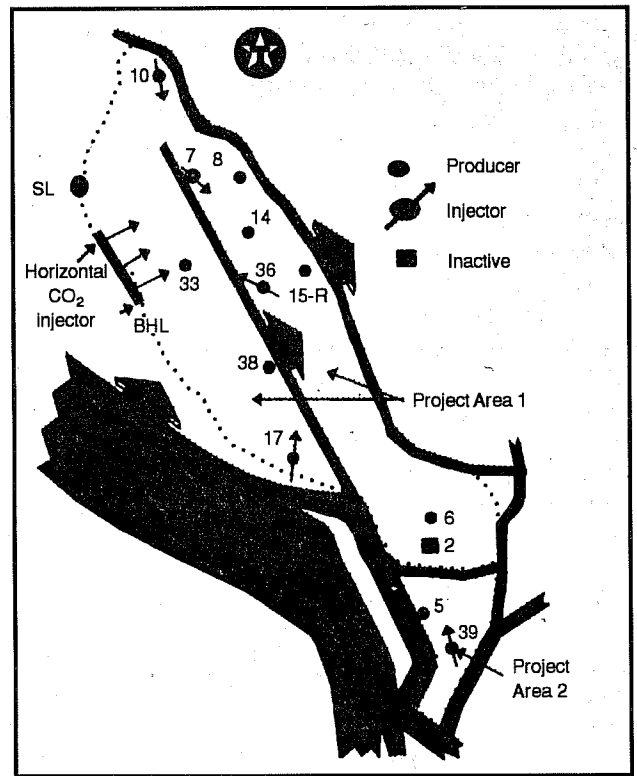


Fig. 1 Map of CO₂ project area, Port Neches Field, Orange County, Tex. Map not to scale.

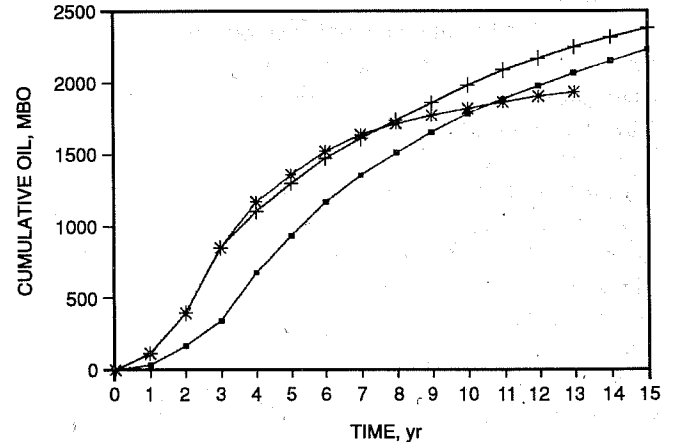


Fig. 2 Advantages of water injection, Port Neches CO₂ project. *, 2000 BWPD for 3 yr. +, 2000 BWPD for entire project. ■, injection of CO₂ only.

this well was high on the structure, it was interpreted that a small gas cap of CO₂ had been formed on top of the structure. The recent test of 217 BOPD, 1139 BWPD, and 2500 MCFPD of CO₂ on the H. J. Kuhn No. 15-R indicates, however, that CO₂ is breaking through very rapidly to the producing wells and that CO₂ injection must be redistributed among the injection wells in a more appropriate manner. Injection of CO₂ into the Stark B No. 7 and Kuhn No. 36 will be reduced

to allow for a reduction in CO₂ production volumes, and the injection will be concentrated in the horizontal injector, the Stark B No. 10, and the H. J. Kuhn No. 17.

When drilling the horizontal CO₂ injection well for the project, many problems surfaced that added to the over-expenditure of the project, but a successful completion was finally made across 250 ft of the sand. An aggressive build rate near the bottom of the intermediate hole prevented the 9⁵/₈-in. casing from being set in the top of the sand. As the shale section directly above the sand became unstable, drilling assemblies were stuck in the open hole on two separate occasions which caused the well to be sidetracked twice. On the last attempt, a 7-in. liner was run in the well to isolate the shale section, which allowed a completion to be made (Fig. 3).

The ability to keep the drilling confined within a 25-ft sand interval in a steeply dipping reservoir limited the amount of horizontal section drilled, which was recognized as a difficult task at the start of the project. The initial penetration of the sand encountered approximately 100 ft of sand before drilling into the shale section. After completion attempts failed because of the sticking of a hole opener in the open hole, a sidetrack was then drilled into 134 ft of the sand. Once this 134 ft of sand was cut, however, the shale section above the sand collapsed, and the drilling assembly containing \$450,000 worth of logging tools was stuck. Attempts to free the assembly were unsuccessful, and a second sidetrack attempt was made. It was on this final attempt that a protective string of casing was run to isolate the shale section. An increase in mud weight from 10.5 to 13.5 ppg allowed the hole to remain open long enough for the running of this 7-in. liner. With the problems previously encountered, the decision was made by Texaco management to drill only 25 ft of sand on the final attempt, if possible, which would limit the risk of sticking the pipe.

Lessons learned from this horizontal well project are: (1) make an attempt to set a protective string of casing at the top of sand before drilling horizontally, (2) if shale sections are exposed in a 90° portion of the hole, consider the use of a higher mud weight to prevent hole instability problems, and (3) ensure that geology is well understood before attempting a horizontal well in a thin, steeply dipping formation.

Figure 4 shows the true vertical depth paths taken by the original hole and sidetrack No. 1 and sidetrack No. 2 penetrations of the sand. The information gained from the first two attempts was useful on the final attempt to keep the well in the

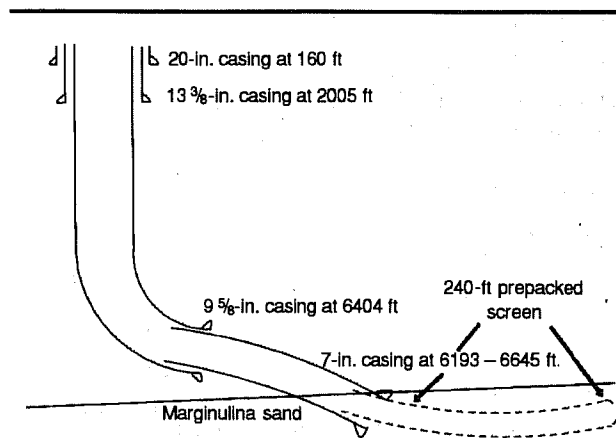


Fig. 3 Diagram of drilling of horizontal CO₂ injection well at Port Neches (Marginulina Area 1) No. 1-H, Orange County, Tex.

sand. Figures 5, 6, and 7 are copies of the open-hole logs run during drilling of the section. The final log is a gamma-ray and penetration rate log only because of the smaller hole that was drilled after the 7-in. liner was set.

Results—Phase III (Technology Transfer)

In addition to the CO₂ screening model, which has been developed by Texaco's research center staff and will be released during 1994, technology transfer work for the project is being conducted by LSU and Science Applications International Corporation (SAIC). LSU has begun gathering information concerning the location of CO₂ sources that can be used to implement other projects similar to the Port Neches CO₂ project and is using the Louisiana Office of Conservation's database to assemble production and reservoir data for FDD reservoirs in Louisiana. This information will be placed on area maps to determine the proximity of the fields to the CO₂ sources. Texaco's CO₂ screening criteria have been provided to LSU to assist the development of tables that will estimate CO₂ recoverable reserves for each field, which will allow oil producers to evaluate CO₂ flooding before the abandonment of fields.

SAIC will begin work during 1994 to develop a topical report that addresses the environmental regulations and constraints that occurred during the implementation phase of the Port Neches CO₂ project.

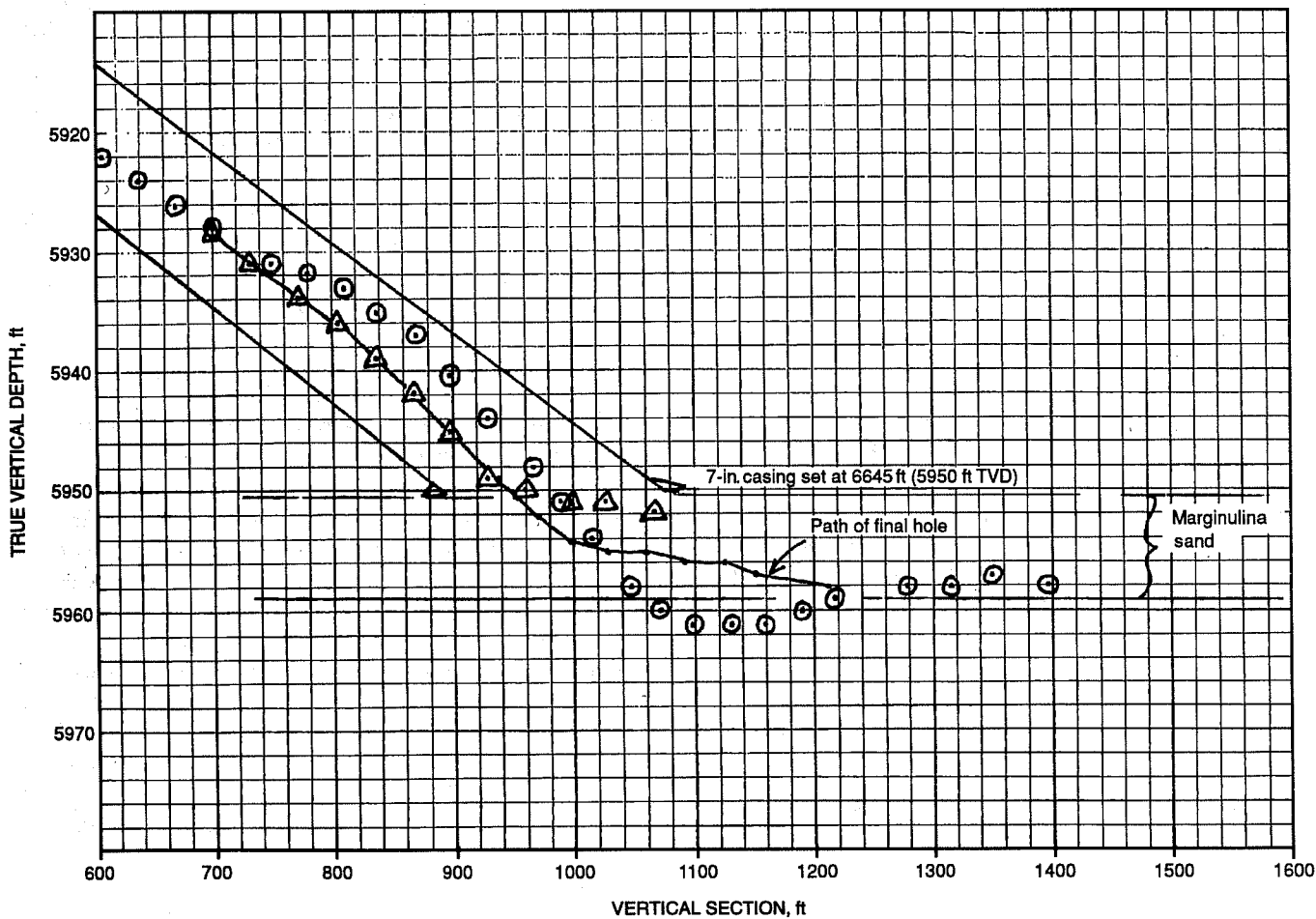


Fig. 4 True vertical depth vs. vertical section. Port Neches (Marginulina Area 1) No. 1-H. Plane of vertical section, 158°. O, original hole. Δ, sidetrack No. 1. —, sidetrack No. 2 (final hole). (Reproduced from best available copy.)

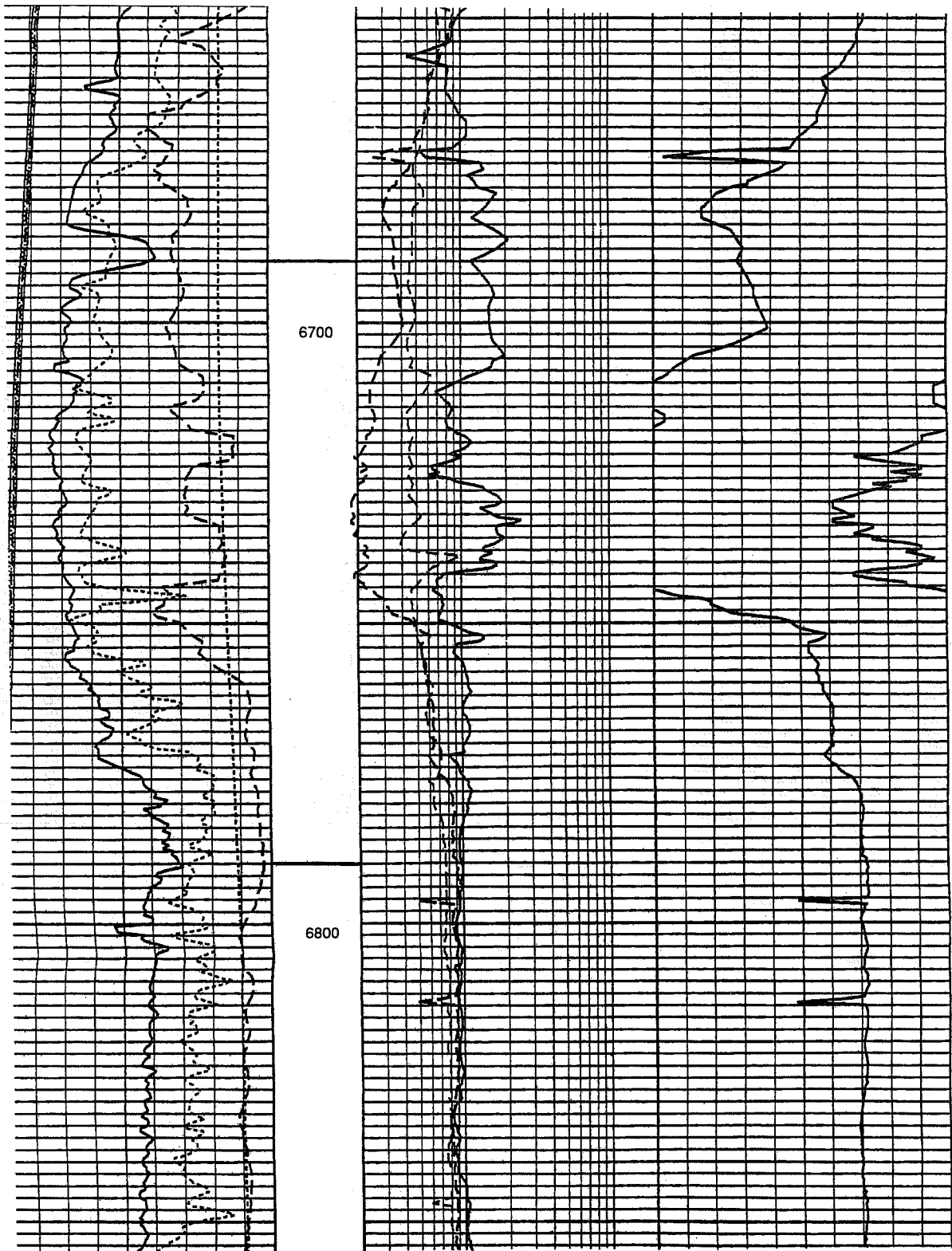
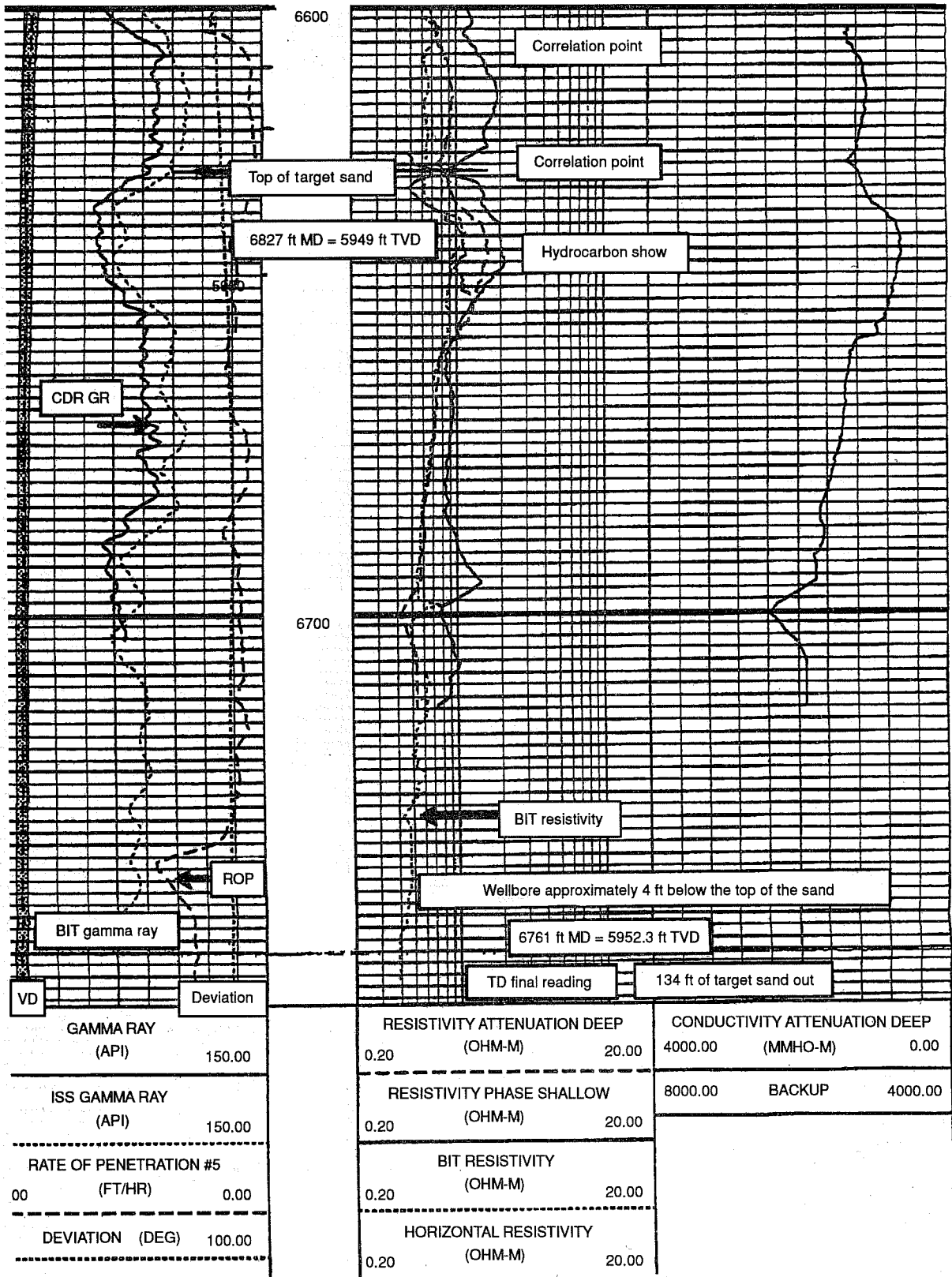


Fig. 5 Dual induction log, original hole, Port Neches (Marginulina Area 1) No. 1-H. (Reproduced from best available copy.)



VD	Deviation	RESISTIVITY ATTENUATION DEEP 0.20 (OHM-M)	20.00	CONDUCTIVITY ATTENUATION DEEP 4000.00 (MMHO-M)	0.00
GAMMA RAY (API) 150.00		RESISTIVITY PHASE SHALLOW 0.20 (OHM-M) 20.00		8000.00	BACKUP 4000.00
ISS GAMMA RAY (API) 150.00		BIT RESISTIVITY (OHM-M) 0.20 20.00			
RATE OF PENETRATION #5 (FT/HR) 00 0.00		HORIZONTAL RESISTIVITY (OHM-M) 0.20 20.00			
DEVIATION (DEG) 100.00					

Fig. 6 Dual induction log, sidetrack No. 1, Port Neches (Marginulina Area 1) No. 1-H. (Reproduced from best available copy.)

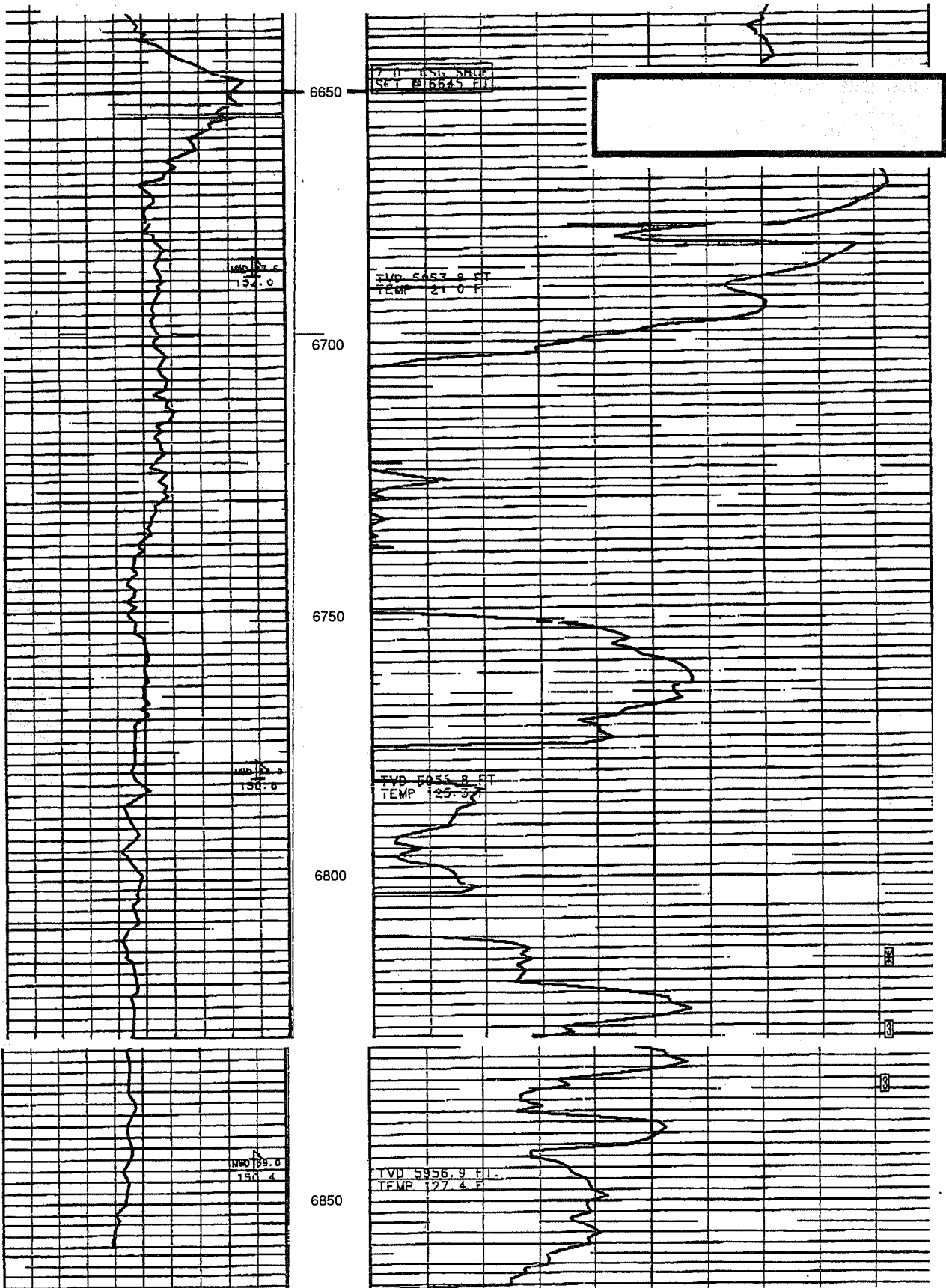


Fig. 7 Gamma-ray log, sidetrack No. 2, Port Neches (Marginulina Area 1) No. 1-H. (Reproduced from best available copy.)

**IMPROVED OIL RECOVERY IN FLUVIAL
DOMINATED DELTAIC RESERVOIRS
OF KANSAS—NEAR-TERM**

Contract No. DE-FC22-93BC14957

**University of Kansas
Lawrence, Kans.**

**Contract Date: June 18, 1993
Anticipated Completion: Dec. 31, 1998
Government Award: \$2,007,450**

**Principal Investigators:
Don W. Green
G. Paul Willhite**

**Project Manager:
Rhonda Lindsey
Bartlesville Project Office**

Reporting Period: Oct. 1—Dec. 31, 1993

Objective

The objective of this project is to address waterflood problems of the type found in Cherokee Group reservoirs in southeastern Kansas and in Morrow sandstone reservoirs in southwestern Kansas. Two demonstration sites operated by different independent oil operators are involved in the project. The Nelson Lease (an existing waterflood) is located in Allen County, Kans., in the Northeastern Savonburg field and is operated by James E. Russell Petroleum, Inc. The Stewart field (on latter stage of primary production) is located in Finney County, Kans., and is operated by Sharon Resources, Inc.

Topics to be addressed will be (1) reservoir management and performance evaluation; (2) waterflood optimization; and (3) the demonstration of recovery processes involving off-the-shelf technologies that can be used to enhance waterflood recovery, increase reserves, and reduce the abandonment rate of these reservoir types.

The reservoir management portion of the project will involve performance evaluation and will include such work as (1) reservoir characterization and the development of a reservoir database, (2) identification of operational problems, (3) identification of near-wellbore problems, (4) identification of unrecovered mobile oil and estimation of recovery factors, and (5) identification of the most efficient and economical recovery process.

The waterflood optimization portion of the project involves only the Nelson Lease. It will be based on the performance evaluation and will involve (1) design and implementation of a water-cleanup system for the waterflood; (2) application of well remedial work, such as polymer gel treatments, to improve vertical sweep efficiency; and

(3) changes in waterflood patterns to increase sweep efficiency.

Finally, plans are to implement an improved recovery process, possibly polymer-augmented waterflooding, on both field demonstration sites.

Summary of Technical Progress

Savonburg Field Project

Engineering and Geological Analyses

The computer database is being modified as additional information becomes available. The geological study is in the final stages of completion. Draft cross sections have been modified on the field. Several meetings were conducted to merge geological and engineering analyses. Several areas of reservoir impermeability were identified and mapped.

Characterization of the field by refining the computer database and cross sections as additional information becomes available will continue next quarter. Patterns with high potential for improvement of production will be identified by calculating the remaining mobile oil in place with the use of the computer database. These potential patterns will be candidates for pattern changes and wellbore cleanups.

Water Plant Development

Several meetings were held on water quality in the field. A list of options was developed, including (1) equipment, (2) specifications of water quality from option, and (3) capital and operating costs. Advantages and disadvantages of each option were identified. Field tests were conducted to characterize the quality of the supply and produced waters. A portable air flotation unit was tested successfully on location.

In the next quarter, a water cleanup process will be designed on the basis of volume requirements and economics. Once a process that will economically clean the brine has been identified, the equipment will be placed on location and tested.

Pattern Changes and Wellbore Cleanup

An analysis of five-spot patterns was conducted to determine the effect of past acid treatments on oil production. Possible workover-wellbore cleanup techniques were identified. In October 1993 injection wells HW-1 and KW-11 were washed and acidized.

The identification of mobile oil saturation will be the basis for pattern changes during the next quarter. New injection lines will be placed to converted injection wells, and pumping units will be placed on converted production wells. Appropriate methods will be used to clean wells exhibiting skin problems. Treatments will be designed on the basis of the problem(s) identified.

Field Operations

Normal field operations have included (1) monitoring wells on a daily basis; (2) repairing waterplant, piping, and

wells as required; (3) collecting daily rate and pressure data; and (4) solving any other daily field operational problem that might occur. Oil production in October 1993 totaled 26.4 bbl/d. Field operations will continue.

Stewart Field Project

Geological and Engineering Analyses

Seismic profiles were shot on the Bulger Lease in sec. 7, T. 23 S, R. 30 W to resolve uncertainties in the net pay map, which is planned to be used in the unitization. Modification of log analysis techniques is in progress. Attempts are being made to modify the calculated Archie equation-derived water saturation data for the wells in the instances where it is believed that the log data are supplying incorrect readings.

Preliminary decline curve analysis from existing production data was completed. With the use of straight exponential decline analysis, calculated remaining primary reserves are 500,000 bbl of oil for an ultimate primary oil recovery of 3,600,000 bbl of oil. Material balance calculation work has continued. It has been determined that uncertainties in fluid and rock properties will not resolve the difference in determining the original oil in place between the volumetric mapping of the net sand and material balance calculations. Either a large volume of the reservoir has yet to be defined or a limited water influx exists within the field.

The hardware and communication links to connect Sharon Resources, Inc., via Internet to the workstation at the University of Kansas to enable transfer of data are complete. The permeability data calculated from the core-log relationship were characterized for the individual wells into different permeability profiles that can be used for sensitivity cases in the simulation. Different case scenarios are being prepared to begin two-dimensional modeling for areas within the field. Simulation of primary depletion and waterflooding was done on initial cases.

The mobility ratio for a conventional waterflood was calculated with available relative permeability data. The mobility ratio is less than 1.0. Thus from these data a mobility problem does not appear to exist between reservoir oil and water.

Preliminary analysis was conducted with the Polymer Flood Predictive Model developed by Scientific Software-

Intercomp for the National Petroleum Council's 1984 survey of U.S. enhanced oil recovery potential. With the use of average reservoir properties, the model does not predict significant incremental amounts of oil recovery for polymer flooding vs. waterflooding.

Following seismic interpretation, plans are to drill a development well at a location to better define the eastern extent of the Morrow reservoir. Mobility ratios and water saturations will be further examined as commercial laboratory data become available. The computerized reservoir simulation of the field will continue during the next quarter.

Laboratory Testing

Representative synthetic formation brine was prepared on the basis of the composite analyses from produced formation water throughout the field. Two cores were cut from the main producing interval from the Sherman No. 3. The permeability to synthetic formation brine was determined at room temperature. The following sequence of brine mixtures was used to test one core for permeability: 100% synthetic brine, 75% synthetic brine-25% proposed injection water, 50% synthetic brine-50% proposed injection water, 25% synthetic brine-75% proposed injection water, and 100% proposed injection water. Initial results indicate a reduction in permeability when the mixture of 75% synthetic brine and 25% of the proposed injection water was injected. No further reductions in permeability were observed.

Additional proposed injection water sensitivity tests will be run on additional cores during the next quarter. Tests will also be conducted at the formation temperature of 125 °F. Preserved cores were sent to a commercial laboratory. Two relative permeability tests will be done on the core from the Scott 4-8. Capillary pressure tests are being done on three samples chosen to represent the three main flow units with varying permeabilities ranging from 50 to 400 mD. The capillary pressure tests will be performed on extracted cores with two samples from the Sherman 3 and one sample from the Meyer 10-1.

Unitization

Regular meetings have been held and the technical committee members have corresponded with each other to debate equity issues necessary for unitization.

INTEGRATED APPROACH TOWARD THE APPLICATION OF HORIZONTAL WELLS TO IMPROVE WATERFLOODING PERFORMANCE

Contract No. DE-FC22-93BC14951

University of Tulsa
Tulsa, Okla.

Contract Date: Jan. 1, 1993
Anticipated Completion: Dec. 31, 1996
Government Award: \$250,973

Principal Investigator:
Balmohan G. Kelkar

Project Manager:
Rhonda Lindsey
Bartlesville Project Office

Reporting Period: Oct. 1–Dec. 31, 1993

Objective

The overall objective of the project is to improve secondary recovery performance of a marginal oil field through the use of a horizontal injection well. The location and direction of the well will be selected on the basis of detailed reservoir description using an integrated approach. With the use of this method, a recovery of 2 to 5% of original oil in place (OOIP) is expected. This should extend the life of the reservoir by at least 10 yr.

The project work is divided into two stages. In Stage I, part of the Glenn Pool field (William B. Self Unit) will be selected, and additional reservoir data will be collected with cross borehole-tomography surveys and formation-microscanner logs through a newly drilled well. Analogous outcrop data will also be used. A detailed reservoir description will be developed on the basis of an integrated approach with the combination of the state-of-the-art data with conventional core and log data. After extensive reservoir simulation studies have been conducted, the location and direction of a horizontal injection well will be selected. The well will be drilled on the basis of an optimized design, and field performance will be monitored for at least six months. If the performance is encouraging, the project will enter into the second budget period of the project.

Stage II, the second budget period of the project, will involve selection of part of the same reservoir (Berryhill Unit, Tract 7), development of the reservoir description using only conventional data, simulation of flow performance using the developed reservoir description, selection of a location and direction of a horizontal injection well, and implementation of the well followed by monitoring of reservoir performance.

Comparison of the results obtained during the two budget periods will allow evaluation of the utility of collecting additional data with state-of-the-art technology. The application of horizontal wells in improving secondary recovery performance of marginal oil fields can also be evaluated.

A successful completion of this project will provide new means of extending the life of marginal oil fields using easily available technology. It will also present a methodology to integrate various qualities and quantities of measured data to develop a detailed reservoir description.

Summary of Technical Progress

The report of technical progress is divided into three sections: (1) preliminary results based on the cross-borehole seismic surveys, (2) geological description of the Self Unit, and (3) petrophysical properties description of the reservoir followed by the flow simulation results. On the basis of a thorough evaluation of the geological and flow simulation results, the initial test well location was finalized and the well was drilled in December 1993. The collected data from the newly drilled well will be evaluated and analyzed.

Geophysical Data Collection

A cross-well seismic test was performed in the Self Unit under Upland Resources management (Kiefer, Southeast Creek County, Okla.) Aug. 24, 1993. Preliminary results of the survey were previously reported,¹ and the analysis has been extended.

As a first step, the cross-well test intervals were tied to lithological descriptions. This will aid in interpretation of specific horizons in the seismic data. Figure 1 shows a detailed

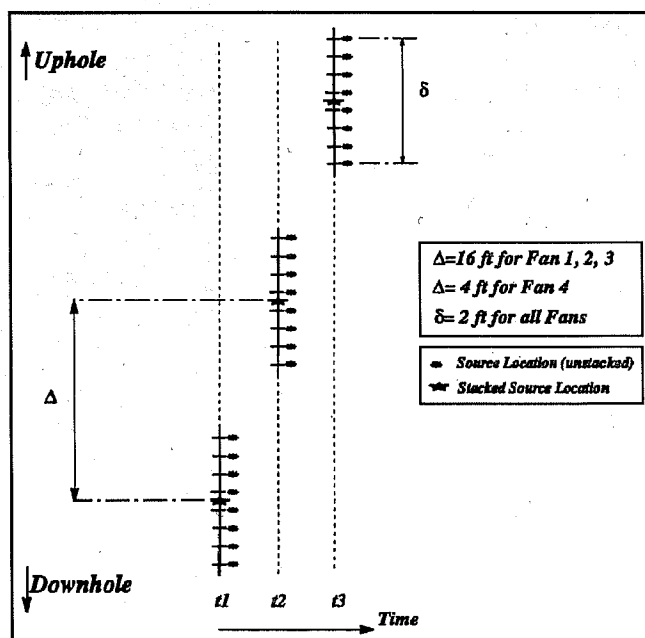


Fig. 1 Source locations at three consecutive time positions.

explanation of the vertical stacking and source level changes for the experiment. The distance between the net source levels in the survey is identified by symbol D. This distance was 16 ft for fans 1, 2, and 3 and 4 ft for fan 4. Actually, each net source level is a composite of several actual source levels spaced 2 ft apart. The outputs from these actual source levels are summed to create a single trace centered on the net source level. This has the effect of supporting random noise.

In the previous quarterly report,¹ a display of four test fans was presented. The signal quality was judged to be good to excellent. On the basis of the data quality and well spacing in the field test (distance of 660 ft), it is anticipated that good data quality will be achieved in the full tomography program where well spacing will be 450 ft.

The field test did not generate enough data coverage for full tomographic inversion in the image plane between source and receiver wells. However, to test the inversion method, event picking, and overlay with lithology, first intervals were picked on all four fans and the velocity tomogram shown in Fig. 2 was computed. The ray coverage for the shoaling fans is clearly seen in the image. Even with this space coverage, there is a clear early indication of velocity range in the area. Seismic

velocities of 11,000 to 14,000 ft/s are evident, with some curious and suspect areas of high velocity. No sonic logs on the Self lease are available. Thus the tomogram is the first glimpse at the velocity structure in Glenn Pool.

Geological Description

Shale maps between reservoir rock (channel-fill and splay sandstones) for each discrete genetic interval (DGI) were constructed in order to assess the potential for vertical connectivity within the Glenn sand across the 160 acres of the Self Unit. DGI A, B, and C appear to be vertically separated by non-reservoir rock (floodplain, level, or upper channel-fill mudstones). Only one well (Shelf No. 71) records a zero thickness of non-reservoir rock between DGI B and C. The aerial distributions of DGI C and D are exclusive of each other; however, they may be connected immediately south of the Unit. By contrast, DGI C, E, F, and G appear to be vertically connected across much wider areas within the boundaries of the Self Unit.

Natural fractures in the Glenn sand are a concern to the operator. Therefore available cores were examined for

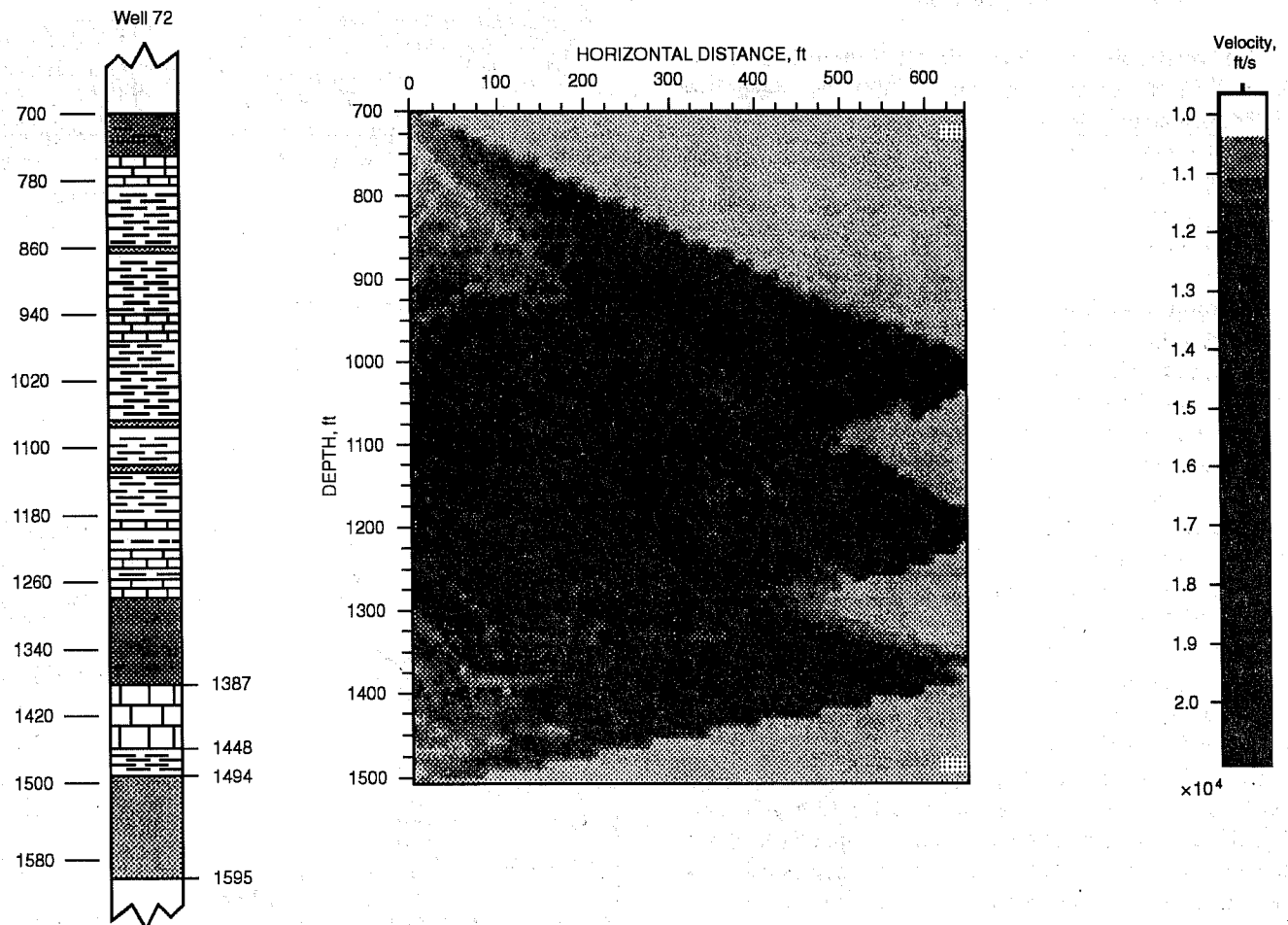


Fig. 2 Velocity tomogram (Glenn Pool test survey).

evidence of natural fractures. No evidence of natural fractures has been identified. This issue will also be addressed in core and microresistivity images collected in the vertical test well.

A vertical test well was drilled through DGI A and C net sand isopach closures (DGI B is predicted to be absent by erosion before DGI A deposition). A total of 153.2 ft of core was recovered in three core runs. Mudrocks above the Glenn sand include the marker interval used in the correlation network and definition of discrete genetic intervals. The entire Glenn sand interval was cut, but the bottom 2 to 4 ft was not recovered in the last core run. Well site observations noted that oil was bleeding from discrete stratigraphic intervals of 1 to 6 ft thick in DGI A, C, D, and E.

Work in progress includes collection and evaluation of data from the Self No. 82 well (vertical test well). The core is being properly archived, including gamma-ray emission scanning and photography. The core is being described for variations in sedimentary textures, structures, and fabrics, as well as other relevant attributes. Subsamples are being collected for porosity, permeability, clay content, and compression and shear velocity measurements. Knowledge gained from the core will be vital to the interpretation and evaluation of the microresistivity images.

Engineering Description and Simulation

A two-step procedure for constructing the reservoir description is being used: constructing the geological facies description followed by defining the petrophysical properties for individual grid blocks consistent with the presence of the appropriate facies. Subsequent to the last

report, some additional data regarding well completion and shut in became available. This resulted in modifications of the well openings and shut ins of the existing and old wells.

Additional initial potential data were received from some of the old wells drilled before 1940. In conducting the flow simulations with the modified data, the simulated initial potential data were compared with the observed initial potential data for many of the wells. Different bottom hole pressures from 200 to 600 psia were tried. It was observed that 400 psia of bottomhole pressure provided the best comparison. The results are shown in Fig. 3. The results for other bottomhole pressures were not significantly different from these results. With the uncertainties involved in how these wells were actually completed, the comparison was deemed satisfactory. The simulation of the entire Self Unit was done with the bottomhole pressure as 400 psia. The comparison between the simulated results and the observed results is shown in Fig. 4. The results match well except for early years. This discrepancy may be explained by the fact that (1) the early production data are estimated on the basis of the cumulative production data available in 1940 and (2) during the early years, all the wells were drilled on the boundary of the Unit, which may have resulted in the drainage of the surrounding leases. In the simulation, it was assumed that the Unit was enclosed. Overall, the results are deemed satisfactory.

On the basis of the simulation results and the resulting saturation profiles, the vertical test well was spudded on Dec. 27, 1993, between wells 59, 63, 81, and 64 (see Fig. 5). New data are being collected from the well.

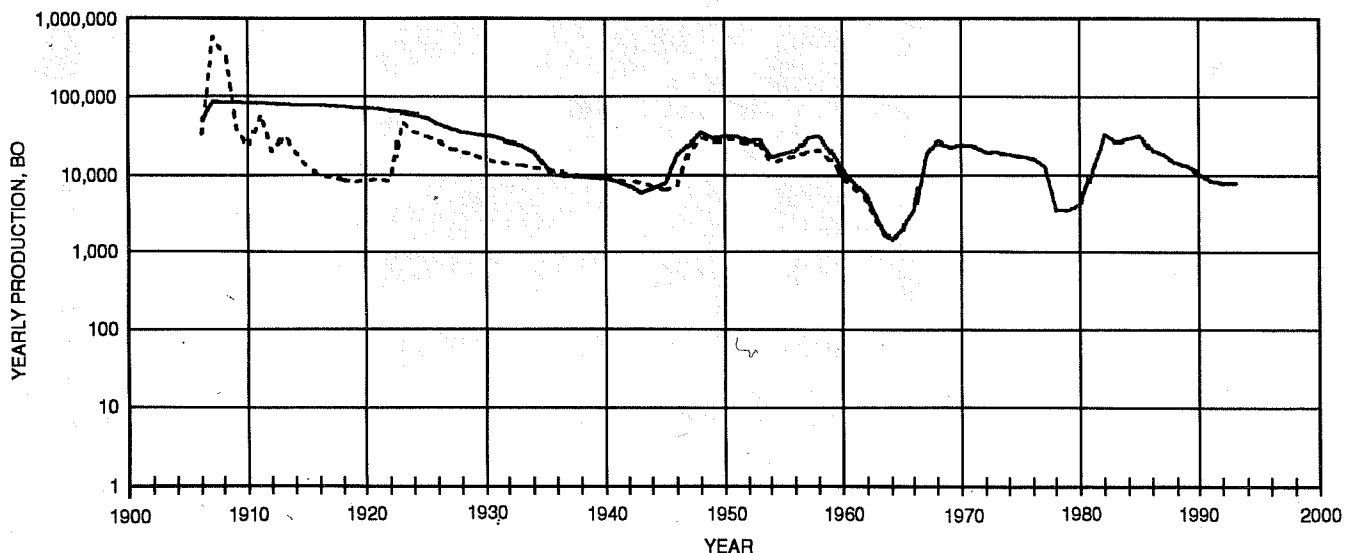


Fig. 3 Simulated and field performance for Self Unit. - - -, simulated. —, field data.

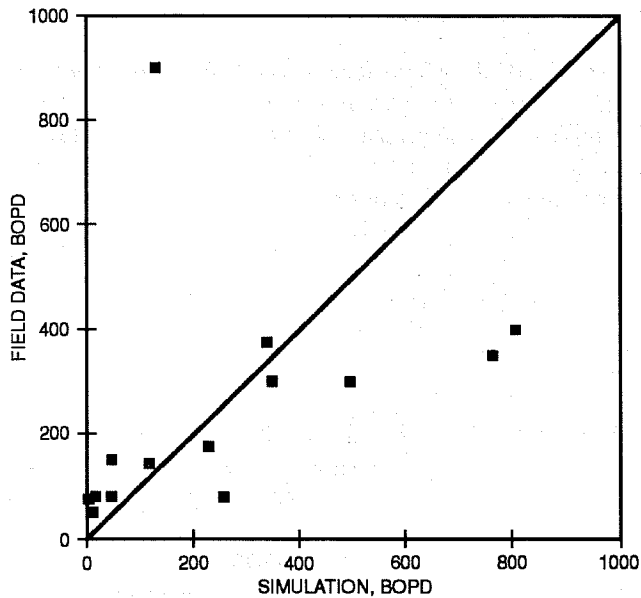


Fig. 4 Initial potential comparison.

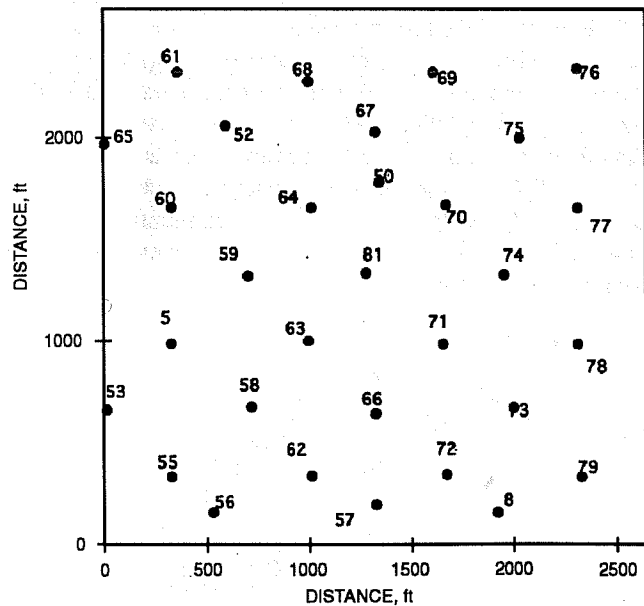


Fig. 5 Well locations.

Reference

1. *Quarterly Report, Integrated Approach Towards the Application of Horizontal Wells to Improve Waterflooding Performance*, Contract No. DE-FC22-93BC14951, July 1–Sept. 30, 1993.

GREEN RIVER FORMATION WATERFLOOD DEMONSTRATION PROJECT, UINTA BASIN, UTAH

Contract No. DE-FC22-93BC14958

Lomax Exploration Company
Salt Lake City, Utah

Contract Date: Oct. 21, 1992
Anticipated Completion: Oct. 20, 1995
Government Award: \$1,304,000

Principal Investigators:

John D. Lomax
Dennis L. Nielson
Millind D. Deo

Project Manager:

Edith Allison
Bartlesville Project Office

Reporting Period: Oct. 1–Dec. 31, 1993

Objective

The project is designed to increase recoverable petroleum reserves in the United States. The Green River formation in Utah's Uinta Basin contains abundant hydrocarbons that are hard to recover by primary means. The successful Lomax Monument Butte Unit waterflood will be evaluated under this contract, and, on the basis of this information, waterfloods will be initiated in nearby Travis and Boundary units. In 1987, Lomax Exploration Co. started a waterflood in the Monument Butte Unit of a Douglas Creek member of the Green River formation. This was a low-energy, geologically heterogeneous reservoir producing a waxy crude oil. Primary production yielded about 5% of the original oil in place (OOIP). As a result of the waterflood project, total production will yield an estimated recovery of 20% OOIP.

Summary of Technical Progress

Field Drilling and Production Results

The Monument Butte Unit No. 10-34 and the Travis Unit No. 14A-28 were put on production the last quarter of 1992. Formation microimaging (FMI) and magnetic resonance imaging logs were used to evaluate these wells as commercially productive. Through Dec. 31, 1993, the Monument Butte No. 10-34 (Nov. 27, 1992, first production) has produced 8,955 bbl of oil and 9,850 Mcf of gas and the Travis No. 14A-28 (Jan. 1, 1993, first production) has produced 7,953 bbl of oil and 23,045 Mcf of gas. The Travis No. 14A-28 was converted into a water injector in October 1993.

On the basis of fracture information provided by the FMI log, the D sand in the Travis No. 14A-28 well was completed. Subsequently, the behind-pipe D sand zones in the Travis Federal No. 14-28 were recompleted in March 1993 and those in the Travis No. 10-28 in May 1993. Through Dec. 31, 1993, the Travis No. 14-28 and No. 10-28 wells have produced 8,846 bbl of oil (43,309 Mcf of gas) and 4,060 bbl of oil (8,943 Mcf of gas), respectively. After the success of the D sand interval in the Travis Unit, water injection was begun in October 1993 in the Travis No. 14A-28. Through Dec. 31, 1993, 10,736 bbl of water has been injected into the Travis No. 14A-28 well at an average injection rate of 37 psi.

Water injection continued throughout the fourth quarter of 1993 to repressure the Lower Douglas Creek member in the Green River formation in the Travis Unit. The average daily water injection rate for the report period in the Travis No. 15-28 was 300 bbl at an average injection rate of 756 psi. Lomax and the Department of Chemical and Fuels Engineering agreed to a slower injection rate in the Travis No. 15-28 because of the fractures found in the logging and coring of the No. 14A-28 well. In October 1993, the Travis No. 3-33 was converted from an oil producer into a water injector to inject into the Lower Douglas Creek member. The average daily water injection rate for the report period was 270 bbl at an average injection rate of 900 psi.

On Nov. 15, 1993, the Monument Butte No. 9-34 well was spudded. The initial objective was to target for completion the D and B sands of the Green River formation. The plan was to convert the No. 9-34 into a water injector. Drilling of the No. 9-34 started on Dec. 1, 1993, and was completed on Dec. 6, 1993, to a depth of 6500 ft. On Dec. 6, 1993, logging of the No. 9-34 was started. On the basis of the results of the logging and coring, 5.5-in. casing was cemented into place in two stages. The D (4992 to 4997 ft; 5000 to 5008 ft) and B (5334 to 5350 ft; 5355 to 5360 ft) sand members were perforated and fractured. Also, on the basis of the logging program, the Castle Peak sand member of the Green River formation was perforated (5854 to 5868 ft; 5902 to 5912 ft) and fractured. All the completed sands were swabbed with bottom-hole pressure tests run. The No. 9-34 well has been put on oil production. From Jan. 9-31, 1994, the No. 9-34 has produced 3232 bbl of oil (140 bbl/d). Apparently the D and B sands have been affected by the waterflood front. The No. 9-34 will be monitored over the next 90 to 120 d to decide what future steps need to be taken to operate the well and waterflood unit.

Reservoir Performance

For the evaluation and prediction of the reservoir performances of the Monument Butte and the Travis Units, a parallel planning approach proposed by Saleri¹ has been adopted. The idea is to improve the reservoir description as more data become available while matching all the previously available data. This approach can be illustrated by comparing the overall reservoir calculations with the reservoir simulation results.

Monument Butte Unit

The OOIP can be projected with the available gas and oil production data if the thermodynamic properties of the oil are established. The oil produced in stock tank barrels (N_p) and the original oil in place (N) are related by Eq. 1 if the water and formation compressibilities are neglected and if there is no initial gas cap in the reservoir.

$$\frac{N_p}{N} = \frac{(B_o - B_{oi}) + B_g(R_{si} - R_s)}{B_o + B_g(R_p - R_s)} \quad (1)$$

where B_{oi} and B_o = initial and final oil formation factors, respectively

R_{si} and R_s = initial and final solution gas/oil ratios (GOR), respectively

R_p = cumulative GOR

B_g = gas formation volume factor

The initial reservoir pressure in the Monument Butte Unit was just over 2300 psia. The initial GOR was about 500 scf/STB, which corresponds to a measured bubble point pressure of 2275 psia. The pressure-volume-temperature (PVT) properties of the Monument Butte fluids were measured and used in the reservoir simulation study, which was reported earlier. A drawdown to about 1200 psia in primary production (end of August 1987) resulted in the production of 419 MSTB of oil and 1.612 MMMscf of gas for a cumulative GOR of 3847 scf/STB. Relevant thermodynamic properties of the Monument Butte fluids are

Property	Value
B_{oi}	1.26 rb/STB
B_o at 1200 psia	1.15 rb/STB
R_{si}	500 scf/STB
R_s at 1200 psia	276 scf/STB
B_g at 1200 psia	0.0024 rb/scf

If Eq. 1 is used, an OOIP of 9.6 MMstb is obtained for the entire Monument Butte Unit. The approach does not consider production of oil from two major sand layers, the D and the B. Reservoir simulation results, reported earlier, used the isopach information for the two sands and arrived at the OOIP by completely independent means. The OOIP by the reservoir simulation approach was 9.3 MMstb, and the average reservoir pressure at the end of the primary was about 1250 psia. The average free gas saturation at the end of the primary was 9.9% by reservoir engineering calculations and 9.7% by reservoir simulation. Thus the overall reservoir engineering calculations and results of the reservoir simulation are in reasonably close agreement. The reservoir simulation is

geologically and physically more sophisticated than the overall reservoir engineering volumetrics.

The idea is thus to ensure data compatibility as more sophisticated reservoir models are constructed. The reservoir model is being improved by increasing the number of grid blocks and thus the model resolution and expanding the unit boundaries to accurately incorporate the geologic and reservoir information generated by drilling well No. 9-34.

Preliminary results indicate that, if variable grid block size representation is used, grid block size has little effect on the overall results. Thus the finer grid reservoir description will be useful only if geologic information is available at the higher resolution. The original unit boundaries placed wells No. 10-34 and No. 9-34 on the edge of the reservoir and too close to the no-flow boundaries of the unit. The reservoir description is being modified to incorporate the geologic information (sand thicknesses, etc.) from the new wells. The modified model must be used to verify and predict the performances of these two wells.

Travis Unit

The preliminary primary production match of the Travis Unit was reported earlier. The reservoir performance of the Travis Unit can be classified into three distinct phases: (1) primary production, (2) waterflooding—1000 bbl/d into No. 15-28, and (3) waterflooding—300 bbl/d into No. 15-28 and 300 bbl/d into No. 3-33.

In primary production (end of December 1990), the Travis Unit, which produces predominantly from the Lower Douglas Creek sand, had yielded 245 MSTB of oil and 1.08 MMscf of gas at a cumulative producing GOR of 4408 scf/STB. The overall reservoir engineering calculations for the Travis Unit will depend on the initial reservoir pressure and the initial producing GOR. There is some uncertainty concerning these two values. A higher initial production GOR than that from the Monument Butte field (550 scf/STB compared with 500 scf/STB) with a depletion down to a pressure of 1200 psia would indicate free gas saturations of about 14% at the end of primary production. These values are about 50% higher than the free gas saturation values for the Monument Butte Unit. This, coupled with the presence of thicker sands in the Travis Unit, may explain a slower than expected response to the waterflood that has been observed.

Injection of 1000 bbl/d of water into No. 15-28 caused water channeling toward No. 14-28 and No. 3-33. The water short-circuiting was also observed while drilling well

No. 14A-28. There are thus reasons to believe that the injection of 1000 bbl/d of water enhanced fracture permeabilities in the directions of No. 14-28 and No. 3-33. In the reservoir model that is being built, the changed reservoir properties must be taken into account.

Lowering the injection rates stopped the water channeling, which indicates at least a partial closure of the opened fractures. The current injection pressures in No. 15-28 and No. 3-33 indicate a gradual pressurization of the reservoir. Successful description and prediction of the Travis Unit performance will require that the model duplicate the preceding observations.

Simulations being performed indicate that the fracture and matrix capillary pressures have profound effects on the waterflood. Altering capillary pressures alters primary production also. A model that will duplicate all three distinct phases of the Travis Unit performance is being developed.

Technology Transfer

The success of the Monument Butte Unit has influenced the start and the development of another waterflood unit in the Uinta Basin, the Wells Draw Unit by Pacific Gas and Electric Resources Co. (PG&E). The PG&E received approval from the State of Utah on Dec. 8, 1993, to unitize 1162 acres. The unit shares a common border with Lomax's Monument Butte and Travis Units. In PG&E's testimony before the State of Utah, it was stated that the waterflood unit will recover an additional 1.3 million bbl of oil that would not be recovered under current pressure-depletion mechanisms.

On Nov. 30, 1993, a speech entitled "The Green River Formation Water Flood Demonstration Project Showing the Development of New Reserves in the Uinta Basin" was presented to the Subcommittee on Renewable Energy, Energy Efficiency and Competitiveness of the U.S. Senate Committee on Energy and Natural Resources in Roswell, N. Mex.²

References

1. N. G. Saleri, Reservoir Performance Forecasting: Acceleration by Parallel Planning, *J. Pet. Technol.*, 45(7): 652-657 (1993).
2. J. D. Lomax, *The Green River Formation Water Flood Demonstration Project Showing the Development of New Reserves in the Uinta Basin*, paper presented at the Meeting of the Subcommittee on Renewable Energy, Energy Efficiency and Competitiveness of the U.S. Senate Committee on Energy and Natural Resources, Roswell, N. Mex., Nov. 30, 1993.

**SECONDARY OIL RECOVERY FROM
SELECTED CARTER SANDSTONE OIL
FIELDS—BLACK WARRIOR BASIN,
ALABAMA**

Contract No. DE-FC22-93BC14952

**Anderman/Smith Operating Company
Denver, Colo.**

**Contract Date: Oct. 21, 1992
Anticipated Completion: Jan. 5, 1996
Government Award: \$369,600**

**Principal Investigator:
James C. Anderson**

**Project Manager:
Gene Pauling
Metalrie Site Office**

Reporting Period: Oct. 1–Dec. 31, 1993

Objectives

The objectives of this project are to (1) increase the ultimate economic recovery of oil from the Carter reservoirs and thereby increase domestic reserves and lessen U.S. dependence on foreign oil; (2) extensively model, test, and monitor the reservoirs to optimize their management; and (3) assimilate and transfer the information and results gathered to other U.S. oil companies to encourage them to attempt similar projects.

Summary of Technical Progress

Central Bluff Unit

Gas production for the unit declined to zero during the quarter. As a result, propane gas is being used to run the pumping unit for the Fowler Brasher 7-9 and Fowler Dodson 8-12 producing wells, where little or no gas is available to dump the heater treaters.

The injection pressure in the Jones 7-16 well continued to increase during the quarter and thus reached 510 psi at a water injection rate of 300 bbl/d. In early November the injection rate was reduced to 250 bbl/d to stabilize the pressure at about 300 to 350 psi. In late November a radioactive injection profile showed that all but the upper 2 ft of perforations was covered with fill in the bottom of the hole. The well was cleaned out to about 60 ft below the perforations, and water injection was subsequently resumed at an average rate between 250 and 275 bbl/d. These injection rates resulted in a rapid increase in the injection pressure from 250 to 560 psi for the Jones 7-16 well.

As a result of waterflood operations at the unit, oil production from the Fowler Brasher 7-9 well increased 40 to 50 STB/d in late October and averaged about 45 STB/d in November with no measurable water production. Production at the Fowler–Dodson 8-12 was more erratic during the same period. In October the oil rate for this well increased to nearly 17 STB/d with no reported water production. In November, however, the oil production rate declined to about 9 STB/d with an associated average water rate of nearly 17 bbl/d. Water analysis showed that this produced water was significantly fresher than the connate water produced before waterflood operations. This provides evidence for early breakthrough of water injected at the Jones 7-16 well and will be an important consideration in the reservoir modeling study being performed for the unit.

The reservoir modeling study of the Central Bluff Unit was initiated this quarter. As with the North Fairview Unit, the objectives of the study are to (1) improve understanding of primary and secondary recovery, (2) check–confirm no-flow boundaries, (3) develop improved reservoir management scheme (e.g., optimal water injection strategy), and (4) forecast oil recovery for various operating strategies.

On the basis of Anderman/Smith's revised geologic evaluation of the unit area, structure and net pay isopach maps were prepared for the Carter C2 sandstone. A reservoir simulation grid (25 × 28 × 1) was constructed to cover an area of about 7250 by 8000 ft, which is about 4.5 times as great as the 300 acres estimated for Central Bluff. A transparency of the grid was overlaid on the structure and isopach maps so that values of elevation and thickness could be digitized at grid-block centers for input to the simulator.

Production and pressure data for the two producing wells (Fowler Brasher 7-9 and Fowler Dodson 8-12) and the injection well (Jones 7-16) will be history matched with the ROAST II simulator. Unlike the North Fairview Unit, no pressure-transient testing was performed on the Central Bluff wells from which to estimate reservoir permeability. Therefore, as with some other parameters for which no data are available, reservoir properties, such as absolute permeability and relative permeability, will be estimated from matching actual field performance. Other reservoir properties, such as the pressure-volume-temperature (PVT) properties, are being evaluated for input to the simulator on the basis of the available measured data.

North Fairview Unit

There has been essentially no change in the waterflood response at the North Fairview Unit during the last quarter. Water injection rates at the Boman 33-5 No. 1 well have been maintained between 200 and 250 bbl/d with a gradual increase in injection pressure from 1240 to 1310 psi by the end of November. Oil production rates from the three producing wells have remained unchanged (i.e., 3 STB/d for Smith 33-6, 2 STB/d for Perkins 33-11, and 1 STB/d for Perkins Young 33-10). Although gas production from the Perkins

33-11 well periodically declined to zero during the three-month period, gas was diverted from the old gathering system to maintain the pumping unit.

During this quarter significant progress has been made on the development of a reservoir characterization for the North Fairview Unit. This characterization is being achieved by adjusting key reservoir properties (such as porosity, absolute permeability, and three-phase relative-permeability relationships) to match actual well performance for the unit. With the use of the ROAST II simulator, good matches have been obtained for the production rates and limited pressure histories for the three producing wells (Smith 33-6, Perkins Young 33-10, and Perkins 33-11) and the injection well (Boman 33-5 No. 1) for a production period in excess of 11 yr (July 1982 to August 1993).

The total oil and gas producing rates for all wells in the unit are shown in Figs. 1 and 2, respectively. As indicated in both figures, good agreement between simulated and observed production rates has been achieved with the reservoir characterization determined from the history match. The total oil producing rate peaked at about 160 STB/d during the second year of production from the unit (representing production from all four wells), with a subsequent decline to less than

40 STB/d by the end of the fourth year. For the last 5 yr, the total oil production rate from the unit has been less than 10 STB/d from the three remaining producing wells (Boman 33-5 No. 1 was shut in about 4.5 yr into production from the North Fairview area).

During this same 11-yr production period, the total gas rate from the North Fairview wells peaked at approximately 200 to 250 Mscf/d and has also shown a relatively steady decline (to less than 50 Mscf/d) with primary depletion of the reservoir. Essentially no water production has occurred from the unit; total water production is reported as less than 750 bbl for the 11-yr period.

For the reservoir permeabilities being used in this study (20 to 85 mD), the decline in both oil and gas production from the North Fairview wells corresponds to a reduction in average reservoir pressure from 1000 to 150 psi at the end of the 11-yr period (Fig. 3). With reservoir energy nearly depleted, waterflood operations for the unit were initiated in June 1993 with water injection at the Boman 33-5 No. 1 well. Since that time, in excess of 25 Mbbbl of water has been injected with no measurable change in either reservoir pressure decline or the production rates from the three offset producing wells. This lack of reservoir response to water injection at the Boman

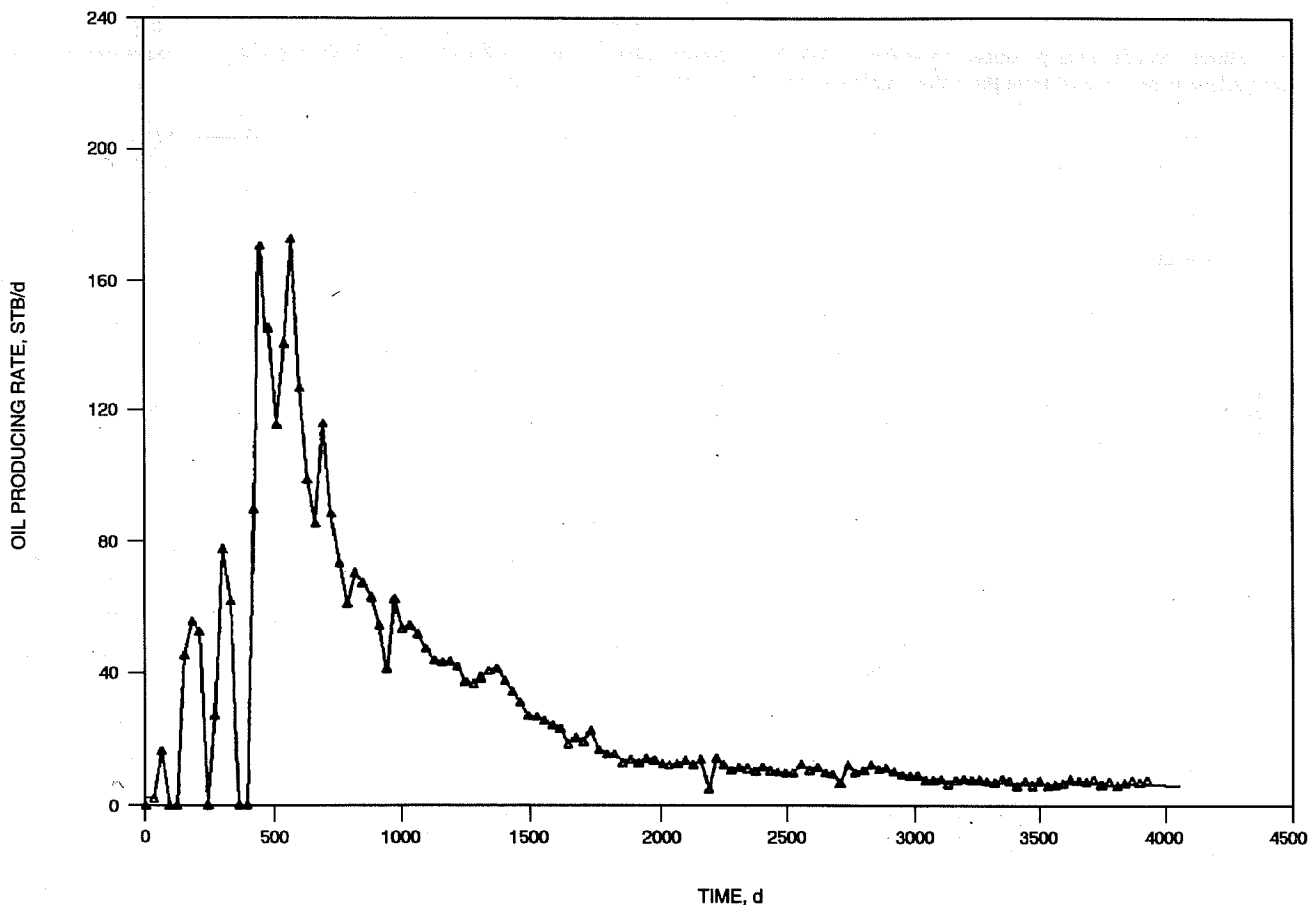


Fig. 1 History match of oil producing rates for all wells in the North Fairview Carter Oil Unit (run No. 8) achieved with the reservoir characterization determined from the history match. —, model oil rate. Δ , actual oil rate.

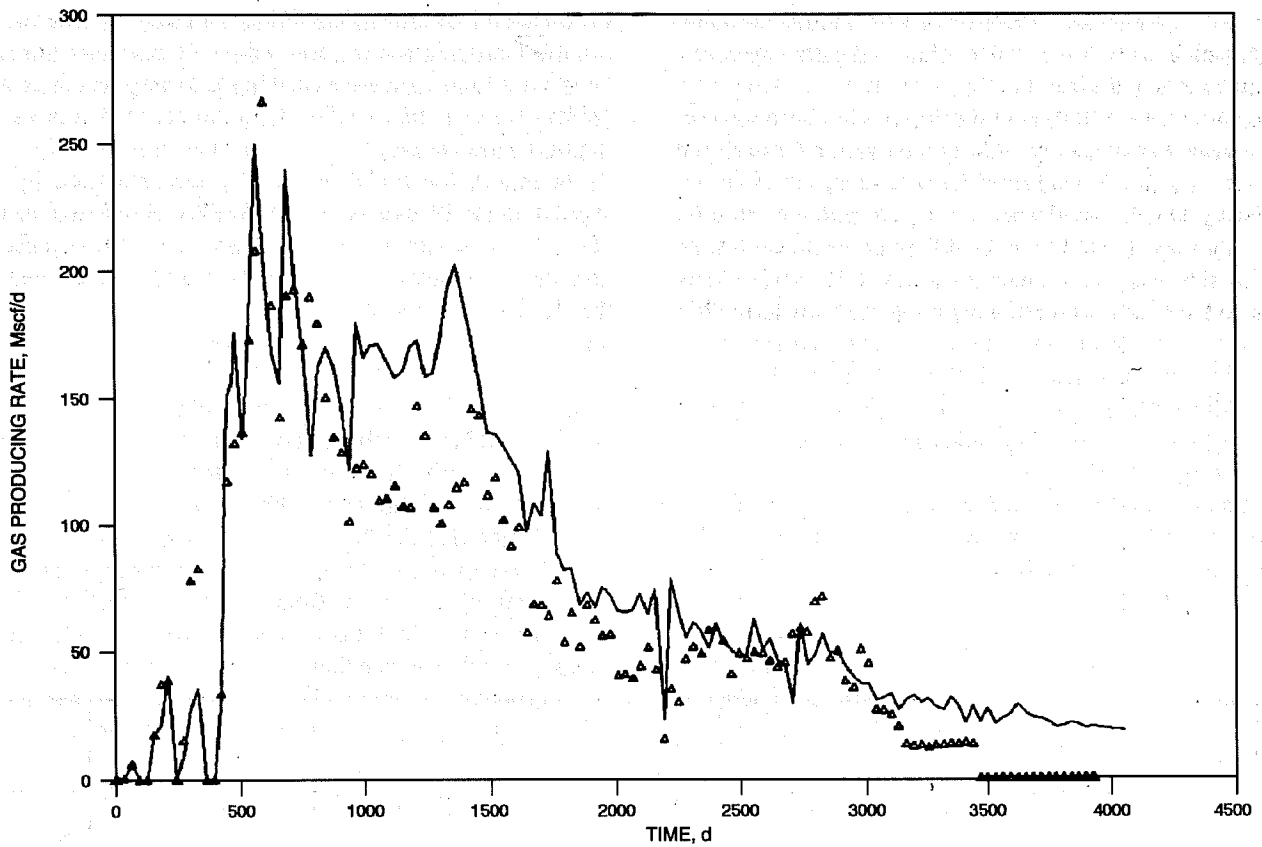


Fig. 2 History match of gas producing rates for all wells in the North Fairview Carter Oil Unit (run No. 8) achieved with the reservoir characterization determined from the history match. —, model gas rate. Δ , actual gas rate.

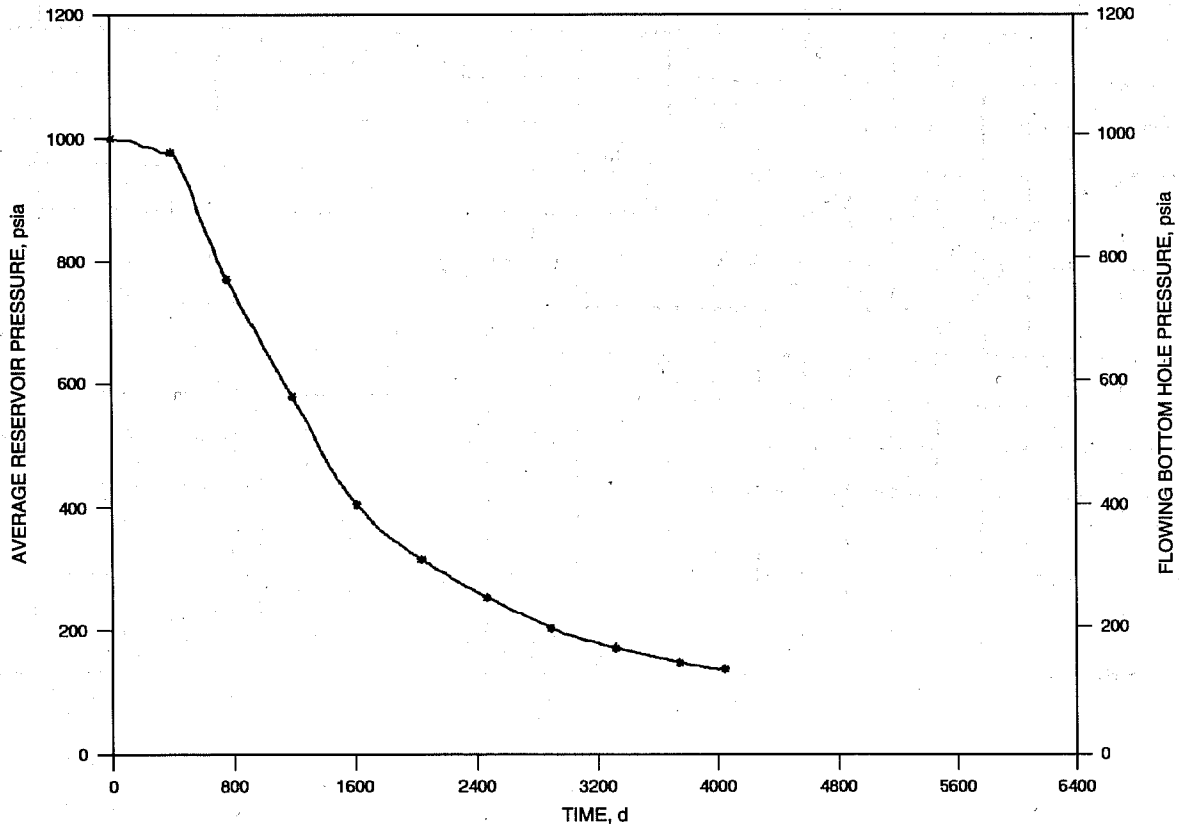


Fig. 3 Reservoir and waterflood pressures for North Fairview Carter Oil Unit (run No. 8). +—+, P_{res} . x—x, P_{wf} .

33-5 No. 1 well provided a valuable check on the simulation results, which also show a lack of change in either reservoir pressure or production rates for this volume of injected water.

The reservoir simulation grid (Fig. 4) was constructed in such a way as to readily adjust (enlarge or reduce) the reservoir's no-flow boundaries if it became apparent during the history match that the reservoir pore volume required further adjustment. On the basis of the history match results thus far, the reservoir boundaries and thickness variations appear to have been well defined during Anderman/Smith's

geologic evaluation. With the reservoir geometry determined for the North Fairview area, values of reservoir porosity between 10 and 19% were used in the history match of well performance. In combination with the net thickness values digitized from the isopach map (thicknesses with 10% porosity or more), the initial fluids in place calculated by the simulator are in excess of 900 MSTB of oil and nearly 400 MMscf of solution gas. Production to date represents about 12% recovery of the original oil in place estimated for the North Fairview Unit.

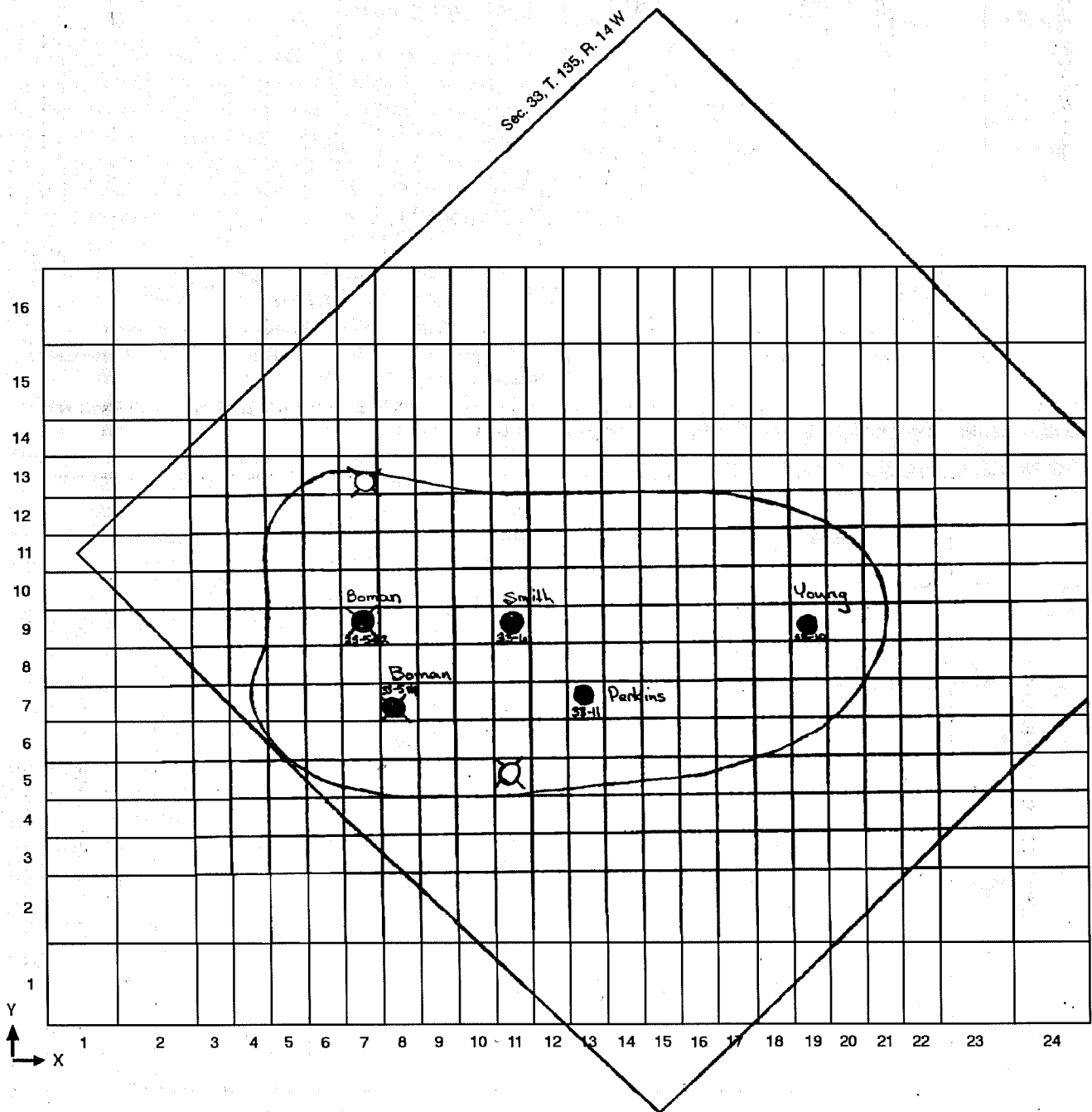


Fig. 4 Reservoir simulation grid of North Fairview Carter Oil Unit.

The focus of the reservoir modeling study so far has been to develop a reservoir characterization that matches the actual 11-yr historical performance period for the North Fairview Unit. This preliminary phase is nearly complete and only requires a few additional simulations to finalize the reservoir characterization. During the next quarter the reservoir characterization will be used to perform several forecast simulations to determine how long it will take to see a pressure response and rate increase for the existing producing wells. In addition, simulations will be performed to further evaluate and improve the existing reservoir management scheme in terms of optimizing the water injection strategy (i.e., selection of additional injection well locations and estimates of water volumes to be injected).

South Bluff Unit

There was no activity at the South Bluff Unit during the reporting period.

**ENHANCED OIL RECOVERY UTILIZING
HIGH-ANGLE WELLS IN THE FRONTIER
FORMATION, BADGER BASIN FIELD,
PARK COUNTY, WYOMING**

Contract No. DE-FC22-93BC14950

**Sierra Energy Company
Reno, Nev.**

**Contract Date: July 10, 1993
Anticipated Completion: Dec. 31, 1994
Government Award: \$1,124,127
(Current year)**

**Principal Investigators:
Richard G. Formann
Jerome P. Walker**

**Project Manager:
Edith Allison
Bartlesville Project Office**

Reporting Period: Oct. 1–Dec. 31, 1993

Objective

The objective of this study of the Frontier Formation in Badger Basin Field, Park County, Wyo., is to use three-dimensional (3-D) seismic and core data to analyze the diagenetic history, rock properties, and the natural fracture system. This will provide the basis for increasing recovery with slant and horizontal wells to intersect oil-bearing fractures.

Summary of Technical Progress

Data Interpretation

Interpretation of the 3-D seismic survey was completed on a Sun Sparcstation 10 workstation (UNIX based), using Landmark Graphics' latest version of Seisworks 3-D software. After the formation tops were tied to the seismic reflectors, normal and reverse faults seen on the survey were picked to constrain the productive structure. Then the following reflectors were picked on a 10 by 10 (inline by crossline) grid: (1) Eagle sandstone member of the Mesaverde Formation, (2) Cody marker, (3) Frontier Formation, (4) 2nd Frontier sand, (5) 3rd Frontier sand, and (6) Lakota Formation (the Pryor conglomerate equivalent). An autopicking routine (ZapIII) was used to fill in the picks throughout the remainder of the survey for the three Frontier reflectors. Each crossline (NW–SE orientation) within the productive area of the field was then checked for quality of the auto picking and edited. The crossline orientation was chosen because it is optimally placed for identification of the normal faulting, which is believed to be key to well productivity. Subsequently, time-structure maps and amplitude maps were constructed for the three Frontier reflectors. Location and wellbore paths were chosen for the slant and horizontal legs. A velocity function, converting time to depth, was used to make a depth-structure map for the slant and horizontal wellbores. (See Figs. 1, 2, and 3.)

Drill Slant Hole

Various service companies, including drilling contractors, well site geologists, mudloggers, and core analysis companies, were contacted and requested to supply bids for their anticipated services. Bids were received for various services. Sierra was prepared to award contracts for these services. Sierra had also picked a location and prepared a drilling plan for the slant/horizontal wellbores. Sierra was ready to submit an Application for Permit to Drill. However, because Sierra entered into an agreement to sell the Badger Basin property, the drilling phase was put on hold.

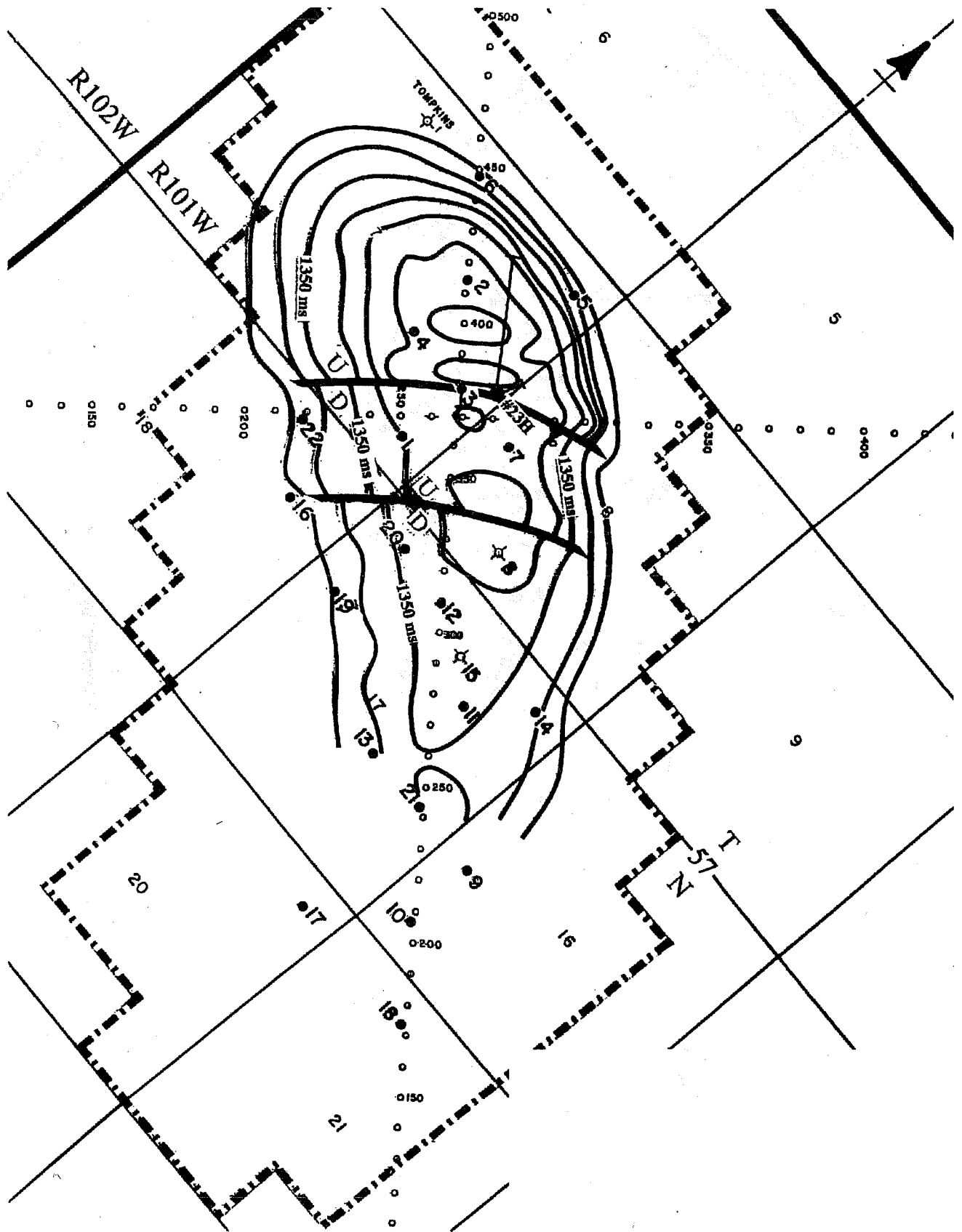


Fig. 1 Time-structure map for the top of the Frontier Formation, Badger Basin Field, Park County, Wyo. C.L., 6 ms (approx. 30 ft). Horizontal scale, 1 in. = 2000 ft. Note: Bottomhole location for the No. 3 Badger Basin Field Unit well is an estimated position, based on expected dips penetrated by the well and absence of any normal-fault cut in the Cody shale or Frontier Formation.

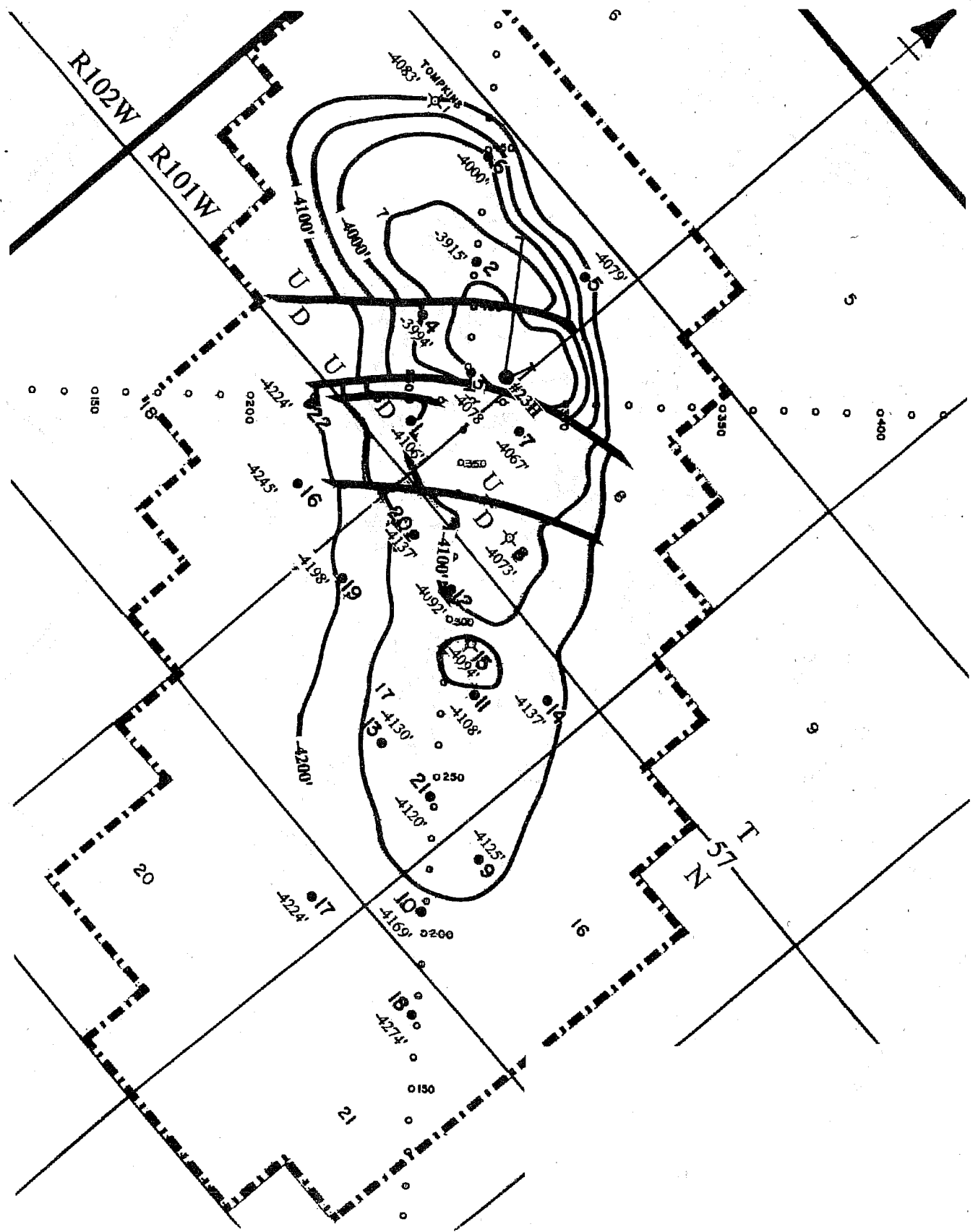


Fig. 2 Depth-structure map for the top of the 2nd Frontier sandstone, Badger Basin Field, Park County, Wyo. C.I., 50 ft. Horizontal scale, 1 in. = 2000 ft. Note: Bottomhole location for the No. 3 Badger Basin Field Unit well is an estimated position, based on expected dips penetrated by the well and absence of any normal-fault cut in the Cody shale or Frontier Formation.

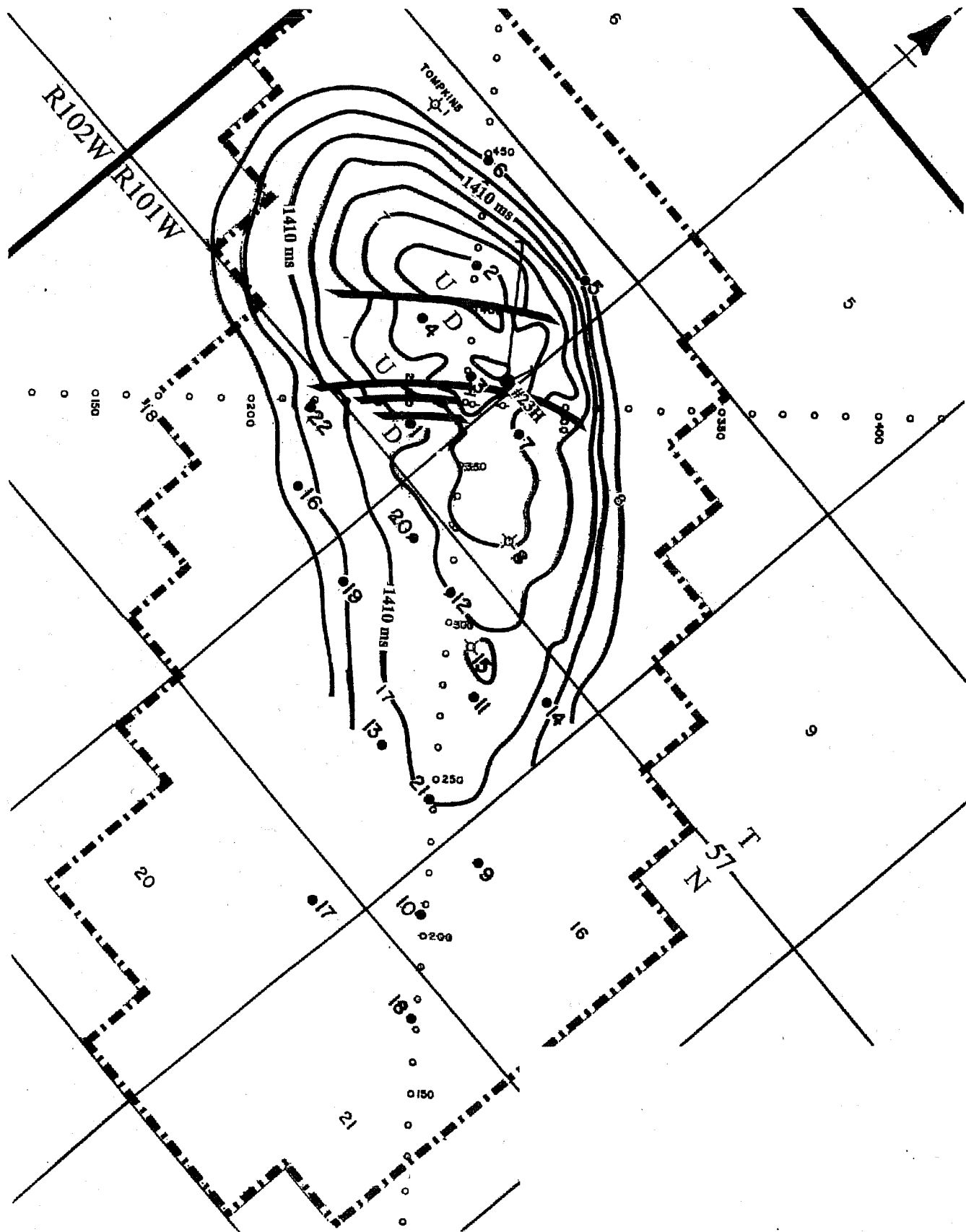


Fig. 3 Time-structure map for the top of the 3rd Frontier sandstone, Badger Basin Field, Park County, Wyo. C.I., 6 ms (approx. 30 ft). Horizontal scale, 1 in. = 2000 ft. Note: Bottomhole location for the No. 3 Badger Basin Field Unit well is an estimated position, based on expected dips penetrated by the well and the absence of any normal-fault cut in the Cody shale or Frontier Formation.

